Ruthenium(II) Complexes as Potential Chemotherapeutic Agents

A Thesis Submitted for the Degree of

Doctor of Philosophy by

Robert Morris, BSc

Department of Chemistry
University of Edinburgh

January 2000

EX BIBL. UNIV. EDINBURGH

Abstract

Five aminophosphine complexes of Ru(II) have been prepared as potential chemotherapeutic agents and characterised by NMR and X-ray crystallography. The chelate ring-opening process of the bidentate aminophosphine ligand in the complex *cis, trans*-[Ru($H_2NCH_2CH_2PPh_2$-*N,P*)$_2Cl_2$] has been investigated by 2D NMR methods. The complex undergoes a ring-opening reaction in coordinating solvents via the cleaving of the Ru-N bond. This exposes a potential binding site on the metal, and leads to the possibility of *in vivo* reactivity.

A range of water-soluble Ru(II)arene complexes of the type [(η^6-arene)$Ru^{II}X$(L-L)]$^+$ [(η^6-arene)$Ru^{II}X(L)_2$]$^+$ and [(η^6-arene)$Ru^{II}X_2L$], arene = benzene, *p*-cymene, alkylbenzoate, biphenyl, L-L = ethylenediamine, L = acetonitrile, isonicotinamide, X= Cl, Br, I, have been synthesised with an aim to produce anticancer active agents. They have been characterised by NMR and X-ray crystallography. The hydrolysis of [(η^6-*p*-cymene)Ru^{II}Cl(en)]$^+$ and [(η^6-biphenyl)Ru^{II}Cl(en)]$^+$ has been followed by HPLC and ESI-MS and an HPLC assay developed for use in studies relating to biological testing.

The reactions of the of Ru(II)arene complex [(η^6-*p*-cymene)Ru^{II}Cl(en)]$^+$ with the nucleotides 5′GMP, 5′CMP, 5′AMP and 5′TMP have been investigated by NMR. The complex [(η^6-*p*-cymene)Ru^{II}Cl(en)]$^+$ binds to 5′GMP at the N^7 of the guanine moiety. On reaction with a 14mer duplex oligonucleotide of known sequence it was found to lower the melting temperature of the duplex significantly to a level comparable to cisplatin. The complex forms mono and bis adducts with the oligonucleotide in a guanine specific manner, as elucidated by HPLC separation, ESI mass spectrometry and enzymatic digestion.

Cytotoxic studies on Ru(II) compounds revealed a significant effect against the ovarian cancer cell line A2780. Cross resistance studies indicate that the complex

$[(\eta^6\text{-}p\text{-cymene})Ru^{II}Cl(en)]^+$ is influenced by the protein p53, but $[(\eta^6\text{-biphenyl})Ru^{II}Cl(en)]^+$ possibly functions as an inhibitor of topoisomerases.

Acknowledgements

A long list of worthy people.

I would like to thank Professor Peter J. Sadler for his supervision and interest in this project over the past few years.

My thanks go to John Millar and Wesley Kerr in the NMR service, Dr. Lorna Eades in Elemental Analysis and Dr. Simon Parsons and his crew for solving the X-ray crystal structures. Thanks also to Dr. Jeff Cummings, Dr. Duncan Jodrell and Rhona Aird in the ICRF at the Western General Hospital for the cytotoxicity studies, Nathan Hughes for the DNA melting temperature work and Haimei Chen for crystallising the biphenyl complex.

The word "thanks" is completely insufficient for Abraha Habtemariam, Socorro Murdoch and Zijian Guo, without whose friendship and help I would definitely not be writing this book. I am extremely grateful, also, to John Parkinson for his NMR expertise and his ability to find time at any time, and distractions from Dave, Beth, Shailja and Michael, which were most welcome.

Fortunately it wasn't all work, and big cheers go to Pat and Rob who shared the pain over the years. Special mention goes to the two scallies Kathryn and Peter for being the perfect hosts, and to Seni, who knows nothing of chemistry, which just makes her all the more appealing.

Finally, I would like to thank my parents Richard and Heather for their support and encouragement at all times from start to finish.

Stars all.

to rico and hedsey-bear

I did my best, it wasn't much
I couldn't feel, so I tried to touch
I've told the truth, I didn't come to fool you
And even though
It all went wrong
I'll stand before the Lord of Song
With nothing on my tongue but Hallelujah

Hallelujah
Leonard Cohen

oh what a cliche
its already done and it took so long
what can i say

she's gone
Ned's Atomic Dustbin

Table of Contents

List of Figures

Chapter 3

Chapter 4

List of Tables

Abbreviations

DHAP	dihydroaminophosphine
DMAP	dimethylaminophosphine
DPEBA	diphenylphosphinoethanebenzylamine
COSY	COrrelation SpectroscopY
HSQC	Heteronuclear Single Quantum Coherence Spectroscopy
TOCSY	TOtal Correlation SpectroscopY
NOESY	Nuclear Overhauser Effect SpectroscopY
TSP	sodium 3-trimethylpropionic acid
HPLC	High Performance Liquid Chromatography
TEAA	Tetra Ethyl Ammonium Acetate
ESI	Electrospray Ionisation
API	Atmospheric Pressure Ionisation
VPD	Venom PhosphoDiesterase
SPD	Spleen PhosphoDiesterase
NP1	Nucleotide Phosphatase 1

Chapter 1

Introduction

1. Introduction

This thesis is mainly concerned with the synthesis of ruthenium(II) complexes and their potential applications as therapeutic agents for the treatment of cancer. Although there are no ruthenium drugs in current clinical use, it is widely considered that this situation will change in the not too distant future. Metals in general have had an increasing role to play in medicinal and biological applications in the last three decades and many reviews and publications have appeared on this subject.[1] This introduction chapter, however, will deal specifically with ruthenium complexes that have been investigated for activity. It begins with a brief introduction to the chemistry of ruthenium and a short introduction to cancer, followed by a summary of data for various ruthenium agents that have appeared in the literature.

1.1 Ruthenium

Ruthenium (atomic number 44, mass no. 101.07) is found in Group VIII of the Periodic table, and along with osmium, rhodium, iridium, palladium and platinum forms the group of metals known as the platinum metals. Ruthenium was discovered in 1844 by Karl Kotchovitch Klaus in the residues left behind after crude platinum from the Urals had been dissolved in aqua regia. This was actually an extension of work by G. W. Osann back in 1826, and Klaus named the new metal ruthenium after the Latin name for Russia, Ruthenia.

Ruthenium is generally found in the metallic state along with other platinum metals and the coinage metals. Major sources are the nickel-copper sulfide ores found in South Africa and Sudbury, Canada, and in the river sands of the Ural mountains. It has an estimated natural abundance of 1×10^{-4} ppm in the earth's crust.[2] Extraction is typically from platinum concentrates obtained as anodic slimes from the electrolytic refinement of nickel. Treatment with aqua regia removes Pt, Pd, and Au, and silver is removed as its soluble nitrate by heating with $PbCO_3$ and treating with nitric acid. The remaining insoluble residue yields Ru, Os, Ir and Rh.

Currently the main use for Ru is as an additive for hardening of platinum and palladium, although the scarcity, and hence high cost, limits its use.

Ruthenium has seven isotopes, ranging from 96 to 104, with ^{102}Ru being the most abundant at 31.6 %. This has the effect of limiting the accuracy of the molecular weight. Its electronic configuration is [Kr] $4d^7\ 5s^1$, it has an electronegativity of 2.2 and is typically metallic, with a hexagonal close packed structure and a high melting point of 2334.[3]

Ruthenium is virtually unaffected by non-oxidising agents, and is at its most reactive with oxidising agents, however it is stable to atmospheric attack. It is capable of reaching the group oxidation state (+8). This is in contrast to iron which is very easily reduced at +6. The lowest oxidation state in which it forms oxides at is +4 RuO_2. RuO_2 is formed from the action of O_2 on Ru metal at 1250° C and it is from this compound that the most commonly used laboratory source of ruthenium, $RuCl_3.3H_2O$, is formed by reduction with concentrated hydrochloric acid. Though containing Ru(III) species such as $RuCl_3.3H_2O$, it also appears to contain some polynuclear Ru(IV) complexes.[3] It is soluble in water, alcohols, acetone and many simple organic solvents and therefore is good for reactions with ligands. This Ru(III) compound can also be reoxidised to RuO_2 by O_2 at the lower temperature of 500 -700° C.

The most relevant oxidation states for bioinorganic chemistry are Ru II, III and IV. Ru(II) forms diamagnetic d^6 complexes which exhibit octahedral geometry with the notable exception of the square-pyramidal complex $RuCl_2(PPh_3)_3$. The reactions of Ru(II) often proceed with retention of configuration, suggesting an associative mechanism.[3] Ru(III) is the best known oxidation state and complexes are always low-spin octahedral with one unpaired electron. They are particularly amenable to nitrogen containing ligands. There are relatively few Ru(IV) complexes in comparison with Ru(II) and Ru(III). They all have octahedral or distorted octahedral configuration. They are potentially useful as DNA oxidising agents as they are conveniently reduced in solution.

1.2 Cancer

Cancer is the second leading cause of death in western countries.[4] It will affect one in three individuals at some stage during their life and causes one in five deaths in the developed world.[4] Cancer is not a new phenomenon, cancer lesions have even been found in dinosaur bones. It is partially due to medical advances in controlling other former major fatal diseases such as tuberculosis, and the increase in pollutants and synthetic materials in the environment today that have become known as carcinogens that it has developed into a more notable risk.

Cancer is not one disease, but many that differ depending on the site and origin of the tumour. Different types of cancers have different characteristics and require different treatment. The nomenclature for these diseases varies. Some are named after the individual who first described the condition e.g. Hodgkin's lymphoma, and some are simply named after the tissue of origin.

Cancer is the abnormal growth, reproduction and spread of body cells. A cancer cell does not know when to stop growing or respond to the normal cell signals telling it when it is time to die. The medical term for a tumour is a neoplasm, a relatively autonomous growth of tissue, and a cancerous tumour is a malignant neoplasm that is potentially dangerous to the host. Malignant tumours have the capability to metastasise, i.e. proliferate secondary tumours to other parts of the body, and these are frequently the lethal aspect of a cancer. There is no clinically used agent at present for the treatment of metastases and it is in this area in particular that ruthenium is hoped to find success.[5] Metastasis may occur when the tumour reaches a critical size and sheds cells into the circulatory system. It may also occur via the lymphatic system, or when improper surgery has resulted in the spreading of cells.

Cancer cells act differently to normal cells. In cultures they can pile up or grow freely while normal cells require to "plate down" and only grow to the thickness of a

monolayer. They are also much more aggressive than normal cells and tend to multiply at a much accelerated rate.

There are three main proposed mechanisms for the formation of a cancerous growth.[6]

1. *Mutation*, involving the loss, rearrangement or substitution of DNA in a cell, although this has been shown to not be always necessary for cancer formation, e.g. mouse tetracarcinoma develops without having any altered genes.
2. *Addition and integration of new viral genetic material* into a cell's genes as a result of tumour producing viruses - known to happen in chickens,[7] hamsters, mice and monkeys.
3. *Epigenesis*, which is when there is no change in the genetic material, but in its expression by the cell.

1.2.1 Treatment of cancers

After diagnosis of a cancer there are a few options left open to the oncologist to decide how to proceed with treatment, depending largely on the cancer type, stage of progression and location. The main ones are surgery, radiation therapy, immunotherapy and chemotherapy.

The first line of attack against tumours is usually surgery. This is particularly beneficial if the tumour has not yet metastasised. However disseminated forms of cancer such as leukaemia cannot be treated surgically. Surgery is always used in conjunction with some other kind of treatment to help prevent remission.

Radiation treatment e.g. with γ-rays from radio-isotopes such as ^{60}Co and X-rays. The radiation is aimed at the site of the tumour to prevent surrounding area damage as the rays are extremely toxic.[6] Radiation sensitisers are used to increase damage to localised areas without having to increase the radiation dose.

Immunotherapy is really a follow-up treatment rather than a first line of attack. This involves the administration of agents that will stimulate the body to destroy the last of the cancer cells left after surgery or radiation therapy. Non-specific agents have been used to generate the immune response in patients as specific immunotherapy (immunisation with the patients own tumour) has been found to be unsuccessful, although specific immunotherapy may develop.[8]

Chemotherapy, the treatment of cancer with drugs, is an area of intense research with great hopes for the future. Unfortunately it is limited in its efficacy by a number of factors. The size of the tumour is very important. Even if the drug therapy managed to kill 99.9 % of a 100 g tumour, this would still leave ~ 10^8 cells, which would probably be too many for a body to cope with. Side effects of drugs can be quite severe due to the similarity between cancerous and normal cells. Drugs particularly affect rapidly dividing cells (like cancers) as they tend to attack the cell at the various points during the cell division process. This leaves healthy rapidly dividing cells such as hair follicles, the gastrointestinal lining and bone marrow cells of the immune system open to attack. This results in some of the typical side-effects experienced with chemotherapy: hair loss, nausea and poor immuno-response.

The main types of drugs in use are:[6]

Antimetabolites: these inhibit a metabolic pathway essential for reproduction or survival of cancer cells.

Alkylating agents: reactive compounds that act upon DNA, RNA and certain enzymes. This group includes the inorganic compounds carboplatin and cisplatin, drugs that was found to be extremely effective in the treatment of testicular cancer.

Antibiotics: a number of antibiotics have shown activity against tumours

Antimitiotic agents: these arrest cells in metaphase of cell division and interfere with the synthesis of transfer RNA.

At present, drug treatments tend to be palliative rather than curative. They work best during the DNA synthesis stage of cell division, which means that fast replicating tumour cells are more susceptible. Young tumours divide more rapidly, growing

exponentially, so early diagnosis gives a much better chance of survival as they are less resistant. But as a tumour ages growth slows and resistance can set in. Often combination treatments are necessary to overcome developing resistance and provide different forms of attack.

Although great progress in the treatment of cancer has been made in the past few decades, it is clear that there is still a great deal of work yet to be done, and it is certain that inorganic chemistry and the development of new treatments based on metals and inorganic compounds has a very important role to play in this research.

1.3 Ruthenium and medicine

The stimulus for investigation into ruthenium complexes as anti-cancer agents was the success of cisplatin in treatments against testicular and ovarian carcinomas and tumours of the bladder and head and neck, although the forefathers of ruthenium pharmacology could be considered as Dwyer and co-workers.[9] In 1965, 4 years before the activity of cisplatin was recognised, they reported the anti-tumour effects of Ru(II) trischelates containing 1,10-phenanthroline.

1.3.1 Ruthenium and selectivity

An advantage of ruthenium is its selectivity for tumour cells. It has been found that ruthenium remains for up to 96 h in tumour tissues with concentrations of four times the rest of the body.[10] The selectivity of ruthenium for tumour cells indicates potential selective cytotoxicity, and is probably linked to transferrin, the iron transport protein found in the blood. Yet the question remains as to how it actually gets to the tumour. One strong possibility is that the ruthenium is picked up in the bloodstream by the iron transport protein transferrin and transported around the body. Transferrin mediated uptake of metal ions in tumour cells is a form of specific intake and is a result of the elevated requirements of tumour cells for nutrients (hence they possess more transferrin receptors than normal cells) due to their accelerated and uncontrolled growth.[11]

There has been previous investigations into the possibility of Ru uptake by transferrin. The diaqua intermediates of the potential anticancer agent *trans*-$[Cl_4(Im)_2Ru]^-$ and its indazole analogue bind to apotransferrin with a 2:1 stoichiometry with the heterocycles remaining attached. The release of the intact complex is promoted by citrate.[17(a)]

Transferrin uptake of *trans*-$[RuCl_4(Ind)_2]^-$ is apparently important to the transport of the complex, despite most of the complex being bound in the bloodstream by the protein albumin.[12] This, and its imidazole analogue *trans*-$[RuCl_4(Im)_2]^-$, do not bind to Al^{III}_2-Tf, suggesting that binding is at the iron binding sites of the protein. Crystallographic evidence shows the imidazole complex binding to a histidine residue at the iron sites.[13] There are also seventeen surface histidine residues in transferrin though, and they also appear to bind the complex, as they do $[Ru(H_2O)(NH_3)_5]^{2+}$.[14,15]

This transferrin uptake of ruthenium in the blood may reduce the toxicity of the drug by preventing it from binding with other molecules in the body until it has been delivered to the tumour cell. It is even possible that the anticancer activity exhibited by many ruthenium agents may, to some extent, be due to a depletion of Fe from cells and proteins.

Transferrins (Tf) are a family of glycoproteins (a protein linked to a polysaccharide) that transport iron around the mammalian vascular system. Iron is an essential element used in dioxygen transport (haemoglobin) and metabolism and participates in a variety of electron transport pathways. Transferrins are bilobal proteins of approx. 80 kDa, each lobe containing a binding site for Fe(III). The lobes are termed the N-lobe and the C-lobe after the chain terminus it contains. Each lobe contains two sub-domains that form a cleft which closes around the iron during binding. The Fe(III) binds with carbonate (CO_3^{2-}) as a synergistic binding ion. The protein first binds carbonate with side-chains from a nearby arginine and threonine residues and two peptide N-Hs in a binding pocket so that the protein is now

organised to bind Fe(III) in an oxygen ligand rich octahedral environment, using two oxygens from the carbonate, two phenolate oxygens from tyrosines, a nitrogen from histidine and a carboxylate from aspartic acid.[16]

The Fe(III) is now solubilised in an otherwise unfavourable environment and is transported through the body to cells where only the iron bound form, and not the unbound (apoTf), is taken up by transferrin receptors on the cell membrane. This indicates the importance of the change in conformation of the protein on metal binding. The receptor is then taken up into an endosomal compartment in the cell, and via H^+ pumps, lowers the compartment pH to 5-6, thereby protonating the tyrosinate oxygens and releasing the iron.[16]

Ruthenium's position below iron in the periodic table means that it may mimic some of its properties. Indeed, both persist mainly as +2 and +3 ions in aqueous solution and both are concentrated in villi of the small intestine and distributed around the body from there. Various Ru-complex - transferrin studies have been performed[17] and binding has been observed. Release of ruthenium is promoted by acidification and presence of a citrate chelating agent, a situation not unlike that of iron being released from transferrin in endosomal compartments of low pH. The crystal structure of a Ru(III) complex bound to lactoferrin has been solved.[17(e)] The complex *trans*-$[RuCl_4Ind_2]^-$ was found to bind to His in the iron binding sites with displacement of chloride but the indazole ligands intact.

Transferrin may promote the concentration of ruthenium in tumour cells due to the higher than normal number of transferrin receptors on tumour cells. This is due to the increased iron requirement, as the cells are growing and dividing at an accelerated rate.

This selective build up in tumour cells means that ruthenium could perhaps be utilised as a diagnostic device, by administration of the radioactive isotope ^{97}Ru. This has a half-life of 2.9 days, which is long enough to allow synthesis and quality control of the radio-pharmaceutical, but sufficiently short that even strongly retained

1.3.3 Ruthenium and metastases

Metastases, secondary tumours proliferated from the primary tumour, are often the cause of death in a case of cancer. These tumours do not respond to the same treatment as the primary neoplasm as they exhibit different clonogenicity and antigenicity. Ruthenium complexes exhibit a significant and specific action against tumour metastases, which is a novel approach as none of the currently available anti-cancer agents exhibit such a property. This was first demonstrated with *cis*- and *trans*-$[RuCl_2(DMSO)_4]$.[25] Presently, [HIm][*trans*-$RuCl_4$(DMSO)Im], (NAMI-A) (Im = imidazole) a complex which has recently entered clinical trials, shows the best antimetastatic activity and has shown activity at low doses and free of a detectable cytotoxicity for primary tumours and the host itself.[26] This will be further discussed in Section 1.4.3.

A difficulty associated with detecting activity for ruthenium compounds *in vitro* is their low cytotoxicity, yet significant effects *in vivo*. An excellent example of this is the lack of effect of NAMI-A on tumour cells *in vitro* as opposed to its excellent effect *in vivo*.[27] This cannot be explained by interactions with the matrix in which the tumour cells are kept in *in vitro*, as shown by the complete inactivity of several compounds up to millimolar concentrations when tested against TLX5 tumour cells kept in sterile Dulbecco's saline, which is calcium and magnesium free.[28] It is possible that a complicated pattern of host interactions may be involved. This would also help explain the metastatic activity. Contrary to first impressions, this lack of cytotoxicity is actually a potentially advantageous factor for the ruthenium drugs as it implies a low, or absent, bone marrow or epithelial toxicity at active dosages.[29]

The initial cytotoxicity studies on complexes were carried out on Ehrlich ascites carcinoma and P388 leukaemia cell-lines. These have low predictivity for human systems but were used as accept or reject screening mechanisms, which led to poor results. Examples of the difficulty in correlating *in vivo* and *in vitro* tests are the high DNA synthesis inhibition of $[RuCl(NH_3)_5]Cl_2$ [30]and its negligible anti-tumour activity, and $[RuCH_3CH_2COO(NH_3)_5]Cl_2$ which exhibits no inhibition of DNA synthesis and good anti-tumour activity.[30]

1.3.4 Ruthenium and nitric oxide

A molecule that has been gaining more recognition recently for its biological relevance is nitric oxide. Formerly almost entirely considered the domain of environmental chemists and catalytic studies, it is now known to play a key part in the regulation of blood pressure, act as a neurotransmitter and also has a role in the macrophagic immune response. It is created in the body by the enzyme nitric oxide synthase which catalyses the transformation of arginine to citrulline. Organonitrates have been used medically for some time as vasodilators and act by releasing nitric oxide. Acetylcholine, a transmitter found at neuro-synapses also releases nitric oxide during its function. Dysfunction in the metabolism of nitric oxide can lead to hypertension, diabetes, epilepsy and septic shock. Septic shock is a condition brought on due to excess nitric oxide and has a greater than 50% mortality rate, therefore there is a need for new drugs to reduce nitric oxide levels. Nitric oxide has a similar coordination chemistry to carbon monoxide and complexes with ruthenium are well known.[31] The Ru-NO bond can exist in both anionic and cationic complexes, in which it is remarkably stable, being able to persist through a variety of oxidation-reduction and substitution reactions. Almost any ligand can be present with NO. NO reacts with Ru(III)-d^5, reducing the Ru(III)→Ru(II) with the ligand formally being NO^+. Ruthenium could therefore conceivably be used as a nitric oxide scavenger. Ruthenium - polyaminocarboxylates[32] are presently being investigated for their activity, particularly K[Ru(Hedta)Cl], see Figure 1.1.. Hedta leaves one coordination site available for NO and, being soluble in water, the complex should remain in the blood. Models of disease activity have indicated the potential therapeutic benefit of ruthenium-polyaminocarboxylates.[32]

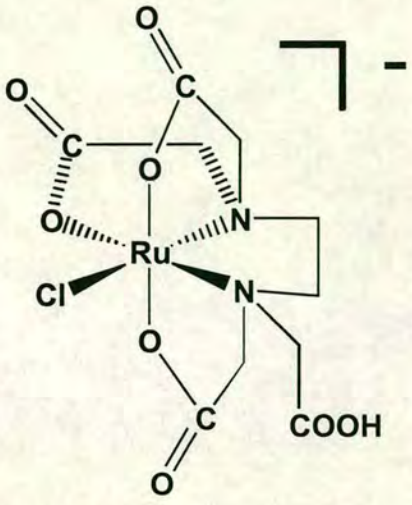

Figure 1.1 Structure of $K[Ru^{III}(Hedta)Cl]$ [32]

Nitric oxide is also toxic towards tumours, due to the formation of metal-nitrosyl bonds.[32] Three key proteins involved in energy metabolism have been identified as the targets of macrophagic attack in tumour cells. All contain non-haem iron as iron-sulphur clusters and it is these irons that are nitrosylated. Ribonucleotide reductase, an enzyme involved in DNA synthesis, is also inhibited.[32]

Ruthenium polyaminocarboxylates are potential antitumour agents as well as NO scavengers. For example, a labile Ru(III) complex with chloride and pdta ligands, pdta = 1,2-propylenediaminetetracetate,[33] shows good antitumour activity, thought to be *via* crosslinking of guanines on DNA. The chlorides are known to dissociate in solution, and in this case, the metal stays in the oxidation state III.[33] This complex can bind to albumin, apotransferrin, and diferric transferrin (pointing to surface binding of the complex), damages nuclear DNA, alters the conformation of plasmid DNA aswell as inhibits DNA recognition and DNA lysis by restriction enzymes.[34] Ru(II) polyaminocarboxylates are known to bind to the C_5-C_6 olefin bond of pyrimidines, and can span the major groove of DNA.[35]

Similarly, perhaps use could be made of ruthenium's coordination chemistry with carbon monoxide. CO is approximately the same size as O_2, and has a greater affinity for haemoglobin and myoglobin than O_2 and tends to bind to them irreversibly. CO has also been linked to Sudden Infant Death syndrome,[36] and epilepsy.[37] It is also thought to play a role as a response mediator in the central nervous system[38] and as a cardiovascular modulator.[39] Ruthenium's high affinity for carbon monoxide suggests a possible role as a scavenger for CO.

Although research into ruthenium drugs was originally intended to try and improve on the activity of cisplatin, it is now clear that due to their different effects and differences in mechanisms, ruthenium agents should be seen as a development of new drugs in their own right.

1.4 Ruthenium Agents

1.4.1 Ruthenium-am(m)ine complexes

Ruthenium-ammine complexes were the first group of ruthenium complexes to undergo screening for anti-tumour activity, and have been previously reviewed.[40] Examples of Ru-ammine complexes are $[RuCl(NH_3)_5]Cl_2$, *cis*-$[RuCl_2(NH_3)_4]Cl$, *fac*-$[RuCl_3(NH_3)_3]$ (Figure 1.2) and Ru-red, a trinuclear cation. Ru-red only exhibits moderate anti-tumour activity but has been shown to inhibit calcium metabolism, which has been linked to suppression of tumour growth.[22]

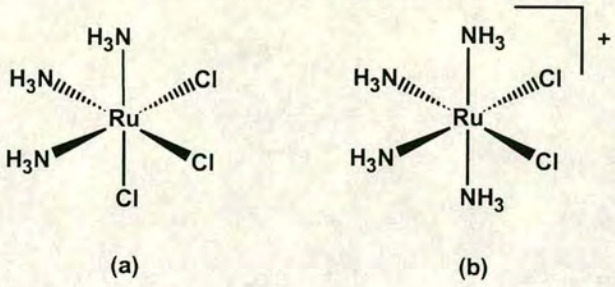

Figure 1.2 Structures of (a) *fac*-$[RuCl_3(NH_3)_3]$ and (b) *cis*-$[RuCl_2(NH_3)_4]^+$

Fac-$[RuCl_3(NH_3)_3]$ is the most active Ru-ammine complex that has been tested and was found to approach the effectiveness of cisplatin on P388 Leukaemia[41] and has similar bacterial elongation properties to cisplatin.[42] Unfortunately, these promising results were coupled with a poor solubility in saline solution[41] and hence were deemed unsuitable for biological application. *Cis*-$[RuCl_2(NH_3)_4]Cl$, on the other hand, has quite a good saline solubility but was never considered effective enough to progress to clinical trials.

Whilst not effective as an anti-tumour agent, $[Ru^{II}(H_2O)(NH_3)_5]^{2+}$ serves as a simple model for monodentate coordination of Ru to DNA and RNA. Rapid binding is observed due to the attraction of the large polyanions to this cation.[43] It was found that the N^7 of guanine was the initial site of attack when exposed in the major groove of B-DNA. Second phase interactions probably occur due to interaction of Ru(II)

with new coordination sites becoming available as the nucleic acid strands separate. Coordination of Ru(III)-pentaammine was also observed on deprotonated exocyclic amines of adenosine and cytidine,[44] and it has been seen to migrate over the N^1, N^3 and N^9 donor sites of 7-methylhypoxanthine and 7-methylguanine, depending on pH.

Clarke's investigations on Ru-ammine complexes led him to propose the theory of activation by reduction, i.e. using Ru(III) as a pro-drug.[41] Indeed, Ru(II) does bind faster to DNA[45] and it has been shown that Ru-ammine complexes can be reduced by a transmembrane electron transport system[46] and that it can be oxidised back to Ru(III) inside a cell, particularly in the case of abundant oxygen,[47] although this situation is not usual in a tumour cell.

Ruthenium am(m)ine complexes can also generate breaks in DNA. In $Ru(NH_3)_5(dG^{N7})$ the Ru(III) acts as a general acid in promoting the hydrolysis of the N-glycosidic bond.[48]

1.4.2 Ruthenium-heterocycle complexes

In order to address the problem of the low solubility of the Ru-ammine anti-cancer agents, Keppler and co-workers decided to develop Ru(III) complexes with fewer N ligands and more halides. These would have an improved solubility due to the ionic charge. The general formula of these is $[HL]_2[RuCl_5L]$ and $[HL][trans\text{-}RuCl_4L_2]$, where L is a heterocyclic base, particularly imidazole and indazole (Figure 1.3). In preliminary tests the imidazole and indazole complexes were found to exhibit a higher activity against P388 leukaemia than cisplatin[49] indicating their potential as anti-cancer agents. Of the two, the indazole derivative has a lower toxicity and a higher activity in models. Both the imidazole and indazole $[HL][trans\text{-}RuCl_4L_2]$ bind covalently to calf thymus DNA and also to the double strand polymers poly(dG-dC) and poly(dA-dT), with a preference for(dG-dC)[50]. In low chloride concentrations the imidazole binds the fastest of the two and, in a reaction ratio of 10:1 nucleotide:[Ru] , after 8 h the imidazole complex was found to be 75 % bound

to (dG-dC) and DNA. Unlike the indazole derivative, the imidazole complex is stable in solution and hence the majority of *in vitro* tests were performed on it.

The original synthesis of [HIm][*trans*-$RuCl_4Im_2$] dates back to the early 1960's.[51] This was further developed by Keppler and co-workers,[52] who recognised the anti-tumour activity and confirmed the structure by X-ray analysis. This complex has a solubility in blood plasma of 10 mM. The (1-methyl), (2-methyl) and (4-methyl) derivatives were also synthesised and specific tumour tests on P388 leukaemia, Walker 256 carcinosarcoma and sarcoma 180 indicated greater effectiveness than 5-fluorouracil in all cases and comparable activity to cisplatin, with the methyl derivatives being the less active of the series. Promising results were also obtained from tests against autochthonous colorectal tumours in rats, reducing tumour volume by up to 90%. These type of tumours are not currently treatable with chemotherapy.

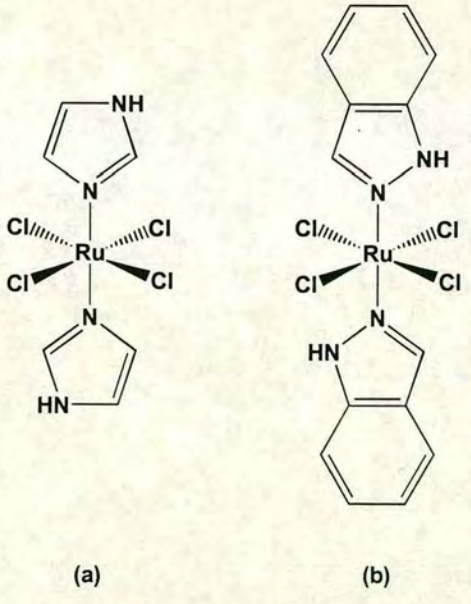

Figure 1.3 Structures of (a) *trans*-$[RuCl_4Im_2]^-$ and (b) *trans*-$[RuCl_4Ind_2]^-$

It was observed that aged aqueous solutions (>20 h) reacted rapidly with DNA and fresh solutions did not.[53] This would imply the necessity of an initial aquation step, similar to cisplatin, to be activated towards DNA. Studies of the process[54] found stepwise aquation with first order kinetics. Initial replacement of a chloride occurs,

and then a second chloride is replaced in either the *cis* or *trans* position. This appeared to occur equally despite the greater *trans* effect[55] associated with oxygen compared to chloride. The half-life of the aquation process was found to be $t_{1/2}$ = 3.4 h at 310 K. $[RuCl_5Im]^{2-}$ undergoes fast aquation[56] to $[RuCl_4(H_2O)Im]^-$. When dissolved in D_2O the initial NMR spectrum shows only this and not $[RuCl_5Im]^{2-}$, the species present in the solid.

The interactions of *trans*-$[RuCl_4Im_2]^-$ and $[RuCl_5Im]^{2-}$ with imidazole and N^6,N^6-dimethyladenine (Figure 1.4) have been studied.[56] Imidazole is good for studies on potentially bioactive molecules as the moiety is present in biology in purine nucleotides and molecules such as histidine. Also, it has several protons available for monitoring reactions by NMR. Dimethyladenine was used to simulate binding of a purine unit, but the 6-NMe_2 creates steric hindrance, and therefore should force binding as the N^7-H tautomer via N^9, and prevents formation of multiple monomeric and polymeric complexes.

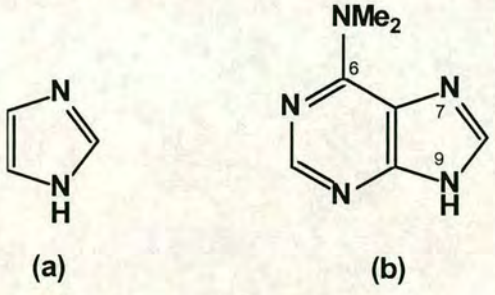

Figure 1.4 Structures of (a) imidazole and (b) N^6,N^6-dimethyladenine

In a 2:1 ratio of imidazole:complex, *trans*-$[RuCl_4Im_2]^-$ forms $[Ru(OH)_2Im_4]^+$ which precipitates as a crystal in coexistence with $[RuCl_4Im_2]^-$. In the presence of excess imidazole the reaction proceeds to $[RuIm_6]^{3+}$.[56] The reaction proceeds slowly at the start, and higher complexes begin to appear at roughly the rate of the first aquation step. The first aquation step is never observed, as the aquated complex is likely to be a short lived intermediate. The rate accelerates after the first reaction with

imidazole. This probably occurs via a base-catalysed process. With excess free imidazole the pH is high so this process is feasible. This implies a reasonable reaction with DNA, showing potential for inter/intra-strand binding.

The mono-imidazole complex $[RuCl_5Im]^{2-}$ exhibits a very high affinity for imidazole, even if the $[HIm]^+$ counter-ion is the only source.[56] Once the bis-imidazole complex is formed it does not revert back to the mono-form due to the inertness of the Ru-N bond. To confirm the inertness of the Ru^{III}-N bond, (C-2) deuterated imidazole was added, but the ^{1}H-NMR signal for H-2 did not disappear. It would have been removed had the Ru-N bond been labile. The bis-imidazole complex was formed in both the *cis* and *trans* configurations and these then underwent successive substitutions of imidazole up to $[RuIm_6]^{3+}$, indicating a high affinity for N bases and therefore probably for DNA.

$[RuCl_4Im_2]^{2-}$ has been found to react in a 1:1 ratio with dimethyladenine,[56] although the reaction never reaches completion. Coordination was probably via the N^7-H - N^9 tautomer (normally the first site of coordination of a metal[57]) with retention of the *trans* configuration of the imidazoles, although no conclusive proof was found. The bis- dimethyladenine -Ru complex was formed in small quantities only when fifteen equivalents of dimethyladenine was used.

Both imidazole and indazole complexes bind to human serum albumin and human serum apotransferrin,[17] and are released by acidification and complexation by citrate. This is important due to the low pH in the endosomal compartment in cells in which transferrin releases its bound iron. Transferrin is potentially a very useful drug delivery system. Circular dichroism spectroscopy has shown both $[RuCl_4Im_2]^{2-}$ and $[RuCl_4Ind_2]^{2-}$ complexes bind specifically around the Fe(III) binding sites of apotransferrin, and that the presence of bicarbonate is necessary. An X-ray crystal structure analysis of the adduct of the indazole complexes with human apolactoferrin[17(e)] has demonstrated that the Ru(III)-indazole complex coordinates to a histidine residue at the unoccupied binding sites, specifically His 253 in the N-lobe and His 597 in the C-lobe, and with lower affinity sites at surface exposed His

residues, primarily His 590 and His 654. The N-heterocycles remain attached to the ruthenium. On binding to HSA the imidazole complex was found to significantly alter the protein's structure, and deleteriously effect the binding of molecules such as warfarin and heme.[58] This binding to transferrin may lead to controlled transport of the ruthenium around body, and hence a high selectivity for tumours.

Anti-proliferative efficacy studies[59] against human colon cancer cell lines have been performed using the free complex, and transferrin and apotransferrin-bound forms of $[RuCl_4Im_2]^-$ and $[RuCl_4Ind_2]^-$. Cisplatin bound to plasma proteins exhibits no significant anti-tumour activity. The apotransferrin bound form of $[RuCl_4Ind_2]^-$ is not as active as the free complex, but the apotransferrin bound form of $[RuCl_4Im_2]^-$ is. This is possibly due to the difference in configurations of the bound apotransferrin due to the different sized heterocycle ligands. The protein-complex with imidazole ligands has the closer configuration to when Fe(III) is bound to transferrin, therefore the transferrin receptors on the cell membrane would be more likely to recognise it.

The speed of binding of $[RuCl_4Ind_2]^-$ to human serum albumin and human serum transferrin is much faster (on a timescale of a few minutes) than cisplatin, whereas the $[RuCl_4Im_2]^-$ binds at a similar rate to cisplatin (a few hours)[17]. This is a possible explanation for the greater toxicity of the imidazole complex as compared to the indazole.

[HIm][*trans*-$RuCl_4$(DMSO)Im] is a ruthenium complex that has shown excellent anti-metastatic activity.[4] It contains both a heterocyclic ligand and a DMSO molecule. This is further discussed in Section 1.4.3.

Spectroscopic and structural studies[60] have indicated imidazole as a moderate π-donor ligand to Ru(III). This effect is not seen with Ru(II) due to the low spin d^6 electron configuration preventing the metal from accepting π–electron density from the imidazole. Electrochemical studies on several imidazole complexes of

ruthenium also suggest that imidazole may also serve as a significant π-acceptor ligand in the presence of anionic ligands. *Cis*-$[(Im)_2(NH_3)_4Ru^{III}]Cl_3$ and $[(Im)_6Ru^{III}]Cl_3$ (Figure 1.5) have been shown to have excellent immunosuppressive properties, and this may well be due to the imidazole ligands tuning the $Ru^{II,III}$ reduction potentials to a range optimal for biological activity, whilst still being small enough to react readily with redox sites in proteins.

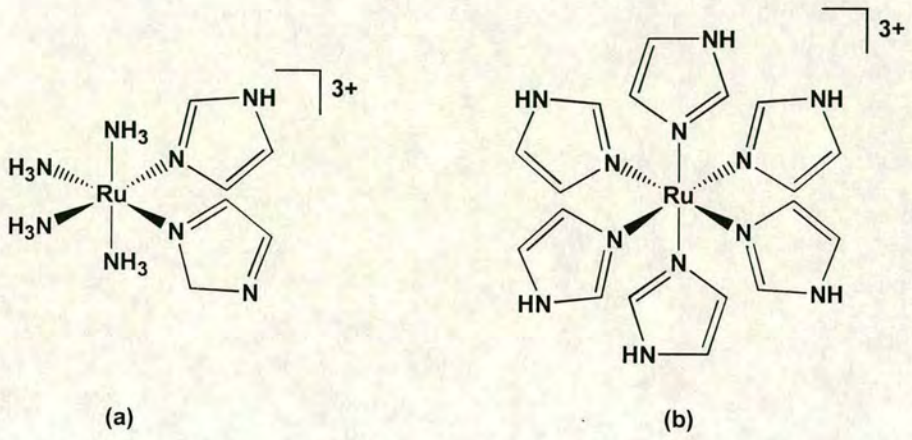

Figure 1.5 Structures of (a) *cis*-$[Ru(NH_3)_4Im_2]^{3+}$ and (b) $[RuIm_6]^{3+}$

1.4.3 Ruthenium sulfoxide Complexes

The ruthenium-sulfoxide complexes that have received the most attention from a biological point of view are *cis*- and *trans*-$[RuCl_2(DMSO)_4]$ (Figure 1.6) The anti-tumour properties of *cis*-$[RuCl_2(DMSO)_4]$ were noticed early on by Giraldi et al in 1977[61]. This complex was obviously selected for its structural similarity to cisplatin and its overall neutrality. An advantage for these complexes is their ease of synthesis.[62] Refluxing $RuCl_3.3H_2O$ in dimethylsulfoxide in air for five minutes, followed by addition of acetone, precipitated the *cis* isomer. From there an equilibrium to the *trans* isomer is easily set up.

$$\textit{cis}\text{-}[RuCl_2(DMSO)_4] \underset{\Delta}{\overset{h\nu}{\rightleftharpoons}} \textit{trans}\text{-}[RuCl_2(DMSO)_4]$$

Other than the configuration of the chlorides, a significant difference between the two isomers is the presence of one oxygen bonded DMSO in the *cis* form, whereas all four DMSOs are sulphur bonded in the *trans*.[67]

Figure 1.6 Structures of (a) *cis*-$[RuCl_2(DMSO)_4]$ and (b) *trans*-$[RuCl_2(DMSO)_4]$

Both *cis*- and *trans*-$[RuCl_2(DMSO)_4]$ have been the focus of much testing. In general both have quite a low toxicity, LD_{50} values of up to 1 g/kg, but this is countered by the need for high therapeutic doses.[40] They have been shown to be mutagenic[63], react *in vitro* with DNA forming covalent bonds, particularly with guanine[64], and have a significant effect on metastasising murine tumours[25], which are cisplatin-resistant. Both show only slight activity against the Lewis lung carcinoma primary tumour, but both are significantly active against its metastases,[65] with the *trans* isomer being the more effective. The *cis* isomer has a similar effectiveness against MCa mammary carcinoma,[25] while the *trans* isomer inhibits both tumour growth and metastases of B16 melanoma in mice. Both are also active against cisplatin-resistant P388 leukaemia.[66]

A possible explanation for the greater effectiveness of the *trans* over the *cis* isomer can be seen from the difference in their chemical behaviour in aqueous solution (Figure 1.7). The steps were followed by conductivity measurements and repetitive electronic absorption scans.[67]

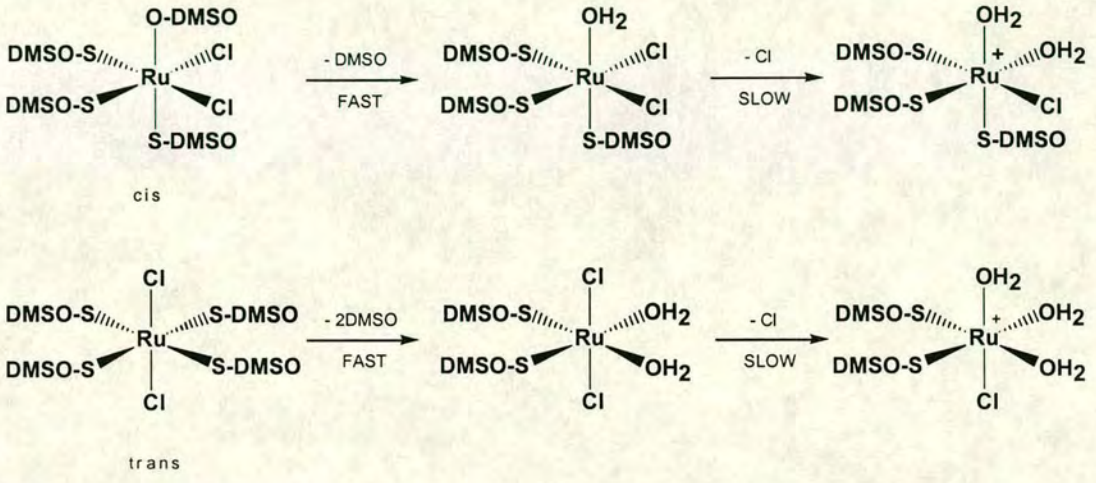

Figure 1.7 Aquation steps of *cis*- (upper) and *trans*-$RuCl_2(DMSO)_4$ [67]

The first step for *cis*-$[RuCl_2(DMSO)_4]$ when dissolved in water is dissociation of the weaker bound *O*-coordinated DMSO, followed by the slow dissociation of a Cl^- anion, to leave a cationic *cis*-diaqua species. The equilibrium was found to be inhibited by a 150 mM concentration of NaCl, simulating extracellular conditions, but unaffected in 3 mM NaCl, simulating internal cell conditions.

The *trans* isomer shows quite different behaviour. On dissolving in H_2O, two *cis* DMSOs are released to form *trans, cis, cis*-$[RuCl_2(DMSO)_2(H_2O)_2]$. This also slowly releases a chloride ion to give a cationic *fac*-triaqua complex. This equilibrium is again inhibited by physiological NaCl concentration.

Therefore, under physiological conditions, the *cis* form has only one coordination site readily available, whereas the *trans* has two sites open in *cis* positions. The significance of the chloride concentration is that as neutral complexes outside the cell, they should be able to cross the cell membrane, and then slowly open another coordination site due to the low [Cl^-] in the cell. The expected increased activity for the *trans* isomer is backed up by it being twenty times more toxic than the *cis*.

The corresponding bromo analogue was also tested, and found to be isostructural, but the chloro version was far more active, pointing to the influence of the halogen.

It is unlikely that the mechanism of anti-metastatic attack of these complexes is the same as their anti-primary tumour attack. Metastases differ from the primary tumour in their drug sensitivity, antigenicity and clonogenic capacity. This led Sava[68] to hypothesise that the host's immune system plays an important part in the anti-metastatic effect. He proposed that the compound has an antigenic effect on the extracellular part of the tumour cells, and in this way induces the host's immune system to kill the tumour. This is only a hypothesis and it must be considered that *trans*-[$RuCl_2(DMSO)_4$] shows similarities in its DNA chemistry to cisplatin. Both bind *in vitro* to plasmid DNA and inhibit the restriction enzymes that would normally cut the DNA at guanine rich sites.

Henn and co-workers[69] have investigated reactions of *cis*- and *trans*-[$RuCl_2(DMSO)_4$] with the monodentate nitrogen ligands NH_3, imidazole and benzimidazole. They concluded, particularly from the benzimidazole derivatives, that the complexes should react quite easily with nitrogen bases. The inertness of the disubstituted derivatives leads to the possibility of long-lived DNA adducts in the absence of efficient repair systems. However, they will be in a variety of environments and they may also react with all such nitrogen ligands present, such as amino acids and proteins, and so large amounts may be deactivated without reaching the target.

Alessio et al[70] reacted *trans*-[$RuCl_2(DMSO)_4$] with 5′-dGMP and found the formation of two diastereomeric monoadducts. The N^7 of the guanine moiety and the α-phosphate group (coordinating through an oxygen) form a chelate to the metal centre. This had only previously been seen in Pt(II)[71] and metallocene[72] chemistry. This relatively favourable coordination precluded formation of bis-nucleotide complexes at pH 7, even with a two-fold excess of 5′-dGMP present. This differs from Pt(II) drugs where excess drug is required to prevent the formation of bis-purine nucleotide complexes.

The phosphodiester groups in DNA should bind to Ru(II) much less strongly than the phosphate monoester groups in nucleotides. Cauci[73] et al investigated the reaction of *trans*-[$RuCl_2(DMSO)_4$] with 2′-deoxyguanosine as a more realistic model of interaction with DNA. They found two diastereomeric monoadducts were formed and one bisadduct, showing the possibility for *cis* coordination of two purine bases in an octahedral transition metal complex. All products were found to coordinate via N^7 of the guanine moiety.

As well as kinetic and thermodynamic factors, the chelate effect appears to be very important as the *trans* isomer reacts irreversibly with d(GpG), forming N^7-N^7 adducts, whereas the monoadducts are reversibly bound.[74] Interestingly, studies[75] using 5′-AMP have found binding by *trans*-[$RuCl_2(DMSO)_4$] to occur only through the phosphate group. No binding to the adenine moiety was observed. However recent investigations[76] into the binding to the dinucleotides GpA, ApG, dGpA and dApG found that bifunctional N^7,N^7 macrochelates were formed in each case, and that chiral N^7,N^7 bifunctional adducts were formed on reaction with an eight nucleotide strand of DNA.

The chirality of metal complexes has been used to probe nucleic acid structure and biochemistry,[77] and chiral complexes could bind more selectively to DNA. There has been some success so far,[78] but most studies have been on pseudo square-planar platinum complexes.[78,79] The chirality for octahedral complexes, however, will be

located on the metal centre, and is potentially more important[77] than the square-planar complexes where the chirality is on the non-leaving ligand.

The first fully characterised chloride, dimethylsulfoxide ruthenium(III) complexes were published by Alessio et al in 1991,[80] [(DMSO)H][*trans*-$RuCl_4(DMSO)_2$] and *mer*-[$Ru(DMSO)_3Cl_3$]. The former is isostructural to the Ru(III) complex with known anti-tumour properties, [HIm][*trans*-$Ru(Im)_2Cl_4$], which shows very good activity toward chemically induced colorectal murine tumour (cisplatin resistant).[81] A series of work has been published involving the synthesis and characterisation of new classes of ruthenium(III) chloride-sulfoxide derivatives and their rhodium analogues[82]. These include derivatives containing a nitrogen ligand[83], of the form Na[*trans*-$RuCl_4(R_2SO)(L)$] and *mer,cis*-[$RuCl_3(R_2SO)(R_2SO)(L)$]. Also synthesised and characterised are the first examples of Ru(III) chloride-(DMSO)-carbonyl complexes.[84] In common with carbonylation of *cis*- and *trans*-[$RuCl_2(DMSO)_4$],[85] coordination of carbon monoxide induces the selective isomerisation of the DMSO *trans* to it from *S*- to *O*-bonding. That leaves the DMSO *trans* to CO weakly bonded and easily replaced by a nitrogen donor ligand. Ru(III) sulfoxide complexes containing a planar N-ligand[86] have also been reported: *mer,cis*-[$RuCl_3$(1Me-Im)$_2$(DMSO-*S*)] and [4Et-PyH][*trans*-$RuCl_4$(4Et-Py)(DMSO-*S*).

Mer-[$RuCl_3(DMSO)_2(NH_3)$] has been tested in mice bearing solid metastasising tumours.[87] In mice bearing the Lewis lung carcinoma, results were achieved that were as effective as cisplatin on primary tumour growth and more potent than it on prolongation of host survival time. Combined treatment with cisplatin provides better results than either complex alone. Slightly lower effects were found for mice bearing MCa mammary carcinoma as compared to cisplatin, but had an equivalent effect in terms of host survival time. Comparisons with [HIm][$RuIm_2Cl_4$] were favourable independent of tumour system used.

Na[*trans*-$RuCl_4$(DMSO)Im] (NAMI) and its indazole analogue[88] (Figure 1.8) are two mixed ligand complexes that are exhibit promising cytotoxic effects and have

good water solubility, particularly the indazole complex. Na[*trans*-$RuCl_4$(DMSO)Im] is particularly effective against solid tumour metastases[26] although it requires a relatively high concentration (> 100 μM) for cytotoxic effects and this depends on the presence of serum and plasma proteins.[89] NAMI is virtually devoid of effect on DNA, yet 80-90 % binds to calf thymus DNA in solution within 24 h at 37° C.[90] It is active against a broad range of tumours, including Lewis lung carcinoma, B16 melanoma and MCa mammary carcinoma.[91] When tested in combination with 5-fluorouracil,[92] it combined its effects against both a solid metastasising tumour, MCa Carcinoma, and a lymphoproliferative type tumour without reducing the activity of the other drug. 5-Fluorouracil was chosen due to its common clinical use against colo-rectal cancers, a type against which ruthenium drugs are seen as being most promising.

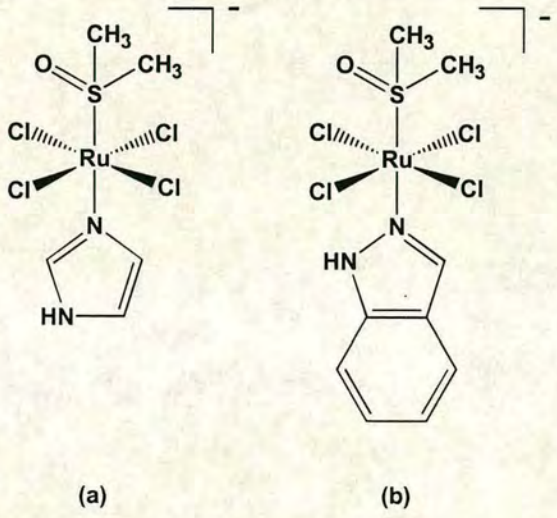

Figure 1.8 Structures of (a) *trans*-[$RuCl_4$(DMSO)Im]$^-$ and (b) *trans*-[$RuCl_4$(DMSO)Ind]$^-$

It is interesting to note that at levels that cause a significant reduction in lung metastases, NAMI greatly alters the ratio between the mRNAs of MMP-2 (a metalloproteinase capable of degrading the extracellular matrix) and TIMP-2 (the specific tissue inhibitor of this enzyme).[93] This corresponds with a pronounced increase of extracellular matrix components in the tumour parenchyma and around tumour blood vessels which probably hinders metastasis formation and blood flow

to the tumour.[94] Overall, NAMI down regulates type-IV collagenolytic activity and the metastatic potential of MCa mammary carcinoma.[95]

NAMI has possibilities for "activation by reduction" to the more active Ru(II) form as it may be readily reduced *in vivo* ($E_{1/2}$= -0.001 V). Its reduction potential is strongly pH dependent and the reduction is favoured at acidic pH values.[83] The complex hydrolyses at a similar rate to cisplatin, with a $t_{1/2}$ value of ca. 3 h at 310 K. Like cisplatin, aquation appears to be a necessary preliminary step for DNA binding.[50] Both analogues hydrolyse in a two step process, involving loss of a chloride followed by successive hydrolytic steps.

The potential of transferrin as a drug delivery system for Na[*trans*-$RuCl_4$(DMSO)Im] and Na[*trans*-$RuCl_4$(DMSO)Ind] has been investigated.[96] The first hydrolysis step of the complexes was not significantly affected by the presence of apotransferrin, although the rate was enhanced. The hydrolysis products do react with apoTf and this interaction occurs concomitantly with the second hydrolysis step, with a 2:1 drug:apoTf stoichiometry. Circular dichroism spectroscopy indicated a tight interaction between the Ru(III) chromophore and the chiral macromolecule, but this is reversible on addition of excess citrate at low pH.

The water solubility of the DMSO/heterocycle complexes along with their cytotoxic activity renders this type of compound attractive for future application, and indeed, after changing the sodium counter-ion of Na[*trans*-$RuCl_4$(DMSO)Im] to $[HIm]^+$, NAMI-A, as it is now known, has become the first Ru^{III} anti-metastatic agent to be introduced into clinical trials.[97] It was found to have improved pharmacological properties over NAMI, and is more stable and reproducible.[98] NAMI-A has been found to be virtually devoid of cytotoxicity against *in vitro* cell lines but causes a marked reduction in lung metastases *in vivo*.[99] It has also been found to be rapidly cleared from the blood by the kidneys[100] and rapidly distributed to the body with only 10 % of the initial dose remaining in the blood after 5 min. NAMI appears to be much less toxic to healthy tissues than cisplatin at equieffective doses, does not modify cell growth and causes a transient cell cycle arrest of tumour cells in the

premitotic G2/M phase, whereas cisplatin causes a dose dependent disruption of cell cycle phases and reduces cell proliferation.[99]

Currently, binuclear ruthenium complexes based on NAMI are being developed.[101] The dimers $Na_2[\{trans\text{-}RuCl_4(DMSO\text{-}S)\}_2(\mu\text{-}L)]$ and $[\{mer,cis\text{-}RuCl_3(DMSO\text{-}S)(DMSO\text{-}O)\}_2(\mu\text{-}L)]$, where L is pyrazine, pyrimidine, 4,4′-bipyridine, 1,2-bis(4-pyridyl)-ethane and 1,3-bis(4-pyridyl)-propane have been synthesised with the aim to investigate their neoplastic ability. They have been found to hydrolyse slowly and maintain their dimeric structure in solution, indicating possible interstrand linking over larger distances than before.

1.4.4 Ruthenium polypyridyl Complexes

Another type of ruthenium complex that has received attention recently is the ruthenium polypyridyl complexes. Although the complexes $[Ru(bpy)_2(ox)]$ and $[RuCl_2(phen)_2]ClO_4$ (ox = oxalate, phen = 1,10 phenanthroline) have previously been shown to be inactive as anti-cancer agents,[41] interest has been retained in these complexes, particularly in their inert covalent binding to DNA.

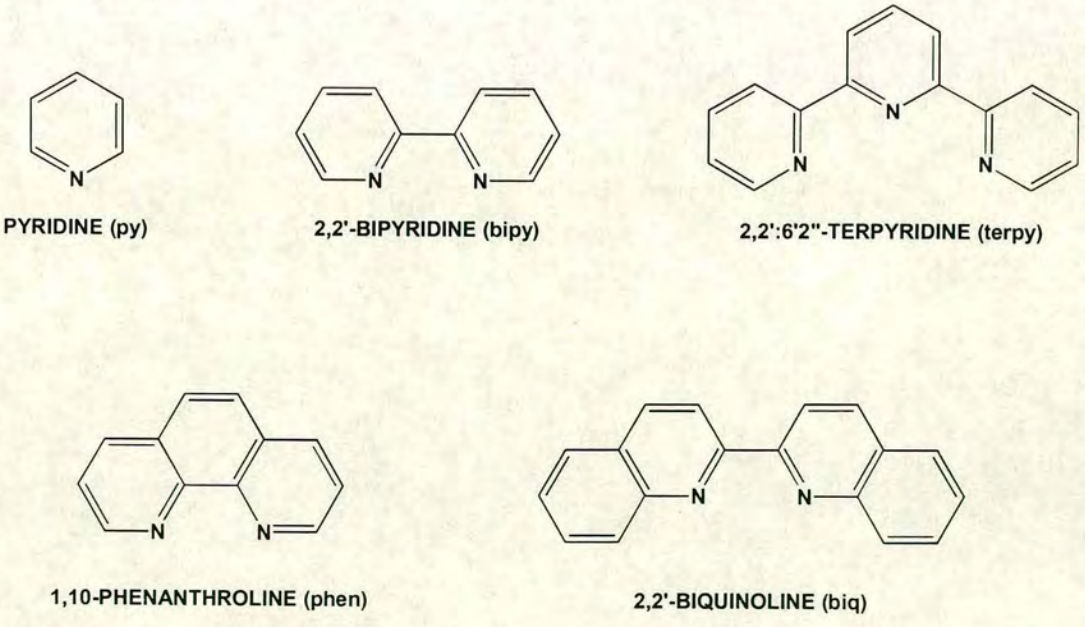

Figure 1.9 Pyridyl ligands cited in the text

Ru(II) polypyridyl complexes have a unique combination of chemical stabilities, redox properties, luminescence emissions and excited state lifetimes[102] that makes them useful. Ruthenium polypyridyl complexes have been used to probe the tertiary structure of nucleic acids,[77(b),(c),103,104,105] binding and hybridisation,[106,107] achieving and probing photosensitised DNA cleavage,[108] and for probing DNA mediated electron transfer.[109]

Ru-polypyridyl complexes show surface binding within a DNA groove,[110,111] and in favourable cases a partial intercalation[112,113] of an extended, fused[114] aromatic ligand between the stacks of nucleotide bases. Full insertion of the intercalating ligand is prevented by the two ligands ancillary to the phosphodiester backbone. Both covalent and intercalating modes probably result from the different types of processes responsible for a decrease in the free energy of the system, such as electrostatic interactions, hydrophobic interactions and hydrogen bonding. Ideally, an intercalating ligand should be attached to a positively charged moiety to "lock" it into place via interactions with the negative phosphate backbone of DNA. Hence, appropriate Ru(II) and Ru(III) complexes are ideal candidates as intercalators.

In 1985 Barton and Lolis[77(a)] reported the enantiomeric selectivity for the Λ isomer of *cis*-$[RuCl_2(phen)_2]$ in covalent binding to B-DNA. The chiral selectivity for intercalative binding shows a preference for the Δ isomer. This gave the compounds special curiosity value. It is possible that new metal based drugs may be designed through understanding the selectivity of DNA-metal binding.

This enantioselectivity for the Λ isomer in covalent binding is backed up by Grover et al[115] who extended the study to a group of seven mono- and diaquapolypyridyl complexes of Ru(II), *cis*-$[Ru(bpy)_2(H_2O)_2]^{2+}$, *cis*-$[Ru(L\text{-}L)_2(py)(H_2O)]^{2+}$, $[Ru(terpy)(L\text{-}L)(H_2O)]^{2+}$, L-L= bpy, phen, (py=pyridine, bpy=2,2′ bipyridine, terpy=2,2′:6′,2″ - terpyridine). They found covalent binding to B-DNA, and, by circular dichroism spectroscopy determined the preferential binding of the Λ form of the complexes. However they found a very low ratio of [bound-metal]:[DNA-

nucleotidephosphate], r_b, ca 0.01-0.02, as compared with that of cisplatin, 0.20.[116] This low r_b is probably due to the higher steric constraints imposed by the octahedral geometry of the ruthenium complexes and the ligands. This is backed up by the finding that the smallest sized complex they tested had the largest r_b.

In further work[117] they found that the monofunctional complexes $[Ru(terpy)(L\text{-}L)(H_2O)]^{2+}$ (L-L=bpy, phen) cannot be oxidised to oxo-Ru(IV) after covalent binding to B-DNA. This suggests that similar to cisplatin, the initial step for covalent binding is the displacement of the aqua ligand. Monofunctional adducts of $[Ru(terpy)(L\text{-}L)(H_2O)]^{2+}$ and *cis*-$[Ru(L\text{-}L)_2(py)(H_2O)]^{2+}$ with calf thymus DNA were indicated by thermal denaturation studies.[118]

On the assumption that purine bases, adenine and guanine, of B-DNA are possible targets for ruthenium compounds, and in particular the N^7 sites which have a nucleophilic character and are available for metal-complex binding when located in the major groove, Van Vliet and co-workers took a variety of pyridyl complexes of ruthenium and tested them for binding to purine DNA-base derivatives. It was found that the reaction of *cis*-$[Ru(bpy)_2Cl_2]$ with 9-methylhypoxanthine (9-mhyp) and 9-ethylguanine (9-egua),[119] both of which are alkylated 6-keto-purines, formed only N^7 monoadducts, and the crystal structure of *cis*-$[RuCl(bpy)_2(9egua\text{-}\kappa^{N7})]Cl.1{\cdot}5H_2O$ was solved. This X-ray structure showed the likelihood of weak interactions between the lone pairs of electrons on guanine carbonyl group with the pyridyl π-systems through space. Although it has been shown before in organic compounds, this is the first example of such an interaction in a coordination compound. This could be important for DNA-(metal-complex) interactions.

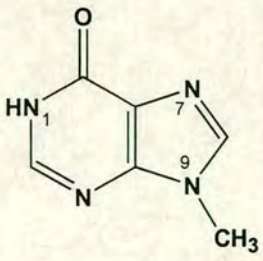

9-METHYLHYPOXANTHINE (9mhyp)

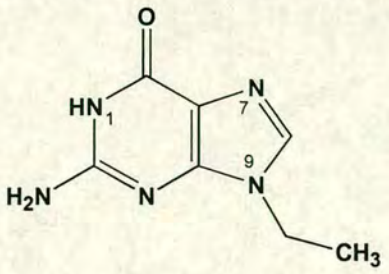

9-ETHYLGUANINE (9egua)

Figure 1.10 Structures of 9-methylhypoxanthine (9mhyp) and 9-ethylguanine (9egua)

Other work includes the reaction of *cis*-[$RuCl_2$(bpy)(biq)], (biq = bisquinoline), binding to imidazole derivatives. Imidazoles are present as fragments in biomolecules like histidine, guanine and adenine. It was found that substitution of one chloro ligand in *cis*-[$RuCl_2$(bpy)(biq)] by an imidazole derivative occurred, and that this takes place at the coordination site opposite to biq, with considerably slower substitution of the second chloro ligand. This implies that biq has a stronger electronic *trans* influence than bpy, and that the steric constraints imposed by biq do not inhibit the approach of an entering ligand. Potential coordinative properties towards certain biomolecules is indicated.

The N^7 site of guanine appears to be the preferred site of attack for Ru(II) in its interactions with DNA. This has been confirmed for *trans*-[$Ru(SO_3)(NH_3)_4(H_2O)$] with a gua-N^7/ade-N^7 binding ratio of 95.[120] This is even more extreme for the pyridyl complex *cis*-[$RuCl_2(bpy)_2$], which reacted only with guanosine at pH 7 and elevated temperature, and not with adenosine, cytosine or thymine.

While the coordination to gua-N^1 at neutral pH has been observed for metals with fast ligand-exchange kinetics,[121] for metals with slow ligand exchange kinetics, like Pt(II), mononuclear N^1 coordination in guanine is observed only at high pH,[122] or when the basicity of N^1 is lowered after prior binding to N^7.[122,123] However, N^1 coordination for ruthenium has only been observed for *cis*-[$RuCl_2(biq)_2$], which was

found to bind at neutral pH to guanosine and 9-substituted guanine bases in a 1:1 ratio.[124]

Mer-[Ru(terpy)Cl_3] exhibits antitumour activity in the L1210 cell line[125] midway between that of cisplatin and carboplatin and is active against human cervix carcinoma HeLa and murine L1210 tumour cell lines. It also exhibits *in vivo* activity against the murine lymphosarcoma LS/BL.[126] It was found in model reactions that with 9-methylhypoxanthine and 9-ethylguanine, two bases coordinate in the *trans* configuration. No other configuration was observed. This indicates the possibility for interstrand crosslinks in DNA, and indeed, it was found to form ~2 % interstrand adducts when reacted with calf-thymus DNA at pH 7, 37° C in the dark.

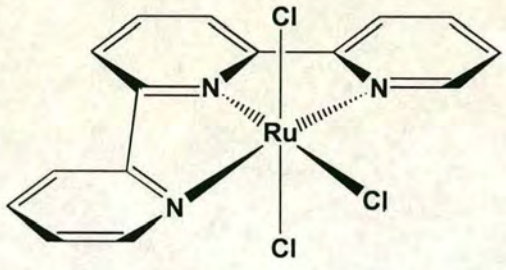

Figure 1.11 Structure of *mer*-[Ru(terpy)Cl_3]

Gupta and co-workers synthesised DNA cleavage agents based on oxo-ruthenium (IV) complexes[115,117] by electrochemical oxidation of aqua-ruthenium(II) forms of $[Ru(terpy)(L)OH_2]^{2+}$, where L= η^2-tpt, phen, dppz, tmentpt = 2,4,6-tripyridyltriazine, dppz = dipyridophenazene, tmen = N,N,N′,N′-tetramethylethylenediamine. All oxidised via $Ru(II)(OH_2)^{2+} \rightarrow Ru(III)OH^{2+} \rightarrow Ru(IV)O^{2+}$ and cleaved DNA. It is possible to study the mechanistic aspects of the cleavage reaction from the point of view of the metal complex with these agents. DNA cleavage was demonstrated by electrocatalytic cleavage upon electrolysis in the presence of the $Ru(II)OH_2$ forms. The electrochemical activation procedure may offer a means of binding functionalities (i.e. oligonucleotides) that would ordinarily undergo self-oxidation.

Although polypyridyl complexes are unlikely to yield a successful anti-cancer agent, they are useful as models of binding to DNA and for probing oligonucleotide structures, and therefore should not be eliminated in the continuing search for effective agents.

1.4.5 Outlook

The success of cisplatin and the continuing need for new and improved agents in the fight against cancer is an inspiration to scientists all over the world. The more we are learning about cancer, its root causes and developmental biochemistry, the more avenues for drug design and creation are being opened. Ruthenium is an excellent candidate for a future clinical treatment, as can be seen from the results achieved so far in a relatively short time, and there is every reason to be optimistic for a bright future for ruthenium agents.

1.4.6 Aims of this thesis

The aim of this thesis is to synthesise Ru(II) complexes with a view to developing effective anticancer agents. There is no general consensus on which the anticancer active oxidation state of ruthenium is, there are many examples of Ru(II), Ru(III) and Ru(IV) complexes in the literature. Bearing in mind the hypothesis that Ru(III) drugs are thought to be reduced to an active Ru(II) form *in vivo*, this work deals specifically with Ru(II) complexes.

In Chapter 3 a series of aminophosphine ruthenium complexes are synthesised and examined for their potential activity. Chapter 4 describes the synthesis of a range of water soluble Ru(II)arene complexes and Chapter 5 deals with one arene complex specifically and investigates its reactivity with mononucleotides and a 14mer oligonucleotide with the aim of elucidating how the complex would interact with DNA. Chapter 6 deals with some preliminary cytotoxicity tests of Ru(II)arene complexes against a human ovarian cancer cell line.

1.5 References

[1] See for example a) Volumes in the series *Metal Ions in Biological Systems*

b) Z. Guo, P.J. Sadler *Angew. Chem. Intl. Ed.* **1999**, 38, 11 and references therein

[2] *The Chemistry of Ruthenium* Seddon & Seddon, Elsevier, **1984**

[3] F.A. Cotton, G. Wilkinson *Adv. Inorganic Chemistry* 4th edition, p.901

[4] G. Sava, A. Bergamo *Anticancer Res.* **1999**, 19, 1117

[5] G. Sava, S. Pacor, A. Bergamo, M. Cocchietto, G. Mestroni, E. Alessio *Chem. Biol. Interact.* **1995**, 95, 109

[6] *Principles of Medicinal Chemistry* W. O. Foye, Lea & Febiger, Philadelphia, **1981**

[7] A.J. Levine, *Chemistry* **1977**, 50, 4, 7

[8] R.D. Smith *The Sciences*, ***1976***, 16, 1, 21

[9] F.P. Dwyer, E. Mayhew, E.M.F. Roe, A. Shulman *Brit J. Cancer* **1965**, 19, 195

[10] M.J. Clarke, M. Stubbs "Interactions of Metallopharmaceuticals with DNA" in *Metal Ions in Biological Systems*, H. Siegel and A. Siegel Eds.; Marcel Dekker, New York **1996**, pp727-780

[11] W.R. Harris *Struct. Bonding* **1998**, 92, 121; F. Kratz, M.T. Schutte *Cancer J.* **1998**, 11, 60; P.J. Sadler *Chem. Rev.* **1999**, 99, 2817

[12] B.K. Keppler in *Metal Complexes in Cancer Chemotherapy*; Ed. B.K. Keppler; VCH Weinheim, germany, **1993**

[13] F. Kratz, B.K. Keppler, L. Messori, C. Smith, E.N. Baker *Metal-based Drugs* **1994**, 1, 169; F. Kratz, M. Hartmann, B. Keppler, L. Messori *J. Biol. Chem.* **1994**, 269, 2581; C.A. Smith, A.J. Sunderland-Smith, B.K. Keppler, F. Kratz, E.N. Baker *J. Biol. Inorg. Chem.* **1996**, 1, 424

[14] D.M. Martin, N.D. Chasteen, J.K. Grady *Biochim. Biophys. Acta* **1991**, 1076, 252

[15] J.E. Biskupiak, K.A. Krohn *J. Nucl. Med.* **1993**, 411

[16] *Principles of Bioinorganic Chemistry* S.J. Lippard , J.M. Berg, **1994**

[17] a) F. Kratz, M. Hartmann, B.K. Keppler, L. Messori *J. Biol. Chem.* **1994**, 269, 2581

b) F. Kratz in *Metal Complexes in Cancer Chemotherapy*, Ed. B.K. Keppler, VCH, Weinheim, Germany, **1993**, p. 391

c) D.M. Martin, N.D. Chasteen, J.K. Grady *Biochem. et Biophys. Acta* **1991**, 1076, 252

d) F. Kratz, L. Messori *J. Inorg. Biochem.* **1993**, 49, 79

e) C.A. Smith, A. J. Sutherland-Smith, B. K. Keppler, F. Kratz, E. N. Baker *J. Biol. Chem.* **1996**, 1, 424

[18] L.C.R. Mangin *Acad. Sci. (Paris)* **1983**, 116, 653

[19] L.H. Anglileri *Strahlentherapie* **1975**, 149, 173

[20] M.A. Corrondo, W.P. Griffith, J.P. Hall, A.C. Skapski *Biochem. et Biophys. Acta* **1980**, 627, 332

[21] P.M. Smith, T. Fealey, J.E. Earley, J.V. Silverton *Inorg. Chem.* **1971**, 10, 1943

[22] L.J. Angileri, C. Marshal, M. Matrat, M.C. Crone-Essanya *Neoplasma* **1986**, 33, 607

[23] *Oxidation-Reduction Potentials* G. Charlot, D. Bézier, J. Courlot , Pergamon Press

[24] M.J. Clarke, S. Butler, D. Rennert, M. Buchbinder, A.D. Kelman *J. Inorg. Biochem.* **1980**, 12, 79

[25] G. Sava, S. Zorzet, T. Giraldi, G. Mestroni, G. Zassinovich *Eur. J. Cancer Clin. Oncol.* **1984**, 20, 841

[26] a) G. Sava, S. Pacor, G. Mestroni, E. Alessio *Clin. Exp. Metast.* 10, 273

b)R. Gagliardi, G. Sava, S. Pacor *Clin. Exp. Metast.* 12, 93

[27] A Bergamo, R. Gagliardi, V. Scarcia, A. Furlani, E. Alessio, G. Mestroni, G. Sava *J. Pharm. Exp. Ther.* **1999**, 289, 559

[28] G. Sava *Unpublished Results*

[29] (a) T. Giraldi, G. Sava, G. Bertoli, G. Mestroni, G. Zassinovich *Cancer Res.*, **1977**, 37, 2662

(b) G. Sava, S. Zorzet, T. Giraldi, G. Mestroni, G. Zassinovich *Eur. J. Clin. Oncol.* **1984**, 20, 841

(c) R. Gagliardi, G. Sava, S. Pacor, G. Mestroni, E. Alessio *Clin. Exp. Metastasis* **1994**, 12, 93

[30] M.J. Clarke *Advances in Chemistry Series* **1997**, 253, 349

[31] F. Bottomley *Coord. Chem. Review* **1978**, 26, 7

[32] S.P. Fricker *Platinum Metals Review* **1995**, 39, 150

[33] F. Gonzalez-Vilchez, R. Vilaplana, G. Blasco, L. Messori *J. Inorg. Biochem.* **1998**, 71, 45

[34] M.J. Clarke, F. Zhu, D.R. Franca *Chem. Rev.* **1999**, 99, 2511

[35] R.E. Shepherd, in *Electron Transfer Reactions*, S. Isied, Ed.; American Chemical Society Symposium Series 253; American Chemical Society: Washington DC, **1997**; 367

[36] G.M. Reid, H. Tervit *Medical Hypotheses* **1999**, 52, 569

[37] C. Montecot, J. Seylaz, E. Pinard *Neuroreport* **1998**, 9, 2341

[38] A.A. Steiner, E. Colombari, L.G.S. Branco *Am. J. Physiol. - Reg. Integ. Comp. Physiol.* **1999**, 46, R499

[39] R.A. Johnson, F. Kozma, E. Colombari *Braz. J. Med. Biol. Res.* **1999**, 32, 1

[40] N. Farrell in *Transition Metal Complexes as Drugs and Chemotherapeutic Agents* Kluwer Acad. Pub., Dordrecht, The Netherlands **1989**, Ch. 6

[41] M.J. Clarke in *Metal Ions in Biological Systems* Vol. 11, ed. H. Siegel, Marcel Dekker Inc., New York, USA **1980**, p.231

[42] J.R. Dunig, J. Danneman, W.D. Behnke, E.E. Mercer *Chem. Biol. Interact.* **1976**, 13, 287

[43] M.J. Clarke, B. Jansen, K.A. Marx, R. Kruger *Inorg. Chim. Acta* **1986**, 124, 13

[44] B.J. Graves, D.J. Hodgson *J. Am. Chem. Soc.* **1979**, 101, 5608

[45] M.J. Clarke *Prog. Clin. Biochem. Med.* **1989**, 10, 25

[46] J.F. Laliberte, I.L. Sun, F.L. Crane, M.J. Clarke *J. Bioenerg. Biomemb.* **1987**, 19, 69

[47] D.M. Stanbury, O. Haas, H. Taube *Inorg. Chem.* **1980**, 19, 518

[48] M.J. Clarke, P.E. Morrissey *Inorg. Chim. Acta* 1984, 80, L69

[49] B.K. Keppler *New J. Chem.* **1990**, 14, 389 and ref. therein

[50] M. Hartmann, T.J. Einhauser, B.K. Keppler *J. Chem. Soc. Chem. Comm.* **1996**, 174

[51] F. Kralik, J. Vrestal *Collect. Czech. Chem. Comm.* **1960**, 1298

[52] B.K. Keppler, W. Rupp, U.M. Juhl, H. Endres, R. Niebl, W. Balzer *Inorg. Chem.* **1987**, 26, 4366

[53] E. Holler, W. Schollen, B.K. Keppler *Drug Res.* **1991**, 41, 1065

[54] O.M. Ní Dhubhghaill, W.R. Hagen, B.K. Keppler, K.G. Lipponer, P.J. Sadler *J. Chem. Soc., Dalton Trans.* **1994**, 3305

[55] F.A. Cotton and G. Wilkinson *Advanced Inorganic Chemistry*, Wiley, New York, 4th edn., 1980, p.1200

[56] C. Anderson, A.L. Beauchamp *Inorg. Chem.* **1995**, 34, 6065

[57] L. Grenier, J.P. Charland, A.L. Beauchamp *Can. J. Chem.* **1988**, 66, 1663

[58] L. Tryndalemiesz, B.K. Keppler, H. Kozlowski *J. Inorg. Biochem.*, **1999**, 73, 123

[59] F. Kratz, B.K. Keppler, M. Hartmann, L. Messori, M.R. Berger *Metal Based Drugs* **1996**, 3, 15

[60] M.J. Clarke, U.M. Bailey, P.E. Doan, C.D. Hiller, K.J. Lachance-Galang, H. Daghlian, S. Mandal, C.M. Bastos, D. Lang *Inorg. Chem.* **1996**, 35, 4896

[61] T. Giraldi, G. Sava, G. Bertoli, G. Mestroni, G. Zassinovich *Cancer Res.* **1977**, 37, 2662

[62] I.P. Evans, A. Spencer, G. Wilkinson *J. Chem. Soc. Dalton Trans.* **1973**, 204

[63] C. Monti-Bragadin, M. Giacca, L. Dolzani, M. Tamoro *Inorg. Chim. Acta* **1987**, 137, 34

[64] S. Caucio, E. Alessio, G. Mestroni, F. Quadrifoglio *Inorg. Chim. Acta* **1987**, 137, 19

[65] G. Sava, S. Pacor, S. Zorzet, E. Alessio, G. Mestroni *Pharmacol. Res.* **1989**, 21, 617

[66] A. Nassi, E. Alessio, G. Mestroni, F. Loseto, D. Giodano, M. Collucia *Anticancer Res.* **1990**, 10, 1411

[67] E. Alessio, G. Mestroni, G. Nardin, W.M. Attia, M. Calligaris, G. Sava, S. Zorzet *Inorg. Chem.* **1988**, 27, 4099

[68] G. Sava, S. Pacor, F. Bregant, V. Ceschia *Anticancer Res.* **1991**, 11, 1103

[69] M. Henn, E. Alessio, G. Mestroni, M. Calligaris, W.M. Attia *Inorg. Chim. Acta* **1991**, 187, 39

[70] E. Alessio, Y. Xu, S. Cauci, G. Mestroni, F. Quadrifoglio, P. Viglino, L.G. Marzilli *J. Am. Chem. Soc* **1989**, 111, 7068

[71] M.D. Reily, L.G. Marzilli *J. Am. Chem. Soc.* **1986**, 108, 8299

[72] L.Y. Kuo, M.G. Kanatzidis, T.J. Marks *J. Am. Chem. Soc.* **1987**, 109, 7207

[73] S. Cauci, P. Viglino, G. Esposito, F. Quadrifoglio *J. Inorg. Biochem.* **1991**, 43, 739

[74] G. Esposito, S. Cauci, F. Fogolari, E. Alessio, M. Scocchi, F. Quadrifoglio, P. Viglino *Biochemistry* **1992**, 31, 7094

[75] Y.N. Tian, P. Yang, Q.S. Li, M.L. Guo, M.G. Zhao *Polyhedron* **1997**, 16, 1993

[76] A. Anagnostopoulou, E. Moldrheim, N. Katsaros, E. Sletten *J. Biol. Inorg. Chem.* **1999**, 4, 199

[77] J.K. Barton, E.J. Lolis, *J. Am. Chem. Soc.* **1985**, 107, 708; J.K. Barton, A.T. Danishefsky, J.M. Goldberg *J. Am. Chem. Soc.* **1984**, 106, 2172; J.K. Barton, L.A. Basile, A.T. Danishefsky, A. Alexandrescu *Proc. Natl. Acad. Sci. USA* **1984**, 81, 1961; J.K. Barton, A.L. Raphael *J. Am. Chem. Soc.* **1984**, 106, 2466

[78] Y. Kidani in *Platinum and Other Metal Coordination Compounds in Cancer Chemotherapy*; M. Nicolini Ed.; Martinus Njhoff: Boston, MA, **1988**, p.555

[79] A.M.J. Fitchtinger, J.L. Van der Veer, J.H.J. den Hartog, P.H.M. Lohman, J. Reedijk *Biochemistry* **1985**, 24, 707

[80] E. Alessio, G. Balducci, M. Calligaris, G. Costa, W.M. Attia, G. Mestroni *Inorg. Chem.* **1991**, 30, 609

[81] B.K. Keppler, W. Rupp *J. Cancer Res. Clin. Oncol* **1986**, 111, 166

[82] G. Mestroni, E. Alessio, A.S. Santi, S. Geremia, A. Bergamo, G. Sava, A. Boccarelli, A. Schettino, M. Colluccia *Inorg. Chim. Acta* **1998**, 273, 62

[83] E. Alessio, G. Balducci, M. Calliagri, C. Costa, W.M. Attia, G. Mestroni *Inorg. Chim. Acta* **1993**, 203, 205

[84] E. Alessio, B. Milani, M. Bolle, G. Mestroni, P. Faleschini, S. Geremia, M. Calligaris *Inorg. Chem.* **1995**, 34, 4716

[85] E. Alessio, B. Milani, M. Bolle, G. Mestroni, P. Faleschini, F. Todone, S. Geremia, M. Calligaris *Inorg. Chem.* **1995**, 34, 4722

[86] S. Geremia, E. Alessio, F. Todone *Inorg. Chim. Acta* **1996**, 253, 87

[87] S. Pacor, G. Sava, V. Geschia, F. Bregant, G. Mestroni, E. Alessio *Chemico-Biol. Interact.* **1991**, 78, 223

[88] G. Mestroni, E. Alessio, G. Sava, S. Pacor, M. Coluccia, A. Boccarelli *Metal Based Drugs* **1994**, 1, 41

[89] G. Sava, S. Pacor, A. Bergamo, M. Cocchietto, G. Mestroni, E. Alessio *Chem. Biol. Interact.* **1995**, 95, 109

[90] G. Sava, E. Alessio, E. Bergamo, G. Mestroni *Top. Biol. Inorg. Chem.* **1999**, 1, 143

[91] G. Sava, S. Pacor, G. Mestroni, E. Alessio *Anticancer Drugs* **1992**, 3, 25

[92] M. Coluccia, G. Sava, G. Salerno, A. Bergamo, S. Pacor, G. Mestroni, E. Alessio *Metal Based Drugs* **1995**, 2, 195

[93] E. Murgonova, A. Tuuttila, U. Bergmann, M. Isupov, Y. Lindquist, G. Schneider, K. Tryggvason *Science* 1999, 284, 1667; P.D. Brown, M. Whittaker *Chem. Rev.* **1999**, 99, 2735

[94] G. Mestroni, E. Alessio, G. Sava P.C.T. Int. Appl. Patent WO 9800431 A1 980108 WO 97-EP3401 970630, IT 96-MI1359 960702, 1996

[95] G. Sava, G. Salerno, A. Bergamo, M. Cocchietto, R. Gagliardi, E. Alessio, G. Mestroni *Metal Based Drugs* **1996**, 3, 67

[96] L. Messori, F. Kratz, E. Alessio *Metal based Drugs* **1996**, 3, 1

[97] E. Alessio, G. Balducci, A. Lutman, G. Mestroni, M. Calligaris, W.M. Attia *Inorg. Chim. Acta* **1993**, 203, 205

[98] G. Sava, R. Gagliardi, M. Cocchietto, K. Clerici, I. Capozzi, M. Marella, E. Alessio, G. Mestroni, R. Milanino *Pathol. Oncol. Res.* **1998**, 4, 30

[99] A. Bergamo, R. Gagliardi, V. Scarcia, A. Furlani, E. Alessio, G. Mestroni, G. Sava *Jnl. Pharm. Exp. Ther.* **1999**, 289, 559

[100] G. Sava, K. Clerici, I. Capozzi, M. Cocchietto, R. Gagliardi, E. Alessio, G. Mestroni, A. Porbellini *Anticancer Drugs* **1999**, 10, 129

[101] E. Iengo, G. Mestroni, S. geremia, M. Calligaris, E. Alessio *J. Chem. Soc. Dalton Trans.* **1999**, 3361

[102] A. Juris, V. Balzani, F. Barigletti, S. Campagne, P. Belser, A. von Zelewsky *Coord. Chem. Rev.* **1988**, 84, 85

[103] C.S. Chow, J.K. Dartan *Method. Enzymology* **1992**, 212, 219

[104] A.E. Friedman, C.V. Kumer, N.J. Turro, J.K. Barton *Nucleic Acids Res.* **1991**, 19, 2595

[105] B. Norden, F. Tjerneld *FEBS Letters* **1976**, 67, 368

[106] A.E. Friedman, J.C. Chambron, J.P. Sauvage, N.J. Turro, J.K. Barton *J. Am. Chem. Soc.* **1990**, *112*, 4960

[107] Y. Jenkins, J.K. Barton *J. Am. Chem. Soc.* **1992**, 114, 8736

[108] C. Sentagne, J.C. Chambron, J.P. Sauvage, N. Paillow *J. Photochem. Photobiol. B: Biol.* **1994**, 26, 165

[109] T.J. Meade, J.F. Kayem *Angew. Chem. Int. Ed. Engl.* **1995**, 34, 352

[110] J.P. Rehmann, J.K. Barton *Biochemistry* **1990**, 29, 1701

[111] M. Eriksson, M. Leijion, C. Hiort, B. Norden, A. Groslund *J. Am Chem. Soc.* **1991**, 19, 2595

[112] R.H. Hartson, J.K. Barton *J. Am Chem. Soc.* **1992**, 114, 5919

[113] A. Friedman, C.V. Kumar, N.J. Turro, J.K. Turro *Nucl. Acids Res.* **1991**, 19, 2595

[114] R.J. Morgan, S. Chaterjee, A.D. Baker, T.C. Strekas *J. Am. Chem. Soc.* **1991**, 30, 2687

[115] N. Grover, N. Gupta, H.H. Thorp *J. Am. Chem. Soc.* **1992**, 114, 3390

[116] J.P. Macquet, J.L. Butour, J.P. Johnson *ACS Symp. Ser.* **1983**, 209, 75

[117] N. Grover, N. Gupta, P. Singh, H.H. Thorp *Inorg. Chem.* **1992**, 31, 2014

[118] N. Grover, T.W. Welch, T.A. Fairley, M. Cory, H.H. Thorp *Inorg. Chem.* **1992**, 33, 3544

[119] P.M. van Vliet, J.G. Haasnoot, J. Reedijk *Inorg. Chem.* **1994**, 33, 1834

[120] G.M. Brown, J.E. Sutton, H. Taube *J. Am. Chem. Soc.* **1978**, 100, 2767

[121] S.H. Kim, R.B. Martin *Inorg. Chim. Acta* **1984**, 91, 19

[122] J.H.J. den Hartog, M.L. Salm, J. Reedijk *Inorg. Chem.* **1984**, 23, 2001

[123] G. Raudachsl-Sieber, H. Schollhorn, U. Thewalt, B. Lippert *J. Am. Chem. Soc.* **1985**, 107, 3591

[124] P.M. van Vliet PhD Thesis, Leiden University, The Netherlands, 1996

[125] P.M. van Vliet, M.S. Sarinten, S.M.S. Toekimin, J.G. Haasnoot, J. Reedijk, O. Nováková, O. Vrána, V. Brabec *Inorg. Chim. Acta* **1995**, 231, 57

[126] O. Nováková, J. Kasparkova, O. Vrána, P.M. van Vliet, J. Reedijk, V. Brabec *Biochemistry* **1995**, 34, 12369

Chapter 2

Materials and methods

2.1 Method theory

2.1.1 Nuclear Magnetic Resonance Spectroscopy

Most elements have at least one naturally occurring magnetic isotope. Nuclear magnetic moments are very sensitive to their environments, and yet interact only weakly with them, and this makes them ideal candidates for analysis. Historically, the first NMR signals were independently observed by two separate physicists back in 1945 for which Bloch and Purcell were jointly awarded the Nobel prize for Physics in 1952.[1,2] The phenomenon of chemical shift was discovered in 1950 and the first commercial NMR spectrometer (a continuous wave, CW, spectrometer) was produced in 1953. In 1970 Fourier Transform (FT) was introduced. Nowadays NMR signals of almost any magnetic nucleus can be routinely detected. A number of textbooks have been published recently explaining the theory of NMR and its application for chemists.[3,4,5,6,7] and can be referred to for a more in-depth look at NMR. A simplified schematic of an NMR machine is shown in Figure 2.1.

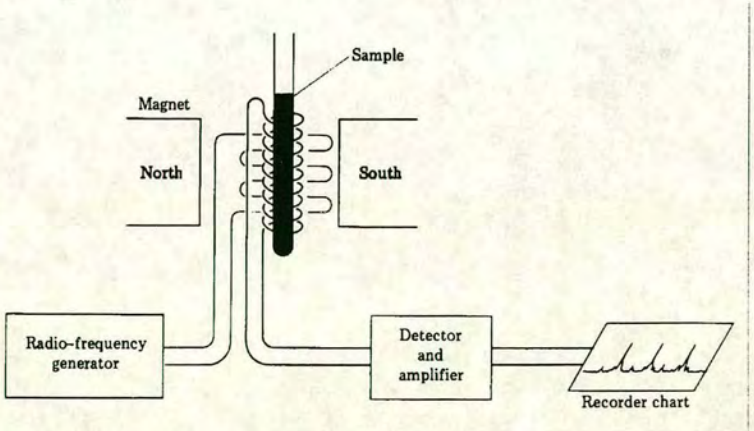

Figure 2.1 Schematic of NMR machine

Nuclear Magnetism

Nuclei possess a spin quantum number I, where $I = 0, ½, 1,$ *etc.*, with $I > 4$ being very rare. Protons, neutrons and electrons all have $I = ½$, and the protons and neutrons determine the I value for a nucleus. A rule of thumb for calculating the I value for individual nuclei is given in Table 2.1 below:

PROTONS	NEUTRONS	*I*
even	even	0
odd	odd	1, 2, 3...
even	odd	1/2, 3/2, 5/2...
odd	even	1/2, 3/2, 5/2...

Table 2.1 Rule of Thumb for Calculating *I* Value

It needs to be noted that this rule is not infallible, due to interactions of the protons and neutrons.

The properties of the nuclei studied in this thesis are given in Table 2.2.

Nucleus	Spin	% Natural Abundance	Magnetogyric Ratio $\gamma / 10^7$ rad T^{-1} s^{-1}	NMR Frequency at 2.35 T (MHz)
^{1}H	½	99.98	26.75	100.00
^{31}P	½	100	10.80	40.48
^{15}N	½	0.37	-2.71	10.13

Table 2.2 NMR Properties of nuclei studied in this thesis

Chemical Shift

The frequency a nucleus resonates at is primarily dependent on the nucleus' magnetogyric ratio, γ, and the applied magnetic field, B_0, it is also dependent on the local electron distribution. It is this what distinguishes between different locations of the same nuclei and is what makes NMR so attractive to chemists. The field experienced by individual nuclei, B, is less than the applied field, B_0. This is because the external field causes electrons to circulate in their orbitals, generating a local field B′ in the opposite direction to B_0. This shields the nucleus from B_0.

$$B = B_0 - B' = B_0(1-\sigma)$$

where σ is denoted the shielding constant. The resonance frequency condition therefore becomes

$$\nu = \frac{\gamma B_0(1-\sigma)}{2\pi}$$

It is common practise to define the chemical shift in terms of the difference in resonance frequencies between the nucleus of interest, ν, and a reference nucleus, ν_{ref}, by means of a dimensionless parameter δ.

$$\delta = 10^6 \frac{(\nu - \nu_{ref})}{\nu_{ref}}$$

Dividing by ν_{ref} means that δ becomes a molecular property independent of the magnetic field, 10^6 scales the value to a more convenient size, and δ values are quoted in *parts per million*, ppm. The δ scale increases from right to left by convention. The left-hand side is known as lowfield (downfield) end or the high frequency end of the spectrum. The opposite is true for the right-hand side.

Integration

The intensity of the signal is generally proportional to the number of protons resonating at that frequency with the result that the area under the peak is proportional to the number of protons being detected. This area is measured by integration.

Spin-spin coupling

Spin-spin coupling causes NMR resonances to split into a small number of components with characteristic relative intensities and spacings. It arises when neighbouring nuclear spins interact with each other due to the tiny magnetic field of one nucleus affecting the other. If the spin of the neighbouring nucleus is aligned with the field, the total effective field at the neighbouring nucleus is slightly larger than it would be otherwise. Therefore the applied field necessary to cause resonance is less. Conversely, if the spin is aligned against the field, the applied field necessary to resonate is more. The consequence of this coupling is that the nucleus comes into resonance at two slightly different values of the applied field. These splittings are separated by the coupling constant, *J*, which is measured in Hz.

Relaxation

Once a physical system is perturbed from its equilibrium condition, and then the perturbing influence is removed, the system will return to its original equilibrium condition in a finite time. The system is said to relax. Spin-lattice relaxation occurs when nuclei in the higher energy state transfer energy to the surrounding lattice. This results in a net loss of energy from the system. Spin-spin relaxation does not result in a net loss of energy from the system, but in loss of phase coherence.

Two-dimensional NMR

2D NMR allows for the collection and presentation of a lot more information than 1D spectra. A 2D spectrum is essentially a contour map, with the two axes being J-

resolved or shift correlated. J-resolved is the separate presentation of chemical shift and coupling information. The chemical shift is plotted on one axis and the multiplicity on the other. A shift-correlated 2D spectrum allows you to establish which nuclei are coupled. The coupling can be either homonuclear or heteronuclear.

COrrelation SpectroscopY (COSY)

In proton spectroscopy it is often valuable to identify all the couplings and connections present in a molecule. Difference decoupling can be a very useful tool for this, but in complicated systems it is difficult to carry out all the necessary decoupling experiments for all the possible connections. Furthermore, when two or more chemical shifts are similar it is impossible to tell what is coupled to what. COSY can reveal all the coupling relationships present in a molecule, or hide them, in a single experiment. Application of a suitable pulse sequence and processing results in a 2D plot, with the conventional 1D spectrum along the diagonal, and crosspeaks identifying nuclei that are coupled to each other.

Heteronuclear Single Quantum Coherence Spectroscopy (HSQC)

This is a form of 2D NMR where the interactions between two different types of nuclei are studied. Two types are used in this thesis. One is [^{1}H, ^{31}P] HSQC, where the coupling between phosphorus nuclei and protons is observed and presented in the form of a 2D map. The other type is [^{1}H, ^{15}N] HSQC. Direct studies of M-N-H studies in aqueous solution has previously proved difficult.[8] Using ^{15}N-edited, either by high concentration (natural abundance) or ^{15}N isotope enriched samples, N-H proton signals are selected and separated according to their ^{15}N chemical shifts.

Ruthenium NMR

Although not a technique utilised in this thesis, it is interesting to pay passing regard to ruthenium NMR. There are two NMR active isotopes of ruthenium, ^{99}Ru (natural abundance = 12.7 %) and ^{101}Ru (natural abundance = 17.1 %). Both isotopes have an I value of 5/2, but ^{99}Ru has a much slower spin-spin relaxation rate than ^{101}Ru[9] and hence gives narrower spectral lines. This favours its use over ^{101}Ru, despite the

latter's higher receptivity. ^{99}Ru is considered a promising nucleus for chemical studies,[10] with the nucleus being sensitive to the environment around the metal centre.[11] It is particularly useful for solid state NMR, [12] for example, for investigating magnetic properties of ruthenium oxides.[13] Solution ^{99}Ru and ^{101}Ru NMR was first reported in 1981[9,14] and since then it has been used to investigate organometallic Ru(II) complexes, both for structural analysis and for distinction of isomers in enantiomeric mixtures.[15]

2.1.2 Electrospray Ionisation Mass Spectrometry

Atmospheric Pressure Ionisation (API) involves the formation of ions from a liquid flow introduced into a source region maintained at atmospheric pressure. There are three main types of API: electrospray, ion-spray,[16] and a heated nebuliser with a corona discharger.[17] The electrospray technique was pioneered by Dole et al[18] in 1971. It is based on the desorption of ions from small droplets with virtually no heat input (low source temperature) and as a result is suitable for highly polar molecules.

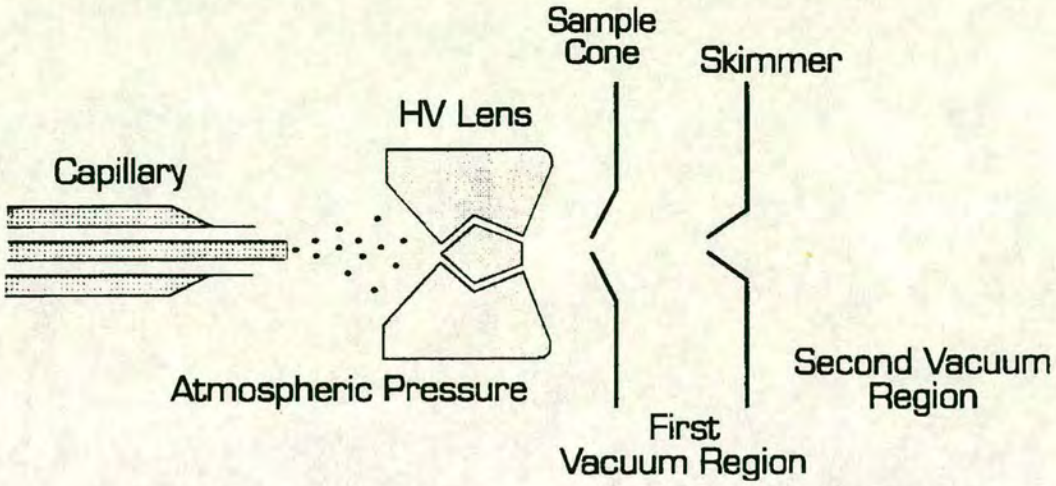

Figure 2.2 Schematic of electrospraying.[19] The capillary sprays onto a counter electrode (HV lens) which is also at atmospheric pressure. Ions are transported into the high vacuum system of the mass spectrometer by use of a nozzle-skimmer arrangement.

An electric field is generated by applying a high (several kV) voltage directly to the spraying capillary, (see Figure 2.2) with a counter electrode located a few mm away. The emerging liquid assumes an equilibrium conical shape (a "Taylor" cone) with a sharp tip from which a stream of droplets is ejected. These droplets are electrostatically charged and a partial separation of positive and negative ions occurs near the capillary tip, allowing detection of either type of ions. Therefore the electrosprayed droplets contain excess ions of one charge. As the solvent evaporates, the electrostatic repulsion produces smaller and smaller droplets until the macromolecule is "expelled" saturated with charges.[20] The formation of multiply charged ions makes the analysis of high molecular weight analytes more accessible to instruments with a limited m/z detection range, e.g. a quadrupole analyser. This means that a large molecule can contain multiple charges. A protein can bear a proton for every 5-17 amino acid residues, thereby yielding peaks at m/z = 600 - 2000, even for 200 kDa proteins. In a similar manner, polynucleotides can yield negative ions of such m/z values by losing a proportionate amount of protons.

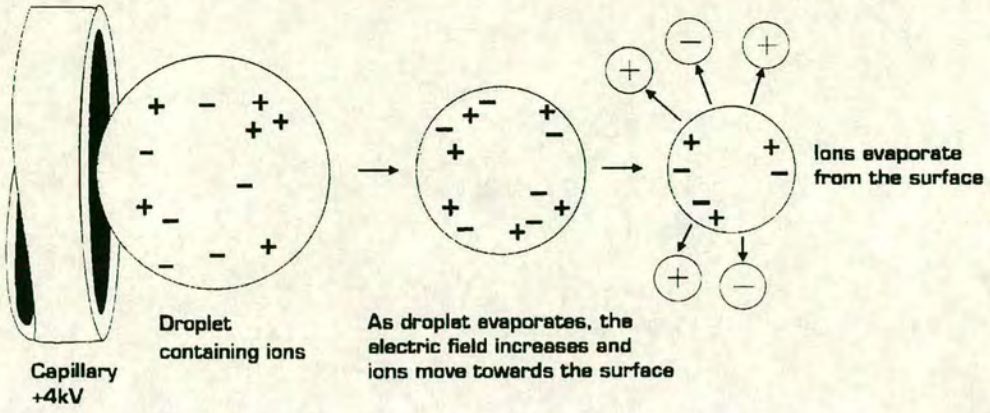

Figure 2.3 Ion evaporation mechanism[19]

Another advantage of ES is that it allows use of solvents such as H_2O or acetonitrile which provide spectra that are relatively free of matrix peaks, and hence improved detection is achieved.

Electrostatic spraying takes place in stages. As the voltage at the capillary increases, the liquid begins to emerge as a succession of large droplets, at which time no ions can be observed. At high voltage, a continuous cone-shaped spray pattern is observed at the needle tip which emits an expanding fog of very small droplets. This stage is influenced by the nature of the solvent, the potential difference and the flow rate. Only a certain volume of liquid can be removed from the tip of the cone by electrical shear force so electrospray flow rates are limited to a few microlitres per minute. At this stage a flow of drying gas, usually warm (60 °C) N_2, is introduced, flowing in the opposite direction between the spraying tip and the sampling orifice. This is to minimise the flow of neutral solvent molecules into the vacuum chamber and aid desolvation of the charged droplets.

Although the electrospray ion formation process is not completely understood,[21] the ions detected in the gas phase are thought to reflect the ions present in solution.[22,23] However it is possible that gas phase reactions can contribute to the ion formation process of electrospray ionization.

A proposed mechanism of gas phase ion formation is field desorption. The radius of the droplet decreases as solvent evaporates resulting in a concurrent build up of the electrical field at the droplet surface. An analyte molecule that has accumulated sufficient charge is then able to evaporate or desorb, from the charged droplet either alone, or associated with one or more solvent molecules.

The field, E, provided by the excess charge, q, on a spherical droplet of radius, r, is given by:

$$E = \frac{eq}{4\pi\varepsilon_o r^2}$$

where ε_o is the permittivity of free space.

If the field needed for ion desorption is E_o, then the limiting charge, q_o, above which ion desorption occurs is given by the following equation:

$$q_o = \frac{4\pi\varepsilon_o E_o r^2}{e}$$

Another mechanism of ion formation is Rayleigh Fission. The Rayleigh limit occurs when charged droplets evaporate until the increased surface charge density confers instability. The maximum charge that can be obtained at the Rayleigh limit, q_r, is given by:

$$q_r = \left(\frac{8\pi}{e}\right)\left(\gamma\varepsilon_o\right)^{1/2} r^{3/2}$$

However, due to local disturbances at the surface of the droplet it may not be possible to distinguish the fission process from field desorption of highly solvated ions.

In summary, electrospray ionisation is a convenient atmospheric pressure, moderate temperature method of analysing macromolecules, such as biomolecules, in solution conditions and within a reasonable detection range.

2.1.3 High Performance Liquid Chromatography (HPLC)

High Performance Liquid Chromatography (HPLC) is the generally accepted name for the liquid analogue to gas chromatography. The stationary phase, a solid surface, a liquid, an ion-exchange resin or a porous polymer, is held in a metal column and the liquid mobile phase is forced through under pressure. Numerous textbooks are available describing the principles of HPLC.[24,25,26]

The emergence of HPLC is considered to have begun with Hubert and Hulsen[27] in 1967, and nowadays modern HPLC analyses are routinely fast and efficient with detection levels as low as 200 pg. As well as at an analytical level, HPLC can also be used on a preparative scale. HPLC also has the advantage of being able to be used "on-line" with various other techniques such as mass-spectrometry. A block diagram of an HPLC system is shown in Figure 2.4 and the parts explained below.

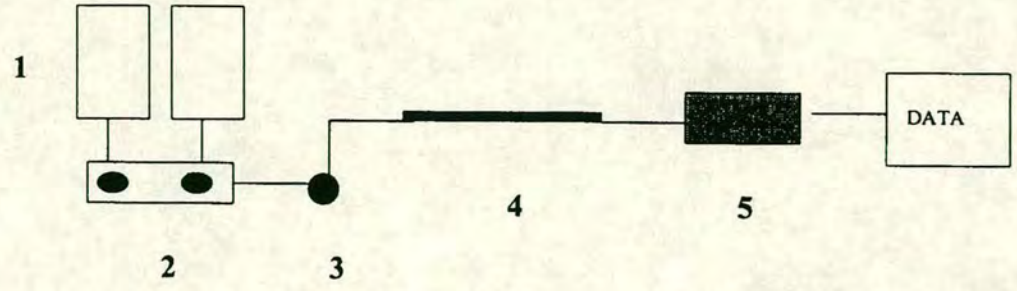

Figure 2.4 Block diagram showing the components of an HPLC system. The labelled parts are explained below.

1. A mobile phase: this is the solvent, or mixture of solvents, used to carry the sample through the system. Mixing chambers are present to allow variations in mixture composition during the course of a run. This results in solvent gradients (constant composition = isocratic) that can be used to draw strongly retained molecules from the column and cut down on time.

2. A pump system: the pump system forces the mobile phase through the system under pressure. Varying the flow rate of the pump varies the pressure.

3. Injection system: The mixture to be analysed is dissolved in a suitable solvent and introduced at this point ("injected") and carried through the column by a continuous flow of the mobile phase. Exact amounts can be controlled by injection size and loop size (20 µl - 2 ml).

4. A column: this is where the separation takes place. The stainless steel column is packed with the "sorptive" particles of large surface area . This is known as the stationary phase. In normal phase chromatography this is traditionally hydrophilic or polar resulting in the retention of ionic or hydrophilic molecules in the column. In reverse-phase chromatography, the stationary phase is hydrophobic or non-polar and typically consists of hydrocarbon chains, e.g. C-8 or C-18, attached to a silicon polymer. The mobile phase carries the sample

through the column under continuous flow and the different components are separated due to their varying interactions/affinities with the stationary phase.

5. A detector: this is usually a UV/Vis detector set to a specific wavelength depending on the substance being analysed. As the sample components emerge from the column the resulting signals are plotted in a chromatogram. The chromatogram is a record of the detector's response as a function of time and indicates the presence of the components as peaks. The eluted components are identified by their retention time (t_r), i.e. time taken for component to elute from the column.

To achieve a separation, it is necessary to manipulate the experimental variables that have the greatest influence on the equilibrium distribution: the composition of the mobile phase, the nature of the stationary phase and, less importantly, the temperature. The forces responsible for solute interactions between the two phases are those that explain solubility: electrostatic, dipole and dispersive (Van der Waals) forces. The mobile and stationary phases are usually chosen to have contrasting polarities.

An explanation of some important terms is given below, and a variety of text-books are available.[24,25,26]

Capacity factor k′

This is a measure of the retention of a compound on a column. It is measured in terms of the number of column void volumes (the total volume of the mobile phase in a packed column) it takes to elute the centre of the peak.

k′ also defines the distribution of a solute between two phases:

$$k' = \frac{\text{amount of solute in the stationary phase}}{\text{amount of solute in the mobile phase}}$$

EX BIBL. UNIV. EDINBURGH

The k′ value is a relative retention measurement which can be calculated from experimental values.

Selectivity

Selectivity is the ability of the column to discriminate between two components.

Column efficiency

This is the measure of the broadening which a solute band experiences during its migration through the column. Generally the efficiency of HPLC columns increases as the particle size of the column decreases.

Resolution

This is the separation between two solute bands. It is defined in terms of the retention times and peak widths:

$$R_s = 2(t_{R2} - t_{R1}/w_1 + w_2)$$

The values of t and w can be measured in volume (ml), distance (cm), or time units (s). It has been shown[28] for column chromatography that the resolution (R_s) can be related to the capacity factor, selectivity, and efficiency.

The main mode of HPLC used in this body of work is reverse-phase HPLC.

2.2 Experimental

2.2.1 High Performance Liquid Chromatography

The following equipment was used: A Hewlett-Packard Series 1100 Chemstation, HP 1100 series quaternary pumps, HP 1100 series vacuum degasser, HP variable wavelength D_2 lamp UV/Vis detector, HP enhanced integrator, Rheodyn sample injector with 25 - 100 µl loops, Hamilton microlitre syringes. All water for HPLC was purified using a Millipore Elix 5 system, followed by an Elgastat UHQ II deioniser, and filtered using PK50, 0.45, 47 mm nylon 66 membranes from Anachem. The data were analysed using HP chemstation for Windows '95. The column and mobile phase used was dependent on the system being studied and is noted in the relevant chapter.

2.2.2 Nuclear Magnetic Resonance Spectroscopy

NMR spectra were recorded on Bruker DMX 500 MHz or Varian Inova 600 MHz spectrometers using 5 mm tubes. The ^{1}H chemical shifts were internally referenced to either TSP (TSP = sodium 3-trimethylsilylpropionic acid) or dioxane (3.767 ppm to TSP). The ^{15}N chemical shifts were externally referenced to 1 M $^{15}NH_4Cl$ in 1.5 M HCl, and the ^{31}P chemical shifts were externally referenced to 30 % H_3PO_4. Typical acquisition conditions for ^{1}H NMR one-dimensional spectra were as follows: 45-60° pulses, 16-32 K data points, 2-3 second relaxation delay, and collection of 32-128 transients. Water resonance was suppressed by presaturation. The two-dimensional gradient selected ^{1}H, ^{1}H-COSY and TOCSY (mixing time of 0.12 s) experiments were carried out using standard sequences. Data sets with 2048 x 512 points were acquired with frequency widths of 8000 Hz in both dimensions and 16 scans per t_1 increment. The t_1 dimension was zero-filled to 2048 data points, and the spectrum was processed with a combination of exponential and Gaussian weighting functions. The two-dimensional [^{1}H-^{31}P] HSQC spectra were recorded using standard sequence and the ^{31}P spins were decoupled by irradiation with the GARP-1 sequence during acquisition.

Some NMR spectra were also recorded at the NMR Service, University of Edinburgh.

2.2.3 Electrospray Mass Spectrometry

Negative and positive ion electrospray mass spectrometry was performed on a Platform II mass spectrometer (Micromass, Manchester, U.K.). The samples were infused at a flow rate of 0.48 ml h^{-1} and the ions produced in an atmospheric pressure ionisation (API)/ESI ion source. The temperature was 363 K and the drying gas flow rate 300 L h^{-1}. The acquisition and deconvolution of were was performed with a Mass Lynx (V. 2.3) Windows NT PC data system using the Max Ent Electrospray software algorithm and calibrated versus a NaI calibration file. ESI-MS was used to detect the hydrolysed ruthenium complexes and its adducts with a 14mer deoxynucleotide DNA strand.

2.2.4 X-Ray Crystallography

X-ray crystal structure analyses were performed by Dr. Simon Parsons at the University of Edinburgh.

2.2.5 Ultraviolet and Visible Spectroscopy

Ultraviolet and visible spectra were obtained on a Perkin-Elmer λ 16 UV-Vis recording spectrophotometer using 1 cm path length quartz cuvettes. The temperature was controlled using a PTP1 Peltier Temperature Programmer. Spectra were normally referenced to solvent alone. Spectra were processed with UVWinlab for Windows '95.

DNA melting-point UV-Vis spectra were recorded on a Perkin Elmer λ 20 UV/Vis Spectrometer using a UV quartz cell with a path length of 10 mm. The temperature was controlled using a PTP1 Peltier Temperature Programmer. The data were

analysed using UV Winlab and PE Templab software for Windows '95 from Perkin Elmer.

2.2.6 Inductively Coupled Plasma Mass Spectrometry

ICP-MS investigations were performed using a PlasmaQuad 3 inductively coupled plasma mass spectrometer from VG Elemental (Winsford UK). The instrumental apparatus included a high efficiency interface (S-Option™), which improves sensitivity by increasing the efficiency of the extraction of ions in the plasma through to the mass spectrometer itself.

2.2.7 CHN Analysis

CHN analyses were performed by the CHN Service at the University of Edinburgh

2.2.8 pH Measurements

All pH measurements were made using a Corning 240 meter equipped with an Aldrich microcombination electrode calibrated with Aldrich buffer solutions pH 4, 7 and 10. Meter readings from D_2O were not corrected for deuterium isotope effects and are termed pH*.

2.2.9 Lyophilisation

All samples for lyophilisation were frozen in liquid nitrogen and lyophilisation carried out at -40 °C using a Modulyo Edwards freeze drier and vacuum pump.

2.2.10 Centrifugation

Centrifugation was carried out using a Sanyo MSE Microcentaur for small volumes and a Beckman GS-15R centrifuge with temperature control for larger volumes and protein work.

2.3 Materials

2.3.1 Solvents

When anhydrous solvent is specified, the solvent was dried in the manner described in Table 2.3.

SOLVENT	DRYING METHOD
ethanol, methanol, propan-2-ol	distilled over Mg/I_2
benzyl alcohol, ethylene glycol	distilled over Na
tert-butyl alcohol	distilled over calcium hydride
chloroform, dichloromethane,	distilled over P_2O_5
acetone	distilled over K_2CO_3
acetonitrile	pre-dried with K_2CO_3 followed by distillation over CaH_2
benzene, toluene	distilled over P_2O_5
diethyl ether	distilled over Na
THF	distilled from Na/benzophenone ketyl

Table 2.3 Methods and reagents used for drying solvents

2.3.2 Reagents

The reagents used in this work, and their sources, are shown in Table 2.4.

REAGENT	COMPANY
$AgBF_4$, NH_4PF_6, isonicotinamide, 4-biphenylcarboxylic acid, 1,4-cyclohexadiene, α-terpinene, $NaBH_4$,	Acros
$LiAlH_4$, Li wire, $Bz_2NCH_2CH_2Cl.HCl$, $H_2NCH_2CH_2Cl.HCl$, $Me_2NCH_2CH_2Cl.HCl$, KO^tBu, Ru ICP standard	Aldrich
benzoic acid, biphenyl	BDH
TEAA buffer	Fluka
$RuCl_3.3H_2O$	Johnson Matthey
$Bz(H)NCH_2CH_2OH$, $C_6H_{11}(H)NCH_2CH_2OH$ PCl_5,	Lancaster
ethylenediamine	Prolabo
nuclease P1	Pharmacia Biotech
9-ethylguanine, , 5′-AMP, 5′-CMP, 5′-GMP 5′-TMP, phosphodiesterase I (5′-VPD), phosphodiesterase II (3′-SPD)	Sigma
$HPPh_2$	Strem

Table 2.4 Reagents and sources

2.4 References

[1] E.M. Purcell, H.C. Torrey, R.V. Pound *Phys. Rev.* **1946**, 69, 37

[2] F. Bloch, W.W. Hansen, M. Packard *Phys. Rev.* **1946**, 69, 127

[3] J.K.M. Sanders, B.K. Hunter *Modern NMR Spectroscopy- a guide for chemists*; OUP, Oxford, 1987

[4] A.E. Derome *NMR Techniques for Chemical Research* Pergamon, Oxford, **1987**

[5] W. Kemp *NMR in Chemistry- a multinuclear introduction* MacMillan, London, **1986**

[6] R. Harris *Nuclear magnetic resonance spectroscopy* John Wiley and Sons, **1986**

[7] *Concepts in magnetic resonance* **1994**, vol. 6

[8] B. Lippert *Prog. Inorg. Chem.* **1989**, 37, 18

[9] C. Brevard, P. Granger *J. Phys. Chem.* **1981**, 75, 4175

[10] *Multinuclear NMR* J. Mason, Plenum Press, **1987**

[11] X.M. Xiao, T. MatsamuraInoue, S. Mizutani *Chem. Lett.* **1997**, 3, 241

[12] K. Ishida, Y. Kawasaki, Y. Kitaoka, K. Asayama, H. Nakamura, J. Flouquet *Phys. Rev. B-Cond. Matter* **1998**, 57, 11054

[13] H. Mukuda, K. Ishida, Y. Kitaoka, K. Asayama, R. Kanno, M. Takano *Phys. Rev. B-Cond. Matter* **1999**, 60, 12279

[14] R.W. Dykstra, A.M. Harrison *J. Magn. Reson.* **1981**, 45, 108

[15] G. Predieri, C. Vignali, G. Denti, S. Serroni *Inorg. Chim. Acta* **1993**, 205, 145

[16] A.P. Bruins, T.R. Covey, J.D. Henion *Anal. Chem.* **1987**, 59, 2642

[17] The A.P.I. Book **1991**, Perkin-Elmer Science

[18] M. Dole, H.L. Cox, J. Gieniec *Adv. Chem. Ser.* **1971**, 125, 73

[19] *Platform Operator Training Course* Micromass, U.K. July **1996**

[20] J.B. Fenn, M. McCann, C.K. Meng, S.F. Wang, C.M. Whitehouse *Science* **1989**, 246, 64

[21] P. Kebarle, L. Tang *Anal. Chem.* **1993**, 65, 972A

[22] R. Guevremont, K.W.M. Siu, J.C.Y. LeBlanc, S.S. Berman *J. Am. Soc. Mass Spectrom.* **1991**, 3, 216

[23] R.D. Smith, K.J. Light-Wahl *Biol. Mass Spectrom.* **1993**, 22, 493

[24] J.J. Kirkland, L.R. Snyder *Introduction to Modern Liquid Chromatography* 2nd edn., Wiley, New York, 1979

[25] C.F. Simpson, Ed., *Techniques in Liquid Chromatography* Wiley, New York, 1984

[26] B.A. Bidlinmeyer, *Practical HPLC Methodology and Applications* Wiley-Interscience, New York, 1992

[27] J.F.K. Hubert, Y.A.R.J. Hulsman *Anal. Chim. Acta* **1967**, 38, 405

[28] J.H. Purnell *J. Chem. Soc.* **1960**, 1268

Chapter 3

Chelate ring-opening aminophosphine complexes of ruthenium

3.1 Introduction

Aminophosphines are bidentate mixed donor ligands containing one soft phosphorus and one hard nitrogen donor. They can act as chelating or pendant ligands in metal complexes.

There are many previous reports relating to the potential use of aminophosphine complexes, mainly with regard to catalysis.[1] However very few studies[2] have investigated the biological activity of the complexes even though they contain *cis* amine ligands, a feature found in many active platinum anti-cancer agents[3] and two *cis* phosphines. Anticancer activity in diphosphines such as 1,2-diphenylphosphinoethane complexes of Cu(I),[4] Ag(I)[5] and Au(I)[5] has been detected. Monophosphine complexes of Au(I) have found use in the treatment of arthritis and auranofin, a PEt_3 complex of gold, is in clinical use.[6] Aminophosphine complexes also possess lipophilic-cationic character and could possibly act by disrupting mitochondrial function.[7]

With metals such as Ru(II), Pt(II) and Pd(II) the hard nitrogen atom would be expected to bind more weakly than the soft phosphorus, offering the possibility of chelate ring-opening and the availability of extra coordination sites. This would be especially pronounced when the P is *trans* to N as the phosphorus exerts a high *trans* influence.[8] This could be particularly useful for the d^6 Ru(II) as the octahedral geometry offers more potential reaction sites than the square-planar d^8 Pt(II) and Pd(II). In addition, M-N bond strength is affected by steric factors to a greater extent than the corresponding M-P bond.[9] Thus, with the appropriate choice of nucleophiles and under a given set of conditions such as pH, $[Cl^-]$ and steric restrictions, equilibria involving the dissociation of the amino groups can occur resulting in ring-opened complexes with a potential binding site on the metal centre, thereby increasing its inherent biological or catalytic activity. A schematic for chelate ring-opening in a coordinating solvent is shown in Figure 3.1.

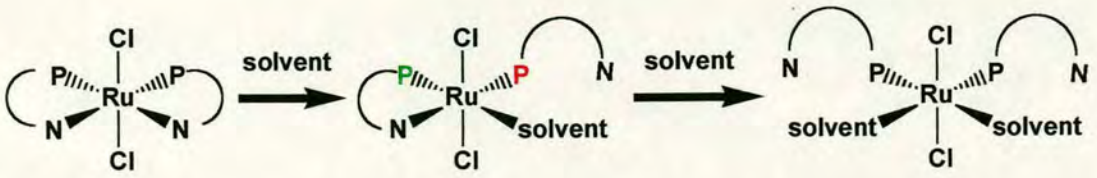

Figure 3.1 Schematic for chelate ring-opening of a bischelated ruthenium aminophosphine complex in a coordinating solvent

It has recently been established that chelate ring-opening reactions of Pt(II) aminophosphine complexes with a two-carbon backbone can be controlled under conditions of biological relevance, and that they readily bind reversibly to the DNA base guanine.[10] It was also shown that complexes of this type can bind rapidly and strongly to thymine, as well as the RNA base uracil, under physiological conditions, in contrast to platinum am(m)ine anti-cancer complexes.[11] The three carbon backbone complex $[PtCl_2(Me_2N(CH_2)_3PPh_2 - P)_2]$ also gave interesting results.[12] In comparison to cisplatin, it was found to coordinate faster to DNA, induced conformational alterations in DNA that were distinctly different from cisplatin, and formed adducts with adenine more frequently than cisplatin. It was reported that both of the above complexes exhibited activity against tumour cells, including those resistant to cisplatin, and this suggests that the mechanism of action of Pt-aminophosphine complexes is different from that of cisplatin and related analogues.

The catalytic activity of ruthenium aminophosphine complexes has been of interest. The idea of using chelating ligands for synthesising complexes for use in homogenous catalysis came about as platinum group metals with phosphines have been found to be good catalysts in a number of reactions.[13] Chelating multidentate phosphine based ligands provide better control over the coordination number and stereochemistry of the resulting complexes, increase basicity at the metal centres and slow down intra- and inter-molecular exchange processes.[14] In particular, ruthenium complexes with chelating P-N ligands have been shown to form dihydrogen complexes.[15,16,17] $[RuCl_2(PPh_3)(DPBA)]$, where DPBA is bis(2-diphenylphosphino)ethyl)benzylamine, has shown in tests to have

where $P_2N_2C_2H_4$ is N, N′-bis[*o*-(diphenylphosphino)benzyl]ethylenediamine has been reported to have excellent activity for the hydrogenation of acrylic acid to propionic acid.[19]

The interactions of ruthenium aminophosphine complexes with H_2S have invoked interest because of the involvement of H_2S in the biological sulphur cycle, the formation of ores, hydrodesulphurisation catalysis and as a source for H_2 and elemental sulphur.[20] The complex $RuCl_2(o\text{-}Ph_2PC_6H_4NMe_2)(P(p\text{-tolyl})_3)(SH_2)$ has been isolated and fully characterised, which is unusual as the H_2S was not oxidised, and low temperatures were not required for stability.

Although some Ru-aminophosphine complexes have been synthesised previously[16,21] there are very few crystal structures in the literature. Ones that have appeared include the five coordinate complex dichloro(*o*-diphenylphosphino-*N,N*-dimethylaniline)-[tris(*p*-tolyl)phosphine]ruthenium(II)[16], *trans*-dichloro-*N,N′*-bis[(*o*-(diphenylphosphino)benzylidene]ethylenediamine-ruthenium(II) where the aminophosphine ligand is tetradentate[22] and the dimeric structure of $[Ru_2Cl_2(P\text{-}N)_4]^-$, where P-N is 1-(diphenyl-phosphino)-2-(2-pyridyl)ethane.[23] A recent paper from this group[24] reported the synthesis and characterisation of the Ru(II) complex *cis, trans*-$[Ru(Me_2NCH_2CH_2PPh_2\text{-}P,N)_2Cl_2]$. It was found that this complex underwent a two step reaction in methanol which involves chloride dissociation followed by P-N chelate ring-opening. Chloride inhibited the solvolysis process, and chloride release appears to be necessary for the chelate ring-opening reaction, although it has been found in a Cp*Ru complex of an aminophosphine ligand that CO(g) caused the ring-opening reaction to occur.[35]

This chapter is concerned with the synthesis and crystal structures of some Ru(II) aminophosphine complexes using the ligands shown in Figure 3.2 and with their potential chelate ring-opening reactions. and hence their possible biological applications.

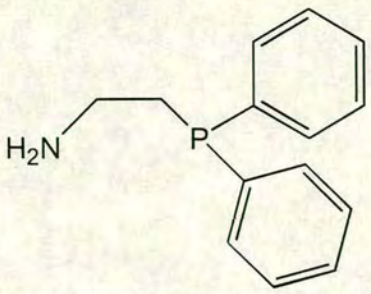

DHAP

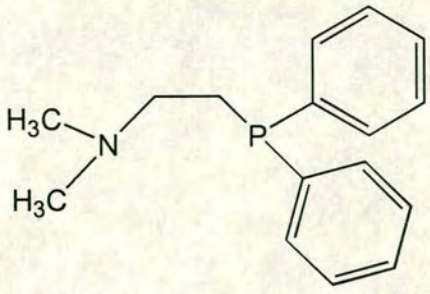

DMAP

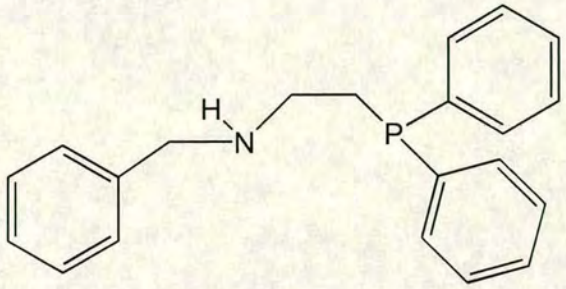

DPEBA

Figure 3.2 Schematics of the ligands used in this section for the synthesis of Ru(II)aminophosphine complexes. DHAP = dihydroaminophosphine, DMAP = dimethylaminophosphine, DPEBA = diphenylphosphinoethanebenzylamine.

3.2 Experimental

For materials and UV-Vis see *Chapter 2 Materials and methods*.

The ^{1}H and ^{31}P $\{^{1}H\}$ NMR spectra were recorded at 298 K on Brüker DMX500 (^{1}H 500 MHz; ^{31}P 202 MHz) and Varian-Inova 600 spectrometers (^{1}H 600 MHz), using 5-mm NMR tubes. The chemical shift references were as follows: ^{1}H, (internal, TSP), ^{31}P (external, 30% H_3PO_4). The 2D Gradient-Selected $^{1}H,^{1}H$-COSY and TOCSY (mixing time of 0.12 s) experiments were carried out using standard sequences. Data sets with 2048 x 512 points were acquired with frequency widths of 8000 Hz in both dimensions and 16 scans per t_1 increment. The t_1 dimension was zero-filled to 2048 data points, and the spectrum was processed with a combination of exponential and Gaussian weighting

functions. The 2D [^{1}H,^{31}P] HSQC NMR spectra were recorded using standard sequence. The ^{31}P-spins were decoupled by irradiation with the GARP-1 sequence during acquisition.

Cyclic voltammetry experiments were carried out in CH_3CN/[n-Bu_4N][BF_4] (0.4 M), with an Autolab PGSTAT20 potentiostat equipped with GPES 4.2 software. The working electrode was a platinum microdisc of diameter 0.5 mm and the potential reported is quoted relative to a Ag/AgCl reference electrode via $FeCp_2/FeCp_2^+$ (0.375 V).

3.2.1 Preparation of ligands

3.2.1.1 Preparation of $H_2NCH_2CH_2PPh_2$ (DHAP)

PPh_2H (5 ml, 5.35 g, 28.76 mmol) was added via syringe under argon to a stirred suspension of Bu^{t}OK (8.5 g, 76 mmol) in freshly dried THF (100 ml). This was stirred at ambient temperature for 40 min after which time $H_2NCH_2CH_2Cl.HCl$ (3.24 g, 28.17 mmol) was added in one portion. The reaction was heated to reflux for 20 h during which time the deep red solution turned almost colourless. The solvent was removed *in vacuo* and the residue taken up in 10 % HCl solution. The solution was washed with benzene and made alkaline with 10 % NaOH solution. The product was extracted into benzene (3 x 50 ml), washed with brine and dried over $MgSO_4$. This was filtered and the solvent removed on the rotary evaporator leaving a colourless oil. This was dissolved in ether and purified on a short column of alumina.

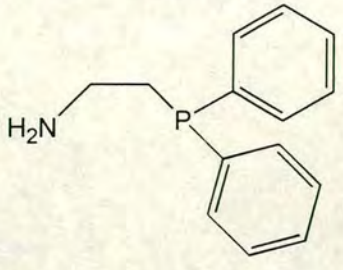

Yield: 3.39 g, 14.8 mmol, 52.4 %

^{1}H NMR ($CDCl_3$): δ 1.51 (2 H, br, s, H_2N), 2.26 (2 H, m, P-CH_2), 2.86 (2 H, m, N-CH_2), 7.1-7.4 (10 H, m, 2 Ph)

$^{31}P\{^{1}H\}$ NMR ($CDCl_3$): δ -21.5

3.2.1.2 Preparation of $Me_2NCH_2CH_2PPh_2$ (DMAP)

This was prepared in an analogous procedure to that described Section 3.2.1.1, replacing $H_2NCH_2CH_2Cl.HCl$ with $Me_2NCH_2CH_2Cl.HCl$

Yield: 4.28 g, 16.4 mmol, 41.3 %

^{1}H NMR ($CDCl_3$): δ 2.24 (6 H, s, N-CH_3), 2.26-2.28 (2 H, m, P-CH_2), 2.38-2.44 (2 H, m, N-CH_2), 7.31-7.34, 7.36-7.48 (10 H, m, Ph)

$^{31}P\{^{1}H\}$ NMR ($CDCl_3$): δ -19.07

3.2.1.3 Preparation of $H(Bz)NCH_2CH_2PPh_2.2HCl$ (DPEBA)

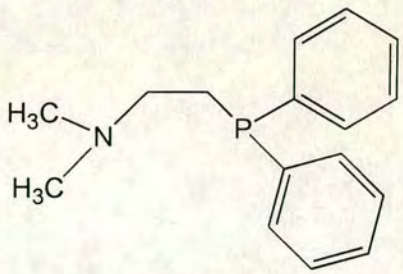

This was prepared by a procedure analogous to Section 3.2.1.1, replacing $H_2NCH_2CH_2Cl.HCl$ with $H(Bz)NCH_2CH_2Cl.HCl$ and with a modification to the work-up. After the THF was removed *in vacuo*, 20 % HCl solution was added, leaving a whitish precipitate. This was filtered, redissolved in $CHCl_3$ and filtered to remove any undissolved particles. The solvent was removed on a rotary evaporator to leave a white powder which was recrystallised from methanol/ether to give shiny white crystals.

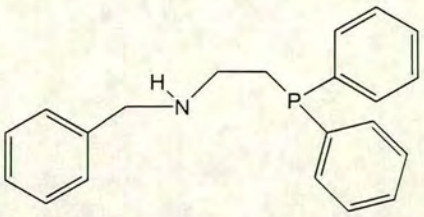

Yield: 5.31 g, 19.4 mmol, 84 %

$C_{21}H_{24}Cl_2NP$ (392.3) Calc. %C = 70.68 %H = 6.45 %N = 3.92

Found %C = 70.41 %H = 6.44 %N = 4.14

^{1}H NMR ($CDCl_3$): δ 2.59 (m, 4 H)), 2.82 (s, br, 2 H), 7.24-7.62 (m)

$^{31}P\{^{1}H\}$ NMR ($CDCl_3$): δ -20.33

3.2.2 Preparation of ruthenium complexes

Cis- and *trans*-$[RuCl_2(DMSO)_4]$,[50] $[(COD)RuCl_2]_x$[25] and $[(\eta^6\text{-}C_6H_6)Ru(CH_3CN)_2Cl][PF_6]$ [26] were synthesised according to the published procedures.

3.2.2.1 Synthesis of *trans*, *cis*-$[RuCl_2(H(Bz)NCH_2CH_2PPh_2\text{-}N, P)_2]$ **1**

cis-$[RuCl_2(DMSO)_4]$ (0.24 g, 0.5 mmol) was stirred in acetone (10 ml) and the ligand DPEBA (0.36 g, 1 mmol) added in one portion. This was sealed and the reaction stirred overnight at ambient temperature. Ether was added to induce precipitation of a pink solid which was collected and recrystallised from acetone/ether.

Yield: 4 mg, 4.9×10^{-3} mmol, 1 %

$C_{42}H_{44}Cl_2N_2P_2Ru$ (810.75) Calc. %C = 62.22 %H = 5.47 %N = 3.46

Found %C = 61.63 %H = 5.80 %N = 3.71

3.2.2.2 Synthesis of *trans*, *cis*-$[RuCl_2(Me_2NCH_2CH_2PPh_2\text{-}N, P)_2]$ **2**

The ligand DMAP (0.36 g, 1.4 mmol) dissolved in benzene (5 ml) was added to a stirred suspension of $[Ru(COD)Cl_2]_x$ (0.39 g, 1.4 mmol) in benzene (10 ml). The reaction was refluxed for 24 h and filtered while hot to remove unreacted ruthenium starting material. The red filtrate was evaporated to dryness and recrystallised from toluene.

Yield: 0.33 g, 0.48 mmol, 34.6 %

$C_{32}H_{40}Cl_2N_2P_2Ru$ (686.57) Calc. %C = 55.98 %H = 5.87 %N = 4.08

Found %C = 55.53 %H = 5.63 %N = 3.92

$^{31}P\{^1H\}$ NMR (d^8-toluene): δ 57

3.2.2.3 Synthesis of *trans*, *cis*-$[RuCl_2(H_2NCH_2CH_2PPh_2\text{-}N, P)_2]$ **3**

The ligand DHAP (1.15 g, 5 mmol) was added in one portion to a stirred suspension of $[Ru(COD)Cl_2]_x$ (0.7 g, 2.5 mmol) in benzene (40 ml) and the mixture refluxed under argon. After 4 h, a yellow precipitate had formed. This was collected after cooling and recrystallised from CH_2Cl_2/ether.

Yield: 0.20 g, 0.32 mmol, 12.8 %

$C_{28}H_{32}Cl_2N_2P_2Ru$ (630.53) Calc. %C = 53.34 %H = 5.12 %N = 4.44

Found %C = 53.95 %H = 5.16 %N = 3.07

$^{31}P\{^1H\}$ NMR (d^6-DMSO): δ 60.7 (d, J = 24.6 Hz), 45.7 (d, J = 24.6 Hz)

3.2.2.4 Synthesis of *trans*, *cis*-$[RuCl_2(DMSO\text{-}S)_2(H_2NCH_2CH_2P(O)Ph_2\text{-}N, O)]$ **4**

Trans-$[RuCl_2(DMSO)_4]$ (0.06 g, 0.13 mmol) was set stirring in freshly dried ethanol (10 ml). DHAP (0.03 g, 0.13 mmol) was added in one portion and the yellow solution stirred overnight. An orange precipitate formed during this time. This was collected and recrystallised from ethanol/ether.

Yield: 6 mg, 9.5 x 10^{-3} mmol, 7.32 %

$^{31}P\{^1H\}$ NMR ($CDCl_3$): δ 51.6 (s)

3.2.2.5 Synthesis of $[(\eta^6\text{-}C_6H_6)Ru(PPh_2CH_2CH_2NMe_2\text{-}N, P)Cl][PF_6]$ **5**

DMAP (0.077 g, 0.23 mmol) dissolved in dry acetonitrile (2 ml) was added in one portion to a solution of $[(\eta^6\text{-}C_6H_6)Ru(CH_3CN)_2Cl][PF_6]$ (0.102 g, 0.23 mmol) in dry acetonitrile (8 ml). The mixture was stirred at ambient temperature for 10 h in a sealed flask with no special precautions to exclude air. The orange solution was evaporated to an orange oil which was taken up in 2 ml $CHCl_3$. Ether was added to induce precipitation and the orange solid was collected, washed with ether and recrystallised as the 0.5 CH_3CN solvate by slow diffusion of ether into an acetonitrile solution.

Yield: 0.085 g, 0.13 mmol, 57.8 %

$C_{23}H_{27.5}ClF_6N_{1.5}P_2Ru$ (637.43) Calc. %C = 43.30 %H = 4.35 %N = 3.29

Found %C = 43.05 %H = 4.40 %N = 3.03

^1H NMR (CD_3CN): δ 5.68 (d, 6H), 3.19 (s, 3H), 3.11 (s, 3H)

$^{31}P\{^1H\}$ NMR (CD_3CN): δ 57.9 (s)

3.2.2.6 Reaction of complex **5** with carbon monoxide

Complex **5** (0.064 g, 0.1 mmol) was dissolved in dry and degassed CH_3CN (5 ml). CO(g) was bubbled through the solution for 15 min, the flask sealed under positive pressure and the reaction stirred for 24 h. Ether (50 ml) was added and the precipitate was collected and dried in vacuo.

3.3 Results and Discussion

3.3.1 Preparation and properties of ligands

The ligands were prepared by the method of Habtemariam.[27] A number of methods have been reported in the literature for the preparation of aminophosphine ligands.[1] The method utilised here has the amino alcohol as the convenient starting material. A large number of aminoalcohols are available commercially or can be prepared from the reduction of amino acids.[28] The chlorination of the amino alcohol, followed by the reaction with the diphenylphosphine anion which was formed *in situ* by the reaction of *tert*-potassium butoxide and diphenylphosphine in THF under argon, afforded the ligand.

The ligands were obtained as viscous oils (DMAP and DHAP) or the hydrochloride salt (DPEBA). The oily ligands were easily purified by passing an ether solution through a short column of alumina or reduced-pressure distillation. The DPEBA was recrystallised from methanol/ether.

The mixed donor ligands DMAP, DHAP and DPEBA are soluble in almost all organic solvents. The ^1H NMR spectra of the ligands in $CDCl_3$ showed the expected peaks with the backbone $-CH_2-$ giving multiplets and the $-NH_2$ a broad peak at δ 1.5 (DHAP). The $^{31}P\{^1H\}$ NMR showed singlet resonances in the region of δ -19 to -22.

3.3.2 Ruthenium(II) complexes

The ruthenium(II) complexes **1-5** were prepared from four different starting materials. *Cis*-$[RuCl_2(DMSO)_4]$ is a very versatile reagent that is known to provide a very good entry point to Ru(II) chemistry. A large number of Ru(II) complexes have been synthesised from it[29] including the chelate-ring opening aminophosphine complex $[RuCl_2(DMAP)_2]$.[24] The easily displaced DMSO ligands make possible the formation of Ru(II) chloride complexes with a variety of ligands.

Trans-$[RuCl_2(DMSO)_4]$ is easily obtained by light catalysed isomerisation from the *cis* form.[50] Although not usually used for synthesis, it was hoped that this compound would facilitate the replacement of only two DMSO molecules by one aminophosphine ligand. Hence, a more water soluble complex may be formed.

The third starting material utilised is $[(COD)RuCl_2]_x$. This is a brown, reasonably insoluble material that is not very well characterised but assumed to be oligomeric. Initially this was used in the hope of making a Ru(II) complex with a coordinated COD ligand as well as an aminophosphine. However the COD proved to be too labile under the conditions used and the ligands were able to replace it. This proved to be a successful starting material, with complexes **3** and **4** being produced from it in low but workable yield.

It was also decided to investigate the possibility of synthesising arene ruthenium aminophosphine complexes. The starting material utilised was $[(\eta^6\text{-}C_6H_6)Ru(CH_3CN)_2Cl][PF_6]$ and was prepared according to the published procedure.[26] It is potentially a very useful entry point to Ru(II) arene complexes.[30]

3.3.2.1 *trans*, *cis*-$[RuCl_2(H(Bz)NCH_2CH_2PPh_2\text{-}N, P)_2]$ **1**

The reaction of *cis*-$[RuCl_2(DMSO)_4]$ with DPEBA as its hydrochloride salt in a 1:2 molar ratio, in acetone, gave rise to complex **1**. The extremely low yield took the form of a few crystals which were suitable for X-ray analysis and the structure was solved. The remaining few crystals were used for elemental analysis. Although *cis*-$[RuCl_2(DMSO)_4]$

is insoluble in acetone, the product should be soluble in acetone and therefore separable from starting material. Attempted preparation in CH_2Cl_2 (c.f. Guo et al[24]) resulted in an air-sensitive, uncharacterisable reddish solid, and the initial crude material from the acetone reaction was similar. However, the attempt to recrystallise the crude product gave only ca. ~4 mg of product. Repeated attempts to synthesise more of the compound all failed.

3.3.2.1.1 X-ray crystal structure of complex **1**

Single crystals of complex **1** suitable for X-ray analysis were grown from an acetone/ether mixture. Compound **1** crystallised in the space group P1 with two molecules in the unit cell. In the molecule the ruthenium is in the formal oxidation state of +2 and is situated in a distorted octahedral coordination environment with two Cl ligands in mutually *trans* positions and two chelated P-N ligands in *cis* positions. The structure can be seen in Figure 3.3. This arrangement seems to be sterically crowded, but is apparently preferred to that in which the two P atoms are mutually *trans* because of their strong *trans* effects.[8] This is in agreement with the previously reported structure of *trans, cis*-$[RuCl_2(DMAP)_2]$.[24] There are no strong intermolecular interactions involved in the crystal packing. A summary of crystal data can be found in Table 3.1 and selected bond-lengths and angles are found in Table 3.2.

The Ru-P (2.247(4) and 2.252(4) Å) and Ru-Cl (2.401(4) and 2.410(4) Å) bond lengths are within the range of values typical for Ru(II) complexes.[24,31]

It was found in *trans, cis*-$[RuCl_2(DMAP)_2]$ by Guo et al[24] that the Ru-N bond lengths (mean = 2.391 Å) were considerably longer (0.2 Å) than values for P-N chelated Ru(II) complexes previously reported, for example, N *trans* to P in complexes such as *trans*-dichloro-bis(diphenylphosphino)pyridineruthenium(II) (2.13 and 2.06 Å),[32] *trans*-dichloro-*N,N*-bis-[*o*-(diphenylphosphino)benzylidene](ethylenediamine)ruthenium(II) (2.17 and 2.16 Å)[22] and dichlorotetra(1-(diphenylphosphino)-2-(2-pyridyl)ethane)diruthenium(II) (2.152 and 2.157 Å).[33] This lengthening of the Ru-N

bond presumably results from the *trans* influence of the P and the steric effects of the methyl substituents on the nitrogen. This increased length indicates a weaker Ru-N bond which would be expected to facilitate chelate ring-opening under certain conditions, a major part of our rationale for investigating Ru(II) aminophosphines. However this effect is not seen for complex **1**, despite the similar geometry and having the potentially more bulky benzyl group on the nitrogens. It is possible that having H as the second substituent on N allows sufficient space to reduce the steric effects. The benzyl groups point away from each other, much like a crab's claws reversed, thereby greatly reducing the steric hindrance. The crystal structures of Pd(II) and Pt(II) complexes with the same ligand (DPEBA) do not contain any metal-N bonds probably because the benzyl groups are too sterically crowding and prevent chelation in these square planar structures.

The less than 180° bond angle for Cl-Ru-Cl (166.98(11)°) probably results from crowding caused by the phenyl substituents on phosphorus. This is less than was found by Guo et al[24] for $[RuCl_2(DMAP)_2]$ (172°). Having the benzyl group as a substituent means that the phenyl ring is one atom removed from nitrogen and hence there is more space for the chloride ligands and therefore the Cl-Ru-Cl angle is able to distort from 180°, as opposed to *cis, trans*-$[Ru(DMAP)_2Cl_2]$. Cl-Ru-Cl bond angles have been reported in the literature as low as 165.4° for *trans*-dichloro-*N,N*-bis-[*o*-(diphenylphosphino)benzylidene](ethylenediamine)ruthenium(II).[22]

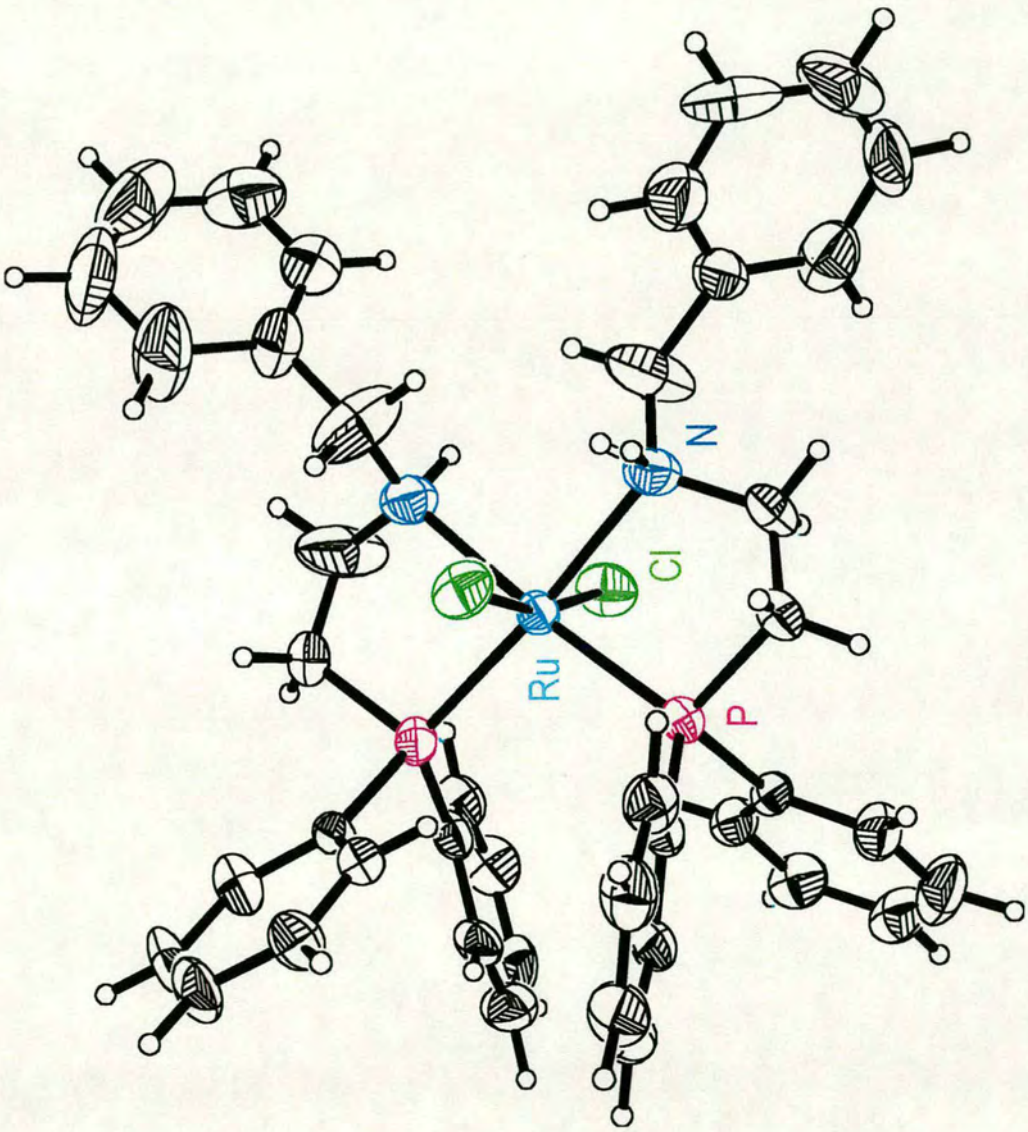

Figure 3.3 Crystal structure of *cis, trans*-[Ru(Bz(H)NCH$_2$CH$_2$PPh$_2$-*N*, *P*)$_2$Cl$_2$] complex **1**

3.3.2.1.2 Conclusions

Complex **1** proved to be an elusive compound, and only a few crystals were obtained despite considerable synthetic effort. The X-ray structure was solved and the complex adopted the expected distorted octahedral geometry with two *trans* chlorides and two aminophosphine ligands chelating in a *cis* configuration. However, the structure did not show the hoped for elongated Ru-N bond length exhibited by *cis, trans*-$[Ru(DMAP)_2Cl_2]$[24] and so no conclusions can be made at this stage as to the potentially hemilabile nature of the chelated ligand. The lack of water solubility of the complex potentially limits any biological uses.

	Complex 1	Complex 3	Complex 4	Complex 5
Empirical Formula	$C_{42}H_{44}Cl_2N_2P_2Ru$	$C_{28}H_{32}Cl_2N_2P_2Ru$	$C_{18}H_{28}Cl_2NO_3PRuS_2$	$C_{23}H_{27.5}ClF_6N_{1.5}P_2Ru$
Formula weight	810.70	630.47	573.47	637.43
Crystal habit	orange block	orange needle	orange block	orange block
Crystal size / mm	0.19 x 0.16 x 0.12	0.20 x 0.06 x 0.06	0.45 x 0.27 x 0.19	0.45 x 0.45 x 0.45
Crystal system	triclinic	triclinic	monoclinic	monoclinic
Space group	P-1	P-1	$P2_1/c$	$P2_1/c$
Volume / $Å^3$	1890.8(18)	1375.5(2)	2344.4(8)	2501.2(12)
Z	2	2	4	4
Density (calc.) / mg m^3	1.424	1.522	1.625	1.693
Absorption coefficient / mm^{-1}	5.700	0.901	1.162	0.921
F(000)	836	644	1168	1284
θ range for data collection / deg	2.86 to 59.99	2.36 to 29.46	2.52 to 22.55	2.53 to 25.06
Reflections collected	5825	10038	5895	4618
Independent reflections	5540	7321	3082	4414
Conventional R (R_1)	0.0764	0.0378	0.1200	0.0369

Table 3.1 Summary of the crystal data for complexes **1**, **3**, **4** and **5**

	1	3	4	5
Ru-P(1)	2.247(4)	2.2552(6)	-	2.3122(11)
Ru-P(2)	2.252(4)	2.2565(6)	-	-
Ru-N(1)	2.212(11)	2.1642(19)	2.20(2)	2.212(3)
Ru-N(2)	2.230(10)	2.1796(18)	-	-
Ru-Cl(1)	2.401(4)	2.4053(6)	2.400(7)	2.3986(11)
Ru-Cl(2)	2.410(4)	2.4192(6)	2.401(7)	-
Ru-O	-	-	2.18(2)	-
Ru-S(1)	-	-	2.200(7)	-
Ru-S(2)	-	-	2.250(5)	-
P(1)-Ru-P(2)	101.48(14)	102.80(2)	-	-
N(1)-Ru-N(2)	93.1(4)	90.73(7)	-	-
Cl(1)-Ru-Cl(2)	166.98(11)	164.31(8)	170.6(2)	-
P(1)-Ru-N(1)	82.5(3)	82.99(5)	-	81.68(9)
P(2)-Ru-N(2)	83.0(3)	83.51(5)	-	-
N(1)-Ru-O(1)	-	-	94.4(6)	-

Table 3.2 Selected bond lengths (Å) and angles (°) for complexes **1**, **3**, **4** and **5**

3.3.2.2 *Trans*, *cis*-$[RuCl_2(Me_2NCH_2CH_2PPh_2$-*N, P*$)_2]$ **2**

The 1:1 reaction of the ligand DMAP and $[Ru(COD)Cl_2]_x$ in refluxing benzene produced the complex *trans*, *cis*-$[RuCl_2(Me_2NCH_2CH_2PPh_2$-*N, P*$)_2]$ **2**. This was not the expected product. It was hoped that this product would contain one coordinated ligand and an η^4-coordinated cyclooctadiene. However, under the conditions used, the COD ligand proved to be too labile and was displaced by two ligands.

Complex **2** is a known complex. Two papers within the space of a few months[24,34] reported on the synthesis, structure and chelate ring-opening of this complex. Presumably because of the reaction conditions and recrystallisation solvent used (toluene), complex **2** had different solubility properties to the previous reports. Unlike the others, this version had a very low solubility in chlorinated solvents, and was actually slightly soluble in ether. It was on attempting to solve the X-ray crystal structure of the molecule that the true product was discovered. With the knowledge of what the structure was, the elemental analysis data fitted, and also, the NMR data corresponded to the literature complexes. On

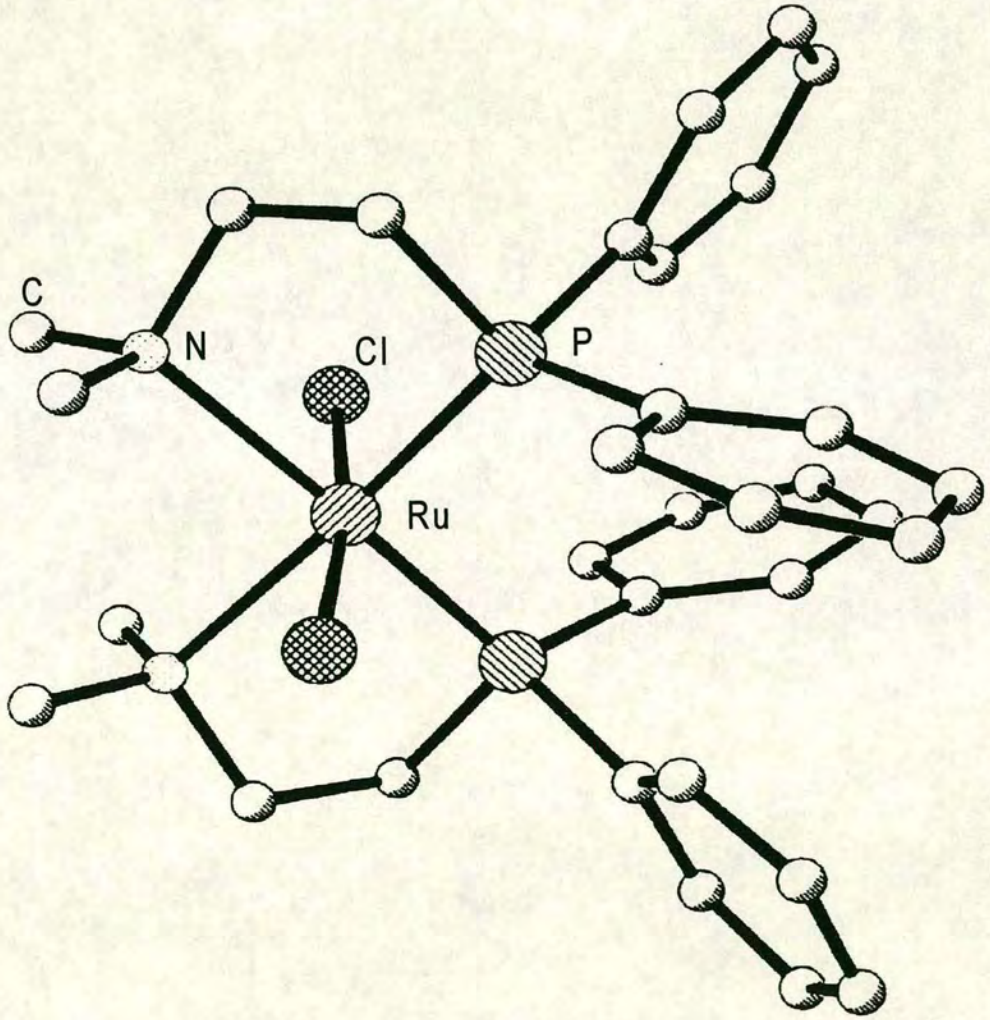

Figure 3.4 Structure of *trans*, *cis*-[$RuCl_2(Me_2NCH_2CH_2PPh_2$-*N, P*)$_2$] complex **2**

literature complexes. On dissolving in methanol, the solution became green with time, and a new singlet arose in the ^{31}P NMR spectrum at $\delta = 33.9$, corresponding to the ring-opened species observed in the literature.[24] Unfortunately, the crystals were of a very poor quality and contained a lot of disordered aromatic toluene. An initial structure was obtained, but the quality of the crystals was such that they were only sufficient to determine connectivity. The structure is shown in Figure 3.4. This procedure was not repeated to try and improve the quality of the crystals as the complex had little new to offer with regards ring-opening or obvious structural novelty, and if anything, was of more limited use due to the restricted solubility.

3.3.2.3 *trans*, *cis*-$[RuCl_2(H_2NCH_2CH_2PPh_2\text{-}N, P)_2]$ **3**

The reaction of $[Ru(COD)Cl_2]_x$ with DHAP in refluxing benzene in a 1:2 molar ratio resulted in the displacement of the COD ligand and the coordination of two DHAP ligands. This yellow compound analysed for $[Ru(DHAP)_2Cl_2]$ by elemental analysis and X-ray crystallography. Complex **3** is only reasonably soluble in coordinating solvents such as DMSO and acetonitrile and sparingly soluble in alcohols. It is insoluble in other organic solvents and water.

3.3.2.3.1 X-ray crystal structure of complex **3**

Crystals suitable for X-ray analysis were grown by the slow evaporation of an ethanolic solution. The complex crystallises in the space group P1 with two molecules in the unit cell. Like complexes **1** and **2**, the Ru has the formal oxidation state of +2 and is situated in a distorted octahedral environment. The two chlorides are in *trans* positions and the aminophosphine ligands chelated in the *cis* positions. No strong intermolecular forces were found in the crystal packing. The structure is shown in Figure 3.5. A summary of the crystal data is given in Table 3.1, and selected bond-lengths and angles are given in Table 3.2.

The lack of steric hindrance from the N-H moieties in the structure is apparent from the Ru-N bond lengths of 2.1642(19) and 2.1796(18) Å which are the shortest Ru-N bond lengths of the complexes **1**, **3**, **4**, **5**, $[RuCl_2(DMAP)_2]$,[24] [Cp*Ru(DMAP)Cl][35] and RuHBz(DMAP). The hydrogens allow the nitrogen to be positioned closer to the metal as compared to bulkier substituents such as a methyl or benzyl. The bite angle of the chelate rings is ca. 83°, indicating a tighter chelate ring than in the other complexes. Also, it can be seen from the N-Ru-N angle of 90.73(7)°, compared with 93.1(4) ° for **1** and 94.6(3)° for *trans, cis*-$[RuCl_2(DMAP)_2]$[24] that the nitrogens are closer together in the structure than in the other bischelated aminophosphine discussed.

The Ru-Cl bond lengths (2.4053(6) and 2.4192(6) Å) are typical for octahedral Ru(II) complexes. The Cl-Ru-Cl bond angle of 164.3° is very low, highly distorted from linearity. The lowest reported in the literature for an octahedral Ru(II) complex with *trans* chlorinde ligands is 165.4°.[22] The distortion is caused by the phenyl groups on the phosphine part of the ligand pushing the chlorides away from them. The extent of the distortion can again be attributed to having two hydrogens on the nitrogens as their low steric hindrance would allow the phenyl groups to push the chlorides further away from them. The phenyl rings of adjacent PPh_2's are almost perpendicular, thus minimising repulsion between them and allowing them to pack closely together.

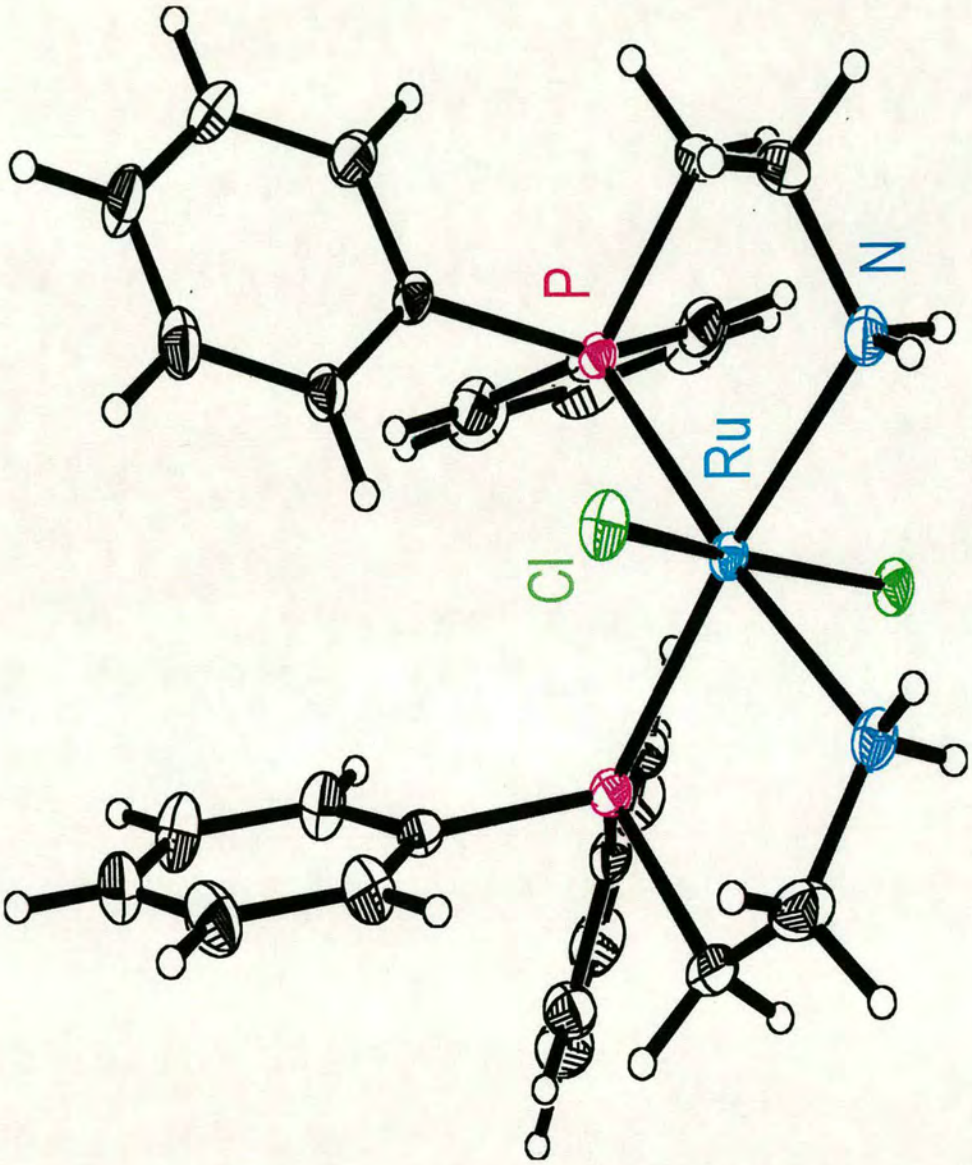

Figure 3.5 Crystal structure of *cis, trans*-[Ru($H_2NCH_2CH_2PPh_2$-*N, P*)Cl_2] complex **3**

3.3.2.3.2 Cyclic voltammetry of complex **3** in CH_3CN

The reduction potential (Ru(III)/Ru(II)) of ruthenium complexes could play an important role in their biological activity. It has been hypothesised that Ru(III) complexes may be prodrugs that are activated *in vivo* by reduction to Ru(II). Therefore, we looked at the electrochemistry of complex **3**. Acetonitrile was used to provide good solubility and allow ease of handling at various temperatures. At one stage, the temperature was lowered to 227 K, which would not have been possible with DMSO.

On analysis, at 298 K and 0.1 Vs^{-1} sweep rate, there were two weak peaks. When the sweep rate was increased to 1 Vs^{-1} a clearer redox couple became visible, with a reversible oxidation at 0.82 V (versus Ag/AgCl) in CH_3CN. The oxidised species appeared to be unstable in solution and very quickly changed into other species, which is why no peak was detected using a slow sweep rate. When the sample was cooled to 227 K, this couple was even clearer. The redox process can tentatively be assigned to the metal centred Ru(II)/Ru(III) couple. The value of 0.82 V is much higher than the corresponding value for $[RuCl_2(DMAP)_2]$[24] which was observed at 0.326 V, and is likely to be too high to be of biological relevance.

3.3.2.3.3 NMR analysis of chelate ring-opening of complex **3**

When dissolved in DMSO, **3** undergoes an instantaneous chelate ring-opening reaction. A fresh solution of **3** in DMSO-d_6 was monitored by NMR. The ring-opening reaction appeared complete by the time that the spectrometer had been prepared and the spectrum acquired. A one ring-open, one ring-closed conformation is strongly suggested by the $^{31}P\{^1H\}$ NMR spectrum. Two doublets are present, one at δ 60.7 and the other at δ 45.7. The J(P-P) coupling constant of 24.6 Hz is indicative of two *cis* phosphorus nuclei.[36] The signal at δ 60.7 corresponds to the expected value for a chelated aminophosphine ligand bound through both P and N.[24,37] If ring-opening of a chelated ligand occurs (Ru-N bond breaks) the ^{31}P signal for the phosphorus of that ligand would be expected to shift to

higher field. This was observed for *trans, cis*-[$RuCl_2$(DMAP)] by Guo et al[24] and also the chemical shift is similar to that observed for the ring-opened Pt(II) complexes of aminophosphine ligands coordinated via P only.[10] This phenomenon has also been observed for the complex [Cp*Ru(DMAP)Cl],[35] for which the ^{31}P shift of the ring-closed form of the complex is δ 60.9 and the ring-opened form appears at higher field at δ 38.9. After one week it was noted that a third signal had arisen in the ^{31}P spectrum of **3** at δ 51.4. This was a singlet, indicating equivalent phosphorus nuclei in the complex. However, even after two months this species never became dominant and a definite assignment was not possible. Of the possible structures it could have arisen from, free ligand could be ruled out as the chemical shift of the phosphorus in the free ligand is ca. -20 ppm. This leaves a Ru-complex with two equivalent ring-opened ligands due to the second ligand ring-opening, or a Ru complex with two equivalent chelated ligands, due to the open ring reclosing. No free ligand was detected at all, therefore complexes with only one ligand, due to loss of a DHAP can be ruled out. The spectrum in CD_3CN is very similar. Thus **3** reacts with DMSO and CH_3CN to give a complex with one chelated aminophosphine ligand and one pendant ligand coordinated only through the P. The ^{1}H NMR spectrum showed a variety of peaks due to the two inequivalent ligands and 2D NMR techniques had to be employed for complete assignment.

2D NMR spectroscopy of complex **3** in DMSO

2D NMR spectroscopy was utilised in order to fully assign the NMR resonances observed. COSY, TOCSY and [^{31}P-^{1}H] HSQC experiments were performed, and from these spectra it was possible to distinguish between the pendant and chelate ligands. The [^{31}P-^{1}H] HSQC spectrum is shown in Figure 3.6 and the COSY spectrum with selected assignments is shown in Figure 3.7, and full spectra are available in Appendix 1. Each experiment had its own piece of the jigsaw to offer, and then by combining all the information obtained from them the full picture could be seen. A table of assignments is given in Table 3.3.

The [^{31}P, ^{1}H] HSQC spectrum, Figure 3.6, allowed assignment of protons coupled to phosphorus, thereby showing at least some of the protons that were linked with either the

ring-opened or ring-closed ligand. The COSY spectrum is a [^{1}H, ^{1}H] 2D spectrum, and this allowed protons which are coupled to each other to be identified, and when combined with the HSQC spectrum assignments could be made for the ring-opened or ring-closed aminophosphine. Finally, the TOCSY experiment allowed the N-H protons to be assigned and provided a complete picture.

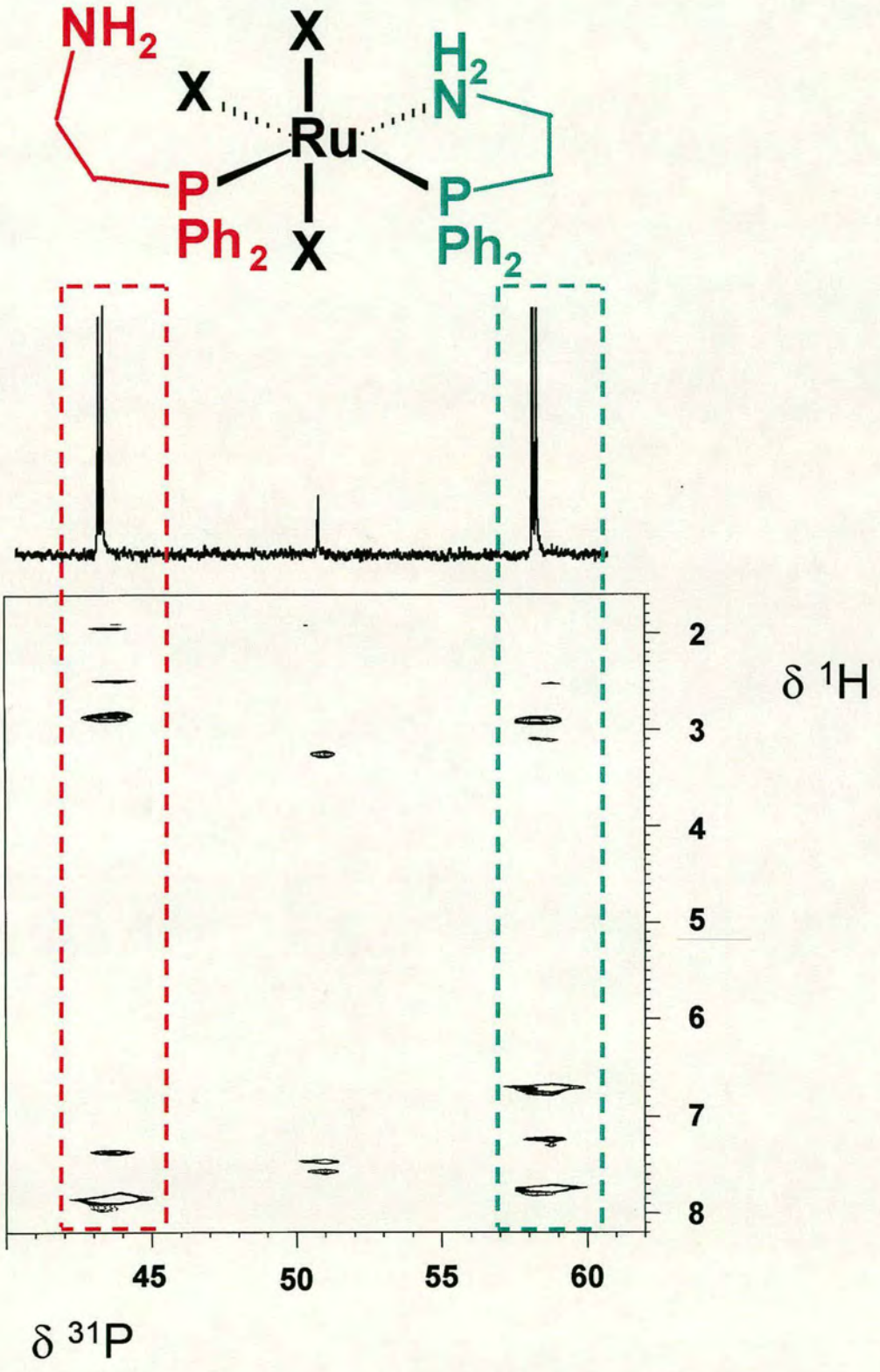

Figure 3.6 ^{31}P-^{1}H HSQC spectrum of complex **3** in DMSO-d_6 after 1 week. The ring-open ligand is shown in red and the chelated ligand in green.

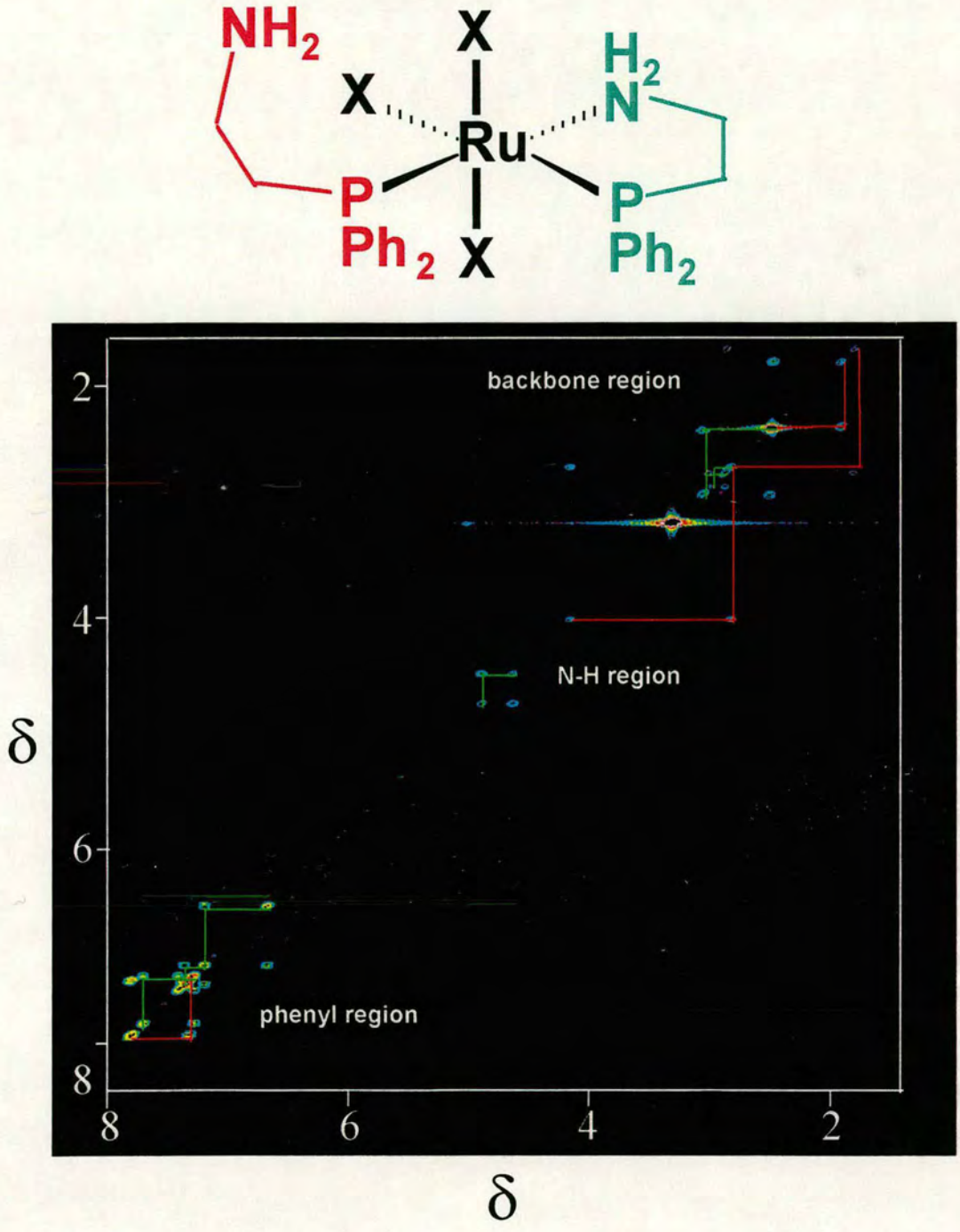

Figure 3.7 ^{1}H-^{1}H COSY spectrum of complex **3** in DMSO-d_6 after 1 week, with selected couplings traced. The ring-open ligand is shown in red and the chelated ligand in green.

The only piece of information lacking is the identity of the ligand coordinated at the vacant site after ring-opening, although as DMSO is the solvent, it is likely to be this. Coordinated DMSO could quite possibly be hidden under the free DMSO peak or the peak from water present as a trace impurity. Coupling information obtainable from the 2D NMR spectra in this regard would not be expected due to the number of bonds that the coupling would have to pass through: 5 bonds to the nearest N-H proton, 6 bonds to the nearest C-H proton or 4 bonds to a ^{31}P, but no corresponding peak is seen in the HSQC spectrum.

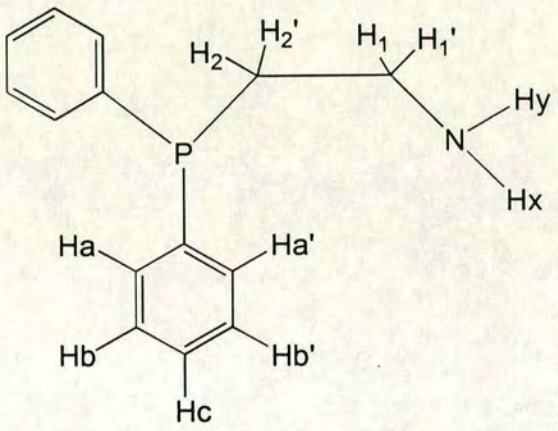

	Chelated ligand δ	*2nd phenyl ring of chelated ligand* / δ	*Pendant ligand* δ
$N\text{-}H_x$	4.97		4.23
$N\text{-}H_y$	4.71		4.23
H_1	3.13		2.89
$H_{1'}$	2.57		1.86
H_2	3.07		2.57
$H_{2'}$	2.95		1.97
H_a, $H_{a'}$	7.78	7.36	7.89
H_b, $H_{b'}$	7.40 - 7.48	7.27	7.40 - 7.48
H_c	7.4 - 7.48	6.75	7.40 - 7.48

Table 3.3 Assignment of the ^1H NMR spectrum of complex **3** in DMSO-d_6 for the chelated and pendant (ring-opened) ligand.

It can be seen from the assignments that the phenyl rings of the chelated ligand are inequivalent. This can be attributed to the pendant ligand "dangling" to one side, hence creating the difference in environment for the chelated ligand. The equivalence of the phenyl protons for the pendant aminophosphine is another argument for being ring-opened as it would now be possible for the Ru-P bond to rotate easily as the rigidity of being chelated is lost, and hence the phenyl protons could be seen as equivalent. Alternatively, the inequivalence of the chelated ligand may arise from the DMSO that is coordinated at the vacated site.

3.3.2.3.4 Conclusions

Hence it has been shown that the ligands present in complex **3** exhibit a hemilabile nature, thereby exposing an available coordination site under certain conditions, in this case in a coordinating solvent. Although the solubility of complex **3** limits its direct use in biological systems, the findings here show the potential of this style of complexes for use in medicine.

3.3.2.4 *Trans*, *cis*-$[RuCl_2(DMSO\text{-}S)_2(H_2NCH_2CH_2P(O)Ph_2\text{-}N, O)]$ **4**

The synthesis of *trans*, *cis*-$[RuCl_2(DMSO\text{-}S)_2(H_2NCH_2CH_2P(O)Ph_2\text{-}N, O)]$, **4**, was unexpected. From a 1:1 molar ratio reaction of *trans*-$[RuCl_2(DMSO)_4]$ with the aminophosphine ligand DHAP, complex **4** was formed in very low yield. The product is of a similar type to that expected, i.e. a Ru complex with one chelated ligand, two Cl ligands and two DMSO ligands. However the P(III) had been oxidised to P(V) at some stage to give the aminophosphine-oxide. The reaction was performed in air, so air oxidation during the reaction may have occured. However since the reaction was carried out in ethanol, a reducing solvent, this seems unlikely. On reanalysing the batch of ligand used for the reaction by ^{31}P NMR, it was discovered that instead of just one peak in the spectrum for the free ligand (δ -21), an extra peak was present as a minor species at δ 32.6. This corresponds well to a P=O resonance. $Ph_3P=O$ produces a resonance at δ = 31.0.[38] Therefore, the ligand had become partially oxidised while being stored, and the ligand used for the reaction was actually a 4:1 mixture of DHAP and DHAP(O). It is this

minor species that gave the product. Therefore it was to be expected that the yield would be low. Ruthenium phosphine oxide complexes can be difficult to isolate due to the lability of phosphine oxides in solution, and they are sometimes formed only as intermediates,[39] for example a Ru(II)terpy complex with $(O)Ph_2PCH_2CH_2PPh_2(O)$ quickly loses the P=O in solution.[38]

There is interest in catalytic systems which involve ruthenium with functionalised phosphine-oxide derivatives.[40] Currently, aminophosphine-oxides are being considered for ruthenium assisted enantioselective transfer hydrogenation of ketones.[41] These have been found to give high yields of product with up to 84 % enantiomeric excess, although no evidence of a Ru-O bond was found. Bisphosphine monoxide ligands are also being used in the development of chiral ruthenium Lewis acids.[42]

The ^{31}P NMR spectrum of complex **4** in $CDCl_3$ shows a singlet at 51.6 ppm. The ^{31}P resonance is deshielded compared to the free ligand, consistent with disruption of the O=P π interaction by Ru-O bonding. Up to 48 h, no other peak arises in the spectrum, indicating that in this case the phosphine oxide remains bound to the metal.

3.3.2.4.1 X-ray crystal structure of complex **4**

The product was obtained as single crystals suitable for X-ray analysis by diffusion of ether into an ethanol solution. The structure of **4** is shown in Figure 3.8. A summary of crystallographic data is given in Table 3.1, and important bond lengths and angles are given in Table 3.2. Compound **4** crystallised in the space group $P2_1/c$ with four molecules in the unit cell. The ruthenium is in the formal oxidation state of +2 and is situated in a distorted octahedral coordination environment. The P of the ligand is P(V), and the ligand forms a six-membered chelate ring, binding to the Ru through the O and the N in *cis* equatorial positions. The two chloride ligands are mutually *trans* in the axial positions and the two DMSO ligands fill the other two equatorial sites. Both DMSO molecules are coordinated through sulfur, and one is *trans* to N and the other is *trans* to O. Sulfur is a mildly π-accepting ligand, and it is reasonable to expect two π-accepting

ligands to be located orthogonal to each other.[43] There are no strong intermolecular interactions in the crystal packing.

The Ru-O bond length is 2.18(2) Å, similar to those in the chelated phosphine-oxide *trans*-[$RuCl_2${*o*-$C_6H_4(PMePh)_2$}{*o*-C_6H_4(PMePh)(P(O)MePh)} which has a Ru-O bond length of 2.166(5) Å,[44] the arene complex [(η^6-*p*-cymene)RuCl(η^2-$Ph_2PCh_2P(O)Ph_2$)][SbF_6] (Ru-O = 2.154(3) Å),[42] and the mixed-valent Ru(II/III) binuclear compound $[Ru_2(\mu\text{-}O_2CC_4H_3S)_4(OPPh_3)_2]^+$ (Ru-O(P) = 2.216(7) Å.[45]

The Ru-S bonds in the two DMSO ligands are significantly different to each other. The longest is the Ru-S *trans* to N, 2.250(5) Å, a value reasonably typical of an *S*-bound DMSO *trans* to a nitrogen, and comparable with 2.229(1) Å for [$RuCl_2$(9-(2-aminoethylamino)ethyl)adenineH)$(DMSO)_2$]Cl.[46] The Ru-S *trans* to oxygen, however, is quite short, 2.200(7) Å, similar to that for $[Ru(DMSO)(NH_3)_5]^{2+}$, 2.188(3) Å.[47] The shortness of the Ru-S bond in the amine complex is attributed by the authors to an M^+=S-O^- component, a conclusion which can be supported by the relatively long S-O bond length of 1.527(7) Å. Complex **4**, on the other hand, has a more typical S-O bonds of 1.48(2) Å, a feature found in *S*-bound DMSO molecules in $[Ru^{II}Cl_3(DMSO)_3]^-$ (1.48 Å mean)[48] and $[Ru(DMSO)_6]^{2+}$ (1.482 Å mean).[49]

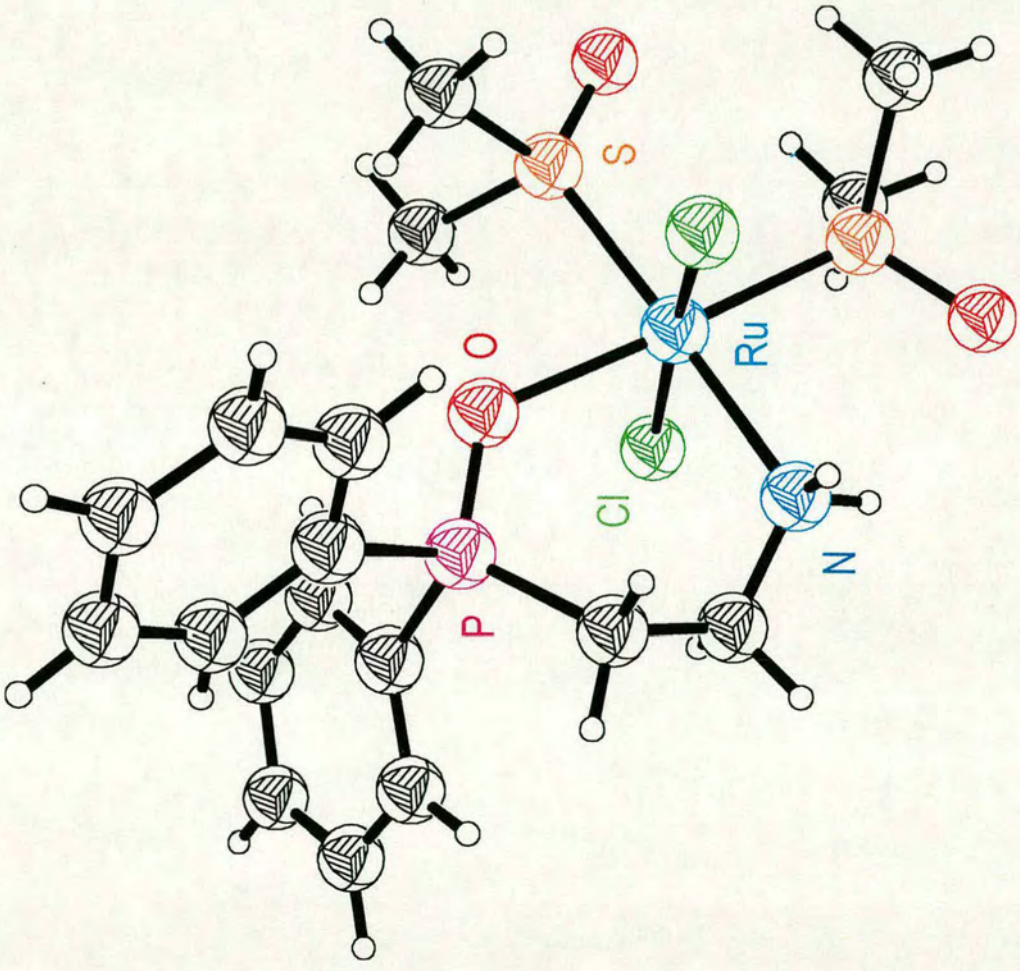

Figure 3.8 Crystal structure of $[Ru(H_2NCH_2CH_2P(O)Ph_2\text{-}N, O)(DMSO\text{-}S)_2Cl_2]$ complex **4**

A more likely explanation for the shortness of the Ru-S bond in complex **4** is that an *S*-bound ligand (weak π-acceptor) *trans* to an O (strong σ-donor) would experience little competition for the metal π-electrons, and so would be able to back-bond more strongly and hence shorten the bond length. The difference in the Ru-S bond lengths may be due to steric interactions between the phenyls on the phosphorus and the DMSO ligand which is inhibiting the approach of one of the DMSOs.

Both Ru-S bonds in complex **4** are shorter than those in *cis*-$[RuCl_2(DMSO)_4]$ (2.267 Å mean), its isomer *trans*-$[RuCl_2(DMSO)_4]$ (2.352 Å mean),[50] and $[Ru(DMSO)_6]^{2+}$ (2.259 Å mean). This can be attributed to less π-accepting ligands being present in complex 4 to compete for the available π-orbitals and π-electron density on the metal. The geometry of the coordinated DMSO ligands is distorted tetrahedral, as would be expected. The greater distortion is in the DMSO *trans* to N. This is caused by the nearby phenyl rings.

The Cl-Ru-Cl angle of 170.6(2)° shows distortion from the true octahedral value of 180°. This distortion, however, is less than in the other aminophosphine complexes **1** and **3** described in this chapter. This is due to the oxygen being the coordinating atom rather than the P, and so the phenyl rings are one atom displaced away from the metal as compared to complexes **1** and **3**, and so the distorting effect will be less. Also, there is only one coordinated aminophosphine-oxide ligand, and so the complex is not as crowded. The Ru-N bond length (2.20(2) Å) is in the expected range.[22,32,33]

3.3.2.4.2 Conclusions

The synthesis of complex **4** was a serendipitous occurrence, caused by a small portion of the ligand having been oxidised by air while stored. While the yield was low, it was also significant that a stable phosphine-oxide has been isolated and the X-ray crystal structure solved. The reactivity and potential biological applications are unknown just now, but the complex looks promising from a point of view of solubility and the groups present. Ru(II) molecules with DMSO ligands are known to be active, and the phosphine oxide offers a new approach to drug design.

3.3.2.5 $[(\eta^6\text{-}C_6H_6)Ru(DMAP\text{-}N, P)Cl][PF_6]$ **5**

The reaction of $[(\eta^6\text{-}C_6H_6)Ru(CH_3CN)_2Cl][PF_6]$ with DMAP in acetonitrile followed by work up produced red crystals of the complex $[(\eta^6\text{-}C_6H_6)Ru(DMAP\text{-}N, P)Cl][PF_6]$ **5** in moderate yield. Complex **5** is soluble in alcohols and coordinating solvents such as DMSO and acetonitrile, but insoluble in water or mixed solvents containing an appreciable (>20 %) water.

3.3.2.5.1 NMR spectroscopy of complex **5**

The ^1H NMR spectrum in CD_3CN shows a doublet for the π-coordinated benzene ring centred at δ 5.68 (J_{CP} = 0.9 Hz) due to coupling to the ^{31}P, implying that all the protons on the benzene ring are equivalent and hence there is free rotation of the π-coordinated benzene ligand. The NMe_2 groups of the ligand give rise to two separate singlet resonances at δ 3.11 and δ 3.19, indicating that the two methyl groups are inequivalent when the ligand is chelated. As the complex has a piano-stool style structure it is likely that the coordination of the N causes one methyl group to point more towards the benzene ring and one to point more away from it, causing inequivalence. The ^{31}P NMR spectrum shows a singlet at δ 58, appropriate for a ring-closed structure. The $^{13}C\{^1H\}$ NMR shows resonances at δ 125-135 for the P-Ph_2 carbons. The η^6-coordinated benzene ring is a doublet, due to coupling to the ^{31}P, at δ 89.3 (J_{CP} = 2.95 Hz), indicative of Ru in the oxidation state +2.[35] The N-CH_2- signal appears as a doublet centred at δ 60.5 (J_{CP} = 2.98 Hz), and the P-CH_2- resonance is a doublet centred at δ 25.6 (J_{CP} = 26.66 Hz). The two N-CH_3 signals are singlets at δ 58.3 and δ 56.5. There was no change in the NMR spectrum after three days incubation at 300 K, so ring-opening of the chelate-ring in a coordinating solvent does not occur.

3.3.2.5.2 X-ray crystal structure of complex **5**

Crystals suitable for X-ray analysis were grown by diffusion of ether into an acetonitrile solution of **5**. Complex **5** crystallised as the acetonitrile solvate in the space-group $P2_1/c$ with four molecules in the unit cell. In the molecule, the ruthenium is in the expected piano-stool type geometry typical for Ru(II) arene complexes. The structure can be seen in Figure 3.9. A summary of crystal data is presented in Table 3.1 and selected bond lengths and angles are in Table 3.2. There are no unusual intermolecular reactions in the unit cell.

The structure of **5** can be compared to that of [Cp*Ru(DMAP)Cl].[35] The Ru-P bond lengths are similar, 2.3122(11) Å for **5**, as compared to 2.289(1) Å for the Cp* complex. The Ru-N bond length, however, is quite different, despite the obvious similarities in the complexes. In **5** it is 2.212(3) Å, significantly shorter than the value of 2.260(2) Å for the Cp* complex. The Ru-Cl bond is also noticeably shorter (2.3986(11) Å as opposed to 2.441(1) Å), but in the region of Ru-Cl bonds for half-sandwich complexes of Ru(II).[51] The reason for this is probably a result of two factors, the steric restrictions imposed by the methyl groups on the Cp*, and also the change in the overall charge on the complex from +1 to 0 as the Cp* is an anionic ligand. The P-Ru-N angle of 81.68(9)° compares well with that of the Cp* complex.

When compared to complexes **1** and **4**, **5** has the longest Ru-P bond, but this is to be expected since the phenyl rings on the P and the benzene ring would interact. The Ru-N and Ru-Cl bond lengths are similar.

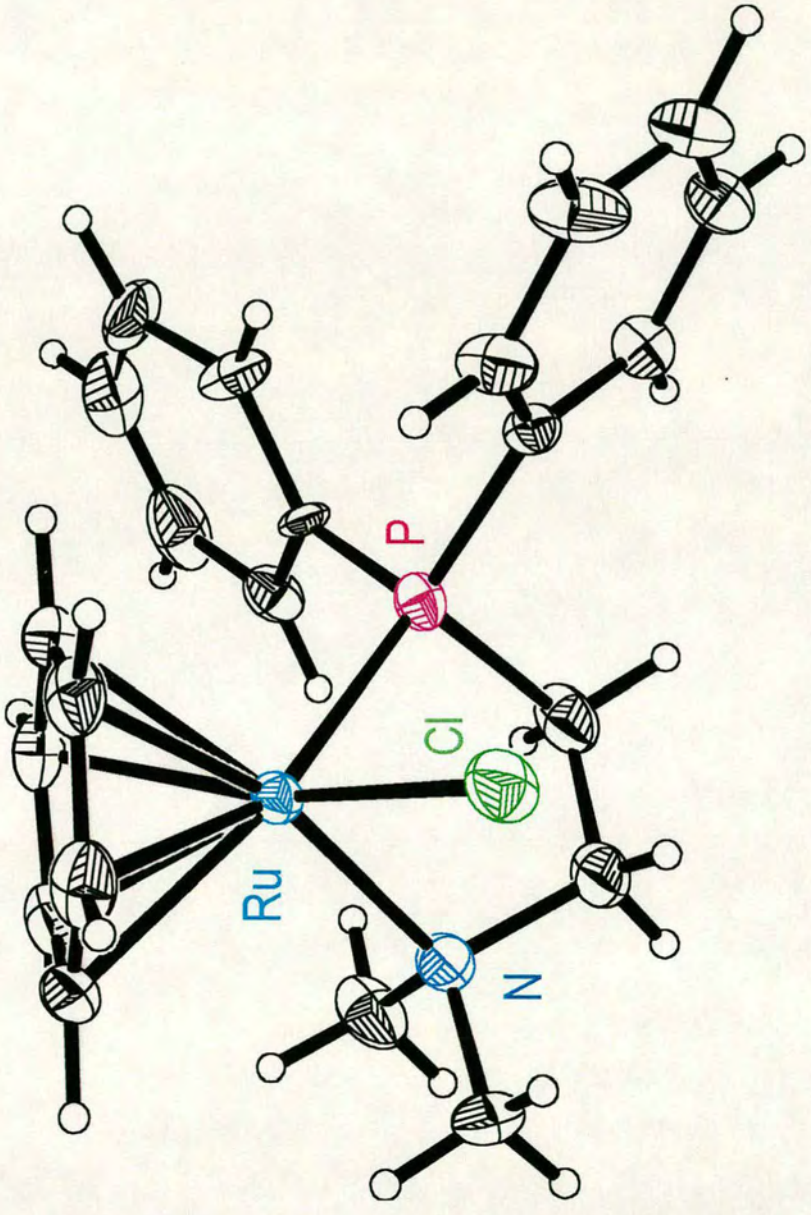

Figure 3.9 Crystal structure of $[(\eta^6\text{-}C_6H_6)Ru(DMAP\text{-}N, P)Cl][PF_6]$ complex **5**. The PF_6^- anion has been omitted for clarity

3.3.2.5.3 UV/Vis spectroscopy of complex **5**

The UV/Vis spectrum of **5** in DMSO undergoes a change with time, see Figure 3.10. The absorbtion band at 326 nm gradually decreases with time and the band at 300 nm increases concomitantly, with an isobestic point at 320 nm. By following the absorbance decrease at 326 nm with time, assuming a first order reaction and treating the data by the Guggenheim method[52] a first order rate-constant of 2.03×10^{-4} s^{-1} was obtained. This change can be attributed to loss of the chloride, and presumably coordination of a DMSO molecule as the change is inhibited by the presence of 100 mM LiCl.

3.3.2.5.4 Reaction of complex **5** with carbon monoxide

In order to investigate the hemilability of the chelated aminophosphine ligand in **5**, a reaction with CO(g) was performed. A similar compound, [Cp*Ru(DMAP)Cl] [35] has been reported to ring-open (Ru-N bond breaks) when saturated and stirred with CO(g). The ring opens, and CO coordinates.

As well as investigating the lability of the ligand, it is interesting from a biological point of view to investigate whether or not CO binds to the complex. CO has a similar size to O_2, and can bind irreversibly to haemoglobin and myoglobin. CO has also been linked to SID (Sudden Infant Death) syndrome,[53] and epilepsy.[54] It is also thought to play a role as a response mediator in the central nervous system[55] and as a cardiovascular modulator.[56]

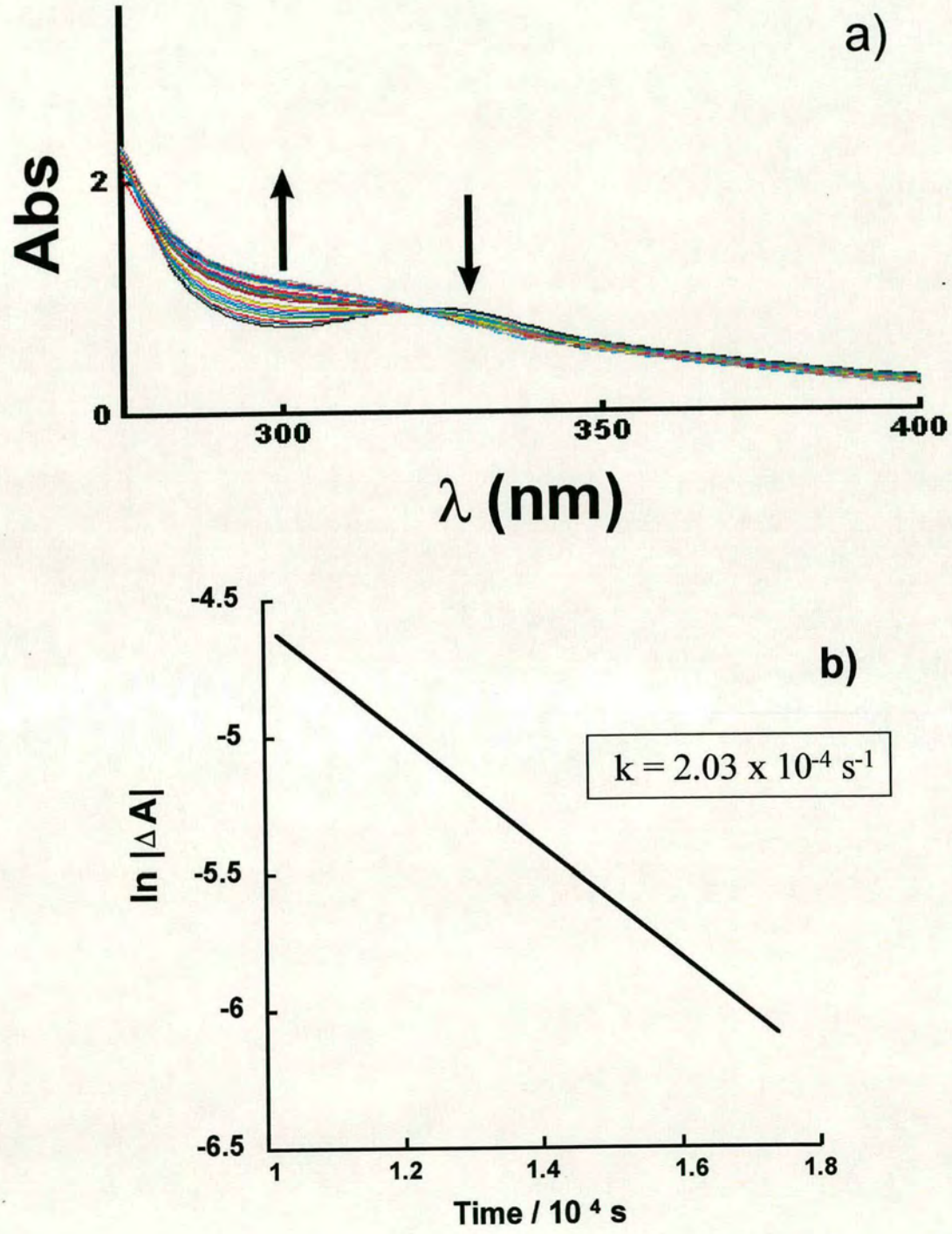

Figure 3.10 a) UV/Vis spectrum of complex **5** in DMSO over a period of 12 h **b)** plot of ln |ΔA| vs time (sec) for the loss of chloride from complex **5** in DMSO

After isolation and drying, the product of the reaction was investigated by IR and NMR spectroscopy. The IR spectrum (KBr disc) showed no peak appropriate to CO bound to a metal. A shift to lower energy compared to free CO[57] (2143 cm^{-1}) would have been expected, if coordinated, due to a lowering of the C-O bond order. This is because CO is a π-acceptor ligand, and accepts electron density back into the π* orbital of the C-O bond. The ^{1}H NMR spectrum of the product in CD_3CN showed no difference to the starting material. Tellingly, the methyl groups ($-N(CH_3)_2$) are still present as two singlets. If the chelate ring had opened via Ru-N bond breakage, we would expect to see the pendant methyl groups as equivalent, and hence a singlet. The ^{13}C NMR spectrum shows no peak appropriate for CO. All peaks in the spectrum correspond to the original complex **5**. The ^{31}P NMR shows a single resonance at δ 57.9, the same value as complex **5**, and appropriate for a ring-closed complex. Hence, we can say that complex **5** does not ring-open in the presence of CO, and does not react it with it at all.

3.3.2.5.5 Conclusions

Complex **5** is a Ru(arene) aminophosphine complex which exhibits the typical piano-stool type geometry. It is insoluble in water and water mixed with other solvents and although there is evidence of loss of the chloride ligand, none could be found to back up the hypothesis of chelate ring-opening. Hence, this complex does not appear to have much biological potential.

3.4 Conclusions

A range of Ru(II)aminophosphine complexes have been synthesised in this chapter. These complexes were generally difficult to synthesise and the result was low yields for complexes **1** and **4**. However, the crystal structures of all compounds were obtained, so the structures of them all could be unambiguously confirmed. Complex **3** was shown to undergo a ring-opening reaction in coordinating solvents, thereby exposing a coordination site at the metal. This was the rationale behind developing these style of complexes. It is hoped that under certain biological conditions the complexes would

ring-open. Unfortunately, these complexes are also insoluble in water, but if the synthesis of water soluble ruthenium aminophosphine complexes was developed, there is no reason at present why these complexes shouldn't become important biological agents.

3.5 References

[1] M. Basset, D.L. Davies, J. Neild, L.J.S. Prouse, D.R. Russell *Polyhedron* **1991**, 10, 501; K. von Issleib, A. Kipke, V. Hanfeld *Z. Anorg. Allg. Chem.* **1978**, 444, 5; K. von Issleib, A. Kipke *Z. Anorg. Allg. Chem.* **1980**, 464, 176; G.K. Anderson, R. Kumar *Inorg. Chem.* **1984**, 23, 4064; M.M.T. Khan, E.R. Rao *Polyhedron* **1987**, 6, 1727; M.M.T. Khan, V.V.S. Reddy, H.C. Bajat *Inorg. Chim. Acta* **1987**, 130, 163; V.V.S. Reddy, S. Vijay *J. Mol. Catal.* **1988**, 45, 73

[2] S. Chatterjee, D.C.R. Hockless, G. Salem, P. Waring *J. Chem. Soc. Dalton Trans.* **1997**, 3889

[3] J. Reedijk *J. Chem. Soc. Chem. Commun.* **1996**, 801

[4] J.S. Lewis, J. Zweit, P.J. Blower *Polyhedron* **1998**, 17, 513

[5] S.J. Berners-Price, R.J. Bowen, P. Galettis, P.C. Healy, M.J. McKeage *Coord. Chem. Rev.* **1999**, 186, 823

[6] S.J. Berners-Price, P.J. Sadler *Structure and Bonding* **1988**, 70, 27

[7] S.J. Berners-Price, R.J. Bowen, M.J. McKeage, P. Galettis, L. Ding, B.C. Baguley, W. Brouwer *J. Inorg. Biochem.* **1997**, 67, 154

[8] F.A. Cotton and G. Wilkinson *Advanced Inorganic Chemistry*, Wiley, New York, 4th edn., 1980, p.1200

[9] A. Togni, L.M. Venanzi *Angew. Chem. Int. Ed. Engl.* **1994**, 33, 497

[10] A. Habtemariam, P.J. Sadler *J. Chem. Soc. Chem. Commun.* **1996**, 1785

[11] N. Margiotta, A. Habtemariam, P.J. Sadler *Angew. Chem. Int. Ed. Engl.* **1997**, 36, 1185

[12] K. Neplechova, J. Kasparkova, O. Vrana, O. Novakova, A. Habtemariam, B. Watchman, P.J. Sadler, V. Brabec *Molecular Pharmacology* **1999**, 56, 20

[13] M.M. Taqui-Khan, A.E. Martell *"Homogenous Catalysis by Metal Complexes"*, Academic Press, New York, **1974**, Vol. 1, II

[14] D.W. Meek *Homogenous Catalysis and Metal Phosphine Complexes* Ed. L. Pignolet, ch. 8, Plenum Press, New York, **1983**

[15] C. Hampton, W.R. Cullen, B.R. James, J.-P. Charland *J. Am. Chem. Soc.* **1988**, 110, 6918; C.R.S.M. Hampton, I.R. Butler, W.R. Cullen, B.R. James, J.-P. Charland, J. Simpson *Inorg. Chem.* **1992**, 31, 5509

[16] C. Mudalige, S.J. Rettig, W.R. Cullen, B.R. James *J. Chem. Soc. Chem. Commun.* **1993**, 830

[17] A.A. Batista, E.A. Polato, S.L. Queiroz, O.R. Nascimento, B.R. James, S.J. Rettig *Inorg. Chim. Acta* **1995**, 230, 111

[18] M.M. Taqui-Khan, H.C. Bajaj, M.R.H. Siddiqui, V. Vijay Sen Reddy, B.T. Khan *J. Chem. Soc. Dalton Trans.* **1985**, 12, 2603

[19] J.X. Gao, H.L. Wan, W.K. Wong, M.C. Tse, W.T. Wong *Polyhedron* **1996**, 15, 1241

[20] D Chandrika Mudalige, E.S. Ma, S.J. Rettig, B. R. James, W.R. Cullen *Inorg. Chem.* **1997**, 36, 5426

[21] M.M.T. Khan, A.P. Reddy *Polyhedron* **1987**, 6, 2009

[22] J.-X. Gao, H.-L. Wan, W.-K. Wong, M.-C. Tse, W.-T. Wong *Polyhedron* **1996**, 15, 1241

[23] L. Costella, A. del Zotta, A. Mezzetti, E. Zangrando, P. Rigo *J. Chem. Soc. Dalton Trans.* **1993**, 3001

[24] Z. Guo, A. Habtemariam, P.J. Sadler, B.R. James *Inorg. Chim. Acta* **1998**, 273, 1

[25] E.W. Abel *J. Chem. Soc.* **1959**, 3178

[26] F.B. McCormick, D.D. Cox, W.B. Gleason *Organometallics* **1993**, 12, 610

[27] A. Habtemariam *Unpublished results*

[28] D.J. Ager, I. Prakash, D.R. Schaad *Chem. Rev.* **1996**, 96, 835; M.J. McKennan, A.J. Meyers, K. Drauz, M. Schwarm *J. Org. Chem.* **1993**, 58, 3568; H.C. Brown, T.P. Stocky *J. Am. Chem. Soc.* **1977**, 99, 8218; A. Abiko, S. Masamune *Tet. Letters* **1992**, 33, 5517; G.A. Smith, R.E. Gawly *Org. Synth.* **1985**, 63, 136

[29] E.B. Boyer, P.A. Harding, S.D. Robinson *J. Chem. Soc. Dalton Trans.* **1986**, 1771; G. Sia, A.L. Rheingold, B.J. Haggerty, D.W. Meek *Inorg. Chem.* **1992**, 31, 900; A. Albinati, Q. Jiang, H. Ruegger, L.M. Venanzi *Inorg. Chem.* 1993, 32, 4940

[30] D.E. Fogg, B.R. James *J. Organomet. Chem.* **1993**, 462, C21

[31] A.G. Orpen, L. Brammer, F.H. Allen, O. Kennard, D.G. Watson, R. Taylor *J. Chem. Soc. Dalton Trans.* **1989**, 83; A.M. Joshi, I.S. Thorburn, S.J. Rettig, B.R. James *Inorg. Chim. Acta* **1992**, 283, 198

[32] D. Drommi, F. Nicolo, C.G. Arena, G. Bruno, F. Faraone, R. Gobetto *Inorg. Chim. Acta* **1994**, 221, 109

[33] L. Costella, A. Del Zotto, A. Mezzetti, E. Zangrando, P. Rigo *J. Chem. Soc. Dalton Trans.* **1993**, 3001

[34] J.Y. Shen, C. Slugovc, P. Wiede, K. Mereiter, R. Schmid, K. Kirchner *Inorg. Chim. Acta* **1998**, 268, 69

[35] K. Merciter, R. Schmid, K. Kirchner *Organometallics* **1997**, 16, 1956

[36] M.M. Taqui-Khan, V. Vijay san Reddy *Inorg. Chem.* **1986**, 25, 208; J.C. Briggs, C.A. McAuliffe, G. Dyer *J. Chem. Soc. Dalton Trans.* **1984**, 423; D.F. Gill, B.E. Mann, B.L. Shaw *J. Chem. Soc. Dalton Trans.* **1973**, 311; G.K. Anderson, R. Turner *Inorg. Chem.* **1984**, 24, 4064

[37] P.E. Garrou *Chem. Rev.* **1981**, 81, 229

[38] A. Dovletoglou, S.A. Adeyemi, M.H. Lynn, D.J. Hodgson, T.J. Meyer *J. Am. Chem. Soc.* **1990**, 112, 8989.

[39] B.A. Mayer, B.K. Sipe, T.J. Mayer *Inorg. Chem.* **1981**, 20, 1475; J.-T. Groves, K.-H. Ahn *Inorg. Chem.* **1987**, 26, 3831; C.-M. Che, K.-Y. Wong *J. Chem. Soc. Dalton Trans.* **1989**, 2065; A. Araneo, A. Trovati *Inorg. Chim. Acta* **1969**, 3, 471; R.S. Tanke, E.M. Holt, R.H. Crabtree *Inorg. Chem.* **1991**, 30, 1714

[40] K.M. Pietrusiewicz *Phosphorus, Sulfur and Silicon* **1996**, 573; P. Kielbasinski, R. Zurawinski, K.M. Pietrusiewicz, M. Zablock *Polish J. Chem.* **1998**, 72, 564

[41] A.M. Maj, K.M. Pietrusiewicz, I. Suisse, F. Agbossou, A. Mortreux *Tet. Asymmetry* **1999**, 10, 831

[42] J.W. Faller, B.P. Patel, M.A. Albrizzio, M. Curtis *Organometallics* **1999**, 18, 3096

[43] M.M. Olmstead, Y. Maisonnat, J.P. Farr, A.L. Balch *Inorg. Chem.* **1981**, 4061

[44] S.R. Hall, B.W. Shelton, A.H. White *Aust. J. Chem* **1983**, 36, 267

[45] M.C. Barral, R. Jiménez, J.L. Priego, E.C. Royer, M.J. Saucedo, F.A. Urbanos *Polyhedron* **1995**, 14, 2419

[46] T. Kawamura, M. Ebihara, H. Katayama, H. Nishikawa, T. Yamaka *J. Chem. Soc. Dalton Trans.* **1991**, 2703

[47] F.C. March, G. Ferguson *Can. J. Chem.* **1971**, 49, 3590

[48] R.S. McMillan, A. Mercer, B.R. James, J. Trotter *J. Chem. Soc. Dalton Trans.* **1995**, 1006

[49] A.R. Davies, F.W.B. Einstein, N.P. Farrell, B.R. James, R.S. McMillan *Inorg. Chem.* **1978**, 17, 1965

[50] E. Alessio, G. Mestroni, G. Nardin, W.M. Attia, M. Calligaris, G. Sava, S. Zorzet *Inorg. Chem.* **1988**, 27, 4099

[51] I. los de Rios, M.J. Tenorio, J. Padilla, M.L. Puerta, P. Valerga *J. Chem. Soc. Dalton Trans.* **1996**, 377

[52] D.P. Shoemaker and C.W. Garland *Experiments in Physical Chemistry*, McGraw-Hill, New York, **1962**, p.222

[53] G.M. Reid, H. Tervit *Medical Hypotheses* **1999**, 52, 569

[54] C. Montecot, J. Seylaz, E. Pinard *Neuroreport* **1998**, 9, 2341

[55] A.A. Steiner, E. Colombari, L.G.S. Branco *Am. J. Physiol. - Reg. Integ. Comp. Physiol* **1999**, 46, R499

[56] R.A. Johnson, F. Kozma, E. Colombari *Braz. J. Med. Biol. Res.* **1999**, 32, 1

[57] K. Nakamoto *Infrared and Raman spectra of inorganic and coordination compounds* **1986**, Wiley, NY

Chapter 4

Synthesis and characterisation of Ru(II)arene complexes

4.1 Introduction

Metal arene π-complexes are of considerable interest for their potential roles in homogenous catalysis, for example in olefin hydrogenation[1] and ring-opening polymerisation reactions,[2] and now, as a result of the work contained in this thesis, in their prospective use as anti-cancer agents.

The first report of π-$C_6H_6RuCl_2$ was in 1967 by Winkhaus and Singer.[3] They presumed that this was a polymeric material and postulated a bidentate benzene ring, an unusual mode of binding for Ru(II), but well known at the time for silver(I) complexes.[4] It was analogous to the structure which had been proposed for $[RuCl_2(diene)]_2$, where diene is norboradiene or cyclooctadiene.[5] The oxidation state of +2 was relatively high, and therefore interesting as most work with arene complexes up until then had been with zerovalent metals.[6]

The synthesis of this π-$C_6H_6RuCl_2$ was taken further and developed by two independent groups, Bennett et al[7] and Zelonka et al,[8] at around the same time. Both syntheses are based on the reaction of $RuCl_3$ and 1, 3-cyclohexadiene in ethanol, with Zelonka et al claiming a wider solubility of their compound as a result of performing the reaction in aqueous ethanol. The complex is now formulated as being dimeric.

It was quickly realised that monomeric Ru(II)-arene complexes could be formed by breaking the dimeric structure and addition of a variety of ligands such as PEt_3 or $P(OEt_3)$.[8] These syntheses have formed the foundation-stone for a large range of work as they act as excellent synthetic precursors and an easy entry point to arene chemistry of both Ru(II) and Ru(0)[9].

The complex $[(p\text{-cymene})RuCl_2]_2$ (*p*-cymene = *para*-isopropyl toluene) was also readily synthesised in high yields by this method using α-terpinene as the arene precursor instead of the cyclohexadiene. This is frequently the reagent of choice in preference to

the benzene complex due to its improved solubility in organic solvents. These two complexes (the benzene and *p*-cymene) also offer a limited route to other arene complexes *via* arene substitution reactions. Possible replacements include toluene, ethylbenzene, cumene and *o*, *m* and *p*-xylene.[7] *p*-Cymene is the most easily replaced yet there is no significant difference in bond length between the two.[10] However, arenes having electron withdrawing substituents such as Cl, F or CO_2Et failed completely to replace a coordinated arene and so an alternative method of synthesis is required to introduce variety on the arene ring.

Ru(arene) complexes were attractive to us for a number of reasons. They are known to keep the metal in the oxidation state of 2+. This is an advantage as it is unknown which is the active form of ruthenium complexes *in vivo*. In fact, Ru(III) complexes have been postulated as prodrugs, being reduced in the hypoxic environment of a tumour to Ru(II).[11,32] The arene ring gives the complex a lipophilic centre. This could be very important for transporting the metal across the cell membrane. It is also known that the (η^6-C_6H_6)Ru(II) bonds resist hydrolysis and are indefinitely stable, at least in the dark, at ordinary acidities, even in water.[12] This style of complex also has potential for variety in two distinct areas, the π-arene ring and also the ligands that provide the "legs" to the piano-stool shape.

Introducing variety on the arene ring allows investigation of structure activity relationships for the arene complexes. If a range of similar complexes is to be tested for anticancer activity, it is of interest to discover which parts of the molecule are important. What effect will changing the arene ring from benzene to *p*-cymene, ester or biphenyl have? Does changing the halide have any influence, as these complexes are likely to find their reactive site upon loss of the halide? And how important is the ancillary ligand (en)? In this chapter a range of complexes are synthesised in order to investigate this. The arene ligand is varied from benzene to *p*-cymene, alkylbenzoate and biphenyl. The halide is changed from chloro to bromo and iodo and the ancillary ligand ranges from acetonitrile to isonicotinamide and ethylenediamine.

All the complexes synthesised in this chapter have good water solubility. Even though the arene ring is lipophilic, the ancillary ligands and the fact that the complexes are generally charged give them their water solubility, up to 40 mM.

4.2 Experimental

$[(\eta^6\text{-}C_6H_6)RuCl_2]_2$ and $[(\eta^6\text{-}p\text{-cymene})RuCl_2]_2$ were prepared according to the literature procedures.[7] $[(\eta^6\text{-}C_6H_6)RuCl(CH_3CN)_2][PF_6]$, complex **7**, was synthesised by the published method.[13]

4.2.1 Preparation of $[(\eta^6\text{-}p\text{-cymene})RuCl_2(\text{isonicotinamide})]$ complex 6

$[(\eta^6\text{-}p\text{-cymene})RuCl_2]_2$ (0.129 g, 0.21 mmol) was stirred in benzene (50 ml), and isonicotinamide (0.052 g, 0.43 mmol) was added in one portion. The mixture was heated to reflux under argon for 4 h during which time a mustard coloured precipitate had formed. This was collected, washed with a little benzene and recrystallised from methanol/ether to give a red crystalline material.

Yield: 0.061 g, 0.14 mmol, 33.8 %

$C_{16}H_{20}Cl_2N_2ORu$ (428.30) Calc. %C = 44.87 %H = 4.71 %N = 6.54

Found %C = 44.65 %H = 4.54 %N = 6.23

4.2.2 Preparation of $[(\eta^6\text{-}C_6H_6)RuBr_2]_2$

$[(\eta^6\text{-}C_6H_6)RuCl_2]_2$ (1 g, 1.99 mmol) was dissolved in the minimum amount of hot water and filtered. Solid KBr (8.75 g, 70 mmol) was added in one portion and the mixture shaken for five minutes. After leaving to stand at ambient temperature overnight, the dark-red precipitate was collected, washed with a little cold water and dried *in vacuo*.

Yield: 0.583 g, 0.86 mmol, 86 %

$C_{12}H_{12}Br_4Ru_2$ (677.97) Calc. %C = 21.26 %H = 1.78

Found %C = 21.03 %H = 1.93

NMR (DMSO-d_6) δ ^{1}H 5.92 (s)

4.2.3 Preparation of [(η^6-C_6H_6)RuBr(CH_3CN)$_2$][PF_6] complex 8

This was prepared in a manner analogous to the literature procedure.[13] [(η^6-C_6H_6)$RuBr_2$]$_2$ (0.4 g, 0.59 mmol) was suspended in dry acetonitrile (50 ml). NH_4PF_6 (0.2 g, 1.23 mmol) in dry acetonitrile (2 ml) was added in one portion and the mixture stirred at ambient temperature. After 1 h, the pale precipitate was filtered off and the remaining red solution evaporated leaving a brownish solid. Hot acetonitrile (2 ml) was added and the brown supernatant liquid removed leaving a clean orange solid. This was dissolved in hot acetonitrile and ether was added to precipitate an orange-gold microcrystalline solid which was collected, washed with ether and dried *in vacuo*.

Yield: 0.29 g, 0.59 mmol, 50 %

$C_{10}H_{12}BrF_6N_2PRu$ (486.18) Calc. %C = 24.70 %H = 2.49 %N = 5.76

Found %C = 24.52 %H = 2.41 %N = 5.48

NMR (CD_3CN) δ ^{1}H 5.97 (s)

4.2.4 Preparation of [(η^6-*p*-cymene)RuCl(CH_3CN)$_2$][PF_6], complex 9

This was prepared in a manner analogous to that described in the literature.[13] reagents and quantities used: NH_4PF_6 (0.18 g, 1.10 mmol), [(η^6-*p*-cymene)$RuCl_2$]$_2$ (0.31 g, 0.51 mmol), dry acetonitrile (30 ml). Recrystallised as bright orange crystals from ether diffusion into an acetonitrile solution.

Yield: 0.28 g, 0.56 mmol, 54.9 %

$C_{14}H_{20}ClF_6N_2PRu$ (497.82) Calc. %C = 33.78 %H = 4.05 %N = 5.62

Found %C = 33.80 %H = 3.91 %N = 5.53

NMR (CD_3CN) δ ^{1}H 5.35 (m, 2H), 5.28 (m, 2H) 1.23 (s, 6 H)

4.2.5 Preparation of $[(\eta^6\text{-}p\text{-cymene})RuBr_2]_2$

The procedure was described in Section 4.2.2. using $[(\eta^6\text{-}p\text{-cymene})RuCl_2]_2$ (0.3 g, 0.48 mmol), KBr (12 g, 10 mmol)

Yield: 0.37 g, 0.47 mmol, 97.9 %

$C_{20}H_{28}Br_4Ru_2$ (790.18)	Calc.	%C = 30.40 %H = 3.57
	Found	%C = 31.05 %H = 3.78
NMR (DMSO-d_6)	δ ^{1}H	5.42 (m, 2H) 5.32 (m, 2H) 2.87 (m, 1H) 2.13 (s 3H), 1.24 (d, 6H)

4.2.6 Preparation of $[(\eta^6\text{-}p\text{-cymene})RuBr(CH_3CN)_2][PF_6]$, complex 10

Procedure analogous to literature.[13] $[(\eta^6\text{-}p\text{-cymene})RuBr_2]_2$ (0.24 g, 0.3 mmol), NH_4PF_6 (0.12 g, 0.74 mmol), 12 ml dry acetonitrile. Final product recrystallised from acetonitrile/ether as deep red crystals.

Yield: 0.28 g, 0.52 mmol, 86.7 %

$C_{14}H_{20}BrF_6N_2PRu$ (542.27)	Calc.	%C = 31.01 %H = 3.72 %N = 5.16
	Found	%C = 31.22 %H = 3.75 %N = 5.09
NMR (CD_3CN)	δ ^{1}H	5.44 (m, 2H) 5.36 (m, 2H) 1.26 (s, 6H)

4.2.7 Preparation of $[(\eta^6\text{-}C_6H_6)RuI_2]_2$

$[(\eta^6\text{-}C_6H_6)RuCl_2]_2$ (1 g, 1.99 mmol) was dissolved in the minimum amount of hot water and filtered. Solid KI (8 g, 50 mmol) was added in one portion. A fine red precipitate formed within one minute of addition. This was collected, washed with a little water and dried *in vacuo*.

Yield: 0.95 g, 1.10 mmol, 55.3 %

$C_{12}H_{12}I_4Ru_2$ (865.97)	Calc.	%C = 16.64 %H = 1.40
	Found	%C = 16.12 %H = 1.25
NMR (DMSO-d_6)	δ ^{1}H	5.83 (s)

4.2.8 Preparation of $[(\eta^6\text{-}C_6H_6)RuCl(H_2NCH_2CH_2NH_2\text{-}N, N)][PF_6]$, complex 11

The synthesis is based on a published procedure.[14] $[(\eta^6\text{-}C_6H_6)RuCl_2]_2$ (0.167 g, 0.33 mmol) was suspended in dry methanol (50 ml) and ethylenediamine (0.06 g, 1 mmol) added in one portion. This was stirred for 3 h, filtered and NH_4PF_6 (0.5 g, 3.07 mmol) added. The volume was slowly reduced to approx. 15 ml on the rotary evaporator. The product formed as a microcrystalline solid on leaving to stand at 277 K. This was collected, washed with ether and recrystallised from methanol/ether.

Yield: 0.128 g, 0.31 mmol, 47.0 %

$C_8H_{14}ClF_6N_2PRu$ (419.69)	Calc. %C = 22.89 %H = 3.36 %N = 6.67
	Found %C = 22.81 %H = 3.24 %N = 6.51
NMR (DMSO-d_6)	δ ^{1}H 6.45 (b, 2H), 5.86 (s, 6H), 4.28 (b, 2H), 2.34(m, 2H), 2.17 (m, 2H)

4.2.9 Preparation of $[(\eta^6\text{-}C_6H_6)RuI(H_2NCH_2CH_2NH_2\text{-}N, N)][PF_6]$, complex 12

The procedure was as described in Section 4.2.8. using $[(\eta^6\text{-}C_6H_6)RuI_2]_2$ (0.48 g, 0.55 mmol), dry methanol (80 ml), ethylenediamine (0.12 g, 2 mmol), NH_4PF_6 (0.5 g, 3.07 mmol)

Yield: 0.41 g, 0.81 mmol, 73.3 %

$C_8H_{14}IF_6N_2PRu$ (511.14)	Calc. %C = 18.80 %H = 2.76 %N = 5.48
	Found %C = 18.52 %H = 2.43 %N = 5.14
NMR (DMSO-d_6)	δ ^{1}H 6.42 (b, 2H), 5.86 (s, 6H), 4.22 (b, 2H), 2.35(m, 2H), 2.15 (m, 2H)

4.2.10 Preparation of [(η^6-*p*-cymene)RuCl($H_2NCH_2CH_2NH_2$-*N,N*)][PF_6], complex 13

The procedure was as described in Section 4.2.8. using [(η^6-*p*-cymene)$RuCl_2$]$_2$ (0.39 g, 0.64 mmol) was stirred in methanol (60 ml) and ethylenediamine (0.12 g, 2.00 mmol) added in one portion. The reaction was stirred for 1.5 h and the green liquid filtered. NH_4PF_6 (0.52 g, 3.2 mmol) was added to the yellow filtrate and the volume reduced to 15 ml. This was left to stand at 277 K for 6 h during which time orange crystals formed. These were collected, washed with a little cold methanol followed by ether and dried *in vacuo*.

Yield 0.23 g, 0.48 mmol, 37.7 %

$C_{12}H_{22}ClF_6N_2PRu$ (475.81)	Calc.	%C = 30.29 %H = 4.66 %N = 5.88
	Found	%C = 30.05 %H = 4.41 %N = 5.98
NMR (DMSO-d_6)	δ ^{1}H	6.13(b, 2H), 5.48 (d, 2H), 5.32 (d, 2H), 4.22 (b, 2H), 2.71 (m, 1H), 2.43 (m, 2H), 2.32 (m, 2H), 2.11(s, 3H), 1.25 (d, 6H)

4.2.11 Preparation of [(η^6-*p*-cymene)RuI_2]$_2$

The procedure was as described in Section 4.2.2. using [(η^6-*p*-cymene)$RuCl_2$]$_2$ (0.44 g, 0.72 mmol), KI (0.92 g, 5.54 mmol).

Yield: 0.68 g, 0.70 mmol, 97.2 %

$C_{20}H_{28}I_4Ru_2$ (978.18)	Calc.	%C = 24.56 %H = 2.89
	Found	%C = 23.94 %H = 2.62
NMR (DMSO-d_6)	δ ^{1}H	5.43 (d, 2H), 5.33 (d, 2H), 2.74 (m, 1H), 2.11(s, 3H), 1.34 (d, 6H)

4.2.12 Preparation of [(η^6-*p*-cymene)RuI($H_2NCH_2CH_2NH_2$-*N,N*)][I], complex 14

The procedure was as described in Section 4.2.8. $[(\eta^6\text{-}p\text{-cymene})RuI_2]_2$ (0.34 g, 0.348 mmol), ethylenediamine (0.06 g, 1mmol), NH_4PF_6 (0.52 g, 3.2 mmol). The volume was reduced to 15 ml and left to stand at 277 K overnight. The red crystals which formed were collected and washed with a little cold methanol, followed by ether, and dried *in vacuo*.

Yield: 0.24 g, 0.44 mmol, 63.2%

$C_{12}H_{22}I_2N_2Ru$ (549.16)	Calc. %C = 26.25 %H = 4.04 %N = 5.10
	Found %C = 26.11 %H = 3.88 %N = 4.93
NMR (DMSO-d_6)	δ ^{1}H 6.15 (b, 2H), 5.51 (d, 2H), 5.35 (d, 2H), 4.24 (b, 2H), 2.69 (m, 1H), 2.37 (m, 2H), 2.29 (m, 2H), 2.08 (s, 3H), 1.33 (d, 6H)

4.2.13 Preparation of [(η^6-*p*-cymene)Ru(en)(9-ethylguanine)][PF_6]$_2$, complex 15

$[(\eta^6\text{-}p\text{-cymene})Ru(en)Cl]^+[PF_6]^-$ **13** (0.057 g, 0.12 mmol) was dissolved in degassed aqueous ethanol (70:30, EtOH:H_2O) (20 ml). 9-Ethylguanine (0.025 g, 0.14 mmol) was dissolved in degassed aq. ethanol (5 ml) and added in one portion. The reaction was sealed and stirred at ambient temperature for 15 h. The solvent was removed *in vacuo* leaving a yellow residue. The residue was taken up in H_2O and loaded on to a short column of CM25 Sephadex cation exchange resin. The column was first eluted with 0.05 M NaCl solution to remove any unreacted 9-egua. The yellow band which eluted with 0.2M NaCl solution was collected and freeze dried. The resulting solid was taken up in ethanol and filtered to remove NaCl. NH_4PF_6 (0.1 g, 0.61 mmol) was added and the solution left to stand for 3 h at 277 K. A yellow microcrystalline material formed which was collected, washed with a little ethanol followed by ether and dried *in vacuo*.

Yield: 15 mg, 0.02 mmol, 16.7 %

$C_{19}H_{31}F_{12}N_7OP_2Ru$ (619.62)	Calc. %C = 36.83 %H = 5.04 %N = 15.82
	Found %C = 36.54 %H = 4.83 %N = 15.46
NMR (D_2O)	δ ^{1}H 8.22 (s, 1H), 6.00 (b, 2H), 5.72 (d, 2H), 5.59 (d, 2H), 4.09 (q, 2H), 2.49 (m, 1H), 2.41 (m, 4H), 2.01(b, 2H), 1.95 (s, 3H), 1.41 (s, 3H), 1.09 (d, 6H)

4.2.14 Preparation of 1,4-dihydrobenzoic acid[15]

Benzoic acid (15.5 g, 0.13 mmol) was added to dry ethanol (100 ml) in a 1 l flask equipped with a mechanical stirrer, Dewar condenser and cooling bath (dry ice/acetone). NH_3 (600 ml) was condensed into the flask and Na metal (8.3 g, 0.36 mmol) added in small pieces over a period of 30 min. When the final blue colour was discharged the mixture was left to stir for 20 min after which time solid NH_4Cl (20 g, 0.22 mol) was carefully added. The cooling bath was removed and the NH_3 allowed to evaporate with stirring, leaving a white residue. The residue was taken up in chilled H_2O (500 ml) and acidified to pH~3 by addition of 10% HCl. This was extracted with ether (4 x 200 ml) and the combined ether layers washed with saturated NaCl solution (1 x 100 ml) and dried over $MgSO_4$. The ether was removed on a rotary evaporator leaving a crude oil which was distilled under reduced pressure giving a clear oil.

Yield: 13.56 g, 109 mmol, 90.8 %

NMR ($CDCl_3$)	δ ^{1}H 11.0 (br, 1H), 5.9 (m, 4H), 3.8 (m, 1H), 2.8 (m, 2H)
IR (neat, NaCl plates, cm^{-1})	3100-2500 (br), 1702 (st), 1640 (med)

4.2.15 Preparation of 3-methoxycarbonylcyclohexa-1, 4-diene

Conc. H_2SO_4 (1 ml) was added to a solution of 1,4-dihydrobenzoic acid (3g, 23.97 mmol) in freshly dried methanol (10 ml). The reaction was heated to reflux in air for 1 h, cooled, poured in to H_2O (25 ml) and extracted with ether (3 x 50 ml). The combined ether layers were washed with 5% $Na[HCO_3]$ solution (50 ml) and saturated NaCl

solution (50 ml) and dried over $MgSO_4$. The ether was removed on the rotary evaporator to leave a colourless oil which was used without further purification.

Yield: 2.60 g, 18.8 mmol, 42.8 %

NMR ($CDCl_3$) δ ^{1}H 5.93 (m, 4H), 3.82 (m, 1H), 3.55 (s, 3H), 2.64 (m, 2H)

IR (neat, NaCl plates, cm^{-1}) 3038-2821 (many sharp signals), 1743.7 (st), 1639.9 (med)

4.2.16 Preparation of $[(\eta^6\text{-}C_6H_5CO_2CH_3)RuCl_2]_2$

3-Methoxycarbonylcyclohexa-1,4-diene (2.6 g, 18.8 mmol) was added to a filtered solution of $RuCl_3.3H_2O$ (1 g, 3.8 mmol) in methanol (50 ml). The reaction was heated to reflux under argon for 8 h. The reaction was cooled, filtered and the volume reduced to 20 ml. After standing for 12 h at 277 K the precipitate was collected, washed with a little methanol followed by ether and dried *in vacuo*.

Yield = 1.08 g, 1.75 mmol, 93.1 %

$C_{16}H_{16}Cl_4O_4Ru_2$ (616.24) Calc. %C = 31.18 %H = 2, 62

Found %C = 31.05 %H = 2.39

NMR ($DMSO\text{-}d_6$) δ ^{1}H 6.72 (d, 2H), 6.31 (t, 1H), 6.04 (m, 2H), 3.92 (s, 3H)

4.2.17 Preparation of $[(\eta^6\text{-}C_6H_5CO_2CH_3)RuCl(H_2NCH_2CH_2NH_2\text{-}N, N)][PF_6]$, complex 16

Ethylenediamine (0.09 g, 1.5 mmol) was added to a stirred suspension of $[(\eta^6\text{-}C_6H_5CO_2CH_3)RuCl_2]_2$ (0.355 g, 0.576 mmol) in methanol (200 ml). After 4 h, the orange solution was filtered and the volume reduced to 20 ml. NH_4PF_6 (0.49 g, 2.3 mmol) was added and the mixture stirred for a further minute. The sealed flask was left to stand overnight at 277 K. The precipitated yellow microcrystalline solid was collected, washed with a little methanol followed by ether and dried *in vacuo*.

Yield 0.22 g, 0.46 mmol, 40.0 %

$C_{10}H_{16}ClN_2O_2PF_6Ru$ (477.75) Calc. %C = 25.14 %H = 3.38 %N = 5.86

	Found %C = 25.18 %H = 3.12 %N = 5.50
NMR (DMSO-d_6)	δ ^{1}H 6.70 (b, 2H), 6.39 (d, 2H), 6.10 (t, 1H), 5.68 (m, 2H), 4.32 (b, 2H), 3.28 (s, 3H), 2.22 (m, 2H), 2.15 (m, 2H)

4.2.18 Reaction of $[(\eta^6\text{-}C_6H_5CO_2CH_3)Ru(en)Cl]^+[PF_6]^-$ with 9-ethylguanine in aqueous ethanol

$[(\eta^6\text{-}C_6H_5CO_2CH_3)Ru(en)Cl][PF_6]$ **16** (0.1 g, 0.24 mmol) and 9-ethylguanine (0.05 g, 0.28 mmol) were mixed in degassed aq. ethanol (70:30, EtOH:H_2O) (25 ml) and stirred at 323 K in a sealed flask for 72 h. The solvent was removed *in vacuo*, the residue taken up in H_2O and loaded on a short column of Sephadex CM25 cation exchange resin. A light green band was eluted with 0.05 M NaCl. This was freeze-dried, the residue taken up in ethanol and filtered free of NaCl. After addition of NH_4PF_6 yellow crystals appeared which analysed for unreacted ruthenium starting complex by NMR and elemental analysis. A blue band was also present on the column but was unretrievable.

4.2.19 Preparation of 1, 4-dihydrobiphenyl[16]

A solution of biphenyl (10 g, 65 mmol) in freshly dried THF (200 ml) was added to NH_3 (400 ml) which had been condensed under argon into a 1 l flask equipped with a Dewar condenser, cooling bath (dry-ice/acetone) and mechanical stirrer. Li wire (1.125 g, 162 mmol) was added in small pieces over a period of 15 min. After a further 15 min stirring, solid NH_4Cl (15 g, 280 mmol) was added and the dark red colour discharged. The reaction was stirred at 213 K for 10 min, then the cooling bath was removed and the NH_3 allowed to evaporate under argon flow with stirring. The remaining residue was taken up in H_2O (200 ml) and acidified to pH~3 with 10 % HCl. This was extracted with ether (4 x 150 ml) and the combined ether layers washed with saturated NaCl solution (1 x 150 ml) and dried over $MgSO_4$. The ether was removed on the rotary evaporator and

the remaining oil distilled under reduced pressure (319 K, 0.2 mmHg) to give a clear oil which was used without further purification.

Yield: 6.45 g, 41.26 mmol, 63.5 %

4.2.20 Preparation of $[(\eta^6\text{-}C_6H_5C_6H_5)RuCl_2]_2$

$RuCl_3.3H_2O$ (2.28 g, 8.70 mmol) was dissolved in dry ethanol (25 ml)and filtered. 1,4-Dihydrobiphenyl (2.43 g, 15.50 mmol) was added in one portion and the solution heated to reflux under argon for 4 h. On cooling a brown solid settled out of solution. This was collected, washed with a little ethanol followed by ether and dried *in vacuo*.

Yield: 2.77 g, 8.49 mmol, 97.6 %

$C_{24}H_{24}Cl_4Ru_2$ (652.36)	Calc. %C = 44.19 %H = 3.71
	Found %C = 44.36 %H = 3.83
NMR (DMSO-d_6)	δ ^{1}H 7.65 (m, 2H), 7.38 (m, 3H), 6.03 (d, 2H), 5.77 (t, 1H), 5.61 (t, 2H)

4.2.21 Preparation of $[(\eta^6\text{-}C_6H_5C_6H_5)RuCl(H_2NCH_2CH_2NH_2\text{-}N, N)][PF_6]$, complex 17

$[(\eta^6\text{-}C_6H_5C_6H_5)RuCl_2]_2$ (0.30 g, 0.46 mmol) was refluxed in H_2O (25 ml) for 1 h. At this time ethylenediamine (0.06 g, 1 mmol) was added to the refluxing suspension. The brown suspension immediately became dark green. This was refluxed for a further 30 min and filtered while hot. NH_4PF_6 (0.5 g, 3 mmol) was added to the yellowish filtrate and the flask briefly shaken. A yellow precipitate began to form almost immediately. The flask was sealed, allowed to cool to ambient temperature and placed in an ice-bath for 3 h. The precipitate was collected, washed with a little water, followed by ethanol, followed by ether and dried *in vacuo*. This was recrystallised from methanol/ether.

Yield:

$C_{14}H_{18}ClF_6N_2PRu$ (495.82)	Calc. %C = 33.91 %H = 3.66 %N = 5.65
	Found %C = 33.86 %H = 3.43 %N = 5.32

NMR (DMSO-d_6) δ ^{1}H 7.78 (m, 2H), 7.50 (m, 3H), 6.48 (b, 2H), 6.17 (d, 2H), 5.89 (t, 1H), 5.79 (t, 2H), 4.18 (b, 2H), 2.31 (m, 2H), 2.21 (m, 2H)

4.2.22 HPLC of aqueous solutions of complexes 13 and 17

The HPLC method used in the analysis of aqueous solutions of complexes **13** and **17** is shown in Table 4.1. The column used is a polymer C_{18}, 5 μm. Detection is at 310 nm.

Solvent A: 50 mM NH_4Acetate, 2 mM pentanesulfonate(PSA)

Solvent B: 100 % CH_3CN

Time / min	% A	% B
0	92.0	8.0
13	56.0	44.0
14	92.0	8.0
18	92.0	8.0

Table 4.1 HPLC method for analysis of aqueous solutions of complexes **13** and **17.**

A = 50 mM NH_4acetate, 2 mM PSA, B = 100 % CH_3CN

4.3 Results and discussion

The synthesis of the Ru(II)arene complexes used in this work are based on a procedure pioneered by Bennett et al[7] in the early 1970s. A cyclohexadiene is refluxed in alcohol with $RuCl_3$ and the Ru(III) is reduced to Ru(II) with concurrent rearomatisation and π-binding of the cyclohexadiene. This forms what is generally assumed to be the dimeric species $[(\eta^6\text{-arene})RuCl_2]_2$ with two bridging chlorides. From this point it is possible to either cleave the dimer in a polar solvent such as methanol, or remove the halides using a reagent such as $AgBF_4$ to promote addition of other ligands.

The most commonly used complexes are the (η^6-benzene) and (η^6-*p*-cymene) complexes. The diene precursors for these (cyclohexadiene and α-terpinene) are both widely available commercially. There is a shortage, however, of commercial derivatised cyclohexadienes. Therefore it is necessary to synthesise them. The synthetic strategy used in this work is reduction of an aromatic system using solvated alkali metals. The general reaction is dissolving an alkali metal in liquid ammonia to create an electron sink to reduce the substrate while also having a proton source present, such as an alcohol, THF or even water,[17] to protonate the generated anions. The reduction of aromatic rings by solutions of alkali metals in liquid ammonia was discovered by Wooster and Godfrey[18] who reacted toluene with sodium in ammonia, followed by addition of water to produce "a highly unsaturated liquid product". This kind of work was taken up and developed further by Birch, and now the Birch reduction is synonymous with reduction of aromatic systems with sodium.[19] By definition, a Birch reduction is one in which the metal, substrate, alcohol and ammonia are present at the onset of the reaction.[20] The reactions, though, are not always straightforward. Experimental variables such as choice of proton source, order of addition and choice of metal are very important.[16]

A schematic for a typical reduction is given in Figure 4.1. A solution of sodium in liquid ammonia contains solvated electrons which add to a benzene ring to give a radical anion. The benzene radical anion is less stable than benzene and the ion reacts readily with a proton donor. Ammonia itself is too weakly acidic to react, but ethanol, for example, is sufficiently acidic to protonate the radical anion. The resulting cyclohexadienyl radical immediately reacts with another solvated electron to form the corresponding cyclohexadienyl anion. This anion is a strong base and reacts immediately with the proton donor to give the cyclohexadiene. Monocyclic benzene derivatives do not readily form anions, even in liquid ammonia, and require the presence of the proton source to displace the initial unfavourable equilibrium to the right.

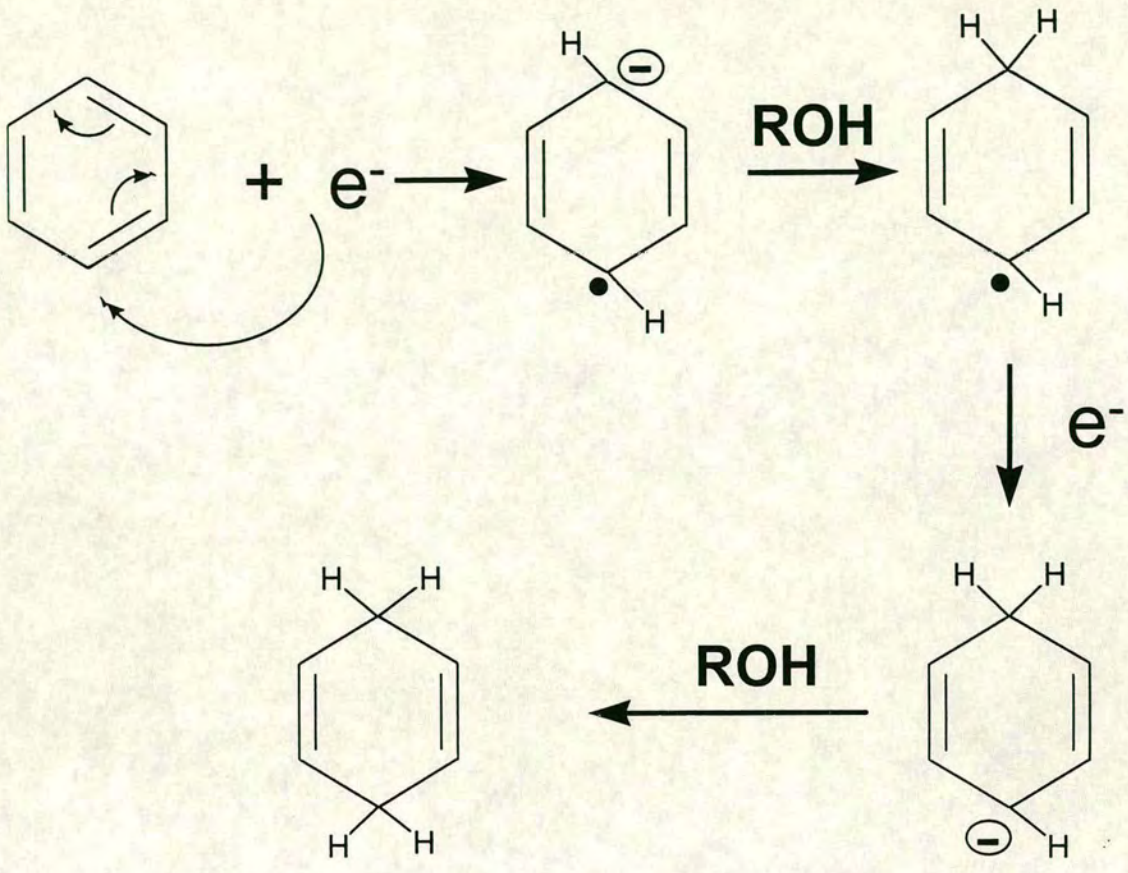

Figure 4.1 Scheme for reduction of an aromatic ring by solvated electrons

4.3.1 [(η^6-*p*-cymene)$RuCl_2$(isonicotinamide)] complex 6

The reaction of [(η^6-*p*-cymene)$RuCl_2$]$_2$ with isonicotinamide in refluxing benzene produced [(η^6-*p*-cymene)$RuCl_2$(isonicotinamide)] **6**. Isonicotinamide consists of a pyridine ring with an amide group at the 4 position, so it has two possible modes of coordination, through the pyridyl nitrogen or the amide functionality.

4.3.1.1 X-ray crystal structure of **6**

Single crystals suitable for X-ray analysis were grown from diffusion of ether into a methanol solution of **6**. Crystal data are shown in Table 4.2 and selected bond lengths

are listed in Table 4.3. The structure is shown in Figure 4.2. The complex crystallises in the space group Cc with four molecules in the unit cell. The structure displays the piano-stool type geometry. The *p*-cymene ring is η^6-coordinated to the ruthenium and the two chlorides and the isonicotinamide make up the "legs" of the stool. The isonicotinamide is coordinated through the pyridyl nitrogen. The Ru-Cl bond lengths are in the region typical for Ru(II) complexes.[28,29] The Ru-N_{isn} bond length of 2.120(8) Å is comparable to the Ru-N_{isn} bond lengths in $[cis\text{-}Ru^{II}(NH_3)_4(isn)_2]^{2+}$ which has a mean Ru-N_{isn} bond length of 2.060(4) Å[21] and the Ru-N bond length in the pyridine complex $[(h^6\text{-}C_6Me_6)RuCl_2(py)]$, 2.1224 Å.[22] It is interesting to note that the Ru-N_{isn} bond length in **6** is not significantly different from the Ru-N_{en} bond lengths in complexes **11**, **13**, **14**, **16** and **18**, see Table 4.3. This implies a lack of $d\pi$-π^* interaction, since back-bonding between the metal and ligand would make the bond shorter, so the pyridine moiety does not act as a π-acceptor. There is an intermolecular hydrogen bond in the unit cell between two molecules, see Figure 4.3. It is between the N-H of the amide on one molecule and the amide oxygen of a second molecule.

	6	11	13	14	16	17
Empirical formula	$C_{16}H_{20}Cl_2N_2ORu$	$C_8H_{14}ClF_6N_2PRu$	$C_{12}H_{22}ClF_6N_2PRu$	$C_{12}H_{22}I_2N_2Ru$	$C_{10}H_{16}ClF_6N_2O_2PRu$	$C_{14}H_{18}ClF_6N_2PRu$
Formula weight	428.31	419.70	475.81	549.19	477.74	495.79
Crystal habit	colourless block	yellow block	orange block	orange block	yellow block	yellow plate
Crystal size / mm	0.43 x 0.23 x 0.16	0.27 x 0.19 x 0.19	0.58 x 0.39 x 0.31	0.39 x 0.25 x 0.19	0.43 x 0.21 x 0.16	0.56 x 0.12 x 0.04
Crystal system	monoclinic	orthorhombic	monoclinic	monoclinic	monoclinic	monoclinic
Space group	Cc	Pnma	P	$P2_1/c$	$P2_1/n$	C_2/c
Volume / $Å^3$	1749.8(10)	1410.1(8)	1726.7(8)	1663.5(5)	1598.8(4)	3509(2)
Z	4	4	4	4	4	8
Density (calc.) / mg m^3	1.626	1.977	1.830	2.193	1.985	1.877
Absorption coefficient / mm^{-1}	1.203	1.469	1.211	4.639	1.318	1.197
F(000)	864	824	952	1032	944	1968
θ range for data collection / deg	2.80 to 25.12	2.65 to 25.03	2.53 to 25.07	2.78 to 25.02	2.67 to 25.03	2.82 to 25.03
Reflections collected	3978	1894	4465	2925	3803	5399
Independent reflections	2530	1345	3047	2925	2715	3080
Conventional R (R_1)	0.0623	0.0416	0.0271	0.0312	0.0400	0.0420

Table 4.2 X-ray crystsllographic data for complexes **6, 11, 13, 14, 16, 17**

	6	11	13	14	16	17
Ru-N_1		2.118(4)	2.130(3)	2.124(5)	2.112(4)	2.110(5)
Ru-N_2		2.118(4)	2.136(3)	2.143(5)	2.116(5)	2.121(5)
Ru-N_{isn}	2.120(8)					
Ru-Cl_1	2.395(3)	2.406(8)	2.4418(8)		2.4035(13)	2.4080(15)
Ru-Cl_2	2.408(3)					
Ru-I				2.7337(7)		
N-Ru-N		78.9(3)	78.98(10)	78.2(2)	79.00(18)	79.20(18)

Table 4.3 Selected bond-lengths Å and angles (°) for complexes **6**, **11**, **13**, **14**,**16**,**18**

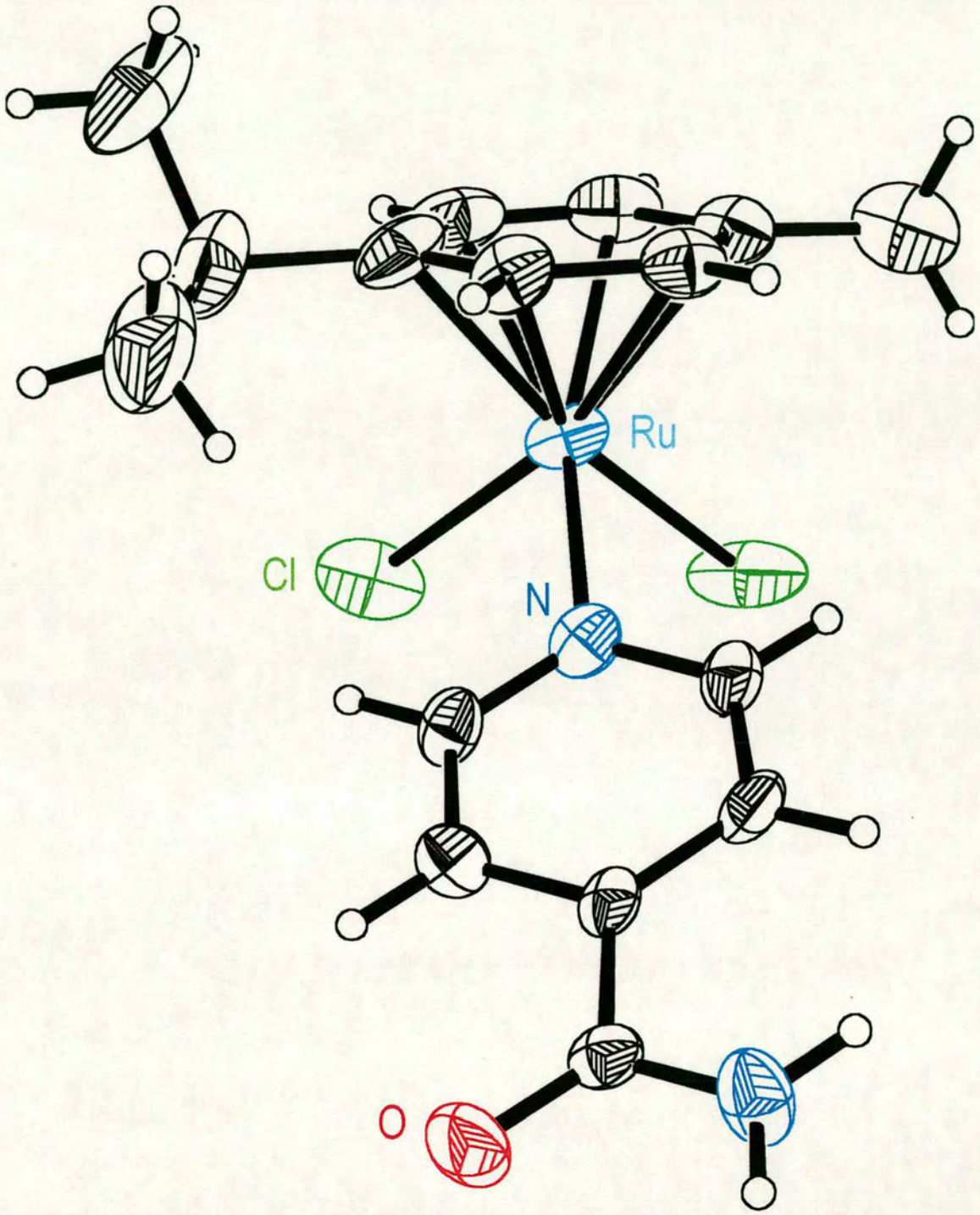

Figure 4.2 X-ray crystal structure of [(η^6-*p*-cymene)$RuCl_2$(isn)] **6**

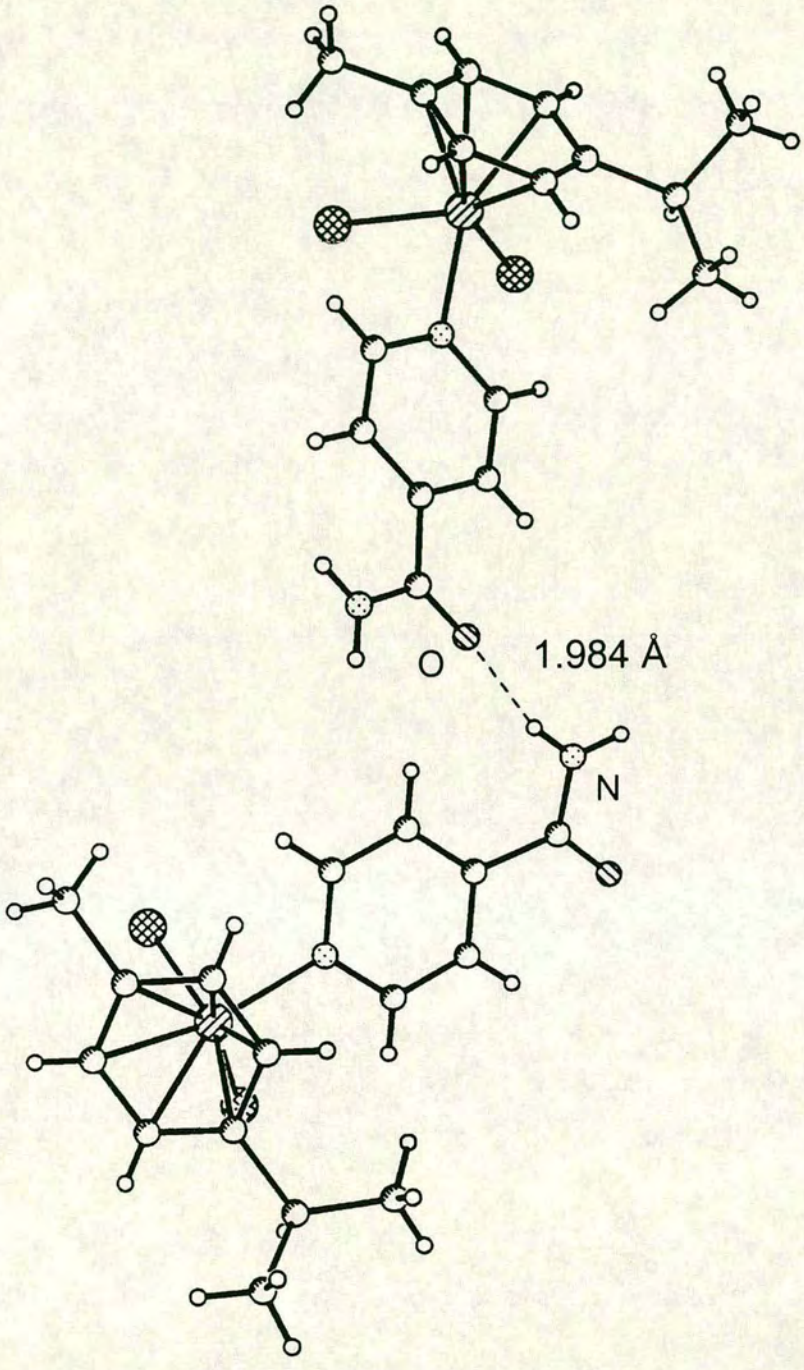

Figure 4.3 Hydrogen bonding between the amide oxygen of one molecule of **6** and an N-H of the amide of another molecule of **6** in the unit cell

4.3.2 Complexes 7, 8, 9 and 10

Complexes **7**, **8**, **9** and **10** were formed from reaction of the appropriate dimer with NH_4PF_6 in acetonitrile, based on a published procedure.[13] NH_4PF_6 is a less aggressive halide extracting agent than, for example, $AgPF_6$, and leaves one chloride behind to form the complexes $[(\eta^6\text{-arene})Ru(CH_3CN)_2X][PF_6]$, where X is the halide. However, the iodide complex could not be isolated.

This type of complex appears in the literature as a synthetic intermediate in Ru(II)arene chemistry. However, due to the water solubility and lability of the ligands, it was thought that these complexes may be biologically interesting in their own right. (see Chapter 6). The complexes have three potentially available coordination sites, so they could form mono-, bi- or even tri-functional adducts with DNA. However, along with this reactivity comes the possible problem of toxicity due to indiscriminate reactions with molecules present in the body. The problem of transport through the body to the tumour site may arise also, as they are likely to react with blood proteins such as HSA (human serum albumin).

4.3.3 $[(\eta^6\text{-}C_6H_6)Ru(en)Cl][PF_6]$, complex 11

$[(\eta^6\text{-}C_6H_6)Ru(en)Cl][PF_6]$ **11** was synthesised from the reaction of $[(\eta^6\text{-}C_6H_6)RuCl_2]_2$ with an excess of ethylenediamine in methanol. The polar methanol promotes the breaking of the dimeric structure allowing coordination of the ethylenediamine. After filtration, NH_4PF_6 was added to provide a substantial counter-ion and the product was isolated in moderate yield. The ^1H NMR spectrum of **11** in DMSO-d_6 shows a singlet at δ 5.86 appropriate for a π-coordinated benzene ring. The ethylenediamine backbone -CH_2- protons appear as two multiplets at δ 2.34 and 2.17 and the NH_2 protons show two broad resonances at δ 6.45 and 4.28.

4.3.3.1 X-ray crystal structure of **11**

Single crystals suitable for X-ray analysis were grown by diffusion of ether into a methanol solution of **11**. The complex crystallised in the space group Pnma with four molecules in the unit cell. A summary of crystal data is given in Table 4.2, selected bond lengths and angles are given in Table 4.3. The structure is shown in Figure 4.4.

The structure is disordered about a mirror plane that runs through the Ru and Cl. The Ru, Cl and the two N atoms fit the mirror plane, however the benzene ring and the backbone of the en ligand are disordered about it. This makes the Ru-C and C-C bond lengths have high esd values (0.016 - 0.018 Å). However the structure has been unambiguously established.

In the molecule the ruthenium has the expected "piano-stool" style geometry typical for Ru(II)arene complexes. The Ru-N bond lengths are 2.118(4) Å and are in the range expected for a nitrogen σ-bonding to a Ru(II) centre. They are statistically similar to the Ru-N bond lengths for $[Ru(en)_3]^{2+}$, which shows a bond length of 2.132(3) Å.[23] This in turn is within two standard deviations of the 2.144(4) Å found in $[Ru^{II}(NH_3)_6]^{2+}$, indicating no important bond length difference between NH_3 and en ligands σ-bonded to Ru(II).[24] The bonds also compare well with those in potentially biologically important oligopeptide ester Ru(II)arene complexes, such as $[(\eta^6\text{-}C_6Me_6)Ru(Cl)(k^2\text{-}L\text{-}AlaGlyGlyGlyOMe)]$ (2.124(12) Å[25] and $[((\eta^6\text{-}C_6H_6)Ru(triglycine\text{-}N, N)Cl]$ (2.118(6) Å.[26]

The N-Ru-N bond angle of 78.9(3)° is slightly less than that found in the octahedrally coordinated complexes $[Ru^{II}(en)_3]^{2+}$ (80.9(3), 81.8(3) and 82.1(3)°)[23] and $[Ru(en)_2(CH_3CN)(PPh_3)]^{2+}$ (80.0(6) and 81.7(7)°)[27] but this is to be expected with the more crowded geometry of the arene complex as opposed to the octahedral ones. The

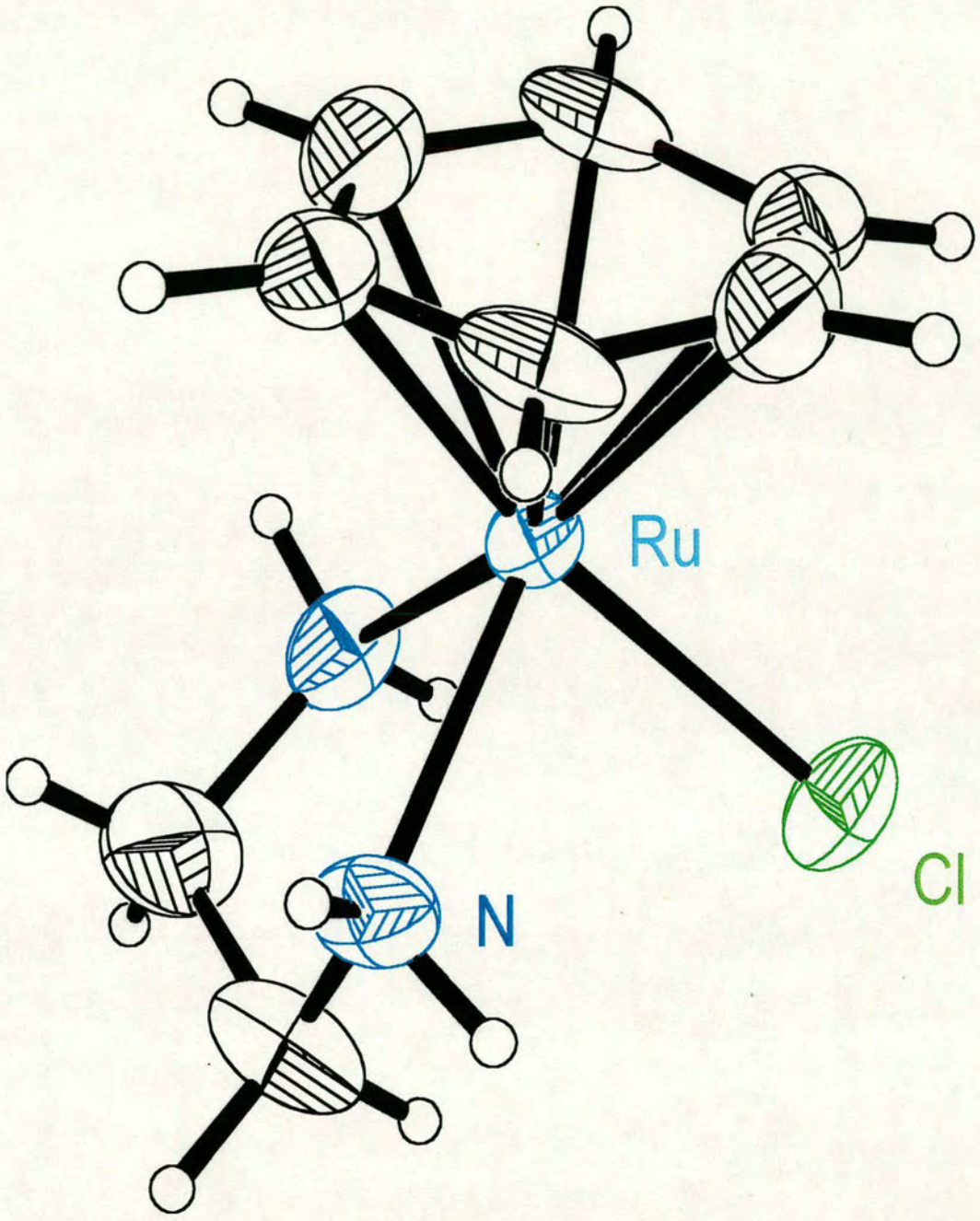

Figure 4.4 X-ray crystal structure of $[(\eta^6\text{-}C_6H_6)RuCl(en)]^+$ **11**. The PF_6^- counter-ion has been omitted for clarity

Ru-Cl bond length of 2.406(8) Å is within the range of values typical for Ru(II) complexes.[28,29]

4.3.4 [(η^6-C_6H_6)Ru(en)I][PF_6], complex 12

Complex **12** was formed from the reaction of [(η^6-C_6H_6)RuI_2] with ethylenediamine in methanol. The iodo version of the ruthenium dimer has a lower solubility than the chloro version and reaction time was longer in a higher volume of solvent. ^{1}H NMR in DMSO-d_6 showed a singlet at δ 5.86 appropriate for a π-coordinated benzene ring. The ethylenediamine backbone protons appear as multiplets at δ 2.35 and 2.15, and the NH_2 protons are two broad resonances at δ 6.42 and 4.22. Unfortunately, crystals suitable for X-ray analysis could not be grown..

4.3.5 [(η^6-*para*-cymene)Ru(en)Cl][PF_6], complex 13

Complex **13** was formed from the reaction of [(η^6-*para*-cymene)$RuCl_2$]$_2$ and ethylenediamine in methanol in a manner similar to **11**, see section 4.3.3. The ^{1}H NMR in DMSO-d_6 showed two doublets with coupling constants of 5.6 Hz at δ 5.48 (2H) and 5.32 (2H), attributable to the four protons of the *p*-cymene ring. The tolyl protons of the arene give rise to a singlet at δ 2.11 (3H), and the isopropyl methyl groups give a doublet at δ 1.25 (J = 6.8 Hz) split by the C-H proton which resonates at δ 2.7 (6H) as a multiplet. The -CH_2- of the ethylenediamine backbone are two broad multiplets at δ 2.43 (2H) and 2.32 (2H) and the NH_2 signals give two broad resonances at δ 6.13 (2H) and 4.22 (2H).

A 2D ^{1}H-^{1}H NOESY experiment allowed the N-H signals to be distinguished. The spectrum is given in Appendix 2. The NH signal of the ethylenediamine ligand to high field has significant NOESY crosspeaks with the protons on the backbone of the ethylenediamine ligand, but not with the arene ring. The signal to low field, however, has significant NOESY crosspeaks with the ethylenediamine backbone and with all the

protons of the *p*-cymene ring. We can assume free rotation of the *p*-cymene ring due to the simplicity of the signals from it. Therefore the NH signals must correspond to one for the NH pointing away from the ring (the signal at high field) and one for the NH pointing upwards toward the ring (the signal to low field) i.e. each signal is for two protons, one from each nitrogen.

As the complex contains a chelated ethylenediamine ring, there is potential for ^{15}N NMR studies. As a preliminary test, to see if it would be of use, an HSQC [^{1}H, ^{15}N] correlation spectrum was obtained in 90 % H_2O:10 % D_2O. This was done at natural abundance with a concentration of 40 mM. ^{15}N is only present in nature at a level of 0.3 % so the high concentration was necessary. For biologically relevant reactions such as DNA binding, ^{15}N isotopically enriched ethylenediamine could be used. The present study was performed to see if there was a significant difference in the shift of the intact complex and the hydrolysed form. A significant shift would mean that bound forms of the complex could be distinguished from unreacted forms. The spectrum is shown in Figure 4.5. The signals from the NH protons in the intact complex are in square boxes and the peaks from the hydrolysed form of the complex are in the oval boxes. There is a separation of 1 ppm in the ^{15}N dimension and a separation of 0.3 ppm in the ^{1}H dimension between the hydrolysed and non-hydrolysed forms. This indicates that ^{15}N NMR studies may be useful in further studies of complex **13**.

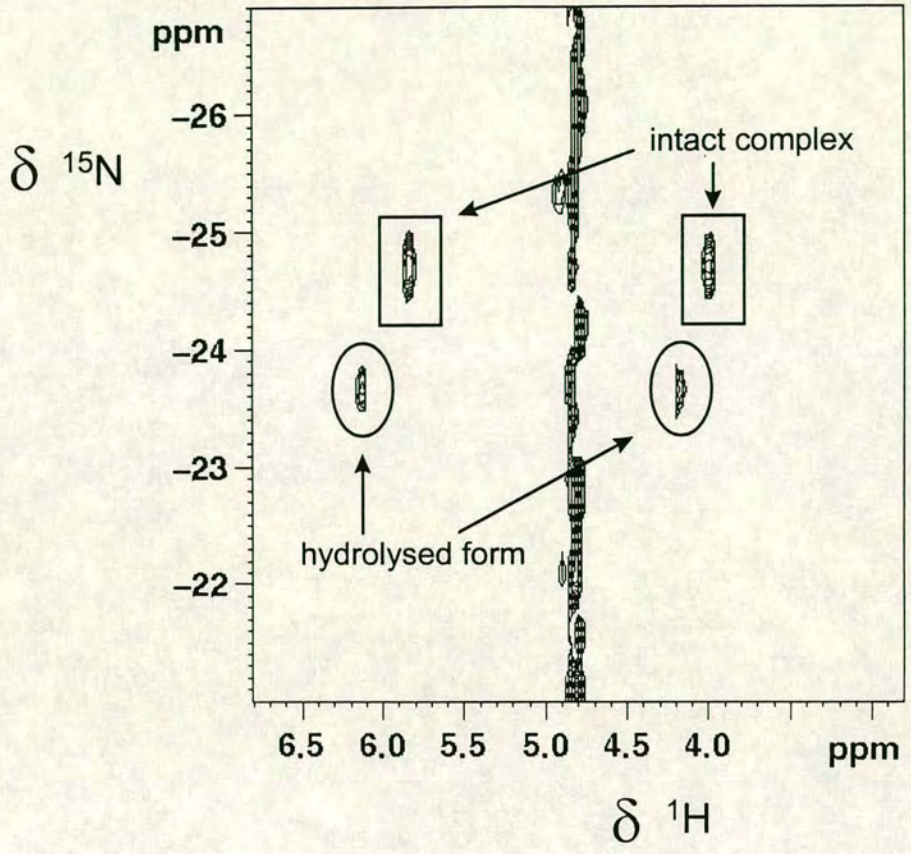

Figure 4.5 HSQC [^{1}H,^{15}N] 2D spectrum of **13** in 90 % H_2O:10 % D_2O after 45 min at 298 K. The ^{1}H dimension is on the horizontal axis and the ^{15}N dimension is on the vertical axis. The signals from the intact complex are denoted by the squares and the signals from the hydrolysed form of the complex are denoted by the ovals.

4.3.5.1 X-ray crystal structure of **13**

Single crystals suitable for X-ray analysis were grown by diffusion of ether into a methanol solution of **13**. Crystal data are listed in Table 4.2 and selected bond lengths and angles are in Table 4.3. The structure is shown in Figure 4.6 and unambiguously confirms the structure. The complex crystallised in the space group P with four molecules in the unit cell. The expected piano-stool type geometry is shown, with the *p*-cymene ring being η^6 coordinated and the chelated ethylenediamine and the chloride

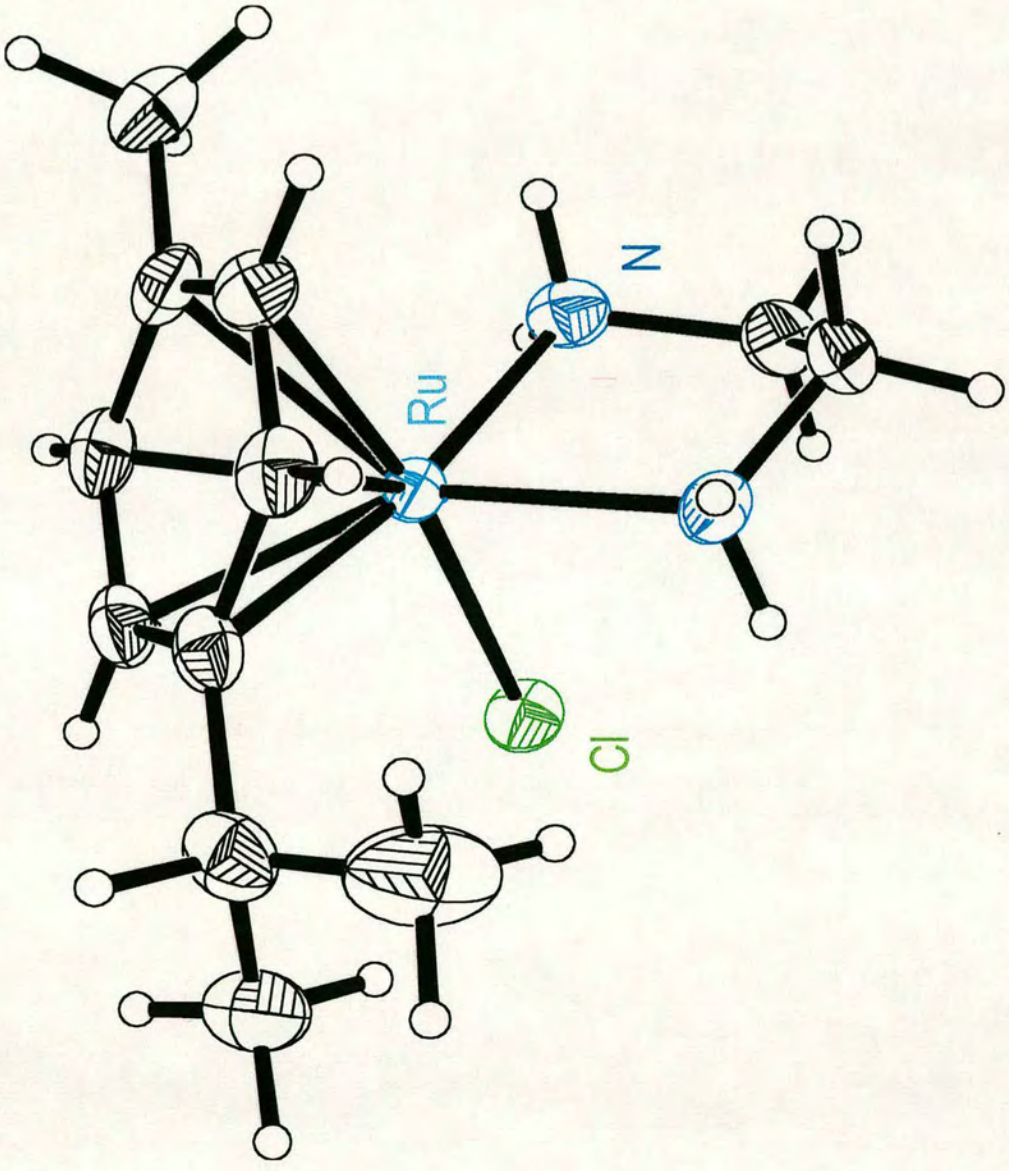

Figure 4.6 X-ray crystal structure of $[(\eta^6\text{-}p\text{-cymene})RuCl(en)]^+$ **13**. The PF_6^- counter-ion has been omitted for clarity

making up the three "legs" of the stool. The Ru-N and Ru-Cl bond lengths and angles can be compared to the same structures as complex **11**, see section 4.3.3.1.

4.3.5.2 Hydrolysis of complex **13**

We are interested in the potential use of the complexes synthesised in this thesis as anticancer agents. As the human system is largely an aqueous one, it is of interest to know how a complex reacts with water in order to give an insight into the biological reactivity of it. From initial cytotoxicity studies on the arene complexes prepared in this thesis, see Chapter 6, complexes **13** and **17** were chosen as lead compounds. With a view to the development of an assay to allow for in-depth biological studies in the future, a HPLC method was developed to study the hydrolysis of complex **13**.

After attempting various types of HPLC methods such as ion-exchange, the successful method turned out to be ion-pairing using pentanesulfonate(PSA). The method is detailed in the experimental section, section 4.2.22.

Three species were detected in the assays, with the peaks eluting at (a)8.4, (b)10 and (c)10.9 min. To assign them, various experiments were performed varying the concentrations of the solutions and by making up the solutions in 100 mM NaCl, a concentration that would prevent or significantly decrease loss of the chloride. These allowed us to assign which peak is the intact complex and which has reacted with water. Figure 4.7 shows the HPLC traces of a 10 mM solution of **13** in A) H_2O and B) 100 mM NaCl. The peaks in the H_2O solution appear in the ratio 3:1:7 in order of elution. The vast reduction in the relative intensities of the peaks (a) and (b) in the NaCl solution (ratios 2:1:21) as compared to the H_2O solution indicates that these peaks correspond to hydrolysed species. Therefore we can assign peak (c) at 10.9 min as the original complex. Fig 4.8 shows the HPLC traces of 0.2 mM solutions of **13** in A) H_2O and B) 100 mM NaCl. This experiment backs up the observations made using the 10 mM solutions. It can be seen that in H_2O the balance of the peaks has been greatly shifted to peaks (a) and (b) (ratio 5:2:1). In the salt solution these peaks are of low intensity.

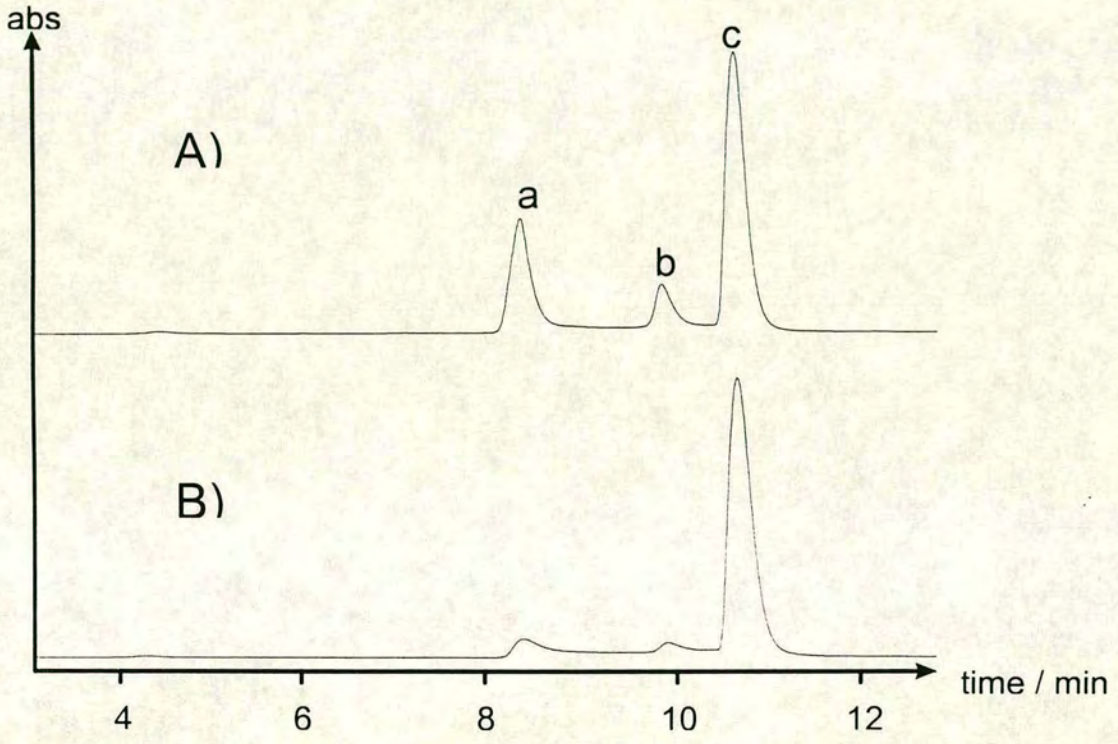

Figure 4.7 HPLC separation of a fresh 10 mM solution of **13** in A) H_2O and B) 100 mM NaCl solution at 295 K. Peaks (a) and (b) correspond to the hydrolysed complex and peak (c) is the intact complex.

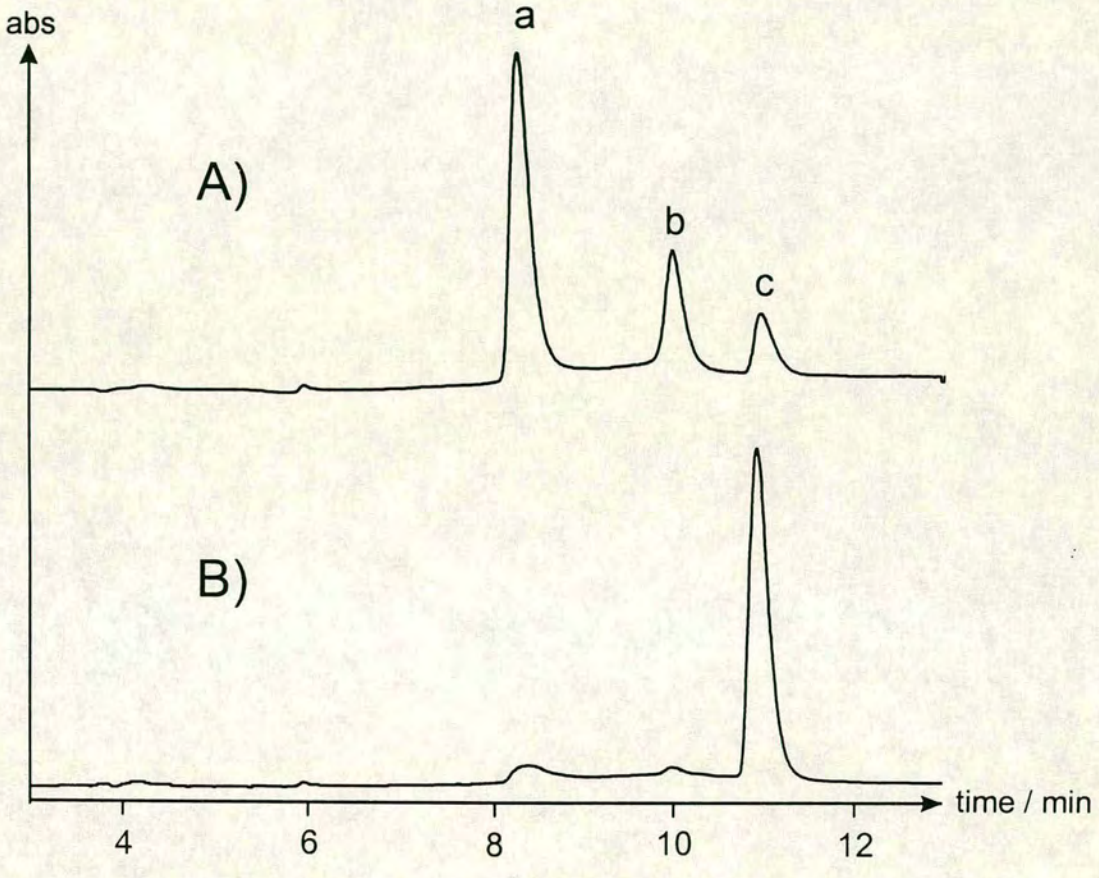

Figure 4.8 HPLC separation of a fresh 0.2 mM solution of **13** in A) H_2O and B) 100 mM NaCl solution at 295 K. Peaks (a) and (b) correspond to the hydrolysed complex and peak (c) is the intact complex

These observations allow the following conclusions to be drawn: peak (c), at 10.9 min, is the original complex, and peaks (a) and (b) are species that have formed after the loss of the chloride. This is known by the significant reduction in the intensity of peaks (a) and (b) in the 100 mM NaCl solution. The high chloride concentration is inhibiting loss of the chloride form the complex. Also, at dilute levels (0.2 mM) practically all the complex has lost a chloride in H_2O whereas at a higher concentration (10 mM) only 36 % of the complex has lost a chloride. Assuming that drug dosage would be in the μM region (see Chapter 6), it is likely that the complex would lose chloride if administered in water.

To confirm assignments and distinguish between the two reacted species, on-line HPLC-electrospray mass spectrometry was performed. However, the experiment resulted in a change of retention times due to different column length and flow rates required for on-line, and peaks (a) and (b) merged into an unseparable broad peak appearing in the mass spectrometer at the same time, see Figure 4.9. It was possible to identify species from these results though. Both peaks showed an ion at m/z 295.4. This corresponds to $[(\eta^6$-*p*-cymene)Ru(en)$]^{2+}$ - H^+ (theor 295.3 amu) due to fragmentation in the mass spectrometer. This is the only fragmentation seen in the experiment and indicates the fragility of the Ru-Cl bond, and hence potential reactivity. Peak (c) at 15 min gives a signal at m/z 331.4, which corresponds to the original complex without its counter-ion (theor. 331.8 amu).

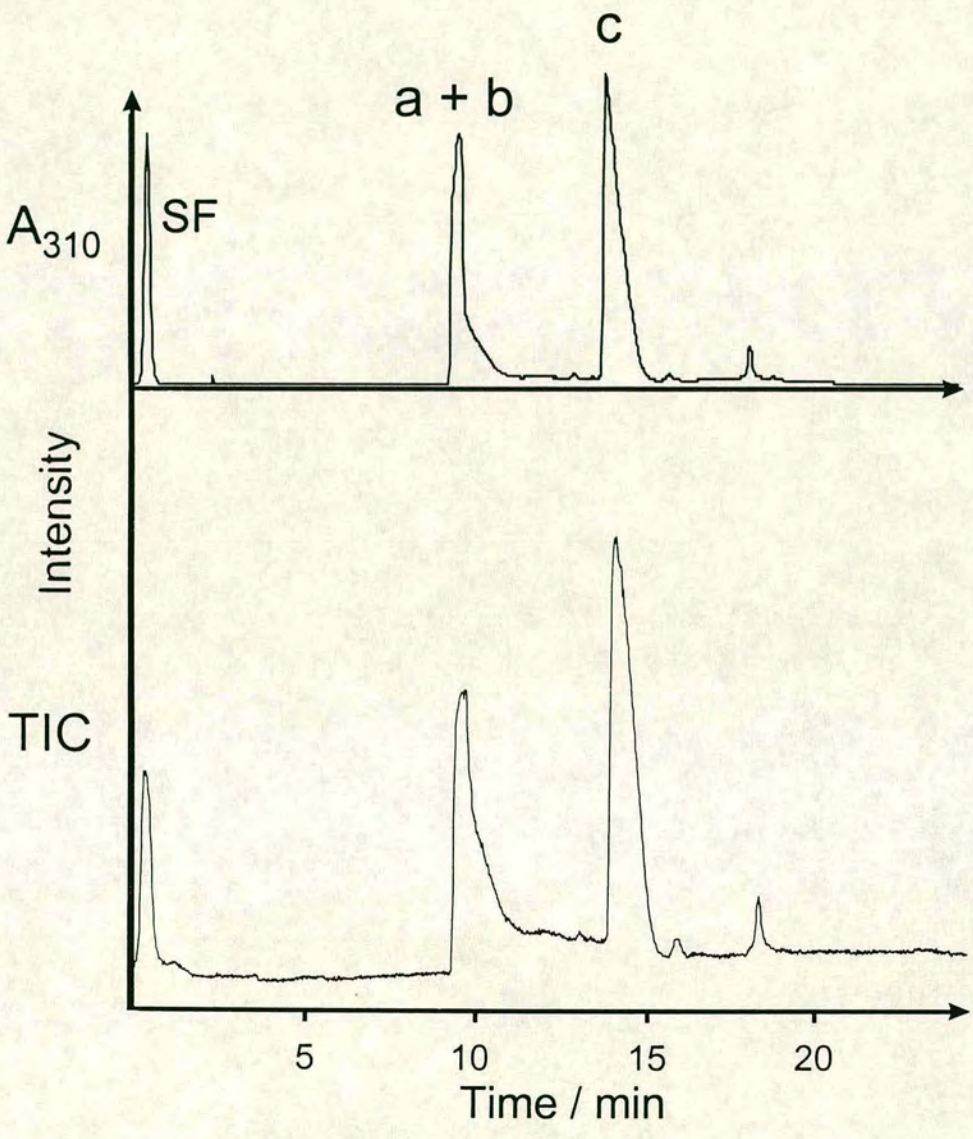

Figure 4.9 On-line HPLC-ESIMS of an aqueous solution of **13**. The top trace is the UV detection at 310 nm of the separation and the Total Ion Count (TIC) detected by the mass spectrometer concomitantly. Peaks (a) and (b) have merged into a single peak. SF is the Solvent Front.

Peak (a + b) at 10 min, produced by the merging of the two peaks, produces the ion at m/z 295.4 and two other ions. One is unexpected at m/z 447.5, but when the HPLC mobile phase was taken into account, it can be assigned as an adduct of the complex with PSA instead of the chloride (theor. 447.4 amu), and therefore an artefact of the HPLC method. There is also a species at m/z 315.1 which is for the hydrolysed form of the complex (theor. 314.3 amu).

4.3.6 [(η^6-*para*-cymene)Ru(en)I][PF_6], complex 14

Complex **14**, [(η^6-*para*-cymene)Ru(en)I][PF_6], was formed from the reaction of [(η^6-*para*-cymene)RuI_2]$_2$ with ethylenediamine in methanol. The ^{1}H NMR in DMSO-d_6 shows two doublets for the *p*-cymene ring protons at δ 5.51 and 5.35, a singlet for the tolyl protons at δ 2.08 and a doublet for the isopropyl methyl protons at δ 1.33 which are coupled to the single isopropyl proton at δ 2.69. The ethylenediamine backbone protons resonate at δ 2.37 and 2.29, and the NH protons give two broad signals at δ 6.15 and 4.24.

4.3.6.1 X-ray crystal structure of **14**

Crystals suitable for X-ray analysis were grown by diffusion of ether into a methanol solution of **14**. Crystal data can be found in Table 4.2 and selected bond lengths and angles are listed in Table 4.3. The complex crystallises in the space group $P2_1/c$ with four molecules in the unit cell. The structure is shown in Figure 4.10 and unambiguously confirms the complex as having piano-stool type geometry. The *p*-cymene is η^6-coordinated and the chelated ethylenediamine and the iodide are the "legs" of the stool. Unexpectedly there is no PF_6^- counter-ion present. Instead the counter-ion is an iodide, presumably the iodide displaced by ethylenediamine upon chelation. Interestingly, the iodide counter-ion links molecules of the complex via intermolecular interactions with hydrogens on the ethylenediamine nitrogens, see Figure 4.11.

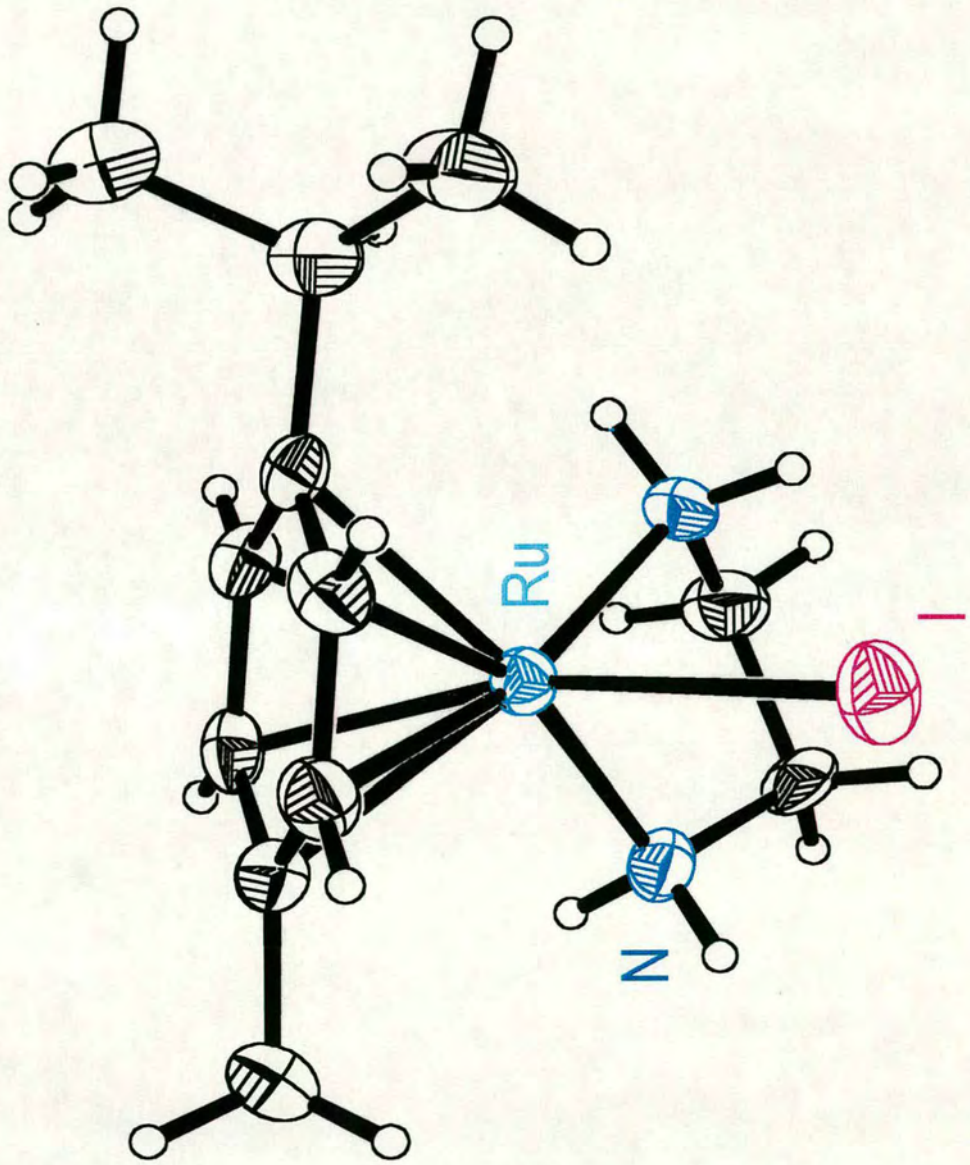

Figure 4.10 X-ray crystal structure of $[(\eta^6\text{-}p\text{-cymene})\text{RuI(en)}]^+$ **14**. The iodide counter-ion has been omitted for clarity

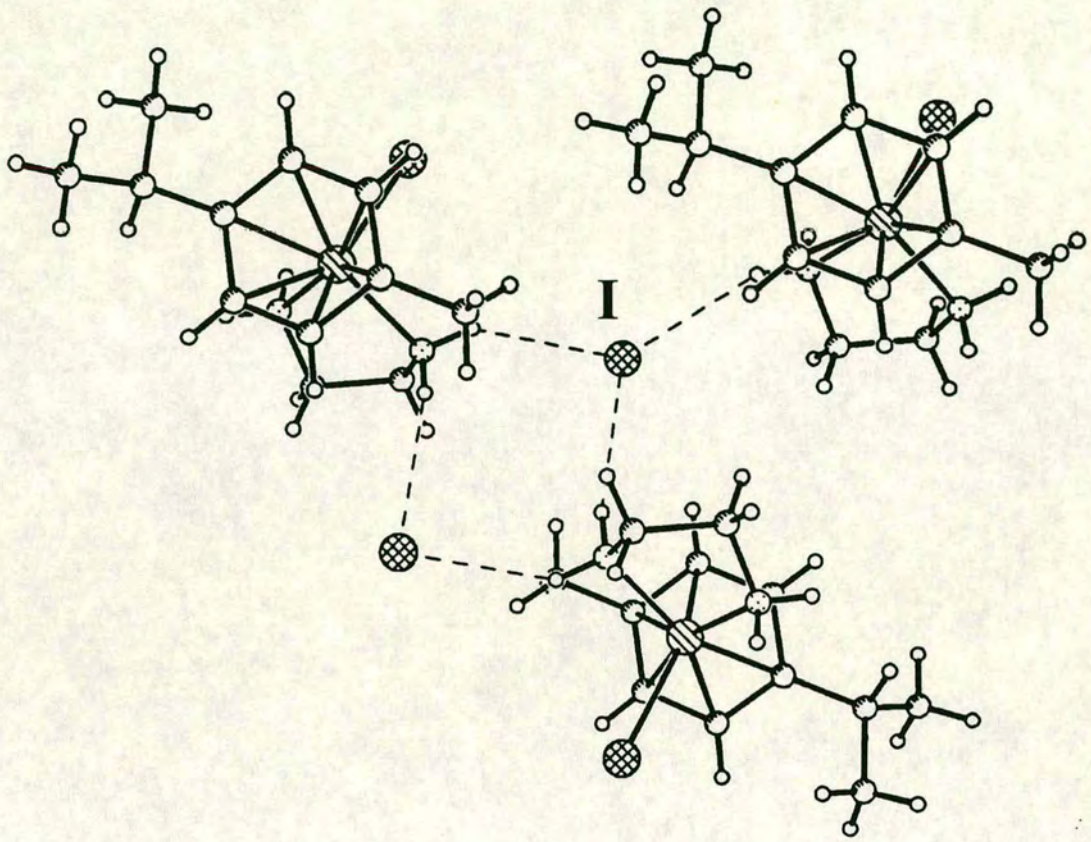

Figure 4.11 Representation showing how the iodide counter-ion links molecules of **14** in the unit cell via N-H of the ethylenediamine moiety.

The Ru-N bond lengths and angles can be compared to the same structures as complex **11**, see section 4.3.3.1. The Ru-I bond length of 2.7337(7) Å compares well with other Ru-arene complexes possessing an iodide such as $[(\eta^6\text{-}C_6H_6)Ru(I)(2\text{-dimethylaminoethyl})\text{-}2\text{-naphthyl}]$, 2.735(1) Å[30] and $[(\eta^5\text{-}C_5H_5)Ru(I)(CNBu^t)]$ which has a Ru-I bond length of 2.717 Å.[31]

4.3.7 [(η^6-*para*-cymene)Ru(en)(9egua)][PF_6]$_2$, complex 15

The reaction of complex **13** with 9-ethylguanine (9egua) in aqueous ethanol, with work-up including ion-exchange chromatography, produced yellow crystals of [(η^6-*para*-cymene)Ru(en)(9egua)][PF_6]$_2$. 9-Ethylguanine is a model compound for the guanine found in DNA, and this might be a possible target for Ru compounds *in vivo*.[32] It is known that when cisplatin is incubated with DNA, intrastrand Pt(GpG-κ^2N^7), G = guanine, chelates are formed in statistically larger amounts than expected. It is with this in mind that the reaction between **13** and 9egua was investigated.

The product was formed in very low yield , hence only preliminary investigations were performed. The ^{1}H NMR is the most insightful piece of information in this case. The spectrum in D_2O is appropriate to complex **13** with an N^7 bound 9-egua molecule replacing the chloride. The *p*-cymene moiety gives rise to two doublets at δ 5.72 and 5.59 (2H each) for the four arene protons, a multiplet at δ 2.49 (1H) and a doublet at δ 1.09 (6H) for the isopropyl group and a singlet at δ 1.95 (3H) for the tolyl group. The ethylenediamine backbone is a multiplet at δ 2.41 (4H). Interestingly there is a large shift in one of the NH signals. The signal for the NH protons pointing away from the *p*-cymene ring (see section 4.3.5) has shifted to higher field, from δ 4.2 to 2.01 This is probably due to the orientation of the ethyl group of the 9-egua. The other NH signal appears at δ 6.00. The fact that the NH does not appear to exchange to ND in D_2O indicates that the ethylenediamine does not ring open as this would allow for exchange processes to occur. The 9-egua ligand resonances are a triplet at δ 1.41 (3H) and a quartet at δ 4.09 (2H) for the ethyl group and a singlet at δ 8.22 for the H^8 proton. In free 9-egua in D_2O the H^8 proton resonates at δ 7.8. The downfield shift of 0.4 ppm upon coordination to the ruthenium indicates that it is bound through the N^7 of the guanine moiety. Coordination of guanine through the N^7 is preferred by most metal ions[33] at neutral pH. This has been shown for 9-egua and Ru(II) in the complex [(η^6-C_6H_6)$RuCl_2$(9egua-kN^7)].[34] Therefore, the complex [(η^6-*para*-cymene)Ru(en)Cl][PF_6] **13** reacts with 9-ethylguanine to form the monoadduct with coordination at the N^7 of the

guanine model, indicating a strong likelihood that this would be the reaction of choice with DNA.

4.3.8 [(η^6-methylbenzoate)Ru(en)Cl][PF_6] complex 16

In order to introduce variety on the arene ring substituent of the complex [(η^6-methylbenzoate)Ru(en)Cl][PF_6] complex **16** was synthesised. Starting from benzoic acid, this was reduced using a Birch style reduction (see section 4.3) to 1,4-dihydrobenzoic acid and this in turn was esterified in methanol to give 3-methoxycarbonylcyclohexa-1,4-diene. On refluxing this with $RuCl_3$ in methanol the dimer [(η^6-methylbenzoate)$RuCl_2$]$_2$ was formed. Reacting this with ethylenediamine in methanol led to the complex [(η^6-methylbenzoate)Ru(en)Cl][PF_6] **16**.

Introducing an ester moiety to the π-coordinated arene ring was of interest for two main reasons. First, the possibility of the complex acting as a prodrug. The activity of hydrolases (for hydrolysis of esters) in cancer cells towards the ester moiety could result in trapping of the complex in the cell. The hydrophobicity of the arene part of the complex should aid passage through cell membranes (composed of lipids), thus raising concentration of the complex in cells. Once in the cell and hydrolysed, the complex may no longer be able to leak out through the membrane, and may be in a more active form. This methodology has previously been attempted with some cisplatin derivatives.[35] They found that the more hydrophobic the ester moiety, and the more susceptible to hydrolysis, the more cytotoxic the complex. Also, by varying the arene ring substituents, we might obtain information as to whether arene is important to activity.

The ^{1}H NMR in DMSO-d_6 showed the appropriate resonances. The protons of the π-coordinated ring gave rise to a doublet at δ 6.39 (2H) for the protons ortho to the ester functionality, a triplet at δ 6.10 (1H) for the para proton and a multiplet at δ 5.68 (2H) for the meta protons. The NH signals and are found at δ 6.70 (2H) and 4.32 (2H) are

broad. The ethylenediamine backbone shows 2 multiplets at δ 2.22 (2H) and 2.15 (2H). The ester methyl signal is a singlet at δ 3.28 (3H).

4.3.8.1 X-ray crystal structure of **16**

Single crystals suitable for X-ray analysis were grown by diffusion of ether into a methanol solution of **16**. Crystal data are given in Table 4.2 and selected bond lengths and angles are listed in Table 4.3. The structure is shown in Figure 4.12 and unambiguously confirms the structure to have the piano stool type geometry. The methylbenzoate is η^6-coordinated and the chelated ethylenediamine and chloro ligands form the "legs" of the stool. The complex crystallises in the space group $P2_1/n$ with four molecules in the unit cell. The Ru-N and Ru-Cl bond lengths and angles are comparable to the similar parameters as complex **11**, see section 4.3.3.1.

Although one of the carbons of the arene ring is substituted with an electron withdrawing ester group, there is no significant difference between this Ru-C bond length (2.181(5) Å) and those for the other ring carbons. Another arene-ester complex of ruthenium[36] $[(\eta^6\text{-}o\text{-}MeC_6H_4CO_2Me)Ru(NMDPP)Cl_2]$, where NMDPP is neomenthyldiphenylphosphine, has been reported to have a longer Ru-C bond to the ester substituted carbon than the unsubstituted carbons but the authors attributed this to the carbon being pseudo-*trans* to a tertiary phosphine and its respective *trans* influence.[37] The C=O double bond length, 1.206(7) Å is comparable to that in $[(\eta^6\text{-}o\text{-}MeC_6H_4CO_2Me)Ru(NMDPP)Cl_2]$, 1.18(4) Å, as is the C-O single bond and the O-CH_3 bond.

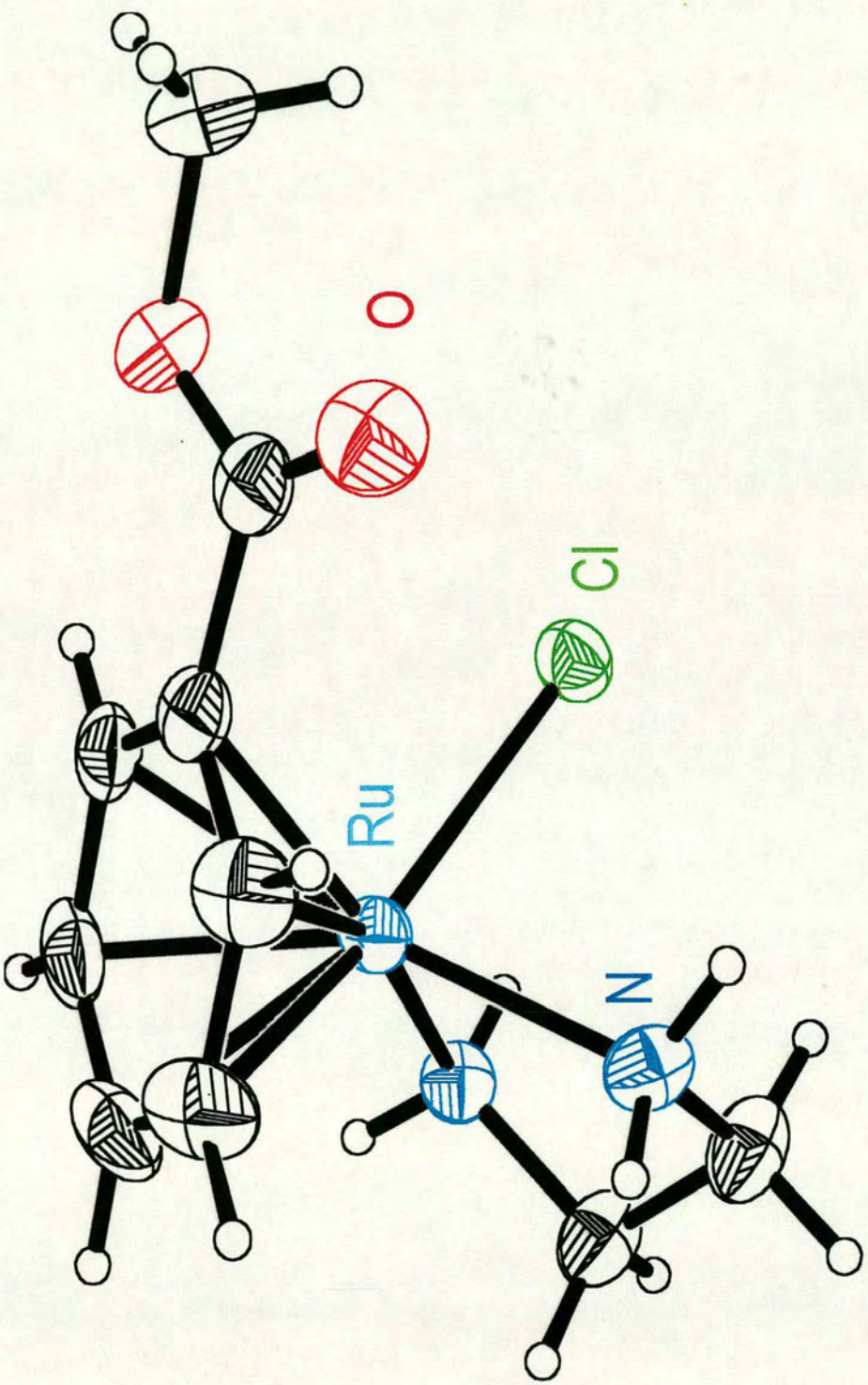

Figure 4.12 X-ray crystal structure of $[(\eta^6\text{-methylbenzoate})RuCl(en)]^+$ **16**. The PF_6^- counter-ion has been omitted for clarity

An attempt was made to react **16** with 9-ethylguanine in aqueous ethanol. After work-up, however, the isolated product turned out to be unreacted **16**. A blue band also appeared on the ion-exchange column, however this would not elute from the column.

4.3.9 [(η^6-biphenyl)Ru(en)Cl][PF_6] complex 17

To introduce another form of variety on the arene ring, the complex [(η^6-biphenyl)Ru(en)Cl][PF_6] **17** was synthesised. Starting with biphenyl, this was reduced using lithium metal in ammonia to form 1,4-dihydrobiphenyl. On refluxing this in ethanol with $RuCl_3$, the dimer [(η^6-biphenyl)$RuCl_2$]$_2$ was formed. This has quite a low general solubility and many variations on syntheses were tried before finally succeeding in producing **17**. The complex was formed by addition of ethylenediamine to a refluxing suspension of [(η^6-biphenyl)$RuCl_2$]$_2$ in H_2O. After filtration and addition of NH_4PF_6, a yellow solid precipitated which was purified from methanol-ether.

The ^{1}H NMR of **17** in DMSO-d_6 was recorded. The coordinated ring of the biphenyl shows a doublet at δ 6.17 (2H), a triplet at δ 5.89 (1H) and a triplet at δ 5.79 (2H). The pendant phenyl ring gives two multiplets at δ 7.78 (2H) and 7.50 (3H). The ethylenediamine backbone $(CH_2)_2$ gives rise to two multiplet resonances at δ 2.31 (2H) and 2.21 (2H) and the N-H resonances appear at δ 6.48 (2H) and 4.18 (2H).

The biphenyl group was chosen for two main reasons. The extra aromatic group increases the hydrophobicity of the complex. Complex **17** is still quite soluble in water (> 20 mM), but the solubility is certainly reduced when compared to other complexes such as **13**. This may have the advantage of leading to a greater partition into the cell membrane which may aid transport into the cell. The biphenyl group is also a potential DNA intercalator. Ru-DNA intercalators have been of interest for probing nucleic acid conformations and in the development of new phototherapeutics.[38] Ru(II) polypyridyl intercalators have a strong affinity for DNA[39] and may act as molecular "light-switches" for double helical DNA.[40] These complexes show no luminescence in aqueous buffer,

but luminesce brightly when intercalated into DNA. Intercalating ruthenium complexes have also been used to study long range fast electron transfer that is mediated by the stacked bases of DNA.[41] On a note more relevant to cancer treatment, an intercalating moiety is believed to be necessary for topoisomerase inhibitors.[42] This point is further discussed in Chapter 6. As the biphenyl is not very large full intercalation is unlikely, but partial intercalation of the pendant phenyl ring is possible, and when combined with the potential covalent binding site on the metal through loss of the chloride, this complex could have some very interesting biological properties.

4.3.9.1 X-ray crystal structure of **17**

Crystals suitable for X-ray analysis were grown from ether diffusion into a benzyl alcohol solution of **17**. The structure is shown in Figure 4.13 and crystal data are shown in Table 4.2. Selected bond lengths and angles are listed in Table 4.3. Figure 4.13 unambiguously confirms that the structure has the piano-stool type geometry, with one ring of the biphenyl η^6 bonded to the metal and the ethylenediamine and the chloride forming the "legs" of the stool. The complex crystallises in the space group C2/c with eight molecules in the unit cell. The Ru-N and Ru-Cl bond lengths and angles are comparable with those in the similar structure of complex **11**, section 4.3.3.1.

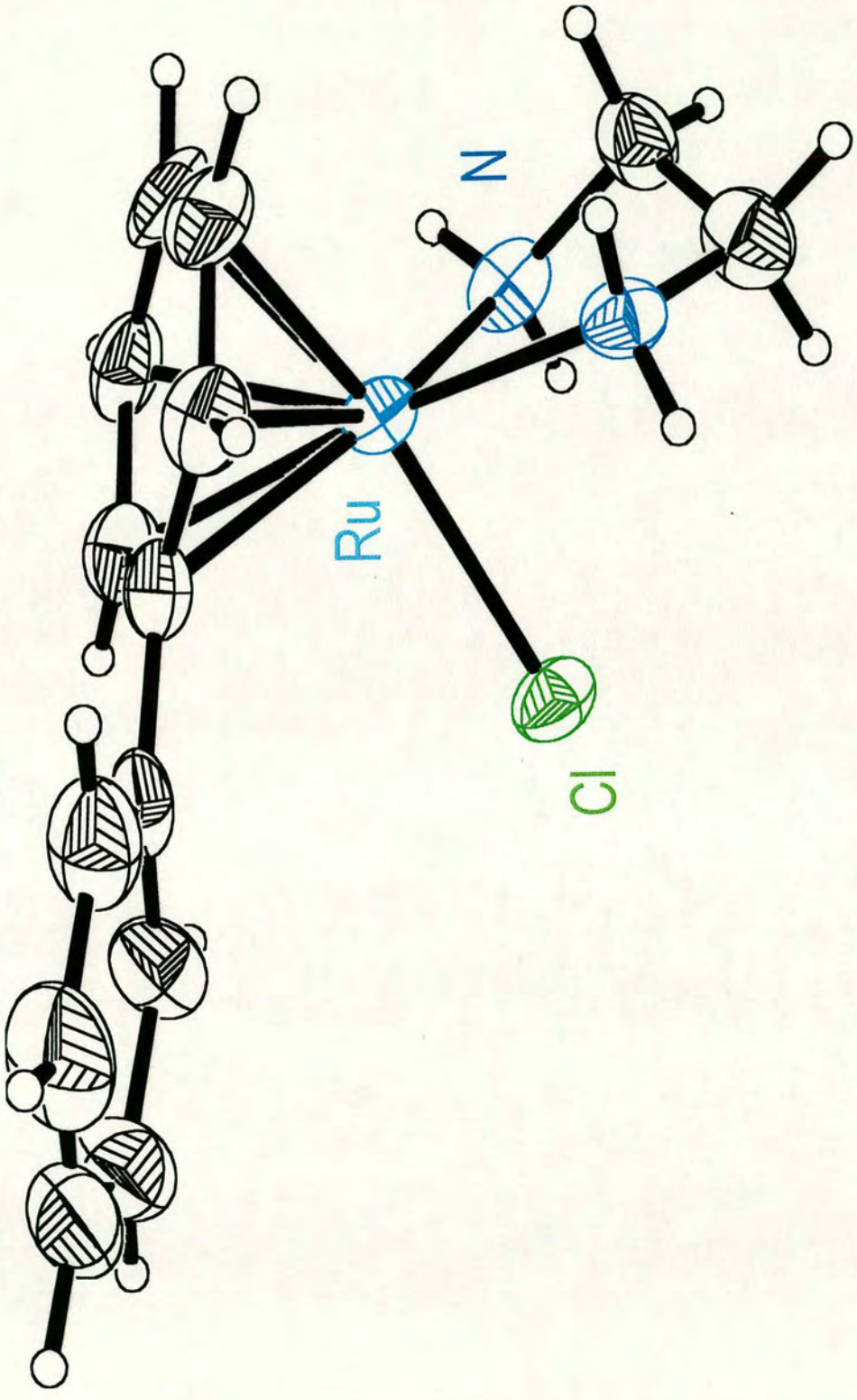

Figure 4.13 X-ray crystal structure of $[(\eta^6\text{-biphenyl})RuCl(en)]^+$ **17**. The PF_6^- counter-ion has been omitted for clarity.

This complex is the first example of a crystal structure of a monoarene complex of ruthenium where the arene is biphenyl. The only other Ru(η^6-biphenyl) complex previously reported is the bis arene [bis(η^6-biphenyl)Ru^{II}][BF_4]$_2$, the biphenyl analogue of ruthenocene. This has actually been reported twice, initially in 1990,[43] when only a cursory description of the structure was made, and again in 1995,[44] when a more thorough analysis was performed. It is interesting to see that both published structures show the two phenyl rings of both biphenyls in the complexes are twisted away from coplanarity, 24.6° for both rings in the early structure, 24.6° and 25.0° for the later one. This phenomenon is also seen in **17**. One phenyl ring is twisted out of the plane by 24.6°. In the solid state, free biphenyl has been found to be planar.[45] The twisting is probably as a result of the way the aromatic rings pack together in the crystal, but it is interesting that the twisting is a consistent occurrence. Another point to note is the length of the bond between the Ru and the substituted carbon, 2.244(6) Å, 0.054 Å longer than the longest of the other Ru-C bonds in the molecule. This also occured in [bis(η^6-biphenyl)Ru^{II}][BF_4]$_2$ [44] where the Ru-C(substituted) bond lengths of 2.271(5) and 2.262(7) Å are also longer than the other Ru-C bonds. As there is no other ligand present which has a *trans* influence, this lengthening must be due to the electron withdrawing effect of the pendant phenyl ring.

4.3.9.2 Hydrolysis of complex **17**

Along with complex **13**, complex **17** was selected as a lead complex for cytotoxicity studies, see Chapter 6. Therefore it is of interest to study the fate of the complex in water, and to develop an HPLC assay to aid further biological investigations. Fortunately the same HPLC method can be used for both **13** and **17**, see section 4.2.22. Like **13**, **17** also gives rise to three peaks in the HPLC trace after dissolution in water, though with different retention times. Peak (a) elutes at 6.7 min, peak (b) at 8.4 min and peak (c) at 9.3 min. Online HPLC-ESI-MS confirmed that peak (c) is the intact complex (chloride still attached), found m/z 351.5, calc. 351.8 amu. Again when studied on-line peaks (a) and (b) merged into a single broad peak. The mass spectrum of this peak

contained an ion at m/z 467.6 which corresponds to a pentanesulfonate taking the place of the chloride (calc. 467.5 amu). The calculated value for the hydrolysed complex, i.e. a water molecule in place of the chloride, is 334.4 amu. The only ion in this region of the spectrum is at m/z 337.3, three units away. This is unexpected, and while it is sure from HPLC studies in H_2O and 100 mM NaCl that **17** loses its chloride in water, exactly what this species is is unknown at the moment.

Like **13**, the proportion of the peaks varies with concentration. At low concentration, 0.1 mM, only 30 % of the complex remains intact. At 10 mM, 60 % of the complex remains intact. This implies that at its IC_{50} levels, which are <10 μM see Chapter 6, if administered in water, the vast majority, if not all, of the complex would have lost its chloride.

4.4 Conclusions

In this chapter the synthesis and characterisation of some Ru(II)arene complexes are described. Arene complexes were chosen as they are known to keep the ruthenium in the oxidation state 2+ under normal conditions and the arene ring would introduce a degree of lipophilicity which could enhance cell-membrane interactions. Substituents were introduced on the arene ring to investigate structure-activity relationships and synethetic routes to derivatised arene complexes were developed. 2D [^{1}H, ^{15}N] HSQC spectroscopy of [(η^6-*p*-cymene)RuCl(en)]$^+$ **13** was studied and the complex appears suitable for further work with isotopically enriched ^{15}N samples. This will be useful for solution structural determination of adducts to biological molecules such as DNA. A HPLC assay was developed for separation of aqueous solutions of two complexes, [(η^6-*p*-cymene)RuCl(en)]$^+$ **13** and [(η^6-biphenyl)RuCl(en)]$^+$ **17**, which have been chosen as lead compounds for anticancer testing and their hydrolysis investigated by a combination of HPLC and ESI-MS. The assay will allow for more in depth analytical work and biological tests.

4.5 References

[1] I. Ogata, R. Iwata, Y. Ikeda *Tet. Lett.* **1970**, 34, 3011

[2] L. Porri, P. Diversi, A. Lucherini, R. Rossi *Makromol. Chem.* **1975**, 176, 3121

[3] G. Winkhaus, H. Singer *J. Organomet. Chem.* **1967**, 7, 487

[4] E.A.H. Griffith, E.C. Amma *J. Am. Chem. Soc.* **1971**, 93, 3167, and ref. therein

[5] E.W. Abel, M.A. Bennett, G.W. Wilkinson *J. Chem. Soc.* **1959**, 3178; M.A. Bennett, G.W. Wilkinson *Chem. and Ind.* **1959**, 1516

[6] H. Zeiss, P.J. Wheatley, H.J.-S. Winkley *Benzenoid Metal Complexes* The Ronald Press Co., New York. **1966**

[7] M.A. Bennett, A.K. Smith *J. Chem. Soc. Dalton Trans.* **1974**, 233

[8] R.A. Zelonka, M.C. Baird *Can. J. Chem.* **1972**, 50, 3063

[9] M.A. Bennett, A.K. Smith, T.N. Huang, T.W Turney *J. Chem. Soc. Chem. Commun.* **1978**, 582; M.A. Bennett, T.N. Huang, T.W. Turney *J. Chem. Soc. Chem. Commun.* **1979**, 312

[10] M.A. Bennett, G.B. Robertson, A.K. Smith *J. Organomet. Chem.* **1972**, 43, C41

[11] A.D. Kelman, M.J. Clarke, S.D. Edmonds, H.J. Peresie *J. Clin. Hematol. Oncol.* **1977**, 7, 274

[12] Y. Hung, W.-J. Kung, H. Taube *Inorg. Chem.* **1981**, 20, 457

[13] F.B. McCormick, D.D. Cox, W.B. Gleason *Organometallics* **1993**, 12, 610

[14] C. Solorzano, M.A. Davis *Inorg. Chim. Acta* **1985**, 97, 135

[15] M.G.B. Drew, C.M. Regan, S.M. Nelson *J. Chem. Soc. Dalton Trans.* **1981**, 1034

[16] R.G. Harvey *Synthesis* **1970**, 4, 161

[17] P.W. Rabideau, D.L. Huser, S.J. Nyikos *Tet. Lett.* **1980**, 21, 1401

[18] C.B. Wooster, K.L. Godfrey *J. Am. Chem. Soc.* **1937**, 59, 596

[19] A.J. Birch *Quart. Rev.* **1950**, 4, 69; A.J. Birch, H. Smith *Quart. Rev.* **1958**, 12, 17

[20] E.M. Kaiser *Synthesis* **1972**, 391

[21] D.E. Richardson, D.D. Walker, J.E. Sutton, K.D. Hodgson, H. Taube *Inorg. Chem.* **1999**, 18, 2216

[22] A.J. Steedman, A.K. Burrell *Acta Crysta. C* **1997**, 53, 864

[23] P.J. Smolenaers, J.K. Beattie, N.D. Hutchinson *Inorg. Chem.* **1981**, 20, 2202

[24] H.L. Stynes, J.A. Ibers *Inorg. Chem.* **1971**, 10, 2304

[25] R. Kramer, M. Maurus, K. Polborn, K. Sunkel, C. Robl, W. Beck *Chem. Eur. J.* **1996**, 2, 1518

[26] W.S. Sheldrick, S. Heeb *J. Organomet. Chem.* **1989**, 377, 357

[27] A. Symala, A.R. Chakravarly *Polyhedron* **1995**, 14, 231

[28] Z. Guo, A. Habtemariam, P.J. Sadler, B.R. James *Inorg. Chim. Acta* **1998**, 273, 1

[29] A.G. Orpen, L. Brammer, F.H. Allen, O. Kennard, D.G. Watson, R. Taylor *J. Chem. Soc. Dalton Trans.* **1989**, 83; A.M. Joshi, I.S. Thorburn, S.J. Rettig, B.R. James *Inorg. Chim. Acta* **1992**, 283, 198; D. Drommi, F. Nicolo, C.G. Arena, G. Bruno, F. Faraone, R. Gobetto *Inorg. Chim. Acta* **1994**, 221, 109

[30] N. Gul, J.H. Nelson *Organometallics* **1999**, 18, 709

[31] J.C.A. Boegens, N.J. Coville, K. Soldenhoff *S. Afr. J. Chem.* **1984**, 37, 153

[32] M.J. Clarke in *Metal Complexes in Cancer Chemotherapy* ed. B.K. Keppler, VCH, Weinheim, **1993**, p.131

[33] B. Lippert *Prog. Inorg. Chem.* **1989**, 37, 1; M.J. Clarke *Prog. Clin. Biochem. Med.* **1989**, 10, 25; J. Reedijk *Inorg. Chim. Acta* **1992**, 198, 873; W.I. Sundquist, S.J. Lippard *Coord. Chem. Rev.* **1990**, 100, 293; S.K. Miller, D.G. van der Veer, L.G. Marzilli *J. Am. Chem. Soc.* **1985**, 107, 1048; A. Terrón *Comments Inorg. Chem.* **1993**, 14, 63

[34] W.S. Sheldrick, S. Heeb *Inorg. Chim. Acta* **1990**, 168, 93

[35] Y. Kageyama, Y. Yamazaki, H. Okuno *J. Inorg. Biochem.* **1998**, 70, 25

[36] P. Salvadori, P. Pertici, F. Marchetti, R. Lazzaroni, G. Vitulli, M.A. Bennett *J. Organomet. Chem.* **1989**, 370, 155

[37] F.A. Cotton and G. Wilkinson *Advanced Inorganic Chemistry*, Wiley, New York, 4th edn., **1980**, p.1200

[38] C.V. Kumar, J.K. Barton, N.J. Turro *J. Am. Chem. Soc.* **1985**, 107, 5518; J.K. Barton, J.M. Goldberg, C.V. Kumar, N.J. Turro *J. Am. Chem. Soc.* **1986**, 108, 2081; A.M. Pyle, J.P. Rehmann, R. Meshoyrer, C.V. Kumar, N.J. Turro, J.K. Barton *J. Am. Chem. Soc.* **1989**, 111, 3051

[39] J. Grant-Collins, A.D. Sleeman, J.R. Aldrich-Wright, I. Greguric, T.W. Hambley *Inorg. Chem.* **1998**, 37, 3133

[40] A.E. Friedman, J.-C. Chambron, J.-P. Sauvage, N.J. Turro, J.K. Barton *J. Am. Chem. Soc.* **1990**, 112, 4960; Y. Jenkins, A.E. Friedman, N.J. Turro, J.K. Barton *Biochemistry* **1992**, 31, 10809

[41] C.J. Murphy, M.R. Arkin, Y. Jenkins, N.D. Ghatlia, S.H. Bossmann, N.J. Turro, J.K. Barton *Science* **1993**, 262, 1025; E.D.A. Stemp, M.R. Arkin, J.K. Barton *J. Am. Chem. Soc.* **1995**, 117, 2375; P. Lincoln, E. Tuite, B. Nordén *J. Am. Chem. Soc.* **1997**, 119, 1454; L.S. Schulman, S.H. Bossmann, N.J. Turro *J. Phys. Chem.* **1995**, 99, 9283; S. Priyadarshy, S.M. Risser, D.N. Beratan *J. Phys. Chem.* **1996**, 100, 17678

[42] T.L. McDonald, E.K. Lehnert, J.T. Lopert, K.C. Chow, W.E. Ross in *DNA Topoisomerases in Cancer* ed. M. Potmesil, K.W. Kohn, Oxford Univ. Press, NY, **1991**, p.199; H. Morjani, J.F. Riou, I. Nabieu, F. Lavelle, M. Manfait *Cancer Res.* **1993**, 53, 4784

[43] K.D. Plitzko, G. Wehrle, B. Gollas, B. Rapko, J. Dannheim, V. Boekelheide *J. Am. Chem. Soc.* **1990**, 112, 6556

[44] L.C. Porter, S. Bodige, H.E. Selnau *Organometallics* **1995**, 14, 4222

[45] G.B. Robertson *Nature* **1961**, 191, 593; G.-P. Charbonneau, Y. Delugeard *Acta Crystallogr.* **1976**, B32, 1420

Chapter 5

Interactions of

[(η^6-*p*-cymene)RuCl(en)]$^+$

with nucleotides and oligonucleotides

5.1 Reactions of [(η^6-*p*-cymene)RuCl(en)]$^+$ 13 with DNA model compounds

Nucleotides and their metal ion complexes are among the most widely used substrates in cell metabolism,[1] both in free form and as subunits of oligonucleotides and DNA. Indeed, it is believed to be a guanine-guanine chelate that gives cisplatin its excellent activity against certain tumours.[51] Unfortunately, it is not a simple matter to monitor reactions of complexes with large pieces of DNA by physical methods, and so low molecular DNA components such as 5′-dGMP are often used. The structures of the nucleotides used in this section are shown in Figure 5.1.

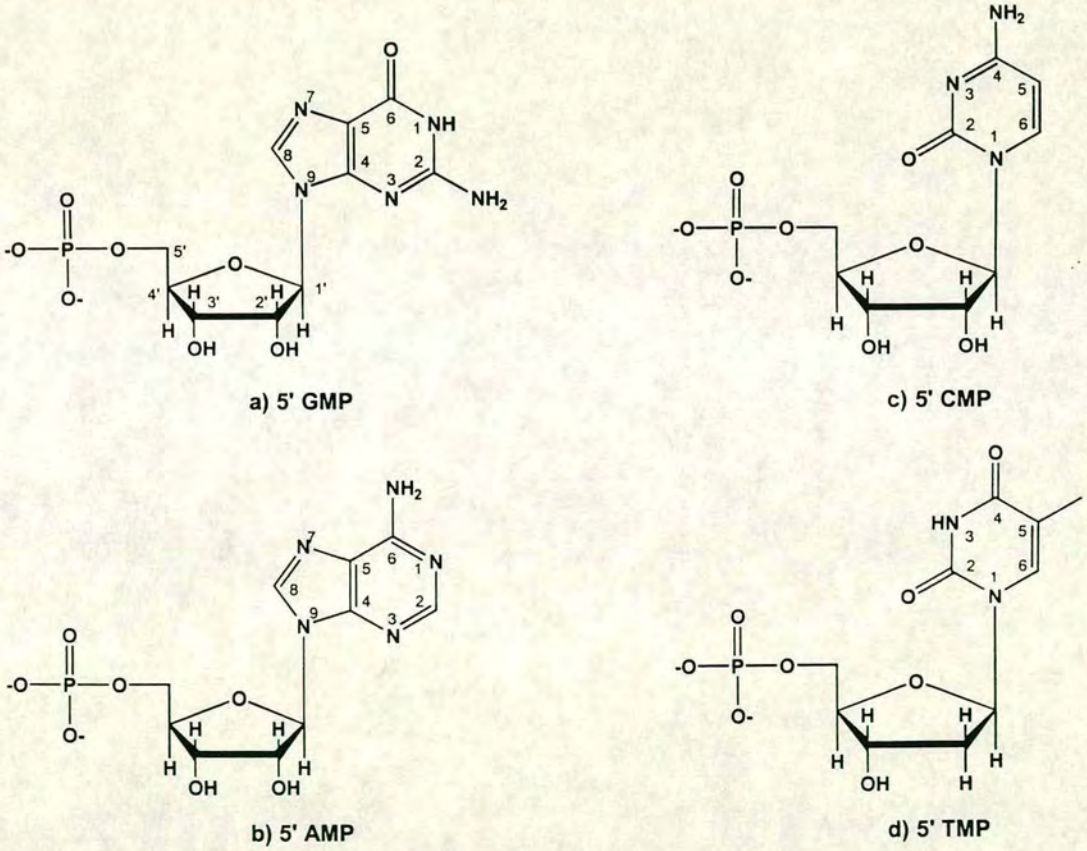

Figure 5.1 Structures of mononucleotides used in this section, including numbering scheme. The numbering scheme for the sugar moiety in (a) is the same for (b), (c) and (d)

In particular, nucleotides, nucleosides and 9-substituted nucleobases can be used to model reactions of complex DNA, but in a less complicated form,[2] and they have often been applied as models in order to understand better the cancerotoxic activity of cisplatin.[3]

With regard to ruthenium, it has been found that there is a direct correlation between cytotoxicity and DNA binding for the ruthenium am(m)ine and imidazole anticancer compounds *cis*-[$Ru^{III}Cl_2(NH_3)_4$]Cl_2 and [HIm][*trans*-[$Ru^{III}(Im)_2Cl_4$] in cell cultures.[4] Also, a number of ammine, amine and heterocyclic complexes of ruthenium inhibit DNA replication,[5] which implies DNA binding. Other effects indicative of DNA binding are mutagenic activity and induction of the SOS repair mechanism,[6] binding to nuclear DNA[4,7] and reduction of RNA synthesis.[6] Polyaminocarboxylate complexes of ruthenium also show anticancer activity which is assumed to be through DNA binding.

Knowing the location of the binding site of the metal to DNA could be crucial for understanding the mechanism of action of a drug. There is strong indication that the N^7 of guanine is the favoured site of binding for ruthenium complexes. It has been shown that bispyridyl compounds of Ru^{II} only bind to the N^7 of the guanine moiety when the model bases 9-methylhypoxanthine and 9-ethylguanine are used (both are models for guanine residues in DNA).[8] Also, *mer*-[$Ru^{III}Cl_3$(terpy)] binds preferentially to N^7 when reacted with guanine analogues,[9] and the reported binding ratio of *trans*-[$Ru(SO_3)(NH_3)_4(H_2O)$] to guanine-N^7/adenine-N^7 is 95.[10]

Unusual binding of Ru^{II} at gua-N^1 has been observed for *cis*-[$RuCl_2(biq)_2$] at neutral pH.[11] Metal coordination at gua-N^1 is not uncommon,[12] although there are no other reports for ruthenium in the literature where the N^1 adduct is a major and isolable adduct. It is unusual at neutral pH as the metal ion has to compete with the proton at that site. For metals with slow ligand exchange kinetics, like Pt^{II}, mononuclear N^1 coordination to guanine is only observed at high pH[13] or when the basicity is lowered due to prior binding at the N^7 site.[14]

ICP-AES studies on the anticancer active complexes *trans*-[Him][$Ru^{III}Cl_4(Im)_2$] and *trans*-[Hind][$Ru^{III}Cl_4(Ind)_2$] and their interactions with synthetic double stranded homopolymers have shown that they exhibit a very definite preference for the poly(dG)•poly(dC) duplex to poly(dA)•poly(dT) duplex.[15]

Studies of the interactions of both *cis*- and *trans*-[$RuCl_2(DMSO)_4$] complexes with nucleosides, nucleotides and DNA *in vitro* suggest that covalent bonds between Ru and DNA occur mainly at the N^7 of guanine.[16] It was noted that reaction of these complexes with 5′-AMP yielded only an adduct through the phosphate group,[17] however a recent study with the dinucleotides ApG, GpA, d(ApG) and d(GpA) resulted in coordination only through N^7 sites on both A and G.[18]

Ruthenium(arene) complexes of guanine and adenine 5′-mono-, di-, and tri-phosphates have been characterised.[19] Reaction of [(η^6-C_6H_6)$Ru(D_2O)_3$]$^{2+}$ with 5′-GMP leads solely to the formation of the N^7 coordinated 1:1 and 1:2 complexes without any other adducts being observed. With 5′-GTP, macrochelate complexes involving N^7 and phosphate groups were formed. Reaction with 5′-AMP resulted in a cyclic trimer being formed, again with coordination at N^7 involved, as well as N^6 and N^1.

Therefore it is of great interest to investigate nucleotide binding properties of the ruthenium(arene) complex [(η^6-*p*-cymene)RuCl(en)]$^+$ **13** , Figure 5.2, in a bid to investigate its potential DNA binding sites and biological activity, and to see whether a prediction of N^7 binding, based on previous literature reports, is correct. In this section the binding **13** to 5′GMP, 5′AMP, 5′CMP and 5′TMP is examined, as well as the effect of changing the pH.

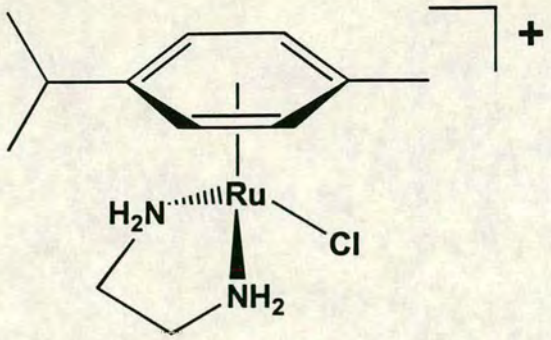

Figure 5.2 The structure of [(η⁶-*p*-cymene)RuCl(en)]⁺ **13**

5.1.1 Experimental

NMR scale reactions of **13** and nucleobases were typically carried out in a 1:1.1 molar ratio (Ru:nucleotide) in D_2O or 90 % H_2O:10 % D_2O. Concentrations were typically in the range of 20 mM. The solutions were incubated at 310 K for 24 h prior to acquisition of spectra. For details on spectra acquisition see Section 2.2.2. pK_a curves were fitted using the Kaleidograph programme and pK_A values determined by first derivatives.

5.1.2 Results and Discussion

The complexes were reacted with the model bases in 90 % H_2O/10 % D_2O or D_2O and the reactions monitored by NMR. Although strictly as DNA models the nucleotides used should be 5′-dNMP (NMP = nucleobase monophosphate) variety, i.e. deoxy, the presence of the hydroxyl group at the 2′ position of the sugar moiety is not expected to affect the reactivity of the compounds. Deductions were made as to binding sites by observing changes in chemical shifts of signals appropriate to binding of the metal centres to sites on the nucleotides. **13** would be expected to only have one binding site available through loss of the chloride. Therefore, assuming a 1:1 reaction, a slight excess of the nucleobase was used in order to have some unreacted material as a reference point when analysing the shifts after the reaction. The affinity of a positively charged metal ion can be expected to parallel that of a proton and is therefore related to the basicity of the site. Diamagnetic

metallation of a nucleotide produces effects quite similar to protonation.[20] Protonation of the base function of a nucleotide normally causes a downfield shift of the nucleobase signals,[12] and from previous ruthenium-nucleotide studies,[9,10,14,16] ruthenation of a base site would be expected to cause the same effect.

The pK_A values of the unsubstituted bases are:[12, 21]

thy-N^3 (9.8) > gua-N^1 (9.4) > cyt-N^3 (4.6) > ade-N^1 (4.1) > gua-N^7 (1.9) > ade-N^7 (-1.6)

From the basicities it is clear to see that in pyrimidine bases, metal binding might occur predominantly at N^3, [21] whereas purine bases exhibit a dichotomy between binding at N^1 or N^7. In slightly acidic and neutral solutions both N^1 and N^7 of adenine remain unprotonated, and hence are available for coordination, but for guanine the $pK_A \sim 9$ for N^1, and so only N^7 is unprotonated and the metal ion has to compete with the proton for binding at N^1. Also, the N^7 sites of G and A do not participate in Watson-Crick base pairing[22] and are sterically accessible for a metal complex when located in the major groove of DNA.

The N^7 of guanine is the most electron rich of the DNA nitrogens[23] and the most basic site of all the nucleobases[24] and hence it has the greatest attraction for transition metal ions (Lewis acids). The N^7 of guanine has stronger σ-donor properties than adenine N^7 and successive guanine residues form the most electronegative regions in DNA. In fact, the preferred binding sites in nucleobases for cisplatin at physiological pH are gua-N^7 > ade-N^7 > ade-N^1 > cyt-N^3.[25]

5.1.2.1 Reaction of complex **13** with 5′GMP

The spectrum of **13** in D_2O is shown in Figure 5.3. The peaks in the spectrum correspond to the presence of two species (a) 60 %, and (b) 40 %. The concentration of this sample is 40 mM. With our knowledge of the hydrolysis process of **13** from HPLC, section 4.3.5.2, we can assign the major species (a) as the intact complex and the minor species (b) as the hydrolysed version. The peaks corresponding to the

arene protons, the tolyl protons, the methyl groups of the *p*-cymene isopropyl group and the NH_2 signals of the ethylenediamine ligand all undergo a downfield shift upon hydrolysis. The fact that we can see the NH_2 groups in D_2O is significant as it indicates a slow exchange between the ^1H and ^2H, which implies a strong Ru-N bond. The smallest of the shifts is for the tolyl singlet (δ 2.22 - 2.26) and the isopropyl methyl doublet (δ 1.28 - 131). This is understandable as they are furthest away from the metal centre and would be less affected by the change in coordination environment. The two doublets for the arene protons shift from δ 5.70 to 5.81 and δ 5.50 to 5.59. The C-H of the isopropyl does not shift sufficiently to distinguish it from the original signal. The multiplet for the CH_2 groups of the ethylenediamine ligand undergoes a slight upfield shift (δ 2.49 - 2.41) upon hydrolysis.

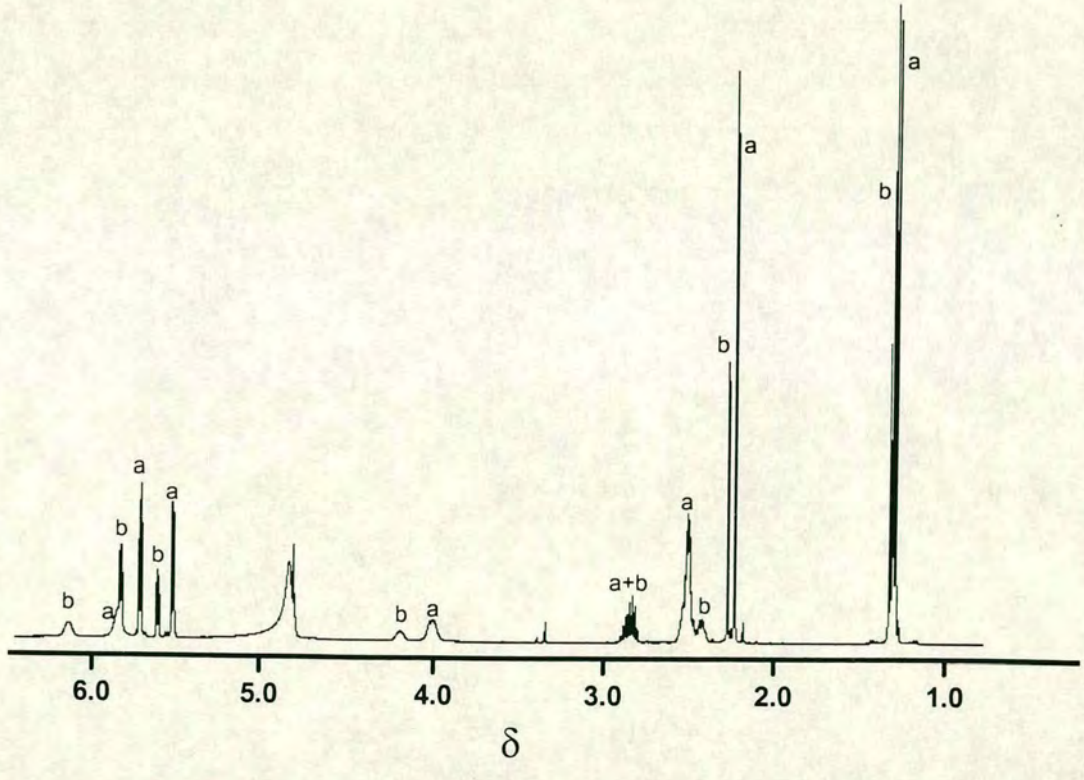

Figure 5.3 ^1H NMR spectrum of a 40 mM solution of complex **13** in D_2O. Peaks labelled (a) correspond to the intact complex, (b) corresponds to the hydrolysed form.

For the reaction of **13** with the mononucleotide 5′GMP, the nucleotide was added to a solution of **13** in 90 % H_2O/10 % D_2O for a 1:1.1 reaction. The concentration of the complex was 20 mM. With knowledge of the hydrolysis of **13** from HPLC, section 4.3.5.2, it can be assumed that the complex was about 60 % intact when the nucleotide was added. The spectrum of the reaction after 24 h incubation at 310 K is shown in Figure 5.4. The reaction is essentially complete as nearly all the free 5′GMP has disappeared (δ 8.13). There are some very minor signals in the spectrum, but the major peaks, marked * in Figure 5.4, are assignable. The doublet for the isopropyl methyl groups of *p*-cymene is at δ 1.15, the singlet for

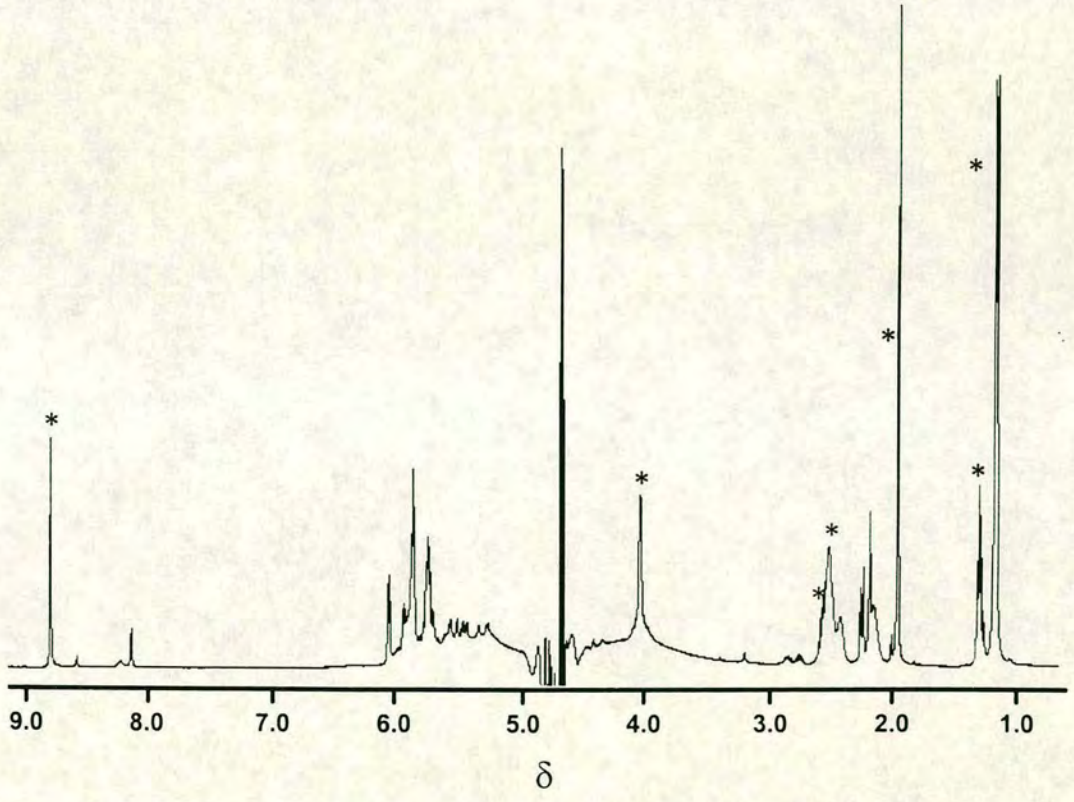

Figure 5.4 ^{1}H NMR spectrum of the reaction of complex **13** with 5′GMP in a 1:1.1 molar ratio in 90 % H_2O/10 % D_2O. The concentration of **13** is 20 mM. The peaks marked (*) correspond to a 1:1 adduct of 13 with 5′ GMP. The very small peaks at δ 8.22 and 8.60 are impurities that were discovered in the 5′GMP

the tolyl group is at δ 1.94 and the H-8 of the guanine moiety is at δ 8.79, shifted downfield from free 5′GMP by 0.66 ppm. This H-8 shift is very indicative of a the nucleotide reacting with the metal at N^7. The CH_2 resonances of the ethylenediamine ligand are two broad multiplets at δ 2.49 and 2.40. They have become slightly resolved into two signals after reaction, as opposed to the one for the complex alone in D_2O. The multiplet for the C-H of the *p*-cymene isopropyl group has shifted underneath this signal. The arene region of the spectrum contains many peaks now, some due to the nucleotide, and is unassignable without detailed 2D NMR studies. The NH_2 signals of the ethylenediamine have decreased to the extent that they are not assignable.

These observations show that the reaction of **13** with 5′GMP results in one major product, a 1:1 adduct, with coordination of the nucleotide occurring through the N^7 of the guanine.

5.1.2.2 pH titration of **13** with 5′GMP

In order to further investigate the binding of **13** to 5′GMP, an NMR pH titration was performed. This involved incubating a 1:1 molar ratio sample of **13** and 5′GMP for 24 h at 310 K and then acquiring the ^1H NMR spectrum of the solution at different pH values. The pH was adjusted by addition of aliquots of either NaOD or DNO_3 and was internally referenced to TSP. By plotting the shift of the H-8 protons against pH, Figure 5.5, pK_A values for the bound nucleotide were determined. 5′GMP is a tribasic species.[26] It binds two protons at the phosphate group and one at the purine moiety. For $H_3(GMP)^+$ the first proton is released from the -P(O)-$(OH)_2$ group, the second from the $H^-(N^7)$ (pK_A 2.48[27]) site and the third one again from the still monoprotonated phosphate group (pK_A 6.25[27]). A fourth proton may be released in the alkaline pH range from the $H(N^1)$ (pK_A 9.49[27]) site. The release of the first proton in $H_3(GMP)^+$ occurs with a pKa of 0.3, and hence is deprotonated under all but the most extreme solution conditions,[27] and is not relevant for this study.

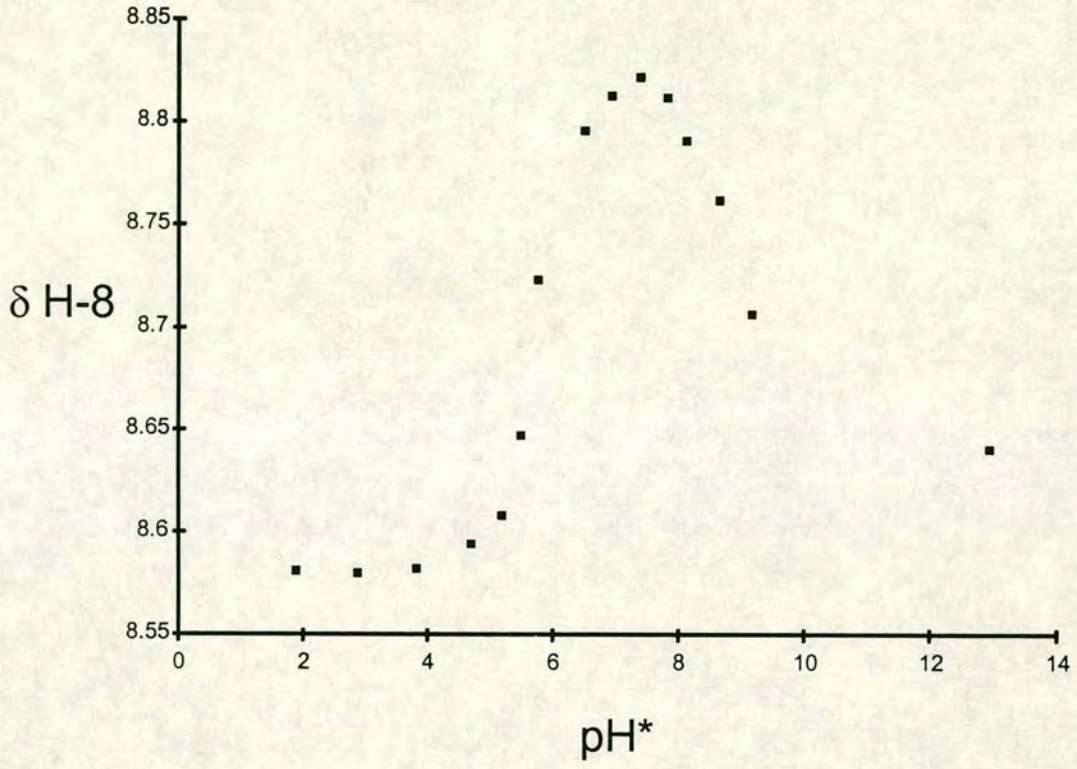

Figure 5.5 Plot of δ H-8 vs pH* of 5'GMP bound to [(η⁶-*p*-cymene)RuCl(en)]⁺ **13**. The steep change in chemical shift in the region δ 5-6 corresponds to the second deprotonation of the phosphate moiety. The change in the region δ 8-9 corresponds to deprotonation of N^1 of the guanine.

The pK_A of the deprotonation of N^7 in GMP is given in the literature as 2.48.[27] It can be seen from Figure 5.5 that this deprotonation is absent in the present case and this is further evidence that the 5′GMP is bound via the N^7. There are two pH dependant effects seen though. The first is attributable to the ionisation of the remaining proton on the phosphate residue. This pK_A of 5.75 for the bound nucleotide is a decrease of 0.5 units form the literature value of 6.25.[27] It is known that protonation of the phosphate group should cause an upfield shift of the nucleobase proton signals[12] and this is what is observed here. As the pH is lowered, the phosphate group becomes protonated and the H-8 proton resonance shifts to higher field. The chemical shift

change that is observed in basic pH can be attributed to protonation of the N^1 of the base. In free 5′GMP, the pK_A of N^1 is 9.49.[27] As diamagnetic metallation produces effects quite similar to protonation,[20] the binding of Ru(II) to the N^7 should have the effect to acidify the proton at N^1, causing a decrease in the pK_A of N^1. This is observed in the present case, with the pK_A of the bound nucleotide being 8.63, almost one unit less than the free molecule. *Trans*-$RuCl_2(DMSO)_4$ lowers the pK_A of N^1 of guanine by almost two units when bound to N^7 [16(b), 28] and the coordination of Pt(II) in cisplatin decreases the pK_A of guanine N^1 by one unit.

5.1.2.3 Reactions of **13** with 5′AMP, 5′CMP and 5′TMP

In order to investigate qualitatively whether or not **13** reacts with the nucleobases 5′AMP, 5′CMP and 5′TMP, NMR scale reactions in a 1:1.1 Ru:nucleotide molar ratio were performed. This is of interest to see if there is potentially more than one binding site on DNA for the complex.

Complex **13** reacts only slightly with 5′AMP in unbuffered solution (pH* = 5. 24). There are two proton NMR probes on 5′AMP, that of the H-8 and H-2. After 24 h incubation at 310 K, only a minor amount, 10 %, of a new species had been formed. This is indicated by the slight downfield shift of the H-8 proton (δ 8.50 to 8.52) and the slight upfield shift of the H-2 (δ 8.26 to 8.21). The major species in the NMR correspond to the intact and the hydrolysed forms of **13**. The ^{31}P NMR shows a shift of 7.24 ppm, from δ 1.12 to 8.36, so coordination to the metal is probably through the phosphate group. It had previously been found that both *cis*- and *trans*-$[RuCl_2(DMSO)_4]$ do not react with the adenine moiety of 5′AMP,[17] just through the phosphate group.

The reaction with 5′CMP (pH* = 6.84), went to 40 % completion after 24 h. Binding appears to be through the phosphate group rather than the base. This is indicated by the upfield shift of the doublet for the H-6 proton from δ 8.08 to 7.93 upon reaction, and of the doublet at for the H-5 proton from δ 6.14 to 6.10. Binding

to the phosphate group of a nucleotide causes upfield shift of the base protons,[12] whereas binding to a base nitrogen would cause a downfield shift, such as that shown by the binding of Pt(II) to the N^3. [29] There is also the presence of two other species in the spectrum, corresponding to the intact complex and the hydrolysed complex. The ^{31}P NMR spectrum also shows a large downfield shift of the signal for the phosphate group from δ 3.42 to 8.54. That **13** reacts to a reasonable extent with 5′CMP is of interest as in Section 5.3 the binding of **13** to a 14mer ODN containing equal amounts of G and C residues is investigated.

Only 20 % of the 5′TMP has reacted after 24 h at 310 K. Again this appears to be through the phosphate group rather than the nitrogenous base. The H-6 proton shows an upfield shift 0.1 ppm, from δ 7.79 to 7.69. Again there is considerable presence of intact and hydrolysed forms of the complex. The ^{31}P NMR spectrum shows that the phosphate group signal has moved from δ 1.97 to 8.53. That the complex did not react with the thymidine moiety of the nucleotide is in agreement with the report that both *cis* and *trans*-[$RuCl_2(DMSO)_4$] did not react at all with thymidine, even after prolonged periods.[30]

It has been shown that complex **13** reacts all four DNA models. However, only 5′GMP binds through the base moiety (via N^7). The other three bases appear to bind through the phosphate group.

5.1.2.4 Reaction of **13** with an equimolar mixture of 5′GMP and 5′CMP

In Section 5.3 the binding of **13** to a 14mer oligonucleotide containing equal numbers of Gs and Cs is investigated. To see which base is the preferred choice of **13**, an NMR sample containing **13**, 5′GMP and 5′CMP in a 1:1:1 ratio was prepared and incubated at 310 K for 24 h and the NMR spectrum acquired. The reaction of **13** with 5′GMP is very much favoured over the reaction of **13** with 5′CMP. This is clear from the ^{1}H spectrum. There was only a negligible amount of unreacted 5′GMP left, and a large singlet at δ 8.76 for the H-8 of reacted nucleotide, Figure 5.6. The downfield shift from δ 8.07 is indicative of binding to the metal at N^7. There is one doublet corresponding to the isopropyl methyl groups (δ 1.08), one singlet for

the tolyl protons (δ 1.88) and the CH_2 groups of the ethylenediamine ligand are two broad multiplets at δ 2.05 and 2.41. The C-H of the isopropyl group has merged with the multiplet at δ 2.41. The N-H signals are not visible anymore. There is no signal for unreacted (intact or hydrolysed) **13**. These signals inform us that there is only one product with between **13** and the nucleotides, and that it is from a 1:1 adduct of

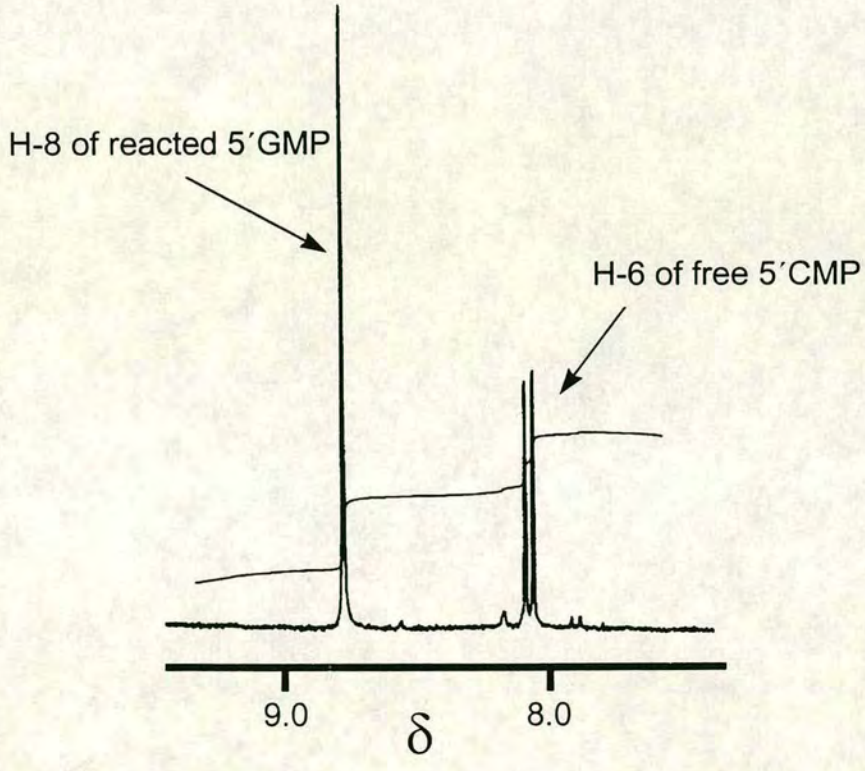

Figure 5.6 ^{1}H NMR spectrum of the equimolar reaction of **13** with 5′GMP and 5′CMP in D_2O. The marked peaks show that the complex has reacted with 5′GMP at the N^7 as the H-8 peak has shifted to lower field as compared to free 5′GMP, but has not reacted with 5′CMP

13 with 5′GMP. The doublet for the H-6 of free 5′CMP remains at δ 8.05, with only a negligible peak appearing upfield at δ 7.9, which would correspond to the metal binding the 5′CMP through the phosphate group, see section 5.1.2.3. Therefore,

when present in equimolar amounts, complex **13** has a much stronger affinity for reaction with 5′GMP than 5′CMP.

5.1.3 Conclusions

Complex **13** [(η^6-*p*-cymene)RuCl(en)]$^+$ reacts with 5′GMP in a 1:1 manner by binding at the N^7 of the guanine moiety. On investigation of the reaction of **13** with the other nucleotides 5′AMP, 5′CMP and 5′TMP it was found that they reacted through the phosphate group rather than the basic nitrogens. A competitive reaction between 5′GMP and 5′CMP with **13** showed that the Ru(II)arene complex strongly preferred binding to the guanine nucleotide. From these studies it can be assumed that the main target for the arene complexes on DNA will be guanine residues.

5.2 Melting Temperature of 14mer oligonucleotide duplex in the presence of [(η^6-para-cymene)Ru(en)Cl][PF_6] 13*

DNA is almost always bound to various metal ions under physiological conditions, e.g. K^+, Mg^{2+}, and these ions play a crucial part in the behaviour of DNA.[31] Various studies using UV and circular dichroism have investigated the interaction of metal-ions and DNA. It has been found that metal ions actively participate in determining the helical, tertiary and quaternary structures of DNA. The differing effects of various ions are due to the nature of the various binding sites and the affinities of the ions for the sites.[32] In the nucleoside, glycosyl links are formed and this blocks the N^9 of the purine and the N^1 of the pyrimidine (in the free purine, unsubstituted N^9 is the most basic site). Hence in DNA the phosphate oxygens and the N^7 site of guanine seem to be the most likely site of metal interaction.[33] Knowing that complex **13** binds to the nucleotides of DNA, see section 5.1, and in particular the N^7 of guanine it is of interest to investigate the structural impact that this has on the DNA duplex.

Cisplatin and other Pt(II) drugs are thought to kill cells as a result of their binding to DNA.[34] Healthy cells are able to remove the adduct by a complicated series of repair mechanisms, however in cancerous cells these mechanisms are unable to function effectively, resulting in apoptosis. NMR studies, in combination with X-ray and gel electrophoretic studies,[35] have found that binding of cisplatin results in the DNA being unwound by 13 - 23 °, and bent by 34 - 55° in the direction of the major groove. The local area of binding becomes A-form while the rest of the molecule remains in the B-form.[35] These changes cause the melting temperature of the DNA to be reduced by 10 - 20 °, depending on the type of DNA being studied. This

* The work in this section formed part of a final year undergraduate project by Nathan Hughes.

indicates a significant destabilisation of the duplex and it is therefore potentially of great importance to the drug/activity relationship.

A series of proteins named HMG (High Mobility Group) proteins bind preferentially to bent DNA-cisplatin adducts.[36] It is postulated that HMG proteins recognise the bent site of cisplatin binding and binds to this region. This step may be critical to the fate of the cell. Various mechanisms have been postulated for this process.[37] The protein may mask the adduct preventing repair, the protein may attract tumour specific regulatory proteins resulting in cell death or the adduct may interfere with ribosomal RNA (rRNA) transcription thus reducing protein synthesis.[38] Such disruption may be crucial in cancer cells where rRNA synthesis is particularly stimulated.

Nucleotides tend to have an overall negative charge as a result of their polyanionic phosphate backbone. The phosphate groups have a $pK_A<1$ and hence are deprotonated under most solution conditions.[27] Positive ions, such as metals, counteract the overall negative charge of the nucleotides and reduction of the phosphate chain repulsion (charge screening) is largely responsible for structural transitions[39] and stabilising of the DNA.[40] Reaction of a positive metal ion with the phosphate group generally means stabilisation of ordered structures[41] whereas reaction with the bases means destabilisation of ordered structures.[42] Although high ionic strength of the medium stabilises the DNA duplex,[47] it is thought that the stability conferred by the positive platinum ion is outweighed by the instability caused by the bending and unwinding. A good method of investigating the extent of the stabilising, or destabilising, effect of a metal ion on a DNA duplex is the process of DNA melting.

Nucleic acids absorb light with a λ_{max} at 260 nm due to π-π^* electron transitions of the purine and pyrimidine rings.[43] When a DNA helix is formed, base stacking is accompanied by a reduction in UV absorption (hypochromicity) compared to the random coil form.[44] This makes UV analysis a convenient method to monitor the formation and breakdown of double helices. If the temperature of a solution

containing double-heliced DNA is slowly raised and the absorbance monitored, it can be seen that the absorbance increases suddenly at a certain temperature due to the dissociation of the ordered helices. The mid-point of the transition is known as the melting temperature (T_m).

Helix-coil interactions are essentially an all or nothing process, and since the absorbance of double stranded DNA is essentially 10 % less than the single stranded form, the transition between the two is easy to monitor. Analysis of the system A(pA)17•U(pU)17 at various temperatures[45] yielded exclusively either dissociated coiled monomers or fully integrated double helices, with only the terminal base pairs in rapid dissociation-recombination.

Certain factors affect T_m. The thermal transition of DNA is greatly influenced by the ionic strength of the solution.[46] Increasing the ionic strength of the medium increases the T_m.[47] Increasing the chain length of the oligonucleotide also increases the T_m, with a steeper slope at the point of inflection, synonymous with enhanced cooperativity. It has also been noted that T_m increases the greater the ratio of GC/AT.[48]

It was of interest to investigate whether binding of complex **13** to the 14mer duplex **I•II** (Figure 5.7) causes any thermal, and hence structural, instability in the helix. The melting point temperature of the Ru-arene adduct was compared to both free DNA 14mer and the cisplatin adduct in solutions of varying ionic strength. The sequence of **I•II** is shown in Figure 5.7 and the sequence is further discussed in Section 5.3.

5′-ATACATGGTACATA-3′ **I**

3′-TATGTACCATGTAT-5′ **II**

Figure 5.7 Oligonucleotide **I** and its complementary strand **II**

5.2.1 Experimental

ODNs **I** and **II** were obtained as HPLC purified sodium salts from Oswel (Southampton, U.K.). Concentrations were determined using UV/Vis spectroscopy (strand **I** ε_{260} = 149.0 $mM^{-1}cm^{-1}$ and strand **II** ε_{260} = 137.2 $mM^{-1}cm^{-1}$). DNA melting-point UV/Vis spectra were recorded on a Perkin Elmer λ 20 UV/Vis spectrometer using a quartz cell with a path length of 10 mm. The temperature was controlled using a PTP1 Peltier Temperature Programmer. The data was analysed using UV Winlab and PE Templab software for Windows 95 from Perkin Elmer. Drug (**13** or cisplatin) and duplex **I•II** were mixed in a 1:1 molar ratio at a concentration of 3 mM and incubated at 310 K for 48 h. The buffer was 10 mM sodium phosphate (pH = 7). Ionic strength was varied (10 - 60 mM) by addition of aliquots of $NaClO_4$ solution.

5.2.2 Results and discussion

In this experiment the melting point of the 14mer oligonucleotide duplex **I•II** was investigated as the free duplex, after incubation (1:1 molar ratio) with complex **13** for 48 h and after incubation (1:1 molar ratio) with cisplatin for 48 h at a range of ionic strengths. This allowed an assessment of the effect of the complex on the thermal stability of the duplex.

The melting points of the free duplex and the drug/duplex mixtures are plotted against the ionic strength of the solution in Figure 5.8. It can be seen that all three follow the pattern that the melting temperature increases with increasing ionic strength.[47] The T_m of the 14mer ranged from 33 - 40 °C over the range of ionic strengths. It can be seen that addition of the Ru(II) complex to the duplex had a thermally destabilising effect on the melting point of the duplex, causing it to be decreased by 5 °C. This indicates that the complex has destabilised the structure of the duplex.

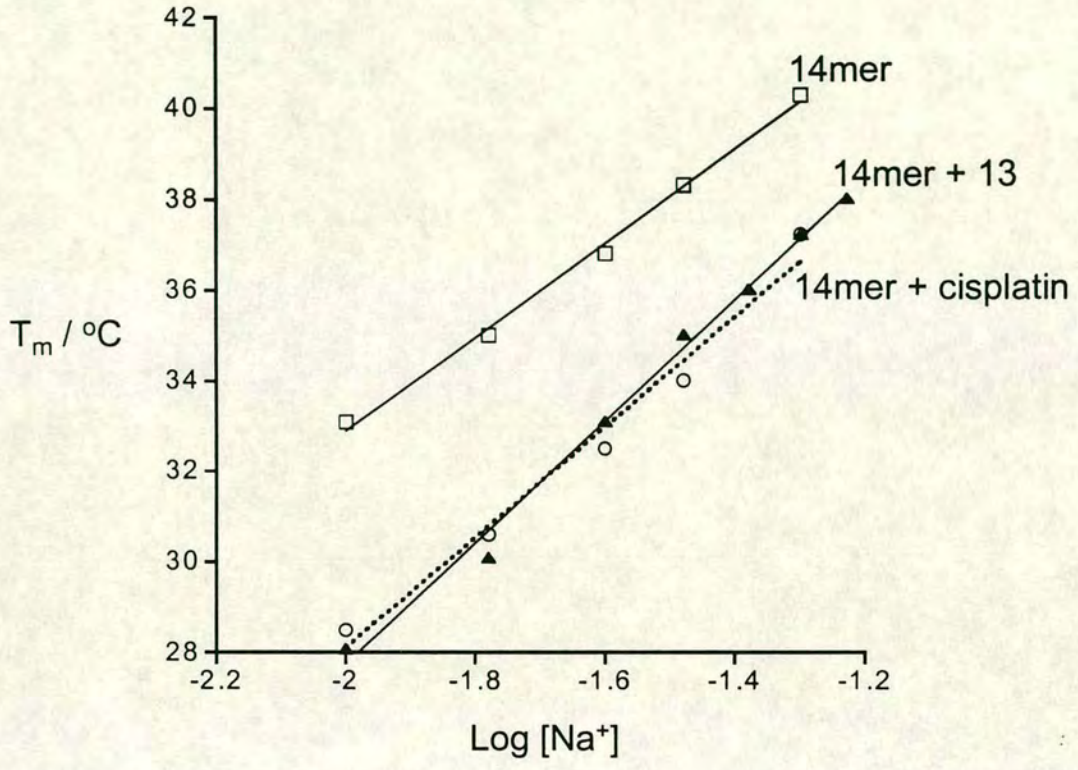

Figure 5.8 Effect of [(η⁶-*p*-cymene)Ru(en)Cl][PF_6] **13** (▲) and cisplatin (o) on the melting temperature (T_m) of the DNA duplex **I•II** ( ), (molar ratio of metal:duplex 1:1). Reaction conditions: 3 mM duplex, 10 mM phosphate buffer (pH = 7)

As a comparison experiment, the duplex **I•II** was also incubated with cisplatin. It is known that cisplatin has a significant structural effect on DNA,[35] and so we would expect it to decrease the T_m of the duplex. This is shown in Figure 5.8. It is remarkable how similar the effects of the two drugs are. Since cisplatin's activity is thought to be linked to DNA binding,[34] the ruthenium complex may also have potential as a chemotherapeutic agent.

In Section 5.3 it is shown that it is possible to isolate the various adducts of **13** to the DNA single strands. An attempt was made to anneal the isolated adduct strands to their complementary strands. The annealing process was monitored by following the

isothermal mixing curves.[49] These showed that the strands did not anneal when the ruthenium complex is bound to a single strand first. Hence more specific melting point investigations were not possible. This was unexpected as the binding of **13** to the duplex did not alter the duplex's melting cooperativity, i.e. have an effect on the two-state melting behaviour of the duplex structure. This work does show conclusively, however, that **13** binds to the duplex ODN in such a manner that it significantly effects the thermal stability of the duplex structure.

5.3 Reaction of [(η^6-para-cymene)Ru(en)Cl][PF_6] 13 with 14mer oligonucleotide

The N^7 site of guanine is the most basic site on the DNA nucleobases.[24] This makes it a strong candidate for interactions with Lewis acids such as the metal centres of metallodrugs. Indeed, DNA is thought to be the most likely bio-target[50] of the potent anti-tumour drug cisplatin, and its efficacy is probably linked to the formation of 1,2-GG or 1,2-AG intrastrand bifunctional adducts.[51,52] A GG bifunctional adduct has been identified by recent X-ray crystallographic work[53] to severely distort the double helix by causing a bend towards the major groove and a widening and flattening of the minor groove, resulting in an unusual juxtaposition of A-like and B-like helical segments. It is possible that this feature could be important for the recognition of Pt-DNA adducts by HMG proteins. HMG (high mobility group) proteins are thought to interfere with cellular repair processes when interacting with Pt-DNA adducts.

Ruthenium complexes have also been found to interact with DNA and nucleotides in a variety of ways, such as covalent binding and intercalation. Indeed, much of the work involving antineoplastic evaluation has found that ruthenium is often selective for N^7 of guanine. Examples of this are Ru^{III} amine and aromatic imine complexes[54,55,56,57,58], and the Ru^{II} complexes *cis* and *trans*-$RuCl_2(DMSO)_4$[59,60,61,62,63] which have been found to favour binding to two adjacent guanine residues. Therefore, it is of interest to investigate the binding of the ruthenium-arene complex [(η^6-*para*-cymene)Ru(en)Cl][PF_6], **13**, see Figure 5.2, to DNA, and to elucidate its binding site.

The DNA strand used in this work is the 14 base single strand oligonucleotide d(ATACATGGTACATA) **I**. This strand (and its complementary d(TATGTACCATGTAT) **II**), see Figure 5.7, was designed for analysis of the bifunctional Pt-GG intrastrand adduct. Its sequence is such that formation of AG intrastrand adducts is not possible. The benefits of the strand in the case of the Ru-arene complex is that it contains a selection of all four nucleotides, and so

investigations will yield information on the base specificity of the complex. It also contains a potential GG chelation site. Complex **13** may form only monoadducts with DNA as it has only one available coordination site through loss of the chloride and therefore differs from metal-drugs such as cisplatin and *cis*-[$RuCl_2(DMSO)_4$].

There is a previous report of the significance of monofunctional DNA adducts. The promising antitumour active *trans* iminoether complex[64] $PtCl_2$(*E*-iminoether$_2$) forms predominantly monofunctional adducts at G residues[65] and induces local distortion in DNA.[66] [Pt(dien)Cl]$^+$ has been widely used to mimic the first binding step of cisplatin, and is itself capable of distorting DNA structure and inducing local DNA denaturation.[67,68,69] Recently, the binding of [Pt(dien)Cl]$^+$ to d(ATACATGGTACATA) has been used to investigate the kinetics of Pt binding to the guanine residues on the 3′ and 5′ end of the strand.[70]

The primary techniques used in this investigation are HPLC and electrospray mass spectrometry (ESI-MS). There are many examples of the use of HPLC in the separation of metallated biomolecules, and is a technique commonly used in bioinorganic chemistry.[71] ESI-MS is a less commonly utilised technique in metal-DNA investigations, yet is extremely powerful and versatile.

ESI-MS has become an important tool for the investigation of large biomolecules since the late 1980s.[72] This soft-ionisation technique is applicable to fragile large molecules such as proteins and oligonucleotides. Its high ionisation efficiency,[73] i.e. [molecular ions produced]/[molecules consumed], makes it a suitably sensitive technique. It has been possible to determine molecular weight, sequence, the site and nature of chemical modification as well as other information.[74,75,76,77] The polyanionic backbone of nucleic acids allows these molecules to be investigated in the ESI-MS negative ion mode. The phosphate groups have pK_A values <1 and will be deprotonated under most solution conditions.[27] However, it has been possible to observe positive ions of oligonucleotides depending on the solution conditions.[78] The solution conditions determine whether or not the purine and pyrimidine bases will be protonated, deprotonated or neutral. This allows for simultaneous analysis of

proteins and oligonucleotides and illustrates the versatility of the technique. Laser desorption mass spectrometry techniques such as MALDI-TOF can also be used for analysis of biomolecules,[79] but nucleic acid analysis is limited due to fragmentation of the DNA occurring during the MALDI process.[80,81] The fragmentation appears to be initiated by protonation of a base followed by cleavage of the N-glycosidic bond, which in turn leads to cleavage of the phosphodiester backbone.[80,81,82] Therefore, electrospray is the technique of choice. ESI-MS has even been used to detect intact DNA duplexes[83,84] and it is possible to detect and characterise non-covalent complexes formed between molecules such as the minor groove binder distamycin A and duplex DNA.[85]

This section describes the separation and characterisation of complex **13**-DNA adducts by HPLC, ESI-MS and after enzymatic digestion.

5.3.1 Instrumentation and Materials

Negative and positive ion electrospray mass spectrometry was performed on a Platform II mass spectrometer (Micromass, Manchester, U.K.). The samples were infused at a flow rate of 0.48 ml h^{-1} and the ions produced in an atmospheric pressure ionisation (API)/ESI ion source. The temperature was 363 K and the drying gas flow rate 300 L h^{-1}. A cone voltage of 40 keV over 0 - 1500 Da was used. The acquisition and deconvolution of data were performed on Mass Lynx (V. 2.3) Windows NT PC data system using the Max Ent Electrospray software algorithm and calibrated versus a NaI calibration file. ESI-MS was used to detect the solvated species of a ruthenium complex and its adducts with the 14 nucleotide DNA strands **I** and **II**.

HPLC was performed with the assistance of Dr. Socorro Murdoch, using a Hewlett-Packard series 1100 Chemstation; including 1100 series Quaternary pumps, 1100 series vacuum degasser and variable wavelength D_2 lamp UV/Vis detector with enhanced integrator. The operating software was HP Chemstation for Windows 95. The chromatographic conditions were optimised on a Nucleosil C_8 300 Å (250 x 4.6 mm ID, 5 μM) stainless steel column (Hichrom U.K.). The detection wavelength

was 254 nm and the relative concentrations of the reaction species were determined from the relative peak areas. Time course reaction was followed at 300 K and all other separations at 298 K.

The 14-nucleotide oligomer with the base sequence of d(ATACATGGTACATA) **I**, and its complementary strand d(TATGTACCATGTAT) **II** were obtained as HPLC purified sodium salts from Oswel (Southampton, U.K.). The calculated molecular masses are 4268.8 and 4250.8 amu respectively. Concentrations were determined using UV/Vis spectroscopy (strand **I** ε_{260} = 149.0 μM^{-1} cm^{-1} and strand **II** ε_{260} = 137.2 μM^{-1} cm^{-1}). Tissue culture water was purchased from Sigma (W-3500).
The phosphodiesterases VPD and SPD were purchased from Sigma and NP1 was purchased from Pharmacia Biotech.

5.3.2 Experimental

5.3.2.1 Sample Preparation

Flame sterilised equipment was used throughout sample preparation so as to avoid bacterial contamination which might lead to DNA degradation. Stock solutions (200 μM of the oligodeoxynucleotide strands and a 6 mM stock solution of the ruthenium complex were made up in double processed tissue culture water. Using dilution techniques, reaction mixtures were made up, sealed in Eppendorf tubes and incubated at 300 K for 48 h. Control 100 μM solutions of **I** or **II** and the ruthenium complex were prepared and incubated at 300 K for 48 h. Aliquots of each sample were diluted x 2 in HPLC grade acetonitrile prior to infusion into the mass spectrometer. The spectrometer was flushed before and between runs with 50:50 v/v CH_3CN:H_2O.

5.3.2.2 HPLC Separation

The following methods were used for the HPLC separation of the ruthenated oligodeoxynucleotide strands:
Solvent A = 20 mM TEAA (tetraethylammonium acetate) in H_2O
Solvent B = 50 / 50 v/v CH_3CN / H_2O

time / min	% A	% B
0	75.5	24.5
5	75.5	24.5
17	60	40
20	60	40
21	75.5	24.5

Table 5.1 Solvent gradient for HPLC separation of 14mer strand **I**

time / min	% A	% B
0	78	22
5	78	22
6	77	23
12.5	67	33
15	67	33
17	60	40
18	60	40
20	78	22

Table 5.2 Solvent gradient for HPLC separation of 14mer strand **II**

5.3.2.3 Enzymatic Digestion of Purified Strands

5.3.2.3.1 Digestions with VPD

Concentrations of purified oligodeoxynucleotides were typically in the region of 25 μM in H_2O. VPD (venom phosphodiesterase) was diluted x 3 in H_2O prior to use, and typically 2 μl of the enzyme solution was added to 200 μl of the ODN solution. The mixtures were incubated at 310 K and aliquots were extracted at various time intervals and diluted x 2 with HPLC grade CH_3CN prior to ESI-MS analysis.

5.3.2.3.2 Digestions with SPD

Digestions with SPD (spleen phosphodiesterase) were performed with the same procedure as VPD.

5.3.2.3.3 Digestions with NP1

1 mg of lyophilised NP1 was dissolved in 10 mM CH_3COONa (pH = 5.2) for optimum activity. An aliquot (2 μl) of this solution was added to 200 μl of 25 μM solutions of purified ODN in H_2O. The mixtures were incubated at 310 K.

5.3.3 Results and Discussion

5.3.3.1 Electrospray mass spectrum of [(η⁶-*para*-cymene)Ru(en)Cl][PF_6] **13**

Ruthenium has a wide isotopic profile, ranging from 96 to 104, with the most abundant species being ^{102}Ru, 31.6 %, see Table 5.3. This wide range aids assignment of peaks in mass spectra due to its characteristic isotope pattern. The predicted pattern for ruthenium is shown below in Figure 5.9, and it can be seen that this matches the patterns observed in the spectrum of the arene complex above. It should be noted that for the high molecular weight compounds, such as the oligonucleotide-Ru adducts studied in this chapter, that the mass of the ruthenium is too small relative to the overall mass to allow observation of the individual isotopomers in the spectrum.

Ru isotope	96	98	99	100	101	102	104
% abundance	5.5	1.9	12.7	12.6	17.1	31.6	18.6

Table 5.3 % Natural abundance of ruthenium isotopes

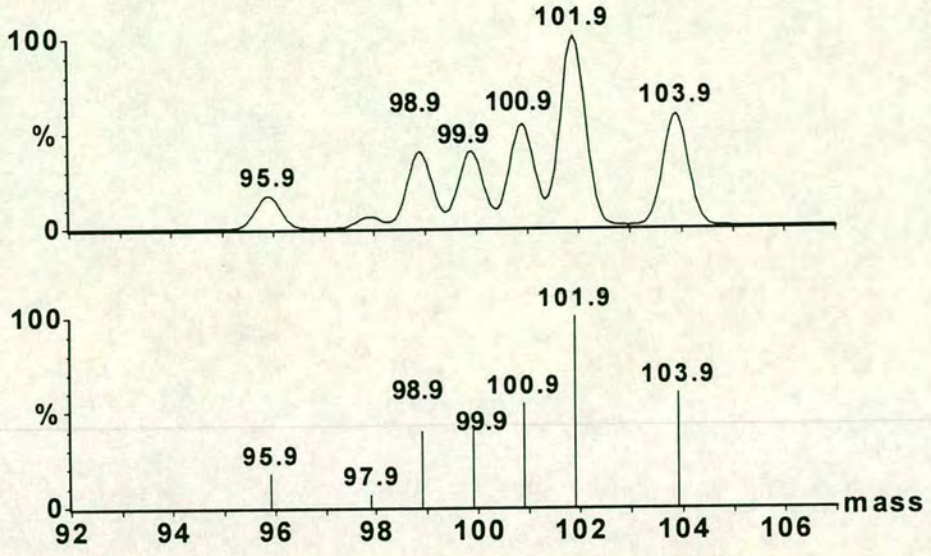

Figure 5.9 Predicted isotope pattern for ruthenium. Top trace is mass spectrum, bottom is line spectrum.

The positive ion electrospray mass spectrum of [(η⁶-para-cymene)Ru(en)Cl][PF_6] **13** is shown in Figure 5.10. This was taken at an intermediate cone voltage of 40 eV. It can be seen that the dominant ions in the spectrum are quasi-molecular ions, i.e. 1+ charge, corresponding to the intact complex (without the PF_6^- counter ion) at 331.1 amu (theor. 331.8), the hydrolysed form of the complex at 315.1 amu (theor. 314.1) and the Ru(arene)(en) moiety at 295.1 amu (theor. for $-H^+$ 295.3). There are also minor 2 + ions at Da/e 148.4 and 167.0. It was found that as the cone voltage was increased these disappeared, and formation of the molecular ions was completely favoured. The lability of the chloride ion is also indicated by the effect of raising the cone voltage. As it was increased, the species at 331.1 became less important and the peak at 295.1 was dominant, showing loss of chloride.

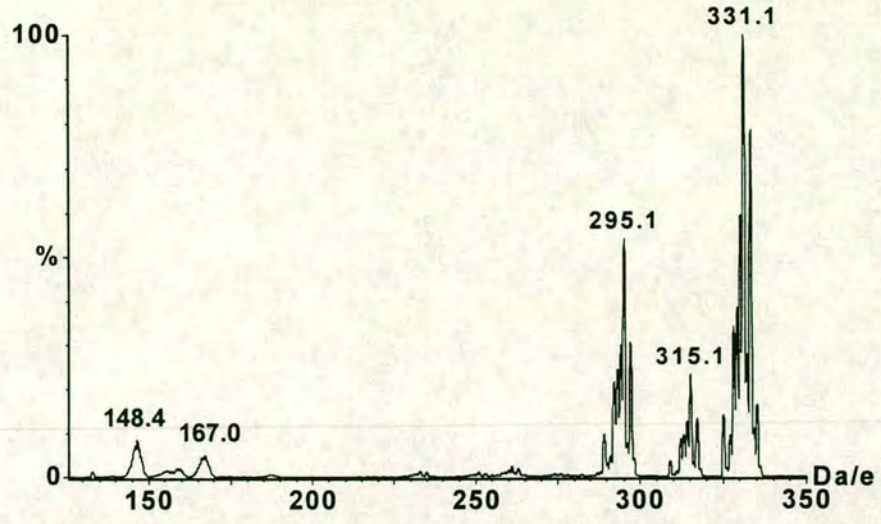

Figure 5.10 Positive ion mass spectrum of an aqueous solution of [(η⁶-para-cymene)Ru(en)Cl][PF_6] **13**

5.3.3.2 Mass spectrum of -GG- strand (**I**)

Sequence of strand **I** = **ATACATGGTACATA**

ODNs contain a phosphate backbone which bears a negative charge at each phosphate group. The pK_A values of these phosphate groups is <1, which means that they are negatively charged under all normal solution conditions. This makes them ideal for analysis by negative ion mode electrospray mass spectrometry. The negative ion mass spectrum of the 14mer strand **I** is shown in Figure 5.11. The spectrum provides an ion series, which can be transformed to determine the molecular mass of the species. The transformed spectrum is shown in the inset. The molecular mass of the transformed species does not correspond to the molecular mass of the free oligonucleotide. Instead, the peak at 4337.1 corresponds to **I** - $3H^-$ + $3Na^-$] (theor. 4335). Strand **I** was supplied as the sodium salt, and it is very common in ESI-MS to find that Na adducts are often the main species detected, rather than protonated species.[86] It can be seen that the most intense peak in the series

corresponds to the 8⁻ ion. This is appropriate for a 14mer strand of DNA in unbuffered aqueous solution.[87]

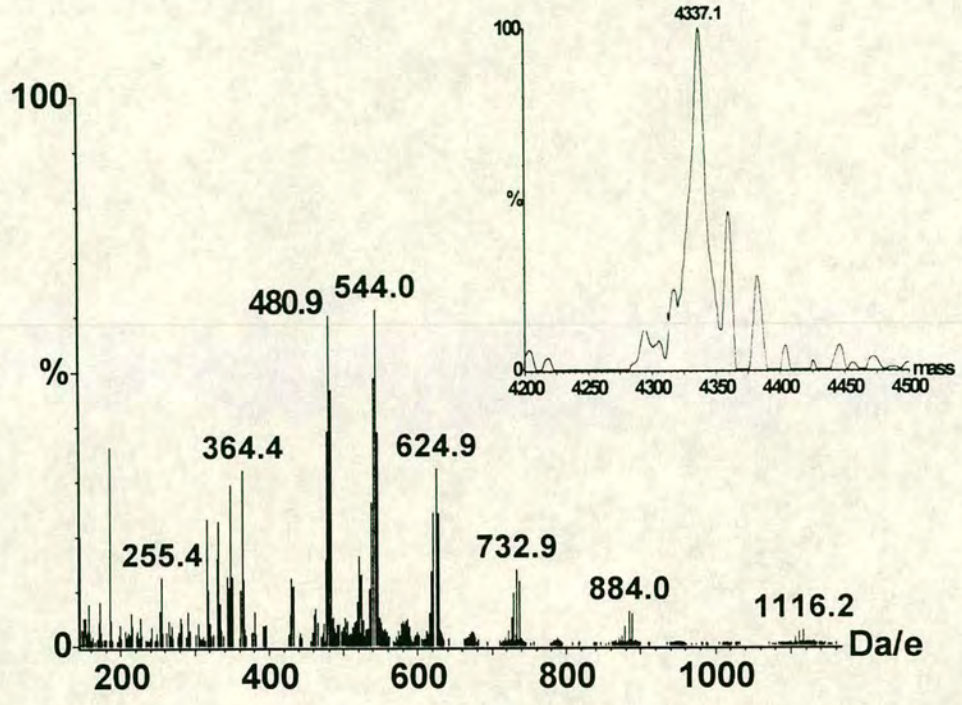

Figure 5.11 Mass spectrum of -GG- strand **I**

5.3.3.3 Mass spectrum of **13** + 14mer strand **I**

Complex **13** was incubated at 310 K for 48 h with a sample of the -GG- **I** strand in a 1:1 molar ratio, and the resulting mixture analysed by negative ion mode ESI-MS. The results proved conclusively that the ruthenium complex binds to the DNA in both a 1:1 and a 2:1 ratio. The spectrum is shown in Figure 5.12. It can be seen that the ionic series corresponding to the free DNA strand is still present, but it is the extra peaks that are of interest. Two new ionic series were detectable and these gave rise to the molecular mass peaks shown in the inset. The molecular masses are appropriate for free DNA (4338 amu) (theor. DNA -3H + 3Na 4335 Da); Ru(arene):DNA, 1:1 (4609.3 amu) (theor. for -2H + 2Na, 4608.9 Da); Ru(arene):DNA, 2:1 (4904.9 amu) (theor. for -2H + 2Na, 4905 Da). It is understandable that free DNA is still present, since although the initial molar ratio was 1:1, some of the DNA strands have 2 bound ruthenium ions. With the

knowledge that the complex does indeed bind to DNA, the process was then investigated in more detail.

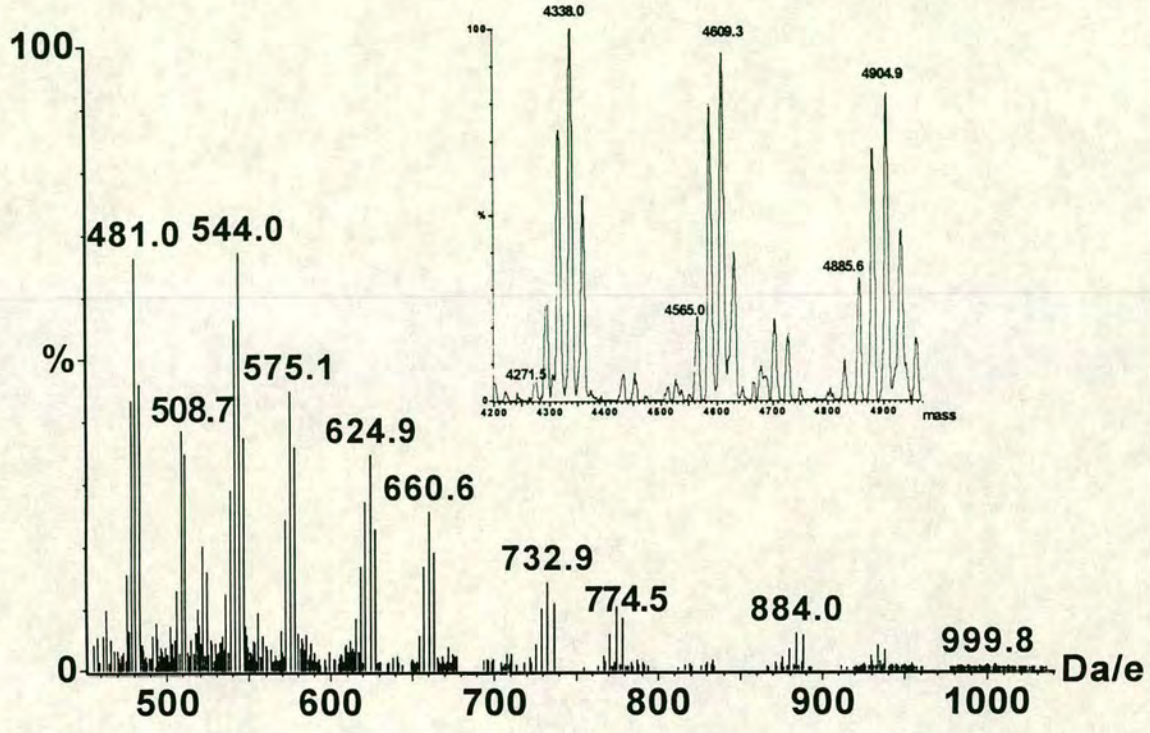

Figure 5.12 Mass spectrum of **13** + 14mer strand **I** (1:1 molar ratio)

5.3.3.4 HPLC separation of **13**-GG strand **I** adducts

HPLC separation of biomolecules is well known.[88] Isolation and purification of biological adducts allows more information about possible modes of binding and mechanisms to be elucidated.

The separation of the Ru(arene)-GG adducts was undertaken on a reverse phase column. Such columns retain hydrophobic entities, which are eluted at various times depending on the solvent system used. In the present case, the buffer tetraethylammonium acetate was used. The tetraethylammonium ion-pairs with the anionic phosphate groups and also has hydrophobic ethyl groups attached. An added advantage of the buffer is that it is volatile, and therefore is lost during lyophilisation, and further purification, is avoided. The speed of the elution of the adducts is controlled by the gradient of the 50/50 CH_3CN/H_2O solvent system. The more

acetonitrile used, the faster the adducts are eluted from the column. However this can be at the expense of separation.

The HPLC trace for the separation and collection of the Ru(arene)-GG adducts and their assignments are shown in Figure 5.13.

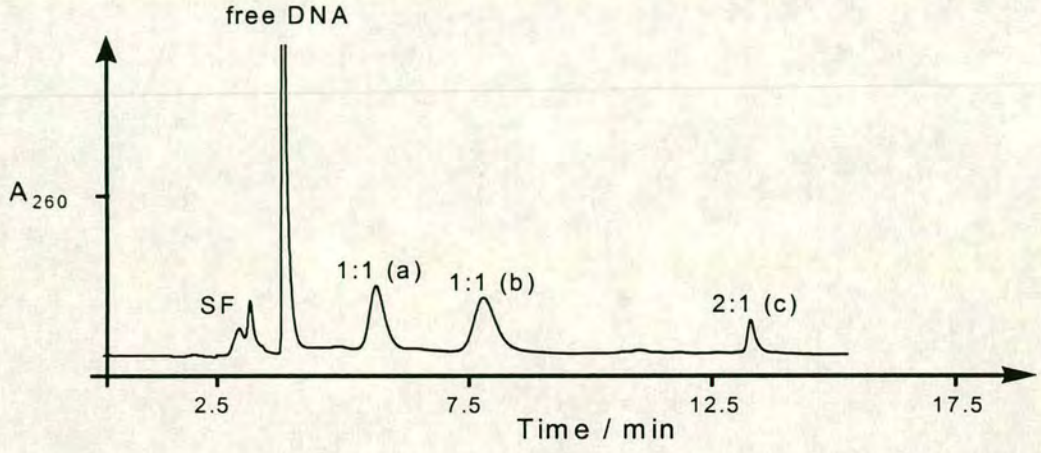

Figure 5.13 HPLC trace of **13**-GG strand **I** adducts. Assignment of peaks: (a) **13**:**I** monoadduct (b) **13**:**I** monoadduct (c) **13**:**I** bisadduct. 13 and the DNA strand **I** were mixed in a 1:1 molar ratio in unbuffered water and incubated at 310 K for 24 h prior to separation.

The initial peak on the trace (SF) is due to the solvent front. All other peaks were conclusively assigned by mass spectrometry following the separation (see next section). By varying the Ru:DNA ratio, incubating for 24 h at 310 K and investigating this by HPLC, it was possible to decide which peak is due to a 1:1 and which peak to a 2:1 adduct. Increasing the amount of ruthenium present caused the size of peak (c) to increase accordingly. When the ratio was 5:1 Ru:DNA, this was the only peak present, see Figure 5.14. There was no free DNA, nor peaks (a) and (b). The method used was changed slightly from the method used to collect fractions, due to pressure change in the machine, hence the differing elution times. This specificity, despite the relatively high ruthenium concentration, lends itself to

the idea that Ru binding is base specific. This base is most likely guanine. This in turn supports the idea that the 1:1 adducts correspond to a 5′G adduct and a 3′G adduct, and that the bis-adduct consists of two ruthenium ions bound at the -GG- hotspot. In this particular strand, only guanine and cytosine appear twice (there are four thymines and four adenines and this would not allow for the specificity observed in the HPLC) and the binding of the complex to guanine is preferred than to cytosine, see section 5.1.2.4.

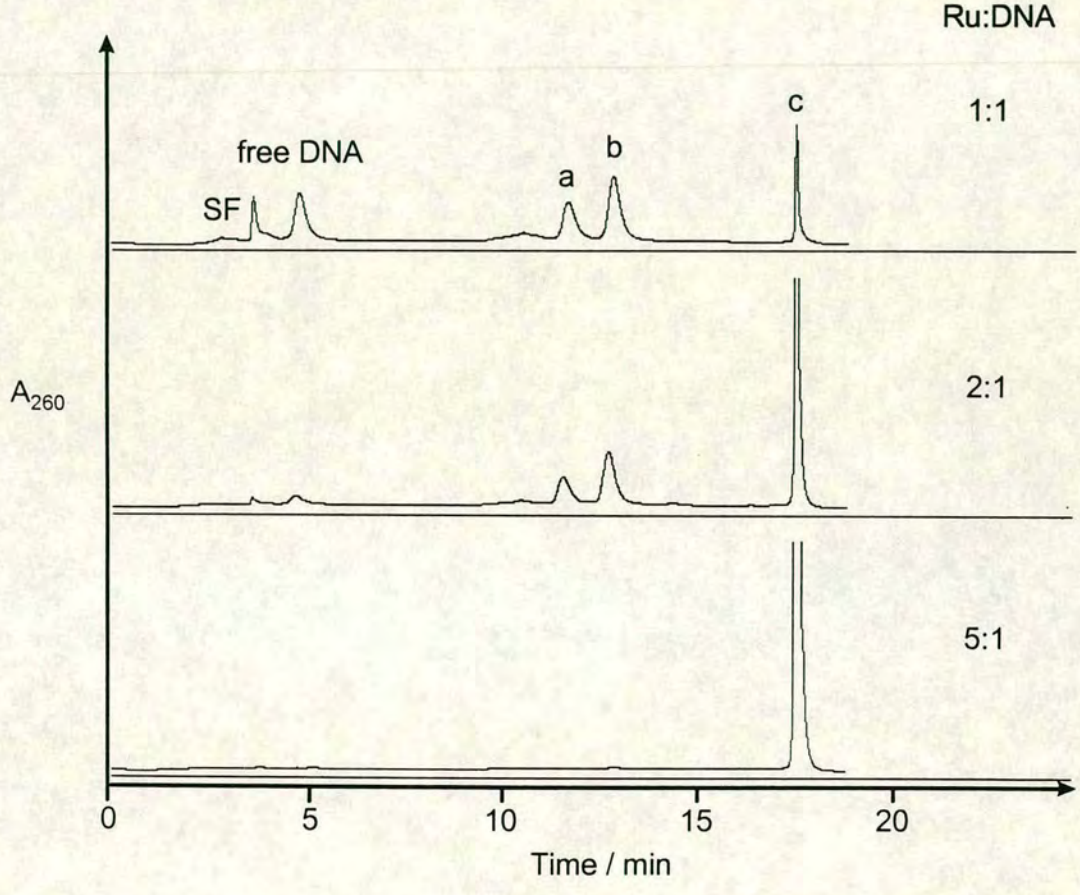

Figure 5.14 HPLC traces of **13**-GG strand **I** adducts at different molar ratios. Mixtures were in unbuffered aqueous solution and incubated for 24 h at 310 K.

5.3.3.5 Mass spectra of purified adducts

The individual fractions were collected, lyophilised and redissolved in H_2O. Aliquots of these were diluted in 50/50 CH_3CN/H_2O to a concentration of 25 μM for

ESI-MS analysis. The spectra obtained agreed with the assignments given to the peaks in the previous section.

Peaks (a) and (b) are 1:1 Ru:DNA adducts. Their spectra are identical and so are shown as one in Figure 5.15. As expected for the two isomers, peaks (a) + (b), the mass spectra are identical as they differ only by the location of the Ru(arene) moiety on the strand. The transformed spectrum (shown as inset) gives the mass value of 4565.9 amu (calc. 4564.9 Da) which corresponds to the 14mer strand **I** with the [(η⁶-*p*-cymene)Ru(en)]$^{2+}$ fragment attached. This would correspond to activation of the complex via hydrolysis which would free the coordination site at the metal, previously occupied by the chloride ligand, for binding to a base on **I**.

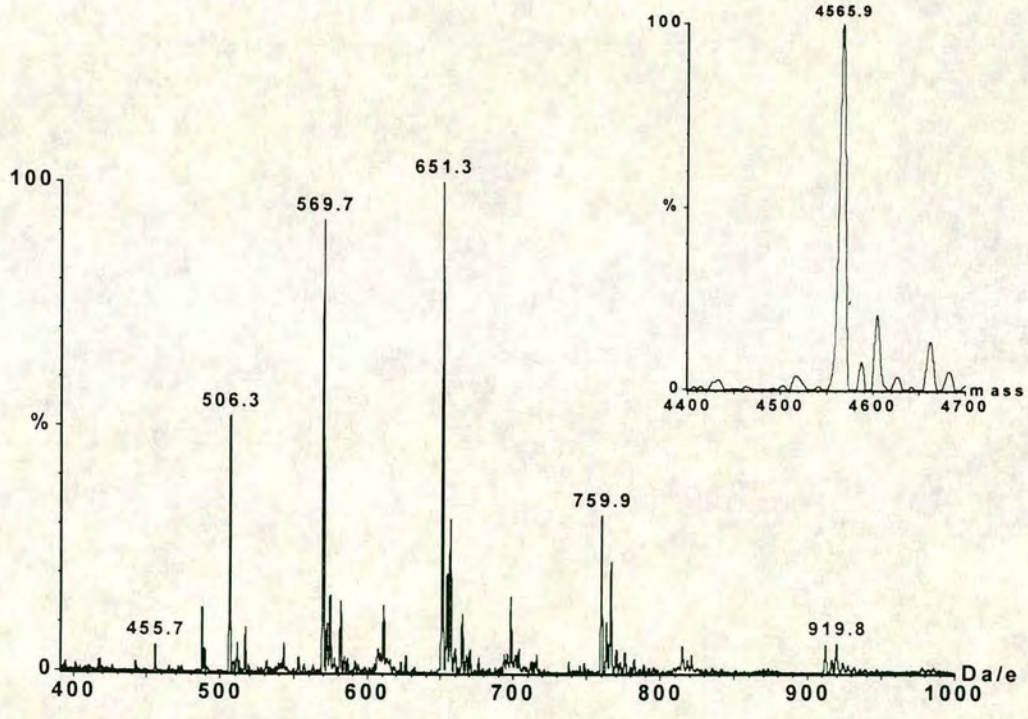

Figure 5.15 Mass spectrum of **13-I** peaks (a) and (b)

The mass spectrum for peak (c) is shown in Figure 5.16. This gives the transformed mass of 4859.4 amu (theor. 4861.0 Da) which is correct for the adduct of **I** with two [(η⁶-*p*-cymene)Ru(en)]$^{2+}$ fragments attached. Therefore it can be conclusively stated that [(η⁶-*p*-cymene)Ru(en)Cl]⁺ binds to the 14mer ODN strand

ATACATGGTACATA in both a 1:1 and 2:1 Ru:DNA manner in aqueous solution, and that there appear to be only two specific sites of binding.

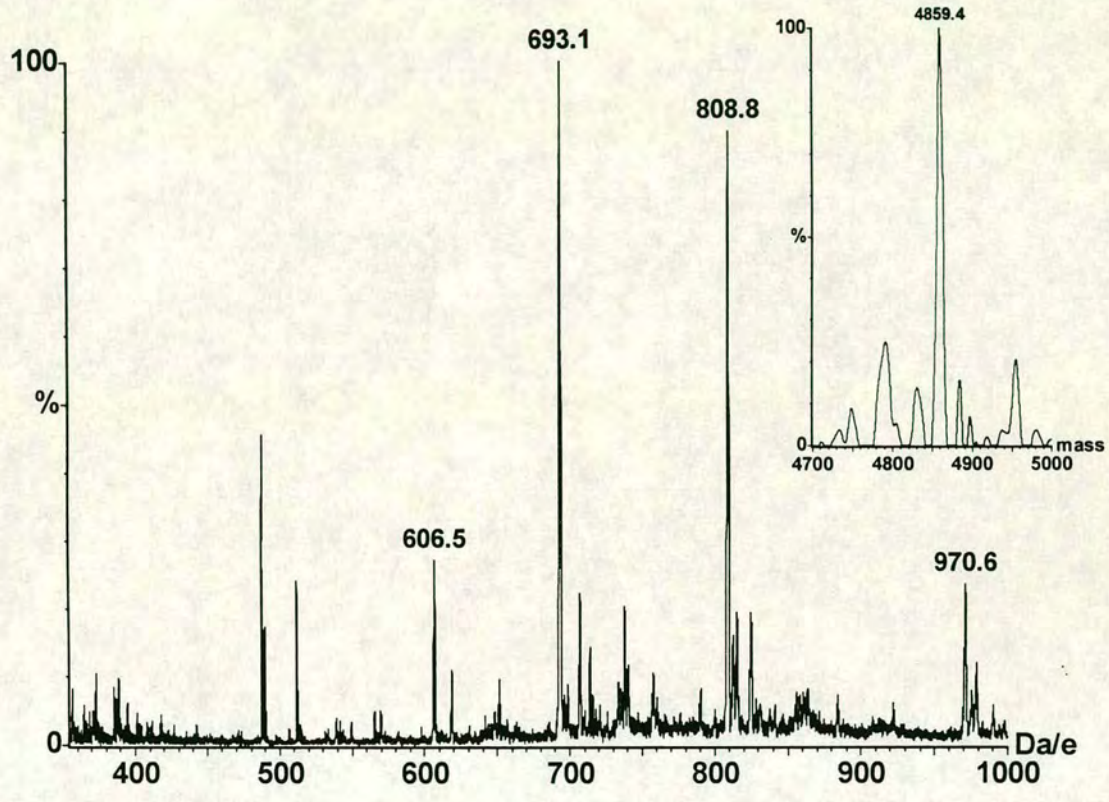

Figure 5.16 Mass spectrum of **13-I** peak (c)

5.3.3.6 Enzymatic digestion of purified Ru(arene)-GG strand I adducts

With the knowledge that the Ru(arene) complex **13** binds specifically, it is of interest to identify the exact sites of binding. One manner of investigation is by enzymatic digestion of the metallated DNA and subsequent analysis of the digestion products. This procedure has previously been used to sequence strands of DNA[89] and also for investigating sites of labelling on DNA.[90] Typical enzymes used include the phosphodiesterases VPD (venom phosphodiesterase) and SPD (spleen phosphodiesterase). Phosphodiesterases hydrolyse phospho-ester bonds. VPD is a 5′-exonuclease, that is, it begins digestion of single strand DNA at the 3′ end and the

products are 5′-mononucleotides. It is extracted from the venom of the South American rattlesnake, *Crotalus Durus Terrifficus*. SPD is a 3′-exonuclease, and sequentially digests the single strands from the 5′ end, creating 3′-mononucleotides. Thus, these two enzymes provide complementary information. Their use is particularly advantageous in the case of labelled DNA as they tend to stop digesting at the site of labelling. A recent example of this is the binding of [Pt(dien)Cl]$^+$ to the 14mer strand ATACATGGTACATA.[70] This study was undertaken to simulate the monofunctional adducts of cisplatin-DNA, and the successful enzymatic digestion of these adducts provided conclusive proof of binding to the guanines of the GG site. Mass spectrometry, electrospray and MALDI-TOF are powerful tools for the analysis of DNA[91], and oligonucleotides up to a 33mer have been sequenced using MALDI-TOF in conjunction with phosphodiesterases.[92] MALDI-TOF is the technique mainly used in the literature, and there is only a limited number of publications on DNA sequencing with electrospray MS, for which DNA size tends to be smaller. These include the partial sequencing[93] and complete sequencing [94]of a 10mer. Recently this has been applied to a 22mer and a biotin-labelled 18mer.[95]

Other enzymes used in this form of analysis are Nuclease P1 (NP1), a non-specific nuclease from penicillium citrinum which hydrolyses DNA and RNA to 5′-mononucleotides.[96]

VPD was the first enzyme utilised. The enzyme was added to a solution of an isolated fraction of Ru(arene)-GG and incubated at 310 K. Aliquots were taken at various time intervals and analysed by ESI-MS. The mass spectra provided ion-series for the various intermediates, with new species appearing as the digestion progressed. Sequence ladders created by combining the transformed spectra of the ions present at various times are shown for peak (a) in Figure 5.17, peak (b) in Figure 5.18 and (c) in Figure 5.19.

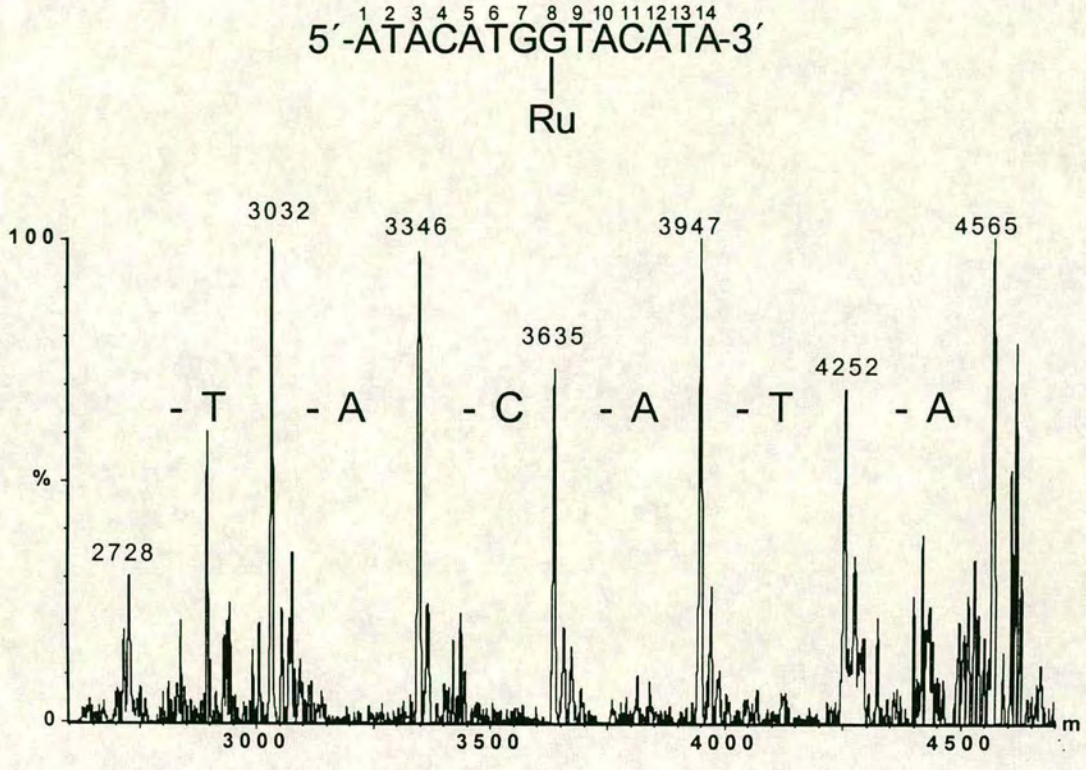

Figure 5.17 VPD digestion ladder of **13-I** peak (a). It should be noted that all these species were not detected at the same time. The ladder is a convenient method of showing the progress of digestion from start (the right-hand side) to the finish (the left-hand side), with each "rung" corresponding to a species present.

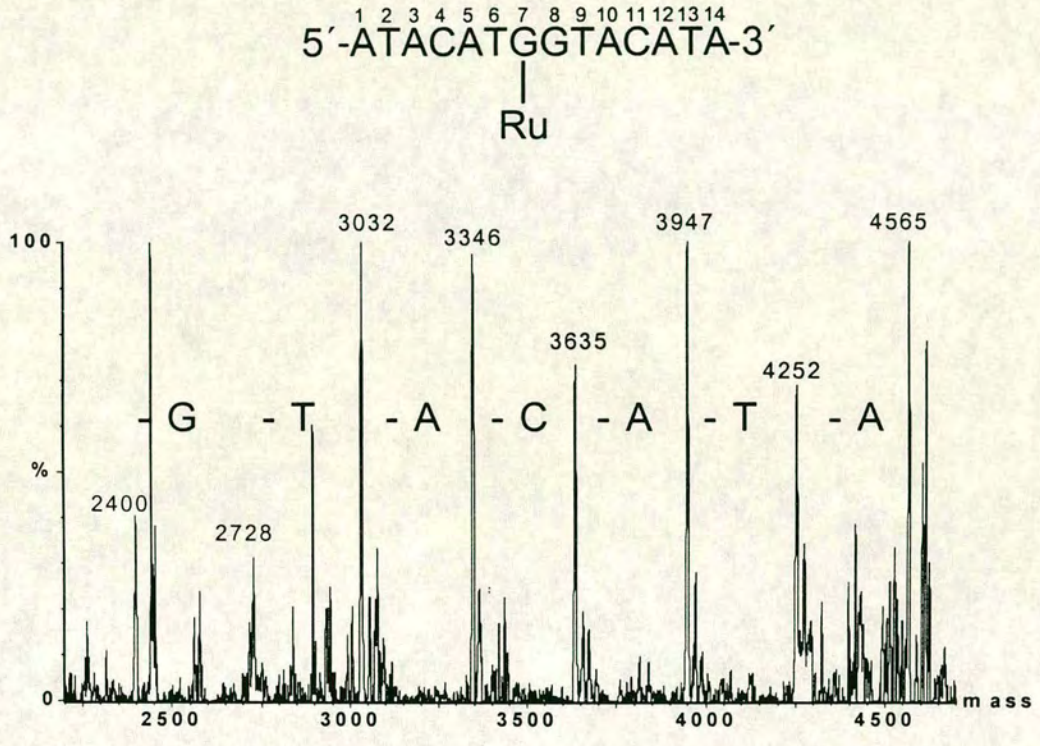

Figure 5.18 VPD digestion ladder of **13-I** peak (b). It should be noted that all these species were not detected at the same time. The ladder is a convenient method of showing the progress of digestion from start (the right-hand side) to the finish (the left-hand side), with each "rung" corresponding to a species present.

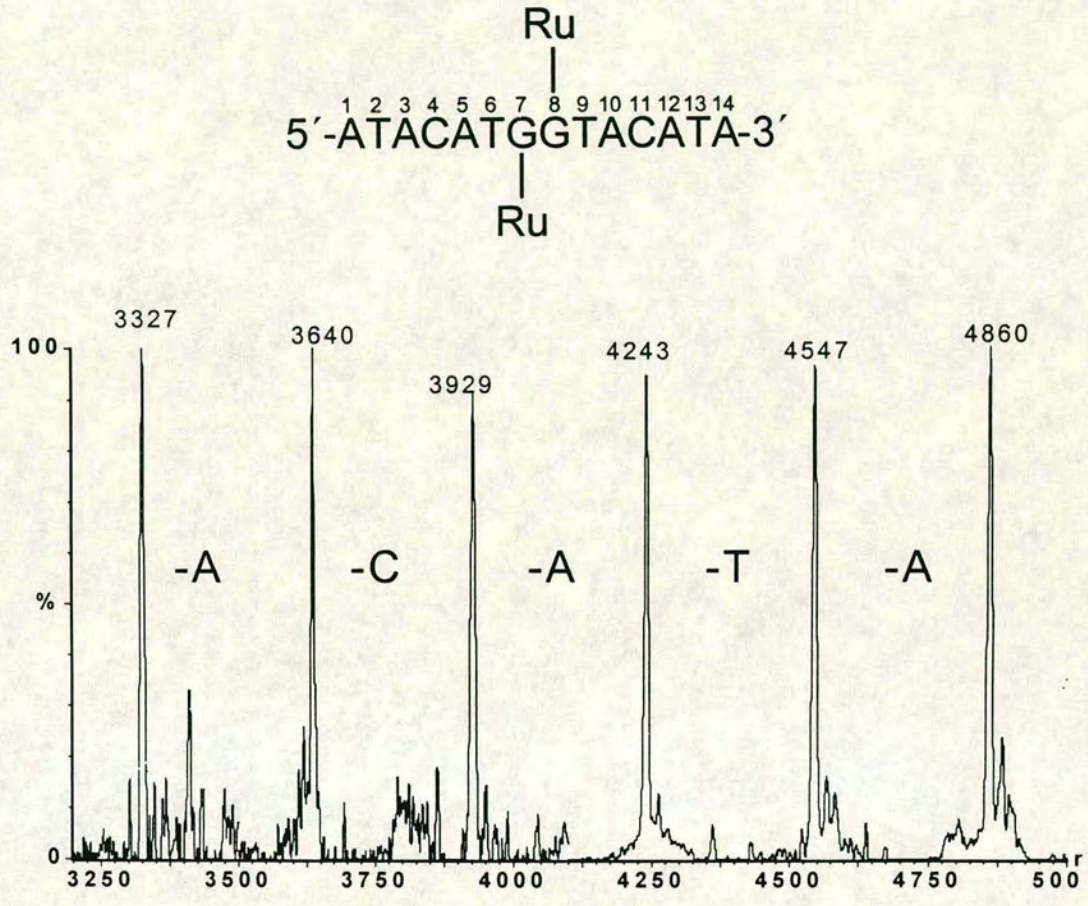

Figure 5.19 VPD digestion ladder of **13-I** peak (c). It should be noted that all these species were not detected at the same time. The ladder is a convenient method of showing the progress of digestion from start (the right-hand side) to the finish (the left-hand side), with each "rung" corresponding to a species present.

It can be seen from the sequence ladders that peak (a), Figure 5.17, digests as far as the T^9, indicating the presence of the ruthenium on the 3′-G^8. Peak (b), Figure 5.18, digests as far as the 3′-G^8, indicating the presence of the ruthenium on the adjacent base, the 5′-G^7. The doubly ruthenated strand, Figure 5.19, only digests as far as A^5, one base before the GG site. This strongly indicates that both Ru ions are on G residues, which is a reasonable assumption to make at this point given the spectra of peaks (a) and (b). It is possible that having two adjacent Ru(arene) fragments has distorted the structure of the strand in that region to such an extent that the enzyme does not recognise it efficiently. There is also precedence for VPD digestion stopping one base prior to a labelling site on DNA.[97]

Although the sequence ladders are quite clear, there are inherent complications due to the nature of the ionisation in the spectroscopy and its low tolerance to detergents and salts. These give rise to noise and unwanted peaks in the spectrum. However as the sequence of the DNA is preset (i.e. known), the possible products are limited, and hence it was possible to identify the real peaks.

These complications are well addressed by Wu et al.[95] As multiply charged ion series predominate with ESI-MS, the regular mass spectrum must be transformed to a reconstructed molecular mass (RMM) spectrum. RMM spectra over ranges greater than 700 Da have not been reported[98] in the sequencing of DNA. This is presumably because interference such as harmonic peaks and chemical noise from 5′-mononucleotides result in poor quality RMMs. Na^+ ion adducts also produce additional peaks in a MS spectrum, which are extremely hard to avoid. The sensitivity drops as a result of spreading the ion current among multiple forms of the DNA, and this complicates the spectral interpretation. Also, as the strand shortens, the presence of mononucleotides increases. These produce very strong signals, not only in the m/z region of 289-329, but also in the m/z region of 600-700 due to the formation of non-specific dimers. Trimers in the region of m/z 900-1000 are also known and these can severely interfere with MW reconstruction.

Although the digestion of the DNA by VPD alone is sufficient to point to binding sites at the guanine residues, it was decided to attempt digestion with another enzyme to provide corroborative evidence. Therefore digestion with the enzyme SPD, which begins from the other end, the 5′ end, was attempted. Problems with this became immediately apparent when it was noticed that the enzyme itself gives a mass spectrum in the negative ion mode which masked every other peak. Even after subtraction of a blank spectrum of the enzyme from the digestion mixture, no assignable peaks were present. No previous mention of this is in the literature, despite many people claiming to have utilised SPD with mass spectrometry.[99]

The digestion of the metallated DNA with the non-specific exonuclease NP1 was also investigated. As expected it successfully completely digested strand **I**, and four strong peaks corresponding to the free mononucleotides CMP (m/z = 306), TMP (m/z = 321), AMP (m/z = 330) and GMP (m/z = 346) were observed. However, no peak corresponding to a metallated nucleotide appeared. No signal could be detected in either positive or negative ion mode mass spectrometry, and concurrently, no free ruthenium complex could be detected. This implies that the labelled base is still intact and that the problem is with the ionisation of the Ru-base adduct. On closer analysis it seems feasible that this should be the case. The Ru complex carries a charge of 2+ and the phosphate group in a mononucleotide carries a charge of 2-. It is possible that this overall neutrality prevented the detection of any charged version of the adduct. An investigation of the Ru-arene with 5′-GMP supported this supposition. After incubating a 1:1 mixture of the two compounds at 310 K for 24 h, no assignable adduct peak could be found in the ESI mass spectrum, positive or negative ion mode. Therefore, this enzyme was of no significant benefit in the determination of the binding site of the ruthenium to the ODN. It does, on the other hand, indicate that the ruthenium is quite strongly bound to the ODN as the strand was fully digested and no free ruthenium was detected.

5.3.3.7 Time course of reaction of **13** with 14mer strand **I** (1:1 molar ratio) at 310 K

The time course for the reaction of **13** with the DNA 14mer strand **I** in a 1:1 molar ratio in unbuffered aqueous solution at 310 K is shown in Figure 5.20. The relative concentrations were calculated from the integrated areas of the HPLC peaks for free DNA and (a), (b) and (c), detected at 260 nm. It can be seen that the reaction is essentially complete after 4 h. It is interesting to note, however, the change in the amount of species (a) and (b) present after this time. Up to 17 h, more of species (a) is present than (b), but after this time there is a shift and a decreases, while (b) becomes more prevalent. This invokes the possibility that Ru(arene) bound to the guanine towards the 5′ end of the ODN (G^8) is the more stable adduct.

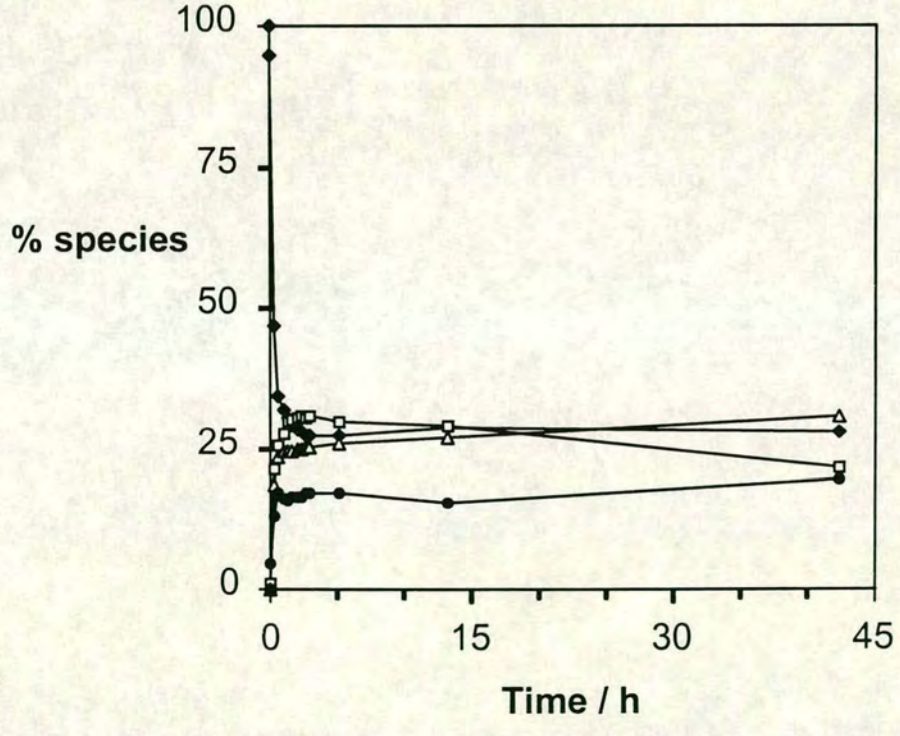

Figure 5.20 Time course for reaction of **13** with 14mer strand **I** (1:1 molar ratio) at 310 K in unbuffered aqueous solution. Detection is at λ = 260 nm. Assignments: free DNA = (♦), (a) = ( ), (b) = (△), (c) = (•)

5.3.3.8 Mass spectrum of **13** and 14mer strand **II**

Sequence of 14mer strand **II**: **TATGTACCATGTAT.**

The ruthenium complex **13** was incubated for 24 h at 310 K with the -CC- 14mer strand **II** (complementary to the -GG- strand **I**) in a 1:1 molar ratio in unbuffered aqueous solution and analysed by ESI mass spectrometry. The results were found to be similar to those for the -GG- strand in that both mono- (found 4568.5 amu, theor. for -1H + 1Na, 4568.9 Da) and bi-ruthenated (found 4837.0 amu, theor. 4843.0 Da) adducts were detected in the reaction mixture as well as free **II** (found 4299.1 amu, theor for -2H + 2Na, 4294.8 Da). This reaction is consistent and reproducible, and again shows that complex **13** is specifically bound to guanine residues. Again there are two guanine residues present in **II**, compared to 6 T and 4 A residues. Binding to either of these would result in a more complicated mixture of products. There are also 2C residues, but binding to guanines is much more favourable for metal-based drugs in general, and for the Ru(arene) complex used here in particular, see section 5.1.2.4.

5.3.3.9 HPLC separation of -CC- strand **II** adducts with complex **13**

Separation of the species present in the reaction mixture of Ru(arene) and **II** was attempted by HPLC methods, see Figure 5.21. Peaks (a) and (b) were collected as one fraction as they could not be separated sufficiently to collect individually, and peak (c) was collected as a single fraction. It seems likely that peaks (a) and (b) are both mono-ruthenated **II** and that peak (c) is the bi-ruthenated species, by comparison with the separation for adducts of strand **I**, see section 5.3.3.4.

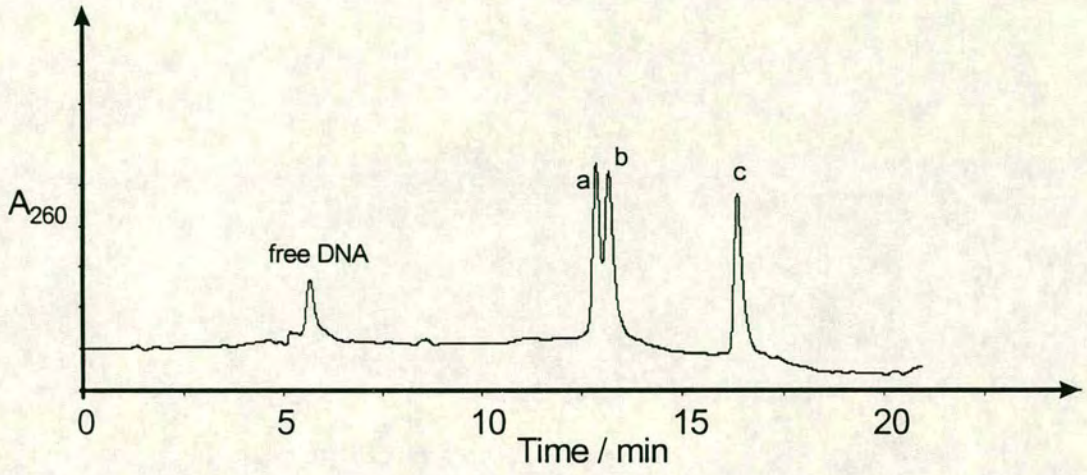

Figure 5.21 HPLC trace for separation of **13** + -CC- strand **II**. A 1:1 molar ratio of **II** and **13** were incubated at 310 K for 24 h prior to separation.

5.3.3.10 Mass spectra of purified adducts

The collected fractions were lyophilised and redissolved in H_2O. Aliquots of these were taken, and diluted in 50/50 CH_3CN/H_2O to a concentration of 25 μM for ESI-MS analysis. The mass spectra show that peaks (a) and (b) combined, Figure 5.22, contain a single species, mono-ruthenated **II**. This corresponds to **II** with a $[(\eta^6\text{-}p\text{-cymene})Ru(en)]^{2+}$ fragment attached (found 4546.8 amu (theor. 4546.9 Da)).

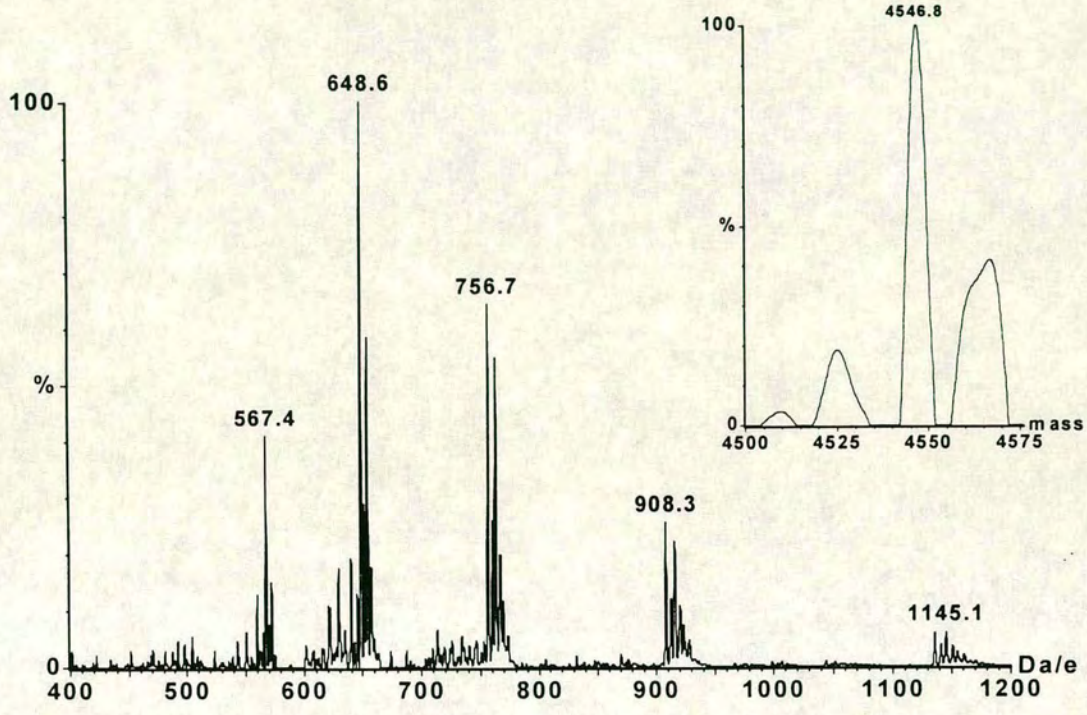

Figure 5.22 Mass spectrum of combined HPLC peaks (a) and (b) from the 1:1 molar ratio reaction of **13** with -CC strand **II**.

The mass spectrum of peak (c), Figure 5.23, is consistent with assignment as **II** with two $[Ru(arene)(en)]^{2+}$ fragments attached, 4840.4 amu (theor. 4843.0 Da).

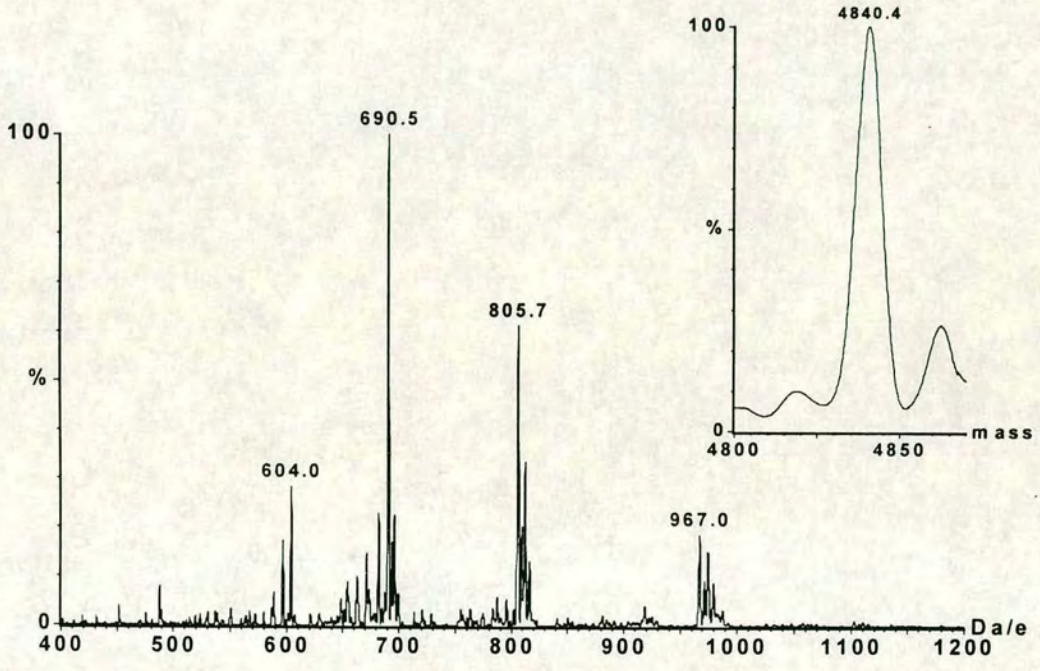

Figure 5.23 Mass spectrum of HPLC peak (c) from reaction of strand **II** with complex **13**.

5.3.3.11 Enzymatic digestion of purified **13**-CC strand adducts

To confirm the Ru binding sites on strand **II**, enzymatic digestion of the isolated fractions with VPD was performed. This enzyme begins digestion at the 3′ end, creating 5′-mononucleotides. If the site of metal binding is guanine, then digestion of the mixed fraction (peaks (a) + (b)) should result in two products: one for TATG-Ru, and one for TATGTACCATG-Ru, two species sufficiently different in their molecular masses, and hence ionic patterns, that they should be easily distinguishable by ESI mass spectrometry.

The digestion ladder for this mixed fraction ((a) + (b)) is shown in Figure 5.24. As can be seen, the digestion did not proceed very far. It seems that only the end two bases, T^{15} and A^{16}, were removed in the reaction. As it is known that VPD sometimes stops one base prior to a labelling,[97] it can be assumed that the ruthenium is indeed bound to a guanine residue. The alternative is that the ruthenium is bound to thymine, but there are four available thymines in **II**, and this does not seem likely.

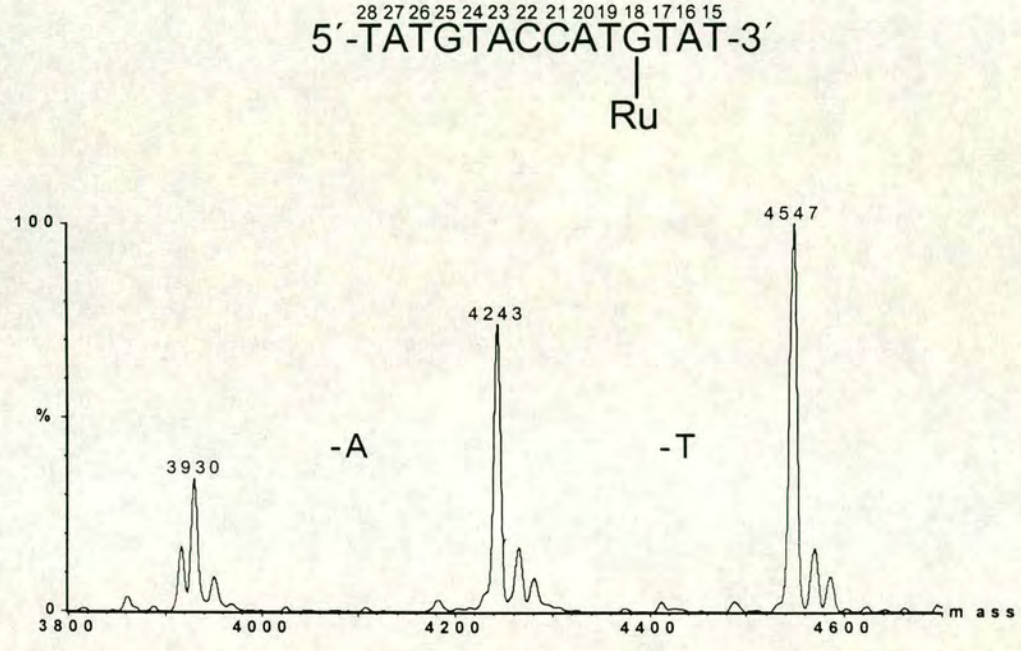

Figure 5.24 VPD digestion ladder of HPLC peaks (a) and (b) combined, separated from reaction of -CC- strand **II** with complex **13**.

An interesting factor in this experiment is the lack of a second post-digestion species, the supposed TATG-Ru, where the ruthenium is located on G^{25}, and the bases T^{15} to T^{24} have been cleaved by the enzyme. The reaction was monitored at various time intervals up to 48 h, with incubation, and no other species were detected at any stage during the reaction, and the -T and -(T-A) ions were present from an early stage. As the HPLC shows two definite peaks in this fraction, it can be assumed that these species are different, and so the mass spectrum of the digestion should have shown

more peaks, corresponding to oligonucleotides of other lengths. This gives rise to the interesting possibility of isomerisation. This would mean that the assumption that one peak is the **II** with a Ru(arene)(en) on the G^{18} towards the 3′-end and the other peak is **II** with a Ru(arene)(en) on the G^{25} towards the 5′-end is correct. After lyophilisation and redissolution of the fraction, the Ru(arene) on the G^{25} may migrate to the possibly more favourable G^{18}, hence only one species arises after enzymatic digestion of the fraction.

The VPD digestion of the bi-ruthenated -CC- strand, peak (c) in the HPLC, is shown in Figure 5.25. The similarity with the digestion of the mixed fraction is easy to see. The digestion proceeds only as far as removal of T^{15} and A^{16}, as would be expected for **II** labelled at the guanine residues. If both guanines are labelled we would still only find the strand digested as far as the first label as the digestion is specifically from the 3′-end.

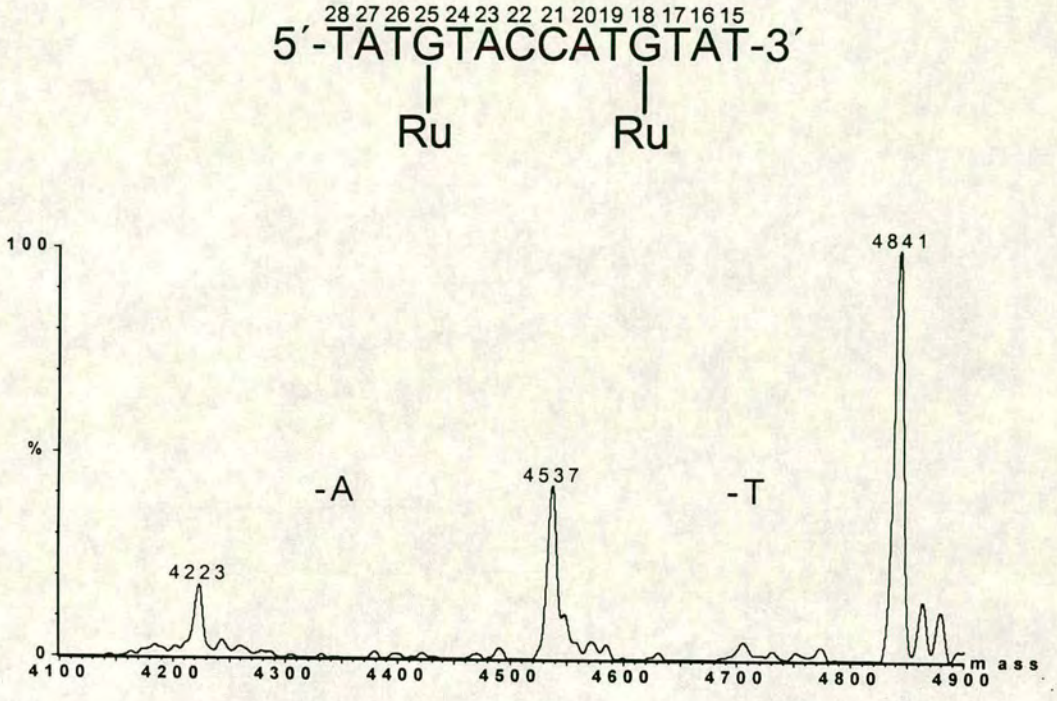

Figure 5.25 VPD digestion ladder of **13-I** peak (c)

5.3.4 Conclusions

In this section it has been shown that the Ru(arene) complex, [(η⁶-para-cymene)Ru(en)Cl]⁺[PF_6]⁻ **13** specifically binds to guanine residues in a 14mer oligodeoxynucleotide strand containing a selection of all four DNA bases. This has been proved using electrospray ionisation mass spectrometry in conjunction with HPLC and enzymatic digestion of the metallated DNA. This is very interesting in the field of metallodrugs as anti-cancer agents as it is known that the highly successful drug cisplatin has a preference for guanine residues in DNA. Also, the fact that the enzyme cannot pass over the bound Ru may be significant for inhibiting the function of repair enzymes in cells.

5.4 References

[1] P.D. Boyer *Biochemistry* **1987**, 26, 8503

[2] N. Farrell *Transition Metal Complexes as Drugs and Chemotherapeutic Agents*, Kluwer Academic Publishers, Dordrecht, The Netherlands, **1989**, p95

[3] J. Reedijk *Inorg. Chim. Acta* **1992**, 198, 873; W.I. Sundquist, S.J. Lippard *Coord. Chem. Rev.* **1990**, 100, 293; S.L. Bruhn, J.H. Toney, S.J. Lippard *Prog. Inorg. Chem.* **1990**, 38, 477; J. Reedijk, A.M.J. Fichtinger-Schepman, A.T. van Oosterom, P. van de Putte *Structure and Bonding* **1987**, 67, 53

[4] D.Frasca, J. Ciampa, J. Emerson, R.S. Umans, M. Clarke *Metal-based Drugs* **1996**, 3, 197

[5] A.D. Kelman, M.J. Clarke, S.D. Edmonds, H.J. Peresie *J. Clin. Hematol. Oncol.* **1977**, 7, 274

[6] R.E. Yasbin, C.R. Matthews, M.J. Clarke *Chem.-Biol. Interact.* **1980**, 30, 355

[7] K.A. Marx, R. Kruger, M.J. Clarke *Mol. Cell. Biochem.* **1989**, 86, 155

[8] P.M. van Vliet, J.G. Haasnoot, J. Reedijk *Inorg. Chem.* **1994**, 33, 1934

[9] P.M. van Vliet, S.M.S. Toekimin, J.G. Haasnoot, J. Reedijk, O. Nováková, O. Vrána, V. Brabec *Inorg. Chim. Acta* **1995**, 231, 57

[10] G.M. Brown, S.E. Sutton, H. Taube *J. Am. Chem. Soc.* **1978**, 100, 2767

[11] P.M. van Vliet *PhD. Thesis* Leiden University, The Netherlands, **1996**

[12] R.B. Martin *Acc. Chem. Res.* **1985**, 18, 32

[13] J.H.J. den Hartog. M.L. Salm, J. Reedijk *Inorg. Chem.* **1984**, 23, 2001

[14] S.L. van der Veer, H. van den Elst, J. Reedijk *Inorg. Chem.* **1987**, 26, 1536; G. Raudascht-Sieber, H. Schöllhorn, U. Thewatt, B. Lippert *J. Am. Chem. Soc.* **1985**, 107, 3591

[15] M. Hartmann, T.J. Einhäuser, B.K. Keppler *J. Chem. Soc. Chem. Commun.* **1996**, 1741

[16] a) G. Mestroni, E. Alessio, M. Calligaris *Prog. Clin. Biochem. Med.* **1989**, 10, 72; S. Cauci, E. Alessio, G. Mestroni, F. Quadrifoglio *Inorg. Chim. Acta* **1987**, 137, 19; b) G. Esposito, S. Cauci, F. Fogolari, E. Alessio, M. Scocchi, F. Quadrifoglio, P. Viglino *Biochemistry* **1992**, 31, 7094

[17] Y.-N. Tian, P. Yang, Q.-S. Li, M.-L. Guo, M.-G. Zhao *Polyhedron* **1997**, 16, 1993

[18] A. Agnostopoulou, E. Moldrheim, N. Katsaros, E. Sletten *J. Biol. Inorg. Chem.* **1999**, 4, 199

[19] S. Korn, W.S. Sheldrick *J. Chem. Soc. Dalton Trans.* **1997**, 2191

[20] D.J. Nelson, P.L. Yeagle, T.L. Miller, R.B. Martin *Bioinorganic Chemistry* **1976**, 5, 353

[21] R.B. Martin, Y.H. Mariam *Met. Ions Biol. Syst* **1979**, 8, 57

[22] J.D. Watson, F.H.C. Crick *Nature* **1953**, 171, 1953

[23] M.J. Clarke, H. Taube *J. Am. Chem. Soc.* **1974**, 96, 5413

[24] A. Pullman, B. Pullman *Q. Rev. Biophys.* **1981**, 14, 289

[25] S. Mansy, G.Y.H. Chu, R.E. Duncan, R.S. Tobias *J. Am. Chem. Soc.* **1978**, 100, 607

[26] B. Song, H. Sigel *Inorg. Chem. 1998*, 37, 2066

[27] H. Sigel, S.S. Massoud, N.A. Corfù *J. Am. Chem. Soc.* **1994**, 116, 2958

[28] S. Cauci, P.Viglino, G. Esposito, F. Quadrifoglio *J. Inorg. Biochem.* **1991**, 43, 739

[29] U. Bierbach, N. Farrell *Inorg. Chem.* **1997**, 36, 3657

[30] J.M. Davey, K.L. Moerman, S.F. Ralph, R. Kanitz, M.M. Sheil *Inorg. Chim. Acta* **1998**, 281, 10

[31] B. Schneider, M. Kabelác *J. Am. Chem. Soc.* **1998**, 120, 161

[32] G.L. Eichhorn, Y.A. Shin *J. Am. Chem. Soc.* **1968**, 90, 7323

[33] A. Laoui, J. Kozelka, J. Chottard *Inorg. Chem.* **1988**, 27, 2751

[34] J. Reedijk *J. Chem. Soc. Chem. Commun.* **1996**, 801

[35] S.E. Sherman, S.J. Lippard *Chem. Rev.* **1987**, 87, 1153; J.H.J. den Hartog, C. Altona, J.H. van Boom, G.A. van der Marel, C.A.G. Haasnoot, J. Reedijk *J. Am. Chem. Soc.* **1984**, 106, 1528; J.H.J. den Hartog, C. Altona, J.H. van Boom, G.A. van der Marel, C.A. Haasnoot, J. Reedijk *J. Biomol. Struct. Dyn.* **1985**, 2, 1137; J.A. Rice, D.M. Crothers, A.L. Pinto, S.J. Lippard *Proc. Natl. Acad. Sci. USA* **1988**, 85, 4158; S.F. Bellon, S.J. Lippard *Biophys. Chem.* **1990**, 35, 179; F. Herman, J. Kozelka, V. Stoven, E. Guittet, J.-P. Girault, T. Huynh-Dinh, J.Igolen, J.-Y. Lallemand, J.-C. Chottard *Eur. J. Biochem.* **1990**, 194, 119; S.F. Bellon, J.H. Coleman, S.J. Lippard *Biochemistry* **1991**, 30, 8026; P.M. Takahara, A.C. Rosenzweig, C.A. Frederick, S.J. Lippard **Nature** 1995, 377, 649; D. Yang, S.S.G.E. van Boom, J. Reedijk, J.H. van Boom, A.H.-J. Wang *Biochemistry* **1995**, 34, 12912

[36] P.M. Pil, S.J. Lippard *Science* **1992**, 256, 234

[37] J. Kasparkova, V. Brabec *Biochemistry* **1995**, 34, 12379

[38] X.Q. Zhai, H. Beckmann, H.M. Santzen, J.M. Essigmann *Biochemistry* **1998**, 37, 16307

[39] D.M. Soumpasis, J. Wiechen, T.M. Jovin *J. Biomol. Struct. Dyn.* **1987**, 4, 535

[40] R. Zaludova, V. Kleinwachter, V. Brabec *Biophys. Chem.* **1996**, 60, 135

[41] J. Shack, R.T. Jenkins, J.M. Thompsett *J. Biol. Chem.* **1953**, 203, 73; R. Thomas *Trans. Faraday Soc. 1954*, 50, 324; R.F. Steiner, R.F. Beers *Biochim. Biophys. Acta* **1956**, 32, 166; K. Fuwa, W.E.C. Wacker, R. Druyon, A.F. Bartholomay, L. Vallee *Proc. Natl. Acad. Sci. USA* **1960**, 46, 1298; W.F. Dove, N. Davidson *J. Mol. Biol.* **1962**, 5, 467

[42] G.L. Eichhorn *Nature* **1962**, 194, 474

[43] A.G. Walton, J. Blackwell *Biopolymers* Academic Press, NY, **1973**, 229

[44] D. Pörschke *Mol. Biol. Biochem. Biophys.* **1977**, 24, 191; V.V. Filimonov, P.L. Privalov *J. Mol. Biol.* **1978**, 122, 465; U. Schernau, S. Marcinowski, T. Ackerman *Z. Phys. Chem. N. F.* **1979**, 117, 11

[45] D. Pörschke, M. Eigen *J. Mol. Biol.* **1971**, 62, 361

[46] J. Marmur, P. Doty *J. Mol. Biol.* **1962**, 5, 109

[47] H.C. Spatz, D.M. Crother *J. Mol. Biol.* **1969**, 42, 191

[48] K.J. Breslauer, R. Frank, H. Blocker, L.A. Marky *Proc. Natl. Acad. Sci. USA* **1986**, 83, 3746

[49] P. Job *Ann. Chim. (Paris)* **1928**, 9, 113; M. Riley, B. Maling, M.J. Chamberlain *J. Mol. Biol.* **1966**, 20, 359

[50] S.J. Lippard, *Science* **1982**, 218, 1075

[51] A.M.J. Fichtinger-Schepman, P.H.M. Lohman, J. Reedijk *Nucleic Acids Res.* **1982**, 10, 5345

[52] A. Eastman *Biochemistry* **1985**, 24, 5027

[53] P.M. Takahara, C.A. Frederick, S.J. Lippard *J. Am. Chem. Soc.* **1996**, 118, 12309

[54] G. Sava, E. Alessio, E. Bergamo, G. Mestroni *Topics Bioinorg. Chem.* (in press)

[55] M.J. Clarke, B. Jansen, K.A. Marx, R. Kruger *Inorg. Chim. Acta* **1986**, 124, 13

[56] K.A. Marx, R. Kruger, M.J. Clarke *Mol. Cell Biochem.* **1989**, 86, 155

[57] J.K. Barton *Pure Appl. Chem.* **1989**, 61, 563

[58] M. Hartmann, K.G. Lipponer, B.K. Keppler *Inorg. Chim. Acta* **1998**, 267, 137

[59] G. Mestroni, E. Alessio, M. Calligaris *Prog. Clin. Biochem. Med.* **1989**, 10, 72

[60] S. Cauci, E. Alessio, G. Mestroni, F. Quadrifoglio *Inorg. Chim. Acta* **1987**, 137, 19

[61] G. Esposito, S. Cauci, F. Fogolari, E. Alessio, M. Scocchi, F. Quadrifoglio, P. Viglino *Biochemistry* **1992**, 31, 7094

[62] S. Cauci, P. Viglino, G. Esposito, F. Quadrifoglio *J. Inorg. Biochem.* **1991**, 43, 739

[63] A. Anagnostopoulou, E. Moldrheim, N. Katsaros, E. Sletten *J. Biol. Inorg. Chem.* **1999**, 4, 199

[64] M. Coluccia, A. Nassi, F. Loseto, A. Boccarelli, M. Mariggio, D. Giordano, F.P. Intini, P. Caputo, G. Natile *J. Med. Chem.* **1993**, 36, 510

[65] V. Brabec, O. Vrana, O. Novakova, V. Kleinwachter, F.P. Intini, M. Coluccia, G. Natile *Nucl. Acids Res.* **1996**, 24, 336

[66] R. Zaludova, A. Zakovska, J. Kasparkova, Z. Balcarova, O. Vrana, M. Coluccia, G. Natile, V. Brabec *Mol. Pharmacol.* **1997**, 52, 354

[67] V. Brabec, J. Reedijk, M. Leng *Biochemistry* **1992**, 31, 12397

[68] V. Brabec, V. Boudny, Z. Balcarová *Biochemistry* **1994**, 33, 1316

[69] G. Admiraal, M. Alink, C. Altona, F.J. Dijt, C.J. van Garderen, R.A.G. de Graaf, J. Reedijk *J. Am. Chem. Soc.* **1992**, 114, 930

[70] P. del S. Murdoch, Z. Guo, J.A. Parkinson, P.J. Sadler *J. Biol. Inorg. Chem.* **1999**, 4, 32

[71] F. Reeder, Z. Guo, P. del S. Murdoch, A. Corazza, T.W. Hambley, S.J. Berners-Price, J.C. Chottard, P.J. Sadler *Eur. J. Biochem.* **1997**, 249, 370

[72] J.B. Fenn, M. Mann, C.K. Meng, S.F. Wong, C.M. Whitehouse *Science* **1989**, 24, 64

[73] R.D. Smith, J.A. Loo, G.G. Edmonds, C.J. Barinaga, H.R. Udseth *Anal. Chem.* **1990**, 62, 882

[74] E. Nordhoff, F. Kerpekar, P. Roepstorff *Mass Spectrom. Rev.* **1996**, 15, 67

[75] P.A. Limbach *Mass Spectrom. Rev.* **1996**, 15, 297

[76] J.A. McCloskey, P.F. Crain *Int. J. Mass Spectrom. Ion. Processes* **1992**, 6, 771

[77] R.D. Smith, J.A. Loo, C.G. Edmonds, L.S. Baringa, H.R. Udseth *Anal. Chem.* **1990**, 62, 882

[78] K.A. Sannes-Lowery, D.P. Mack, P. Hu, H.Y. Mei, J.A. Loo *J. Am. Soc. Mass Spectrom.* **1997**, 8, 90

[79] M. Karas, D. Bachmann, U. Bahr, F. Hillenkamp *Int. J. Mass Spectrom. Ion. Processes* **1987**, 78, 53

[80] L. Zhu, G.R. Parr, M.C. Fitzgerald, C.M. Nelson, L.M. Smith *J. Am. Chem. Soc.* **1995**, 117, 6048

[81] W. Tang, L. Zhu, L.M. Smith *Anal. Chem.* **1997**, 69, 302

[82] F. Kirpekar, E. Nordhoff, K. Kristiansen, P. Roepstorff, S. Hahner, F. Hillenkamp *Rapid Commun. Mass Spectrom.* **1995**, 9, 525

[83] K.J. Lightwahl, D.L. Springer, B.E. Winger, C.G. Edmonds, D.G. Camp, B.D. Thrall, R.D. Smith *J. Am. Chem. Soc.* **1993**, 115, 803

[84] B. Ganem, Y.T. Li, J.D. Henion *Tet. Lett.* **1993**, 34, 1445

[85] D.C. Gale, R.D. Smith *J. Am. Soc. Mass Spectrom.* **1995**, 6, 1154

[86] R.D. Smith, J.A. Loo, C.G. Edmonds, C.J. Barinaga, H.R. Udseth *Anal. Chem.* **1990**, 62, 882; K. Bleicher, E. Bayer Biol. *Mass Spectrom.* **1994**, 23, 320

[87] R.H. Griffey, H. Sasmor, M.J. Greig *J. Am. Soc. Mass Spectrom.* **1997**, 8, 155

[88] Z. Guo, T.W. Hambley, P. del S. Murdoch, P.J. Sadler, U. Frey *J. Chem. Soc. Dalton Trans.* **1997**, 469

[89] E. Nordhoff, F. Kerpekar, P. Poepstroff *Mass Spectrom. Rev.* **1996**, 15, 67

[90] H. Troujman, J.C. Chottard *Anal. Biochem.* **1997**, 252, 177

[91] P.A. Limbach *Mass Spectrom. Rev.* **1996**, 15, 297; K.K. Murray, *J. Mass Spectrom.* **1996**, 31, 1203

[92] I.P. Smirnov, M.T. Roskey, P. Juhasz, E.J. Takch, S.A. Martin, L.A. Haff *Anal. Biochem.* **1996**, 238(1), 19

[93] P.A. Limbach, J.A. McCloskey, P.F. Crain *Nucleic Acids Symp. Ser.* **1993**, 31, 127

[94] R.P. Glover, G.M.A. Sweetnam, P.B. Farmer, G.C.K. Roberts *Rapid Commun. Mass Spectrom.* **1995**, 9, 897

[95] H. Wu, C. Chan, H. Aboleneen *Anal. Biochem.* **1998**, 263, 129

[96] Y. Furuichi, K. Miura *Nature* **1975**, 253, 374

[97] H. Wu, R.L. Morgan, H. Aboleneen *J. Am. Soc. Mass Spectrom.* **1998**, 9, 660

[98] D.P. Little, R.A. Chorush, J.P. Speir, M.W. Senko, N.L. Kelleher, F.W. McLafferty *J. Am. Chem. Soc.* **1994**, 116, 4893

[99] H. Wu, R.L. Morgan, H. Aboleneen *J. Am. Soc. Mass Spectrom.* **1998**, 9, 660

Chapter 6

Cytotoxicity tests of Ru(II)arene complexes

6.1 Introduction*

Cisplatin is one of the most widely used drugs in anticancer therapy[1] and has proven to be very effective in clinical therapy of several human solid tumours such as testicular carcinomas, ovarian tumours, head and neck cancers, bladder tumours and osteocarcomas, however it only shows a weak effect against many other malignancies of relevant social incidence such as breast cancers, lung cancer and colo/rectal adenocarcinomas.[2] Thus, there is much room for the development of new antitumour agents. The current trend for organisations such as the National Cancer Institute is to use. as a first selection process, tumour cell lines of histologically defined solid tumour entities which are used to determine the cytotoxic activity of the compounds tested and those qualifying go on to *in vivo* testing.[3]

Some ruthenium compounds have shown promising effects in these form of cell line tests. *Mer*-[Ru(terpy)Cl_3] shows a very high cytotoxicity against leukaemia and human cervical cell lines.[4] In cell-free media, this complex was found to coordinate to DNA preferentially at G residues, and this suggests a cisplatin type mechanism of action.[4] *cis* and *trans*-[$RuCl_2(DMSO)_4$] were found to exert an anti-leukaemic effect on a cisplatin resistant cell line, which indicates a lack of cross resistance and hence a different mechanism of action, despite binding preferentially to Gs in DNA.[5] [(η^6-C_6H_6)$RuCl_2$(metronidazole)] is cytotoxic towards *E. Coli*, more so in fact than free metronidazole (metronidazole is a nitromidazole, a range of compounds which sensitise hypoxic tumour cells to radiation).[6] Other Ru(arene) complexes such as [$Ru(cp)_2Cl]^+$ [7]and its ring-oxidised analogue [Ru(cpO)(cp)Cl]$^+$, [8] however, show weak cytotoxicity, in the region of 100 μM, whereas the osmium analogue has very good cytotoxicity against several cancer cell lines.[7]

* This work was performed in collaboration with Dr. Duncan Jodrell, Dr. Jeff Cummings and Rhona Aird of the ICRF, Western General Hospital, Edinburgh.

Yet the property that renders ruthenium complexes unique among anticancer agents is principally the lack of evident cell cytotoxicity at doses that increase lifetime expectancy in tumour-bearing hosts.[9] Na[*trans*-$RuCl_4$(DMSO)Im], NAMI, a ruthenium 3+ complex that is very effective against metastases is not cytotoxic towards tumour cells[10] and NAMI-A, [HIm][*trans*-$RuCl_4$(DMSO)Im], the more recent version of NAMI, is virtually devoid of *in vitro* toxicity in doses >100 μM against a cell line against which cisplatin is effective.[11] Yet, despite their lack of cytotoxicity, both NAMI and NAMI-A are effective in both preventing formation of metastases and in reducing their growth when already present at the beginning of drug treatment.[9(b)] Metastases represent the greatest obstacle to post-surgery and/or radiotherapy cures, in that they often show a low chemosensitivity to the available anticancer drugs.[12]

Perhaps lack of penetration of the cell membrane is the reason for the lack of direct cytotoxicity, and hence the compounds bind to extracellular components. Here Ru interactions may deprive tumour cells of normal cell-cell and cell-matrix contacts which are essential for cell growth, division and formation of metastases.[13] This idea is supported by a study performed on a series of eighteen Ru(III) complexes that are structurally related to NAMI. These complexes only showed *in vitro* cytotoxicity at concentrations $>10^{-4}$ M, yet reduced the formation of metastases by a mechanism unrelated to direct tumour cell cytotoxicity.[9(b)] The absence of direct cell toxicity may actually be an advantage as it may decrease the side effects on healthy tissues.[9(c)] NAMI, in fact, has very low side-effects on normal cells of host tissues such as liver, kidney and lung epithelia.[14] Any cytotoxicity which has been found, however, seems to be related to the lipophilicity of the compound, suggesting that lipophilicity allows the compound to enter the cell and exert its cytotoxic action.[9(b)] This fits in well with part of our rationale for using Ru(arene) complexes. The arene ring should confer a degree of lipophilicity on our compounds, and increase interactions with the cell membrane. It was also noted in the publication that cytotoxic compounds can also be anti-metastatic,[9(b)] so although cytotoxicity is not necessary for anti-metastatic activity, the two may be related.

With the knowledge that ruthenium complexes do not always exhibit cytotoxicity against cell lines, preliminary tests were performed on a selection of complexes prepared in Chapter 4. These tests were considered worthwhile as $[(\eta^6\text{-}p\text{-cymene})RuCl(en)]^+$ **13** has been shown to bind to DNA in a G specific manner, section 5.3, and the arene ring confers a degree of lipophilicity on the complexes that should aid passage through the cell membrane. Tests were performed against human ovarian cancer cell lines, and their cisplatin resistant and adriamycin resistant strains, with a view to obtaining an insight into cytotoxic effects of the complexes and possible mechanisms of action.

6.2 Experimental

The compounds were tested on 24-well trays by Rhona Aird, Dr. Jeff Cummings and Dr. Duncan Jodrell at the ICRF Unit of the Western General Hospital, Edinburgh. Cells growing in a flask were harvested just before they become confluent, counted using a haemocytometer and diluted down with medium (cell-culture medium containing 5 % foetal calf serum) to a concentration of 1 x 10^4 cells ml^{-1}. The cells were then seeded in the 24-well trays at a density of 1 x 10^4 cells per well (i.e. 1 ml of the diluted cell suspension was added to each well). The cells were then left to plate down and grow for 72 h before the drug was added.

The Ru complexes were weighed out and made up to a concentration of 1 mg ml^{-1} with deionised water and then sonicated until dissolved. The appropriate volume of the Ru solution was added to 5 ml of medium to make it up to a concentration of 100 μM stock solutions for each drug. This 100 μM solution was then serially diluted to make up 10 μM, 1 μM and 0.1 μM solutions. The medium was removed from the cells and replaced with 1 ml of the medium dosed with drug. Each concentration was made up in duplicate. A set of control wells were left on each plate, containing medium without drug. The cells were exposed to the drugs for 24 h and then washed with phosphate

buffered saline before fresh medium was added. The cells were allowed to grow for a further three days before being counted using a Coulter counter.

To prepare the cells for counting the medium was removed and 1 ml of PBS was added to the cells. An aliquot of 250 μl of trypsin was added and the cells left in an incubator for a few minutes to allow the monolayers to detach. Once trypsinised, 250 μl of media was added to each well to neutralise the trypsin. An aliquot of 200 μl of this suspension was then added to 10ml of NaCl for counting.

Resistance was derived in the cisplatin resistant A2780cis and adriamycin resistant A2780AD cell lines by stepwise exposure of A2780 to increasing concentrations of the respective drug. PE01 cisplatin resistance was obtained in a similar manner.

6.3 Results and discussion

Potential ruthenium anticancer agents are often compared to cisplatin as they both contain a heavy transition metal of Group VIII. The management of ovarian cancer has been improved by the introduction of cisplatin into clinical use[15] and for these reasons we performed the cytotoxicity tests reported here. The cell line used was A2780, an ovarian cancer cell line. This is a cell line quite commonly used for cytotoxicity tests of platinum drugs in its original form, or its cisplatin or adriamycin resistant form.[16] This cell line has also been used as screens for cytotoxic gold(III) compounds.[17] In this chapter, complexes **6**, **8**, **9**, **11**, **12**, **13**, **14**, **16** and **17** (see Table 6.1) were tested for cytotoxicity against the A2780 cell line. Any positively-charged complex has the counter-ion PF_6^-, except for **14**, which has an iodide counter-ion. NH_4PF_6 has previously been shown to be devoid of cytotoxic activity[8] therefore any cytotoxic effect can be attributed to the ruthenium complex.

Complex	Formula
6	[(η^6-*p*-cymene)$RuCl_2$(isn)]
8	[(η^6-benzene)RuCl(MeCN)]$^+$
9	[(η^6-*p*-cymene)RuCl(MeCN)]$^+$
11	[(η^6-benzene)RuCl(en)]$^+$
12	[(η^6-benzene)RuI(en)]$^+$
13	[(η^6-*p*-cymene)RuCl(en)]$^+$
14	[(η^6-*p*-cymene)RuI(en)]$^+$
16	[(η^6-methylbenzoate)RuCl(en)]$^+$
17	[(η^6-biphenyl)RuCl(en)]$^+$

Table 6.1 A list of Ru(arene) complexes tested in this chapter. The positive metal complexes have PF_6^- as the counter-ion with the exception of **14** which has an iodide counter-ion.

A graph showing the IC_{50} of the complexes on the A2780 cell line is shown in Figure 6.1. IC_{50} is the concentration at which the complex causes death of 50 % of the cancer cells as compared to the control (no ruthenium).

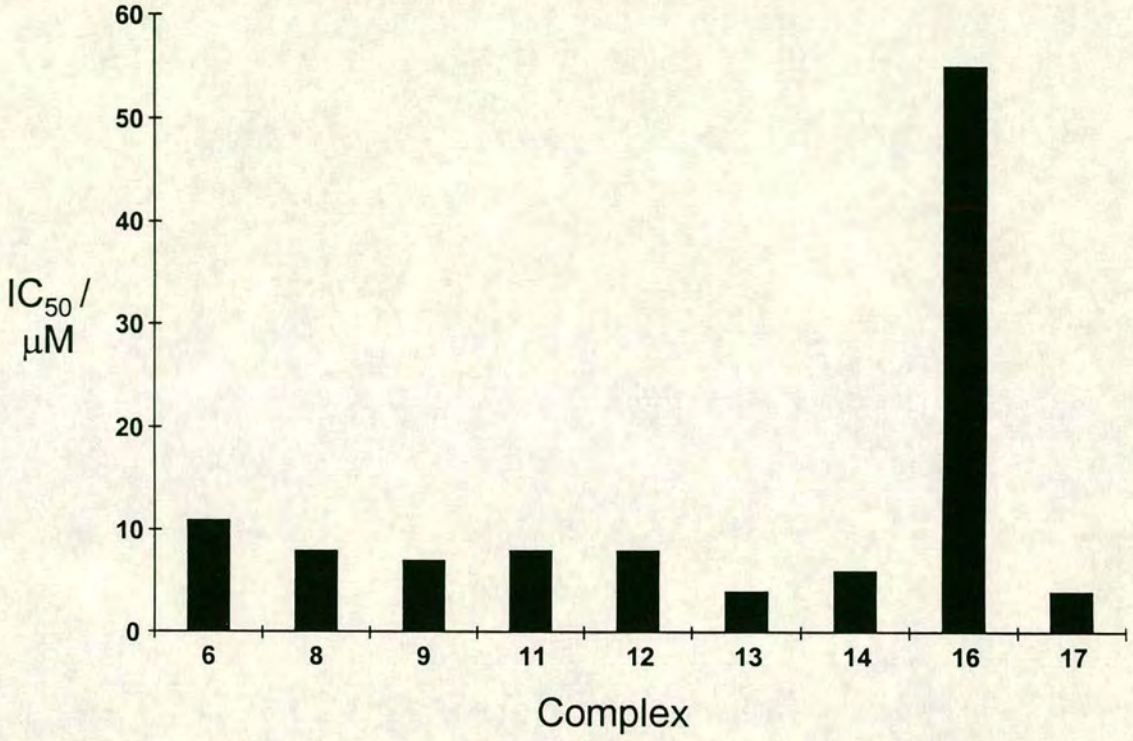

Figure 6.1 Bar chart showing the IC_{50} values in μM for the Ru(arene) complexes tested against the ovarian cancer cell line A2780. Cisplatin showed an IC_{50} value of 0.6 μM and carboplatin showed an IC_{50} value of 5 μM against the same cell line. Figures shown are a mean of two tests. The formulae of the complexes is given in Table 6.1.

It can be seen from Figure 6.1 that all the complexes with the exception of **16** exhibit a reasonable activity. Although the value for cisplatin is a factor of ten less (IC_{50} = 0.6 μM), the values are close to carboplatin, another clinically used anticancer drug. By comparison of the results from each complex we can draw certain conclusions. Firstly, the difference in cytotoxicity brought about by changing the halide from Cl to I is negligible. This can be seen by comparing the results for **11** and **12**, and **13** and **14**. Secondly, changing from a complex that is likely to form polyfunctional adducts to one that is likely to produce only monofunctional adducts actually brings about a decrease in

the IC_{50} value. This is demonstrated by the lower IC_{50} values of the ethylenediamine complexes **11, 12, 13, 14** and **17** (the monofunctional complexes) as compared to **6, 8** and **9** (the polyfunctional complexes). Where a really noticeable effect occurs is on varying the arene ring. It is not so much in changing from benzene to *p*-cymene (**11** and **12** to **13** and **14**), but there is a decrease in the IC_{50} value. On changing to the methylbenzoate group, however, the complex becomes virtually inactive, with an IC_{50} of almost 100 μM. This change has to be due to the ester moiety on the arene ring as the complex is otherwise identical to **11**, **13** and **17**. Thus, the proposed idea of **16** acting as a prodrug which is hydrolysed in the cell by hydrolase enzymes to an active species appears not to be beneficial. Possibly the complex hydrolyses prior to entering the cell and this hinders its uptake. It should be remembered, however, that cytotoxicity tests have proven to be misleading in the past for Ru compounds and the complex may still find an effect as an antimetastatic agent.[9(b)] The final complex, **17**, is the biphenyl complex. This is the most active of the group against A2780. These results show the merit in introducing variation on the arene ring in an attempt to increase the cytotoxicity of the Ru(arene) complexes.

From these initial tests, complexes **13** and **17** were selected as lead compounds due to their low IC_{50} values and their different arene moieties, for further investigations of the mechanism of action.

6.3.1 Further cytotoxicity tests of [(η^6-*p*-cymene)RuCl(en)]$^+$ 13

The results of some further cytotoxicity tests with [(η^6-*p*-cymene)RuCl(en)]$^+$ **13** are shown in Figure 6.2. The complex exhibits good cytotoxicity against the parent cell line A2780, IC_{50} 6 μM, with a lesser effect against the cell line that is mutant for p53, IC_{50} 16

μM. The cell line containing the mutant vector, but not the mutant itself experienced a decrease in cytotoxicity as compared to the parent line, but the complex was still more effective against this than the mutant cell line, with an IC_{50} of 9 μM. When tested against another ovarian cancer cell line, PE01, and its cisplatin resistant analogue, PE01cDDP, the complex exhibited a low cytotoxicity, with IC_{50} values of 70 and 82 μM, respectively.

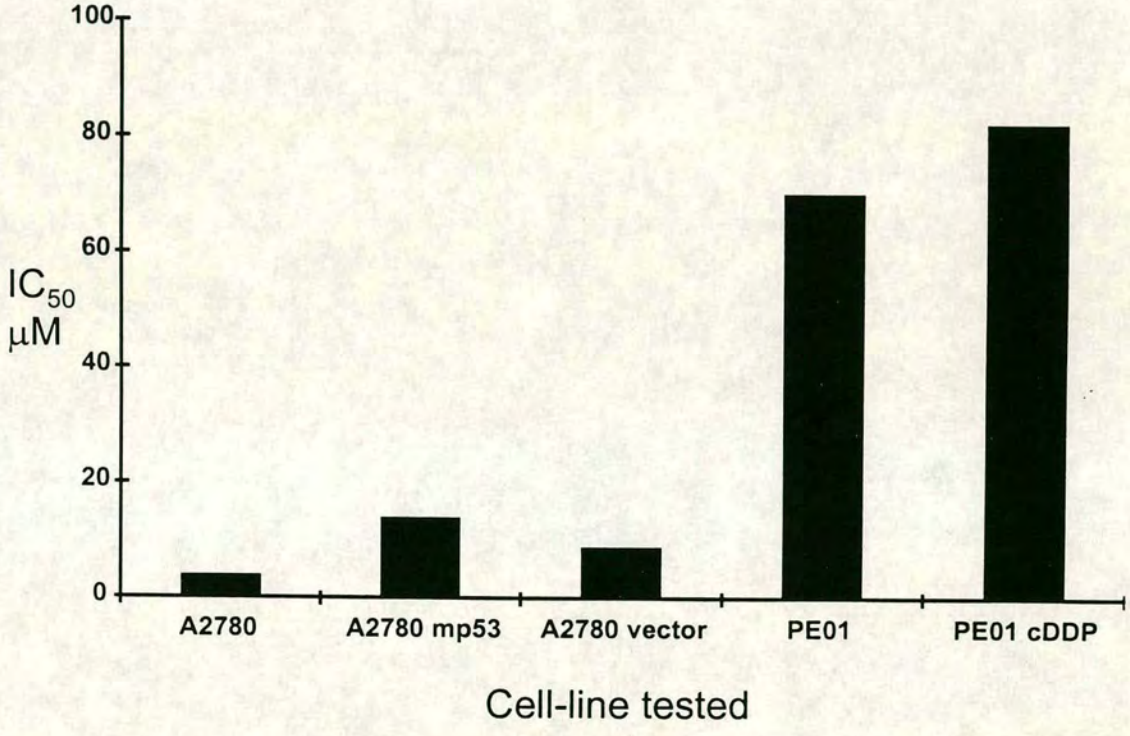

Figure 6.2 Bar chart showing the IC_{50} values of $[(\eta^6\text{-}p\text{-cymene})RuCl(en)]^+$ **13** against a series of cell lines. A2780 is the parent cell line, A2780 mp53 is the parent cell line mutant in p53, A2780 vector is the A2780 cell line containing the vector of the p53 mutant, but not the mutant, PE01 is another ovarian cancer cell line and PE01 cDDP is the PE01 cell line with acquired resistance to cisplatin. Cisplatin displayed IC_{50} values of 0.6, 2.2, 0.6, 5 and 44 μM for the cell lines, from left to right.

The implications of these results is that it is likely that $[(\eta^6\text{-}p\text{-cymene})RuCl(en)]^+$ **13** has a mechanism influenced by p53. This can be inferred because of the decrease in activity against the cell line that is mutant for p53, i.e. p53 does not function properly in this cell line. As a control, the complex was tested against a cell line which contains the vector that transfers the mutation to the cell line, but without the actual mutation. Against this cell line, there is a slight decrease in cytotoxicity, but not as much as in the p53 mutant cell line. Cisplatin shows a p53 influence against this cell line, as shown by the IC_{50} values of 0.6 mM against the parent cell line and 2.2 mM against the p53 mutant. Against PE01, the complex has such a low toxicity, that the fact that it is slightly worse towards the cell line which has become resistant to cisplatin is insufficient to gain any insights into the complex's activity.

Mutation of several specific genes involved in the control of cell growth and apoptosis is part of the process involved in the development of a malignant tumour.[18] Mutation or deletion of p53 has been shown to be one of the most common features of human cancer.[19] Its normal function is important in preventing cells from turning malignant. p53 protein is normally only present in the cell in minute levels and is generally thought to be inactive. However, when the cell starts to divide uncontrollably or its DNA is damaged, the protein becomes switched on and p53 levels rise,[20] and for this reason p53 is thought to act as a "molecular policeman" and has been termed the guardian of the genome.[21] When it has been activated, p53 may switch off replication to allow time for cell repair, or if this repair fails, it can trigger apoptosis, so preventing development of damaged cells.[22] Certain radiation and chemotherapy treatments are thought to function to some degree by triggering apoptosis and the function of p53 is important in this respect. Tumour cells which are mutant for p53 cannot perform this function are genetically unstable and can easily accumulate mutations.[22] Mice which do not possess wild-type p53 (WT p53) develop normally, but are very susceptible to tumours.[23] Intracellular levels of p53 increase dramatically in response to a variety of DNA damaging agents.[24] p53 is also thought to play a role in controlling DNA replication[25]

and transcription.[26] DNA binding is necessary for its tumour suppression activity[27] and it can bind DNA in a sequence specific manner.[28]

Mutations of the p53 gene are associated with development of resistance to cisplatin in human ovarian cancer cells,[29] and one proposed reason for the efficacy of cisplatin in testicular cancers is the low frequency of p53 mutations in this type of tumour.[30] Cisplatin has also been found to suppress growth of oesophageal cancer cells that are wild-type for p53, but not for the mutant strain.[31] Interestingly, and encouragingly for future treatments, reintroduction of WT-p53 into the human ovarian cisplatin resistant cancer cells resulted in a resensitisation.[32] It has been proposed that interperitoneal dosing with WT-p53 gene therapy could be beneficial in combination with cisplatin for treatment of ovarian tumours expressing mutant p53.[32] It is important to note, though, that some cells which are devoid of functional p53 function can be killed by cisplatin by a p53 independent route.[33]

Other platinum drugs have been found to have their activity linked to p53. Carboplatin has been found to stimulate an increase in p53 levels in tumour cells and trigger apoptosis.[34] JM216, an orally administered drug currently on clinical trials induces p53 in human ovarian cancer cell lines, including a line with induced cisplatin resistance. This is relevant as JM216 is thought to exert its cytotoxic effects through induction of apoptosis.[35]

Not all metal drugs are effected in the same way as cisplatin. [1,2-diaminocyclohexane-diactetato-dichloroPt(IV)] can actually reactivate WT-p53 in ovarian tumour cell lines, yet cell lines which are devoid of or mutant for p53 are cross resistant to it.[36] Peculiarly, a charged trinuclear platinum complex has been reported to be very active against mutant p53 cell lines, yet experiences a ten-fold reduction in cellular chemosensitivity for WT-p53.[37] These results emphasise the point that there is no general mechanism by which the cytotoxicity of metal-based drugs can be attributed.

6.3.2 Further cytotoxicity tests of [(η^6-biphenyl)RuCl(en)]$^+$ 17

Figure 6.3 shows IC_{50} values for [(η^6-biphenyl)RuCl(en)]$^+$ **17** against a series of A2780 cell lines. The IC_{50} values of this complex increase only very slightly from the parent cell line to the p53 mutant cell line, 5 μM to 6 μM, and the vector cell line has a lower IC_{50} value of 4 μM. There is no difference between the cytotoxic effect of complex **17** against the parent cell line and the cisplatin resistant cell line A2780 cis, but the complex is reasonably inactive, with an IC_{50} value of 70 μM against the adriamycin resistant cell line A2780 AD.

These results indicate a lack of p53 influence in the mechanism of action for complex **17**. If there was a p53 influence, it would be expected that there would be a more significant increase in the IC_{50} value for **17** against the cell line mutant for p53. Interestingly, the complex does not appear to share cross resistance with cisplatin. While cisplatin showed a four-fold increase in IC_{50} value against the A2780 with induced resistance, **17** showed no change from the parent cell line. This is promising as ideally an anticancer agent should possess a different mechanism of action to cisplatin. The most significant result from this test comes from the adriamycin resistant cell line. Adriamycin is an anticancer agent whose efficacy is linked to topoisomerase-II inhibiton.[43] The fact that the cytotoxic activity of complex **17** is severely reduced in this cell line is an exciting result and points to a cross resistance with adriamycin, and an unusual mechanism of action for a metallodrug.

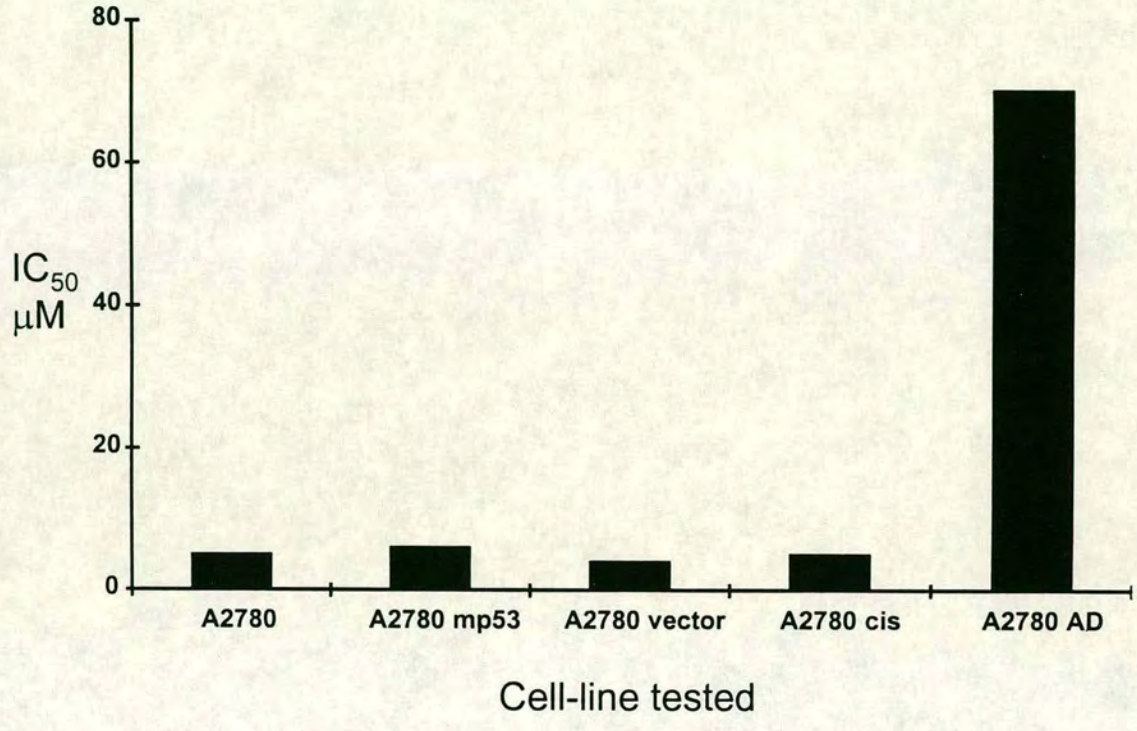

Figure 6.3 Bar chart showing IC_{50} values for $[(\eta^6\text{-biphenyl})RuCl(en)]^+$ **17** against a series of A2780 ovarian cancer cell-lines showing different properties. A2780 is the parent cell line, A2780 mp53 is the parent cell line mutant in p53, A2780 vector is the A2780 cell line containing the vector of the p53 mutant, but not the mutant, A2780 cis is the cell line with acquired cisplatin resistance and A2780 AD is the cell line with acquired resistance to adriamycin. Cisplatin displayed IC_{50} values of 0.6, 2.2, 6, 4 μM for the respective cell lines. Doxorubicin showed IC_{50} values of 0.2 μM for A2780, 0.2 μM for A2780 cis and 22 μM for A2780 AD. Doxorubicin is an alternative name for adriamycin.

Topoisomerases are a group of enzymes that can interconvert different topological isomers of DNA. The faithful replication and segregation of chromosomes as part of the cell division cycle requires that topological changes be imposed upon cellular DNA and topoisomerases catalyse these changes. [38] They relieve the torsional stress in unwinding DNA and resolve topological problems that arise during the various processes such as transcription, recombination, replication and chromosome partitioning during cell replication.[39] Type I topoisomerases only introduce breaks on one strand of the duplex, while a type II topoisomerases catalyse a double strand break.[40] These are vital enzymes for all organisms from bacteria to humans.[38] Many antibacterial and antitumour drugs are known to target topoisomerases I and II and effect their catalytic cycle.[41] The chemotherapeutic actions of many of these drugs correlate with their abilities to stabilise the covalent topoisomerase II-DNA cleavage complex,[42] thereby shifting the equilibrium of the enzymes DNA cleavage/religation cycle toward the cleavage event.[43] Drugs may also act at other steps of the catalytic cycle such as inhibiting the DNA religation step[43] or enhancing the enzyme's forward rate of cleavage.[44]

Anticancer drugs that target topoisomerase II are grouped in two categories depending on their DNA binding properties: binding, but nonintercalative,[45] and intercalating.[42(a),(b),(c)] The majority of the clinically effective topoisomerase poisons work through the cleavable complex, bind to DNA with high affinity (usually by intercalation) and induce extensive site specific damage.[42(c)] Most of these drugs, however, are not selective enzyme inhibitors, but exhibit secondary mechanisms of action that contribute to their host toxicity.[46] A structure-activity relationship for these drugs has recently been proposed.[47] The model suggests that a polycyclic ring is necessary for intercalation into DNA, and a further aromatic ring substitution, with a sterically unhindered hydroxy or amino function, is necessary to extend out of the plane of the DNA and interact with a hydrophobic pocket of the enzyme. Our complex [(η^6-biphenyl)RuCl(en)]$^+$ **13** could be viewed in a similar manner. The pendant ring of the biphenyl could act as the

intercalating moiety and the positive metal ion could bind to the DNA or enzyme, in a covalent or ionic manner, and hold the complex in place.

The platinum drugs used at present appear to have no inhibitory effect on topoisomerase. In fact, cisplatin resistant cell lines have been shown to have an associated increased topo-II activity[48] and cells with increased topo-II levels contribute to the cisplatin resistance, but cells with reduced levels of topo-II were found to be more sensitive to cisplatin.[49] Cisplatin and topo-II inhibitors have been found to have a synergistic effect when used together against cisplatin resistant cell lines.[50] Oxaliplatin, too, has been used in conjunction with a topo-I inhibitor, SN-38, with synergistic results.[51]

Recently a publication[52] reported that two ruthenium(II) complexes interfered with the catalytic effect of topoisomerase II, and the authors attempt to elucidate their molecular mechanism of action and relative neoplastic activity. The Ru(arene) complex [(η^6-C_6H_6)$RuCl_2$(DMSO)] was found to inhibit the DNA relaxation activity of topo-II by cleavable complex formation. It should be noted, though, that the characterisation of this complex, and the second complex tested [Ru^{II}(*trans*, bis-salicylaldoximato)] was not convincing. This view is supported by Clarke in his recent review.[53] The Ru-saldox complex was found to not induce cleavable complex formation, even though its DNA binding and antiproliferative effects are similar to the Ru(arene) complex. These complexes are relatively inactive though, doses >150 μM were required to give 50 % inhibition of cell proliferation. They also tested the complexes for their effect on the melting temperature T_m of calf thymus DNA. They report that, for the arene complex, the T_m increases with increasing drug concentration. This is in contrast to the work done on the effect of [(η^6-*p*-cymene)RuCl(en)]$^+$ **13** in section 5.2, where **13** caused a lowering of the T_m of an oligonucleotide duplex. The published results[52] imply an ionic interaction of the complex with the phosphate backbone, which would stabilise the duplex due to charge screening[54] rather than destabilise it by covalent binding to the nitrogenous bases.[55] Although this publication points to a topo-II inhibition by a Ru(arene) complex, the characterisation of the complex itself was very poor, and the

doses required for efficacy are very high. Complex **17**, on the other hand, is well characterised by NMR and X-ray crystal structure and shows efficacy at a much lower dosage, hence showing more potential for development.

6.4 Conclusions

Preliminary cytotoxic studies were performed on nine Ru(arene) complexes against a human ovarian cancer cell line. All complexes except one showed good activity. An important structural lead to take from these investigations is that varying the arene ring of the complex can have a significant effect on the activity of the complex. Two lead complexes, $[(\eta^6\text{-}p\text{-cymene})RuCl(en)]^+$ **13** and $[(\eta^6\text{-biphenyl})RuCl(en)]^+$ **17**, were chosen for some further studies. Interestingly the two complexes appear to display different mechanisms of action. Complex **13** appears to be p53 influenced and possibly cross resistant with cisplatin. Complex **17** does not seem to be influenced by p53, but instead shows a cross resistance with adriamycin, a topoisomerase-II inhibitor. This is potentially a very exciting result for a metallodrug.

It should be noted that these are preliminary results and repeats of cell cytotoxicity studies need to be performed to provide confirmation. On the basis of this study though, **17** has been chosen for more in-depth biological testing. This includes investigating accumulation of the complex in the cell, binding to DNA and testing in tumour models. The HPLC assay developed in Chapter 4 will be of assistance in these tests.

These complexes have great potential for structural variety and hopefully further investigations will elucidate structure-activity relationships. These tests mark the start of an exciting body of work linking chemistry and medicine, and hopefully it will prove to be of benefit in the treatment of cancer in the future.

6.5 References

[1] (a) P.J. Loehrer, L.H. Einhorn *Ann. Intern. Med.* **1984**, 100, 731; (b) M. Sum *Science* **1983**, 222, 145

[2] E. Holler in *Metal complexes in cancer chemotherapy* ed. B.K. Keppler, VCH, Weinheim, **1993**, 37; N. Farrell *Transition metal complexes as drugs and chemotherapeutic agents* Kluwer Acad. Pub., Dordrecht, **1989**

[3] M.C. Alley, D.A. Scudiero, A. Monks, A.C. Hursey, M.J. Czerwinski, D.L. Fine, B.J. Abbott, J.G. Mayo, R.H. Shoemaker, M.R. Boyd *Cancer Res.* **1988**, 48, 589

[4] O. Nováková, J. Kaspárková, O. Vrána, P.M. van Vliet, J. Reedijk, V. Brabec *Biochemistry* **1995**, 34, 12369

[5] M. Coluccia, G. Sava, F. Loseto, A. Nassi, A. Boccarelli, D. Giordano, E. Alessio, G. Mestroni *Eur. J. Cancer* **1993**, 13, 1873

[6] L.D. Dale, J.H. Tocher, T.M. Dyson, D.E. Edwards, D.A. Tocher *Anticancer Drug Design* **1992**, 7, 3

[7] Y. Yamazaki, M.Goto, Y. Kageyama, T. Tomohiro, H. Okuno *Zeit. Naturforsch.* **1996**, 51, 301

[8] Y. Yamazaki, M. Goto, K. Kobayashi, Y. Ogawa, T. Shimura, S. Oka, H. Okuna *Bioorg. Med. Chem. Lett.* **1994**, 4, 483

[9] (a) G. Sava in *Metal compounds in cancer therapy* ed. S. Fricker, Chapman and Hall, London, p.65; (b) G. Sava, S. Pacor, A. Bergamo, M. Cocchietto, G. Mestroni, E. Alessio *Chem. Biol. Interact.* **1995**, 95, 109; (c) I Capozzi, K. Clerici, M. Cochietto, G. Salerno, A. Bergamo, G. Sava *Chem. Biol. Interact.* **1998**, 113, 51

[10] G. Sava, I. Capozzi, A. Bergamo, R. Gagliardi, M. Cocchietto, L. Masiero, M. Onisto, E. Alessio, G. Mestroni, S. Garbisa *Int. J. Cancer* **1996**, 68, 60

[11] A. Bergamo, R. Gagliardi, V. Scarcia, A. Furlani, E. Alessio, G. Mestroni, G. Sava *J. Pharm. Exp. Ther.* **1999**, 289, 559

[12] J.E. Talmadge *Cancer Metast. Rev.* **1983**, 2, 25

[13] S.B. Fox, G.D. Turner, R.D. Leek, R.M. Whitehouse, K.C. Galter, A.L. Huris *Breast Cancer Res. Treat.* **1995**, 36, 219; D. Schadendorf, J. Haidel, C. Gawlik, L. Suter, B.M. Czarnetzki *J. Natl. Cancer Inst.* **1995**, 87, 366; V. Umarsky, V. Schirmmacher, M. Rocha *J. Mol. Med.* **1996**, 74, 353

[14] R. Gagliardi, G. Sava, S. Pacor *Clin. Exp. Metast.* **1994**, 12, 93

[15] W.J. Zeller, S. Frühauf, G. Chen, B.K. Keppler, E. Frei, M. Kaufmann *Eur. J. Cancer* **1991**, 27, 62

[16] see for example: M. Coluccia, A. Nassi, A. Boccarelli, D. Giordano, N. Cardellicchio, D. Locker, M. Leng, M. Sivo, F.P. Intini, G. Natile *J. Inorg. Biochem.* **1999**, 77, 31; A. Ercoli, A. Battaglia, G. Raspaglio, A. Fattorossi, A. Alimonti, F. Petrucci, S. Caroli, S. Mancuso, G. Scambia *Int. J. Cancer* **2000**, 85, 98; M. Coluccia, A. Nassi, A. Boccarelli, D. Giordano, N. Cardellicchio, F.P. Intini, G. Natile,

A. Barletta, A. Paradiso *Int. J. Oncol.* **1999**, 15, 1039; K.M. Henkels, J.J. Turchi *Cancer Res.* **1999**, 59, 3077

[17] B. Bruni, A. Guerri, G. Marcon, L. Messori, P. Orioli *Croatica Chem. Acta* **1999**, 72, 221; S. Carotti, A. Guerri, T. Mazzei, L. Messori, E. Mini, P. Orioli *Inorg. Chim. Acta* **1998**, 281, 90

[18] http://www.dundee.ac.uk/biochemistry/dpl.html

[19] (a) M. Hollstein, D. Sidransky, B. Vogelstein, C. Harris *Science* **1991**, 253, 49; (b) D. Lane, S. Benchimol *Oncogene* **1990**, 4, 1; (c) A.J. Levine, J. Momand, C.A. Finlay *Nature* **1991**, 351, 453

[20] X. Lu, D.P. Lane *Cell* **1993**, 75, 765

[21] D.P. Lane *Nature* **1992**, 358, 15

[22] R.E. Yonish *Nature* **1991**, 353, 345

[23] L.A. Donehower, M. Harvey, B.L. Slagle, M.J. McArthur, C.A. Montgomery Jr., J.S. Butel, A. Bradley *Nature* **1992**, 356, 215

[24] P.A. Hall, P.H. McKee, H.D. Menage, R. Dover, D.P. Lane *Oncogene* **1993**, 8, 203; (b) (a) M.B. Kastan, O. Onyekwere, D. Sidransky, B. Vogelstein, R.W. Craig *Cancer Res.* **1991**, 51, 6304; (c) X. Lu, S.H. Park, T.C. Thompson, D.P. Lane *Cell* **1992**, 70, 153; (d) W. Maltzman, L. Czyzyk *Mol. Cell. Biol.* **1984**, 4, 1689

[25] P.N. Friedman, S.E. Kern, B. Vogelstein, C. Prives *Proc. Natl. Acad. Sci. USA* **1990**, 87, 9275

[26] S. Fields, S.J. Jang *Science* **1990**, 249, 1046

[27] T.R. Hupp, D.W. Meek, C.A. Midgely, D.P. Lane *Cell* **1992**, 71

[28] (a) S. E. Kern, J.E. Pietenpol, S. Thiagalingam, A. Seymour, K.W. Kinzler, B. Vogelstein *Science* **1992**, 256, 827; (b) W.S. El-Deiry, S.E. Kern, J.A. Pietenpol, K.W. Kinzler, B. Vogelstein *Nature Genet.* **1992**, 1, 45

[29] K.M. Song, Z.W. Li, P. Seth, K.H. Cowan, B.K. Sinha *Oncol. Res.* **1997**, 9, 603

[30] D.B. Zamble, T. Jacks, S.J. Lippard *Proc. Natl. Acad, Sci. USA* **1998**, 95, 6163

[31] H. Matsubara, M. Kimura, M. Sugaya, Y. Koide, Y. Gunji, K. Takegama, T. Asano, T. Ochiai, K. Isono, S. Sakiyama, M. Tagawa *Int. J. Oncol.* **1999**, 14, 1081

[32] K.M. Song, K.H. Cowan, B.K. Sinha *Oncol. Res.* **1999**, 11, 153

[33] X.H. Wang, Y. Liu, L.S.N. Chow, S.C.H. Wong, S.W. Tsao, D.L.W. Kwong, J. Wang, J.S.T Sham, J.M. Nicholls *Int. J. Oncol.* **1999**, 15, 1097

[34] V. DiFelice, M. Lauricella, M. Giuliano, S. Emanuele, R. Vento, G. Tesoriere *Int. J. Oncol.* **1998**, 13, 225

[35] C.F. O'Neill, B. Koberle, J.R.W. Masters, L.R. Kelland *Brit. J. Cancer* **1999**, 81, 1294

[36] Z.H. Ziddik, G.S. Hagopian, G. Thai, S. Tomisaki, T. Toyomasu, A.R. Khokhar *J. Inorg. Biochem.* **1999**, 77, 65

[37] G. Pratesi, P. Perego, D. Polizzi, S.C. Righetti, R. Supino, C. Caserini, C. Manzotti, F.C. Giulani, G. Pezzoni, S. Tognella, S. Spinelli, N. Farrell, F. Zunino *Brit. J. Cancer* **1999**, 80, 1912

[38] P.M. Watt, I.D. Hickson *Biochem. J.* **1994**, 303, 681

[39] (a) J.C. Wang *Ann. Rev. Biochem.* **1985**, 54, 665; (b) R. Sternglanz *Curr. Opin. Cell Biol.* **1989**, 1, 533; (c) C.A. Austin, L.M. Fisher *Sci. Progress* **1990**, 74, 147; (d) N. Osherhoff, E.L. Zechiedrich, K.C. Gale *BioEssays* **1991**, 13, 269

[40] J.J. Champoux *Ann. Rev. Biochem.* **1978**, 47, 449; N.R Cozzarelli *Cell* **1980**, 22, 327; N.R. Cozzarelli *Science* **1980**, 207, 953; M. Gellert *Ann. Rev. Biochem.* **1981**, 50, 879

[41] (a) W.T. Beck, M.K. Danks *Semin. Cancer Biol.* **1991**, 2, 235; (b) G. Capranico, F. Zunino *Eur. J. Cancer* **1992**, 28A, 2055; (c) D.J. Fernandes, C.V. Catapano, A.J. Townsend in *Mechanisms of drug resistance in oncology* **1993**, Marcel Dekker, NY; (d) Y. Pommier *Cancer Chemother. Pharmacol.* **1993**, 32, 103; (e) W.T. Beck, M.K. Danks, J.S. Wolverton, R. Kim, M. Chen *Adv. Enz. Reg.* **1993**, 33, 113; (f) A.H. Corbett, N. Osherhoff *Chem. Res. Toxicol.* **1993**, 6, 586; (g) A.Y. Chen, L.F. Liu *Ann. Rev. Pharm. Toxic.* **1994**, 34, 191; (g) Y. Pommier, P. Pourquier, Y. Fan, D. Strumberg *Biochim. Biophys. Acta* **1998**, 1400, 83; (h) D.A. Burden, N. Osherhoff *Biochim. Biphys. Acta* **1998**, 1400, 139; (i) J.M. Fortune, N. Osherhoff *Prog. Nucl. Acid Res. Mol. Biol.* **2000** in press

[42] (a) L.A. Zwelling *Cancer Metast. Rev.* **1985**, 4, 263; (b) B.S. Glisson, W.E. Ross *Pharmacol. Ther.* **1987**, 32, 89; (c) L.F. Liu *Ann. Rev. Biochem* **1989**, 58, 351

[43] M.J. Robinson, N. Osherhoff *Biochemistry* **1990**, 29, 2511

[44] M.J. Robinson, B.A. Martin, T.D. Gootz, P.R. McGuirk, M. Moynihan, J.A. Sutcliffe, N. Osherhoff *J. Biol. Chem.* **1991**, 266, 14585; B.S. Sorensen, J. Sinding, A.H. Andersen, J. Alsner, P.B. Jensen, O. Westergaard *J. Mol. Biol.* **1992**, 228, 778

[45] W. Ross, T. Rowe, B. Glisson, J. Yalowich, L.F. Liu *Cancer Res.* **1984**, 44, 5857; K.-C. Chow, T.L. Macdonald, W.E. Ross *Mol. Pharmacol* **1988**, 34, 467

[46] J. Cummings, J.F. Smyth *Ann. Oncol.* **1993**, 4, 533

[47] T.L. Macdonald, E.K. :Lehnert, J.T. Loper, K.C. Chow, W.E. Ross *Cancer* **1991**, 199; H. Morjani, J.-F. Riou, I. Nabiev, F. Lavelle, M. Manfait *Cancer Res.* **1993**, 53, 4784

[48] J.M. Barrett, P. Calson, A.K. Larsen, B. Salles *Mol. Pharm.* **1994**, 46, 431

[49] A.K. Larsen, C. Gobert, C. Gilbert, J. Markovits, K. Bujanowski, A. Skladanowski *Acta Biochim. Pol.* **1998**, 45, 535

[50] Y. Minagawa, J. Kigawa, T. Irie, Y. Kanamori, H. Hamochi, X.S. Cheng, N. Terakawa *Jap. J. Cancer Res.* **1997**, 88, 1218

[51] C. Erlichman, S. Boerner, S.H. Kaufmann *Clin. Cancer. Res.* **1999**, 5, 615

[52] Y.N. Gopal, D. Jayaraju, A.K. Kondapi *Biochemistry* **1999**, 38, 4382

[53] M.J. Clarke, F.C. Zhu, D.R. Frasca *Chem. Rev.* **1999**, 99, 2511

[54] D.M. Soumpasis, J. Wiechen, T.M. Jovin *J. Biomol. Struct. Dyn.* **1987**, 4, 535

[55] G.L. Eichhorn *Nature* **1962**, 194, 474

Appendix 1

[^{1}H, ^{1}H] COSY spectrum of [$RuCl_2(H_2NCH_2CH_2PPh_2$-*N,P*)] **3** in DMSO-d_6

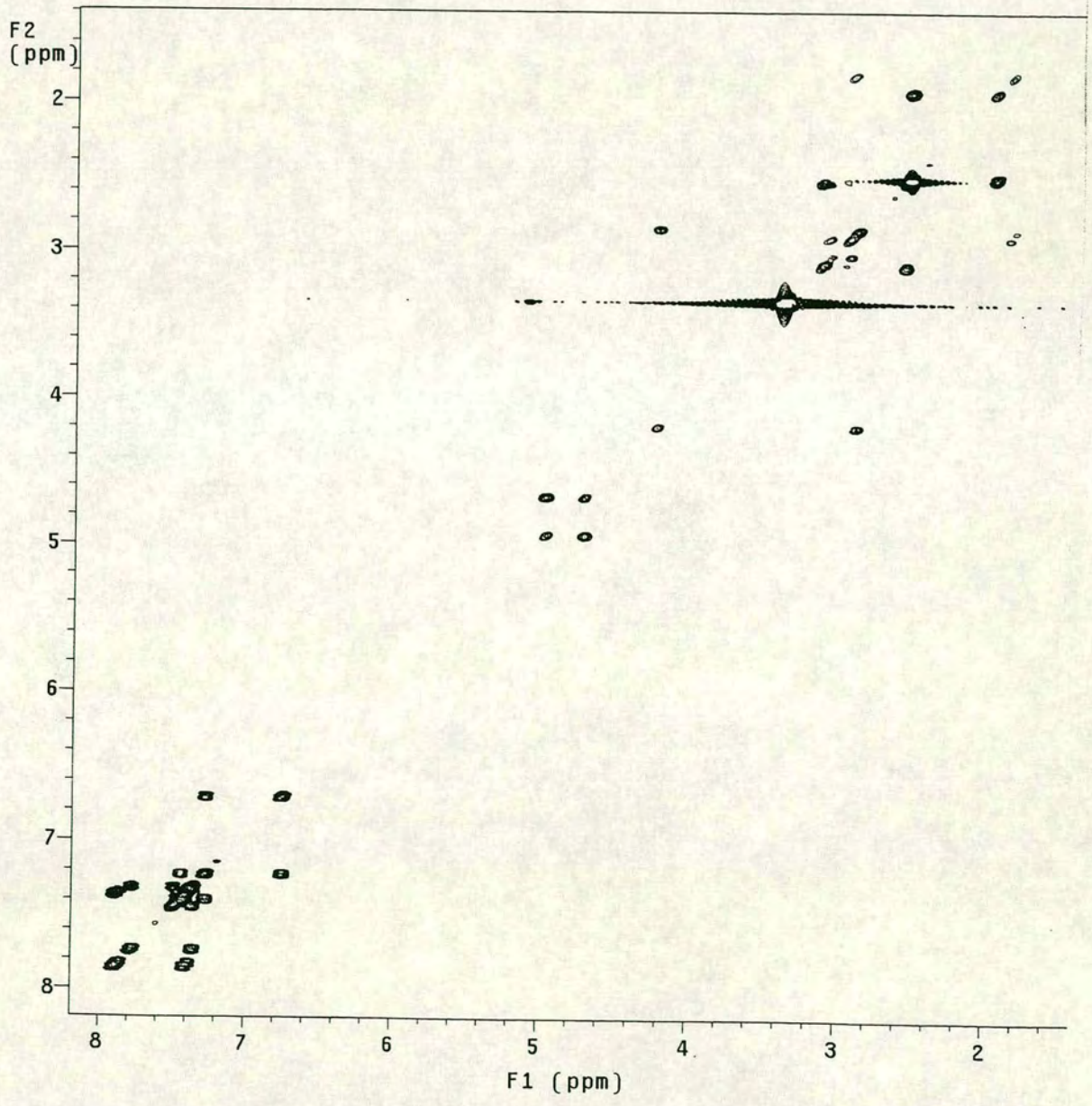

[^{1}H, ^{1}H] TOCSY spectrum of [$RuCl_2(H_2NCH_2CH_2PPh_2$-*N,P*)] **3** in DMSO-d_6

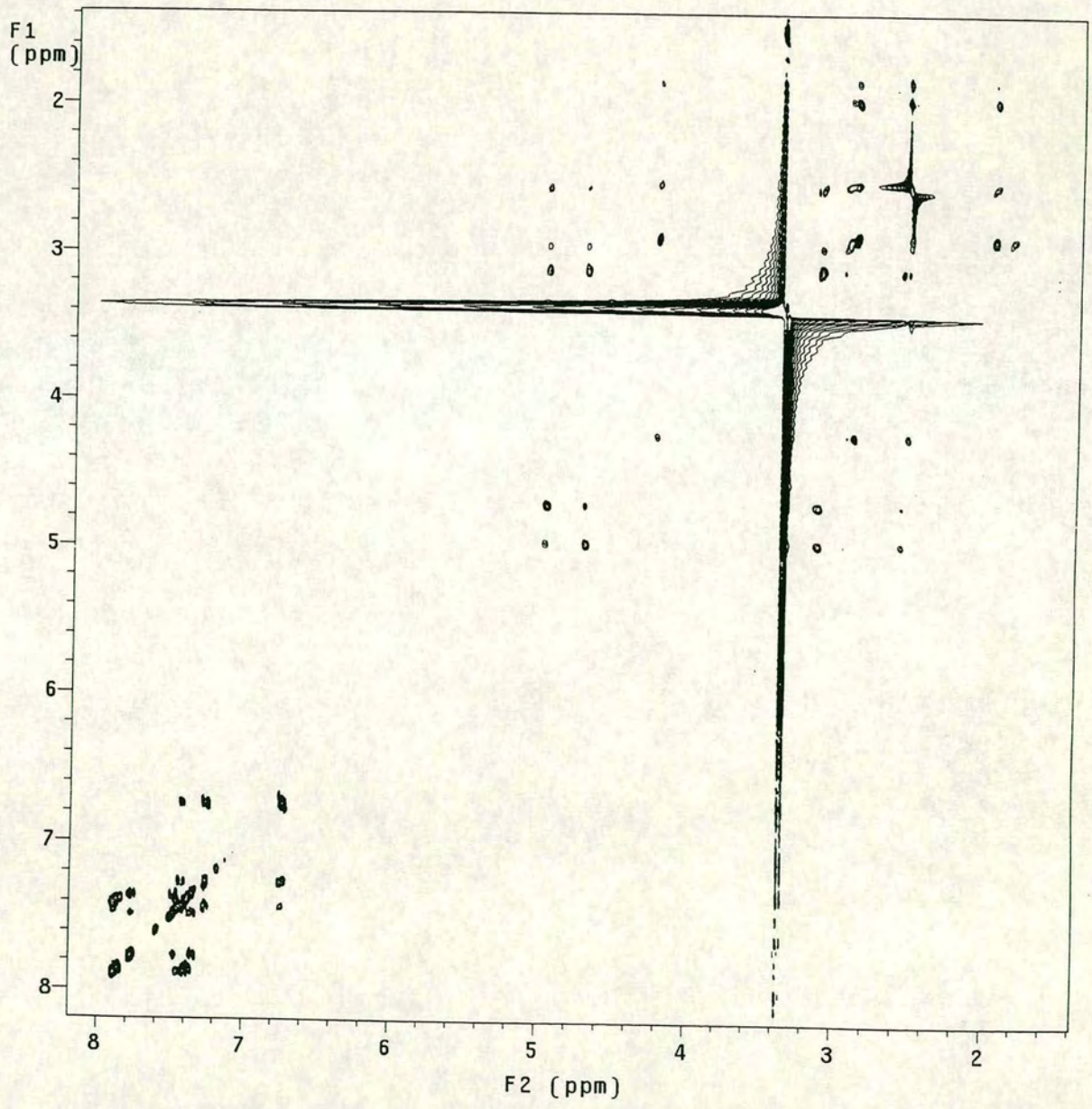

Appendix 2

NOESY spectrum of [(η^6-*p*-cymene)RuCl(en)]$^+$ **13** in D_2O